UNIVERSITY OF SOUTHAMPTON

FACULTY OF NATURAL AND ENVIRONMENTAL SCIENCES

Biological Sciences

The role of tetrapyrroles in plastid-to-nucleus retrograde signalling in *Arabidopsis thaliana*

by

Sylwia Monika Kacprzak

Thesis for the degree of Doctor of Philosophy in Biological Sciences

March 2018

UNIVERSITY OF SOUTHAMPTON

ABSTRACT

FACULTY OF NATURAL AND ENVIRONMENTAL SCIENCES

Doctor of Philosophy

THE ROLE OF TETRAPYRROLES IN PLASTID-TO-NUCLEUS RETROGRADE SIGNALLING IN *ARABIDOPSIS THALIANA*

By Sylwia Monika Kacprzak

Since the majority of chloroplast proteins are encoded in the nucleus it is critical that the chloroplast can communicate with the nucleus to regulate their synthesis. Biogenic chloroplast-to-nucleus signalling pathways have been described at a response level through changes in nuclear gene expression, but the signalling components are essentially unknown. Various biogenic signals have been proposed including a recently hypothesized positive heme-related signal, a singlet oxygen ($^1O_2$)-mediated inhibitory signal resulting from mis-regulation of chlorophyll synthesis, and signals derived from chloroplast gene expression. Chloroplasts have also been implicated as a sensor of many environmental signals and must also convey this information to the nucleus. This project was undertaken to increase our understanding on mechanisms by which plastids signal to the nucleus during seedling development.

Inhibition of photosynthetic gene expression after treatment with 2'2- dipyridyl (DP) and rescue of nuclear gene expression in the *gun6-1D* mutant following growth on norflurazon (NF), both support the model for plastid retrograde signalling with ferrochelatase 1 (FC1)-derived heme functioning as a positive plastid signal. One approach that has been taken was to identify new components of the chloroplast-to-nucleus signalling pathways in the model plant *Arabidopsis thaliana*. While most of the treatments blocking chloroplast functions result in a down-regulation of nuclear gene expression, it was found that white light (WL)-grown seedlings of the chloroplast translation mutant *prpl11-1* displayed elevated expression of some tetrapyrrole and photosynthesis-related genes (for example *HEMA1*, *CP12-2*). qPCR analyses showed that this phenotype was only partially reduced when chloroplast signalling was blocked by NF and lost when heme synthesis was blocked with DP. Physiological analyses showed *prpl11* mutants have disturbed tetrapyrrole metabolism with reduced Pchlide, 5-aminolevulinic acid (ALA) synthesis and total heme levels and were unable to accumulate Pchlide after additional ALA feeding. This is partially supportive of a role for PRPL11 as a regulator redirecting tetrapyrrole distribution towards the heme branch. PRPL11 overexpressing plants were constructed to identify putative PRPL11-interacting proteins and preliminary evidence suggests an interaction of PRPL11 with Mg-chelatase. Mutant and overexpressor lines of *GUN1* were also shown to affect tetrapyrrole metabolism and the elevated gene expression on NF and Lin seen for *gun1* was lost after treatment with DP. This analysis revealed GUN1 is a negative regulator of tetrapyrrole synthesis and its retrograde signalling phenotype is tetrapyrrole dependent. The possible integration of tetrapyrrole synthesis and chloroplast protein synthesis in retrograde signalling to the nucleus is proposed.

Feeding ALA to dark-grown seedlings resulted in $^1O_2$ production in WL and blocked the induction of photosynthetic gene expression. Inhibition of these genes was also detected in *flu, fc2-1* and *fc2-2* mutants transferred from D to WL supporting the role of $^1O_2$ in initiating an inhibitory retrograde signal. Genome-wide comparison of gene expression changes resulting from norflurazon (NF), a far red light pre-treatment, and multiple abiotic stresses showed partial similarity between $^1O_2$-dependent plastid signalling pathways and heat stress, and a strong overlap between drought stress and NF-induced transcriptomic changes. Further physiological analysis supports an interaction between these treatments. For example, exposure to heat shock blocked the induction of $^1O_2$ marker genes and induction of selected drought and salt stress genes was inhibited when chloroplast signalling was blocked. Furthermore, this response was rescued in known retrograde signalling mutants.

Contents

Declaration Of Authorship 1

Acknowledgements 3

Abbreviations 5

Chapter 1 Introduction 13

1.1 Chloroplast structure 13

1.2 Chloroplast genomes 14

1.3 Protein import into the chloroplast 16

1.4 Chloroplast gene expression 19

1.4.1 Chloroplast transcription 19

1.4.2 Chloroplast post-transcriptional regulation 22

1.4.3 Chloroplast translation 23

1.5 Chloroplast biogenesis 25

1.6 Tetrapyrrole biosynthesis in plants 28

1.6.1 ALA formation 28

1.6.2 Porphyrin synthesis 30

1.6.3 Chlorophyll synthesis 30

1.6.4 Heme synthesis 31

1.6.5 Phytochromobilin synthesis 31

1.7 Plastid retrograde signalling 31

1.7.1 Historical overview 32

1.7.2 *genomes uncoupled (gun)* mutants 34

1.7.3 An inhibitory signal resulting from mis-regulation of chlorophyll synthesis 37

1.8 The response to abiotic stresses 38

1.9 Role of chloroplast signals in response to abiotic stress 42

1.10 Project aims 46

Chapter 2 Materials and methods 49

2.1 Plant material, growth conditions and treatments 49

2.2 Basic physiology and biochemistry 51

2.2.1 Pigment measurements 51

2.2.1.1 Chlorophyll and carotenoids 51

2.2.1.2 Chlorophyll fluorescence measurements 51

2.2.1.3 Protochlorophyllide measurements 52

2.2.1.4 Heme detection by chemiluminescence 52

2.2.2 Measurement of 5-aminolevulinic acid synthesis 53
2.2.3 ROS detection by fluorescence microscopy 53
2.2.4 Trypan blue staining 54
2.3 Analysis of gene expression by quantitative real-time PCR (qPCR) 54
2.3.1 Total RNA isolation from seedlings 54
2.3.2 First strand cDNA synthesis 55
2.3.3 Quantitative real-time PCR 56
2.4 Genomic PCR and High-fidelity PCR 58
2.5 Gene cloning and transformation 60
2.6 *Arabidopsis* transformation 61
2.7 Selection of *Arabidopsis* transformants 62
2.8 Protein extraction and immuno-blot analysis 62
2.9 TAP-tag protein purification for pull-down analysis 64
2.10 Transcriptome data analysis 65
Chapter 3 Retrograde regulation of photosynthetic gene expression 67
3.1 Introduction 67
3.2 Results 69
3.2.1 Expression profiles of the *HEMA1* and *LHCB2.1* genes on NF after transfer to WL 69
3.2.2 Verification of the *gun* phenotype in the *gun6-1D* mutant 71
3.2.3 The effect of altering tetrapyrrole synthesis on retrograde signalling 72
3.2.4 The effect of heme synthesis inhibition on nuclear gene expression 75
3.2.5 The role of the sigma factors SIG2 and SIG6 in tetrapyrrole synthesis and retrograde signalling 80
3.2.6 Regulation of the tetrapyrrole biosynthesis pathway by GUN1 85
3.2.7 Seedlings lacking ABI4 or PTM do not show a *gun* phenotype 91
3.3 Discussion 99
3.3.1 Heme synthesis is required for the production of a positive retrograde signal . 99
3.3.2 ABI4 and PTM are not required for biogenic retrograde signalling 101
3.3.3 GUN1 affects tetrapyrrole synthesis 104
Chapter 4 The role of plastid ribosomal protein L11 (PRPL11) in plastid to nucleus retrograde signalling 107
4.1 Introduction 107
4.2 Results 109
4.2.1 The role of PRPL11 and MRPL11 in regulation of nuclear gene expression 109
4.2.2 PRPL11 alters tetrapyrrole metabolism 120

4.2.3 Construction of PRPL11 overexpressing lines 126
4.2.4 Identification of putative PRPL11 interacting proteins 131
4.2.5 Interaction of plastid translation-dependent signalling with tetrapyrrole signalling 136
4.3 Discussion 139
4.3.1 Loss of PRPL11 promotes nuclear gene expression 139
4.3.2 PRPL11 affects tetrapyrrole metabolism 141
4.3.3 PRPL11 may interact with Mg-chelatase 142
Chapter 5 The role of singlet oxygen in retrograde signalling 143
5.1 Introduction 143
5.2 Results 146
5.2.1 Induction of singlet oxygen signalling with ALA treatment 146
5.2.2 Induction of singlet oxygen response by FR pre-treatment 154
5.2.3 Singlet oxygen signalling is dependent on Mg-porphyrin synthesis after ALA treatment 158
5.2.4 Environmental regulation of singlet oxygen signalling 161
5.2.5 Induction of inhibitory retrograde signalling in *flu* 164
5.2.6 Genetic regulation of ALA-induced singlet oxygen signalling 169
5.2.7 CAS is not involved in singlet oxygen-mediated retrograde signalling in young seedlings 174
5.3 Discussion 176
5.3.1 ALA treatment blocks nuclear gene expression in WL but not in the dark 176
5.3.2 ALA treatment induces $^1O_2$ in WL in *Arabidopsis* seedlings 178
5.3.3 ALA treatment supports the role of $^1O_2$ in plastid to nucleus communication. 179
Chapter 6 Role of plastid retrograde signalling in the response of *Arabidopsis* seedlings to abiotic stress 183
6.1 Introduction 183
6.2 Results 185
6.2.1 The effect of abiotic stresses on expression of tetrapyrrole pathway genes ... 185
6.2.2 Bioinformatics analysis of the interaction between singlet oxygen signalling and heat stress signalling 188
6.2.3 Interaction of heat stress signalling and singlet oxygen signalling 193
6.2.4 Interaction of retrograde signalling with drought and salt stresses 205
6.3 Discussion 211
6.3.1 Possible role of tetrapyrrole signalling in abiotic stress signalling 211
6.3.2 The role of tetrapyrrole signalling in drought and salt stresses 212

6.3.3 Heat stress impacts on $^1O_2$–dependent inhibitory retrograde signalling 214
Chapter 7 Final discussion 217
7.1 Regulation of the plastid-to-nucleus retrograde signalling 217
7.2 Integration of plastid retrograde signalling with plant responses to abiotic stresses.... 224
Chapter 8 References 227

Declaration Of Authorship

I SYLWIA MONIKA KACPRZAK

Declare that this thesis entitled THE ROLE OF TETRAPYRROLES IN PLASTID-TO-NUCLEUS RETROGRADE SIGNALLING IN *ARABIDOPSIS THALIANA* and the work presented in it are my own and has been generated by me as the result of my own original research.

I confirm that:

1. This work was done wholly or mainly while in candidature for a research degree at this University;
2. Where any part of this thesis has previously been submitted for a degree or any other qualification at this University or any other institution, this has been clearly stated;
3. Where I have consulted the published work of others, this is always clearly attributed;
4. Where I have quoted from the work of others, the source is always given. With the exception of such quotations, this thesis is entirely my own work;
5. I have acknowledged all main sources of help;
6. Where the thesis is based on work done by myself jointly with others, I have made clear exactly what was done by others and what I have contributed myself;
7. Parts of this work have been published as:

Page M.T., Kacprzak S.M., Mochizuki N., Okamoto H., Smith A.G., Terry M.J. (2017). Seedlings Lacking the PTM Protein Do Not Show a genomes uncoupled (gun) Mutant Phenotype. Plant Physiol. 174: 21-26.

Signed: .....

Date: .....

Acknowledgements

Firstly, thanks to Gatsby Charitable Foundation for founding this project and providing stimulating intellectual environment.

I would like to thank my supervisor Prof. Matthew Terry for giving me an opportunity to conduct my PhD research in his group, for his experimental guidance and support in worse days.

Also big thank you to Dr Haruko Okamoto for general support, good ideas and help with plasmid production and protein purification. I would like to thank Prof. Dario Leister and Dr Tatjana Kleine for inviting me to visit their research group, for their generosity with seed stocks and use of their antibodies.

Thank you to the all people in the lab for experimental suggestions and all good time we shared together.

Lastly, thank you to my friends and family for their understanding, love and support in challenging time.

Abbreviations

ABA	Abscisic acid
ABI4	Abscisic acid insensitive
accD	Gene for Acetyl-CoA-Carboxylase
ACT2	Actin 2
ADF2	Actin depolymerizing factor 2
ALA	5-aminolevulinic acid
Ala	Alanine
Amp	Ampicillin
AOX1	Alternative Oxidase 1
APX	Ascorbate peroxidase
Arabidopsis	*Arabidopsis thaliana*
ARC	Accumulation And Replication Of Chloroplasts
Arg	Arginine
ATP	Adenosine triphosphate
A. tumefaciens	*Agrobacterium tumefaciens*
BAP1	Bon Association Protein 1
β-CC	β –cyclocitral
bHLH	basic/Helix-Loop-Helix
bp	base pair
C	Cytidine
°C	Grad Celsius
$CaCl_2$	Calcium chloride
CAO	Chlorophyll *a* oxygenase
CAS	Calcium sensing receptor
CAT2	Catalase 2
CBF1	C-Repeat/Dre Binding Factor 1,
cDNA	complementary DNA
CF1	Chloroplast Coupling Factor-1
CHLD	Magnesium chelatase subunit D
CHLH	Magnesium chelatase subunit H
CHLI	Magnesium chelatase subunit I
CHLM	Magnesium protoporphyrin methyltransferase
Chlide	Chlorophyllide

ClpC	Gene for ATP-dependent Clp protease ATP-binding subunit
ClpP	Gene for ATP dependent Clp protease
Col	Columbia ecotype
COP	Constitutively Photomorphogenic
COR15A	Cold Regulated 15A
CORR	Co-Location For Redox Regulation
cox1	Gene for Cytochrome c Oxidoreductase 1
CP12	CP12 Domain-Containing Protein
CPO	Coporphyrinogen II Oxidase
C. reinhardi	*Chlamydomonas reinhardi*
CSK	Chloroplast Sensor Kinase
C(t)	Cycle threshold
C-terminal	Carboxyl terminal
DAB	Diaminobenzidine tetrahydrochloride
DET	De-etiolated
DMSO	Dimethyl sulfoxide
DNA	Deoxyribonucleic acid
DNase	Desoxyribonuclease
DP	2'2-dipyridyl
DTT	Dithiothreitol
E. coli	*Escherichia coli*
et al.	*et alii*
EDTA	Ethylene diamin tetraacetic acid
EMS	Ethylmethane sulphonate
ERF6	Ethylene Responsive Element Binding Factor 6
EX1/2	Executer1/2
FC	Ferrochelatase gene
FER1	Ferretin 1
FLU	Fluorescent in blue light
FNR	Ferredoxin-$NADP^+$ reductase
FR	Far red
FUS	fusca
g	Gram
g	Gravity force
GFP	Green Fluorescent Protein

Glu-TR	Glutamyl-tRNA reductase enzyme
GLK	Golden2-like
γ-Ray	Gamma radiation
GSA	Glutamate-1-semialdehyde
GST	Glutamyl-tRNA synthetase
GTP	Guanosine-5'-triphosphate
GTPase	GTP-binding protein
GUN	Genome Uncoupled
h	hour
HCl	Hydrogen chloride
HEMA	Glutamyl-tRNA reductase gene
HEPES	4-(2-hydroxyethyl)-1-piperazineethanesulfonic acid
HFR1	Long Hypocotyl In Far-Red1
HiFi	High fidelity
HO	Heme oxygenase
H_2O_2	Hydrogen peroxide
H_2DCFDA	2',7'-Dichlorodihydrofluorescein diacetate
HRP	Horseradish peroxidase
HSFA2	Heat Shock Transcription Factor A
HSP17.4	Heat Shock Protein 17.4
HSP	Heat Shock Protein
Hyg	Hygromycin B
HY5	Long Hypocotyl5
IgG	Immunoglobulin G
IR	Inverted repeats
Kan	Kanamycin
kb	Kilobase pair
KCl	Potassium chloride
kDa	Kilo Dalton
KIN1	Kinase 1
LAF1	Long After Far-Red Light 1
LB	Lysogeny broth
LC-MS/MS	Liquid chromatography-tandem mass spectrometry
LHCB	Light-harvesting chlorophyll a/b binding protein
LHCII	Light-harvesting complex II

Lin	Lincomycin
LOESS	Local weighted regression
LS	Linsmaier and Skoog
LSC	Large single copy region
LTI30	Low Temperature Induced 30
Lys	Lysine
M	Mole(s) per liter
m	Milli
MAS5	Microarray Affymetrix Suite 5
MEcPP	Methylerythritol cyclodiphosphate
MES	2-(N-Morpholino) ethanesulfonic acid
$MgCl_2$	Magnesium chloride
$MgSO_4$	Magnesium sulfate
min	Minute
ml	Milliliter
mm	Millimeter
Mg-Chel	Magenesium chelatase
Mg-PMT	Magnesium-protoporphyrin IX methyltransferase
Mg-protoIX	Magnesium protoporphyrin IX
Mg-protoME	Magnesium-protoporphyrin IX monomethylester
mol	Mole
mRNA	Messenger RNA
MRP	Mitochondrial Ribosomal Protein
MS	Murashige and Skoog
NaCl	Sodium chloride
NADPH	Nicotinamide Adenine Dinucleotide Phosphat
NASC	Nottingham *Arabidopsis* Stock Centre
NaF	Sodium fluoride
Na_3VO_4	Sodium orthovanadate
NBT	Nitroblue tetrazolium
NDA1/2	Alternative NAD(P)H Dehydrogenase 1/2
NDB2	NAD(P)H Dehydrogenase B2
ndh	Gene for NADH-dehydrogenase
NEP	Nuclear-encoded RNA polymerase
NF	Norflurazon

NOD	Nodulin-like protein transcript
NP-40	Nonyl phenoxypolyethoxylethanol
NPQ4	Nonphotochemical Quenching 4
nt	Nucleotide
N-terminal	Amino terminal
ORF	Open reading frame
$^1O_2$	Singlet oxygen
PAGE	Polyacrylamide gel electrophoresis
PAM	Pulse Amplitude Modulation
PAP	Phosphoadenosine phosphate
PAPP5	Phytochrome Associated Protein Phosphatase 5
PAPs	Proteins associated with PEP
Pchlide	Protochlorophyllide
PCR	Polymerase Chain Reaction
PE	Primer efficiency
PEP	Plastid-encoded RNA polymerase
Pfr	Far-red light absorbing form of phytochrome
PHOT	Phototropin
PHY	Phytochrome
PIF	Phytochrome interacting factor
PLB	Prolamellar body
PNPase	Polynucleotide phosphorylase
POR	Protoporphyrin oxidoreductase
PPR	pentatricopeptide repeat
PQ	Plastoquinone
PRF1	Profilin 1
PRP	Plastid Ribosomal Protein
ProtoIX	Protoporphyrin IX
PSI/II	Photosystem I/II
psbA	Gene for Photosystem II Reaction Center Protein A
psbB	Gene for Photosystem II Reaction Center Protein B
PSBQ	Photosystem II Subunit Q
PSRP	Plastid Specific Ribosomal Protein
PTM	PHD transcription factor with transmembrane domains
PVDF	Polyvinylidene difluoride

qRT-PCR	Quantitative Real Time PCR
rbcL	Gene for RuBisCO
RD29B	Responsive To Desiccation 29B
RMA	Robust Multi-Array Average
RNA	Ribonucleic acid
RNAi	RNA interference
RNase	Ribonuklease
ROS	Reactive oxygen species
rpm	Rotations per minute
RpoT	RNA polymerase of the phage T3/T7 type
rpoB	Gene for RNA polymerase subunit β
rRNA	Ribosomal RNA
RT	Room temperature
RT-PCR	Reverse transcription polymerase chain reaction
RuBisCO	Ribulose-1,5-bisphosphate carboxylase oxygenase
s	Second
SDS	Sodium Dodecyl Sulphate
Sec	Secretory pathway
Ser	Serine
SIG	Sigma factor
SOSG	Singlet Oxygen Sensor Green
Spec	Spectinomycin
SPP	Stromal Processing Peptidase
SRP	Signal Recognition Pathway
SSC	Small single copy region
TAC	Transcriptional Active Chromosome
TAE	Tris-Acetate-EDTA
TAP	Tandem Affinity Purification
TAT	Twin-Arginine Translocation
Taq	DNA polymerase enzyme isolated from *Thermus aquaticus*
TBS	Tris-buffered saline
T-DNA	Transfer DNA
TEV	Tobacco Etch Virus protease
Thr	Threonine
TIC	Translocon Of The Inner Envelope Of Chloroplasts

TOC	Translocon Of The Outer Envelope Of Chloroplasts
Tris	Tris (hydroxymethyl) - aminomethane
Tm	Melting temperature
tRNA	Transfer RNA
$tRNA^{Glu}$	Glutamic acid transfer RNA
U	Uridine
UPOX1	Upregulated By Oxidative Stress 1
UTR	Untranslated region
V	Volt
v/v	Volume per volume
w/v	Weight per volume
WLc	Continuous white light
WT	Wild Type
YLS8	Yellow-Leaf-Specific Gene 8
µl	Microliter
µg	Microgram

Chapter 1 Introduction

1.1 Chloroplast structure

Chloroplasts are one of the most important members of a group of plant organelles termed plastids. Plants produce different types of plastids that vary in structure, tissue specificity and function. Chloroplasts are lens shaped, chlorophyll-containing plastids governing many fundamental metabolic functions including photosynthesis, starch synthesis, synthesis of lipids, amino acids, hormones and some secondary metabolites. Each chloroplast is enclosed by a double membrane envelope encompassing an aqueous matrix (stroma) and a complex inner membranous system (thylakoids). Thylakoids are arranged into two distinct domains: tightly stacked thylakoid grana interconnected by unstacked thylakoids called stromal lamellae (Albertsson et al., 2001; Figure 1.1). The envelope membrane regulates protein, metabolite and ion transport. Within the stroma matrix there are ribosomes, circular DNA, plastoglobuli, starch grains and enzymes for multiple metabolic reactions including amino acid and fatty acid synthesis, glycolysis, nitrogen fixation, and enzymes for the Calvin cycle reactions (Peltier et al., 2006). Protein complexes that harvest light energy and carry out the light reactions of photosynthesis are localised in thylakoids. However, they are unevenly distributed within the thylakoids to maximize light capture, balance energy distribution between the two photosystems and protect from potential light-induced damage. Within the stromal lamellae, the non-appressed part of the membrane grana, and the granal margins there are components of the cyclic electron transport chain, ATP synthase, ferredoxin and photosystem I (PSI) proteins: photosystem II (PSII) complexes mostly reside in the appressed regions of thylakoid grana (Albertsson et al., 2001; Chuartzman et al., 2008). Under different light conditions, one of the main light harvesting complexes LHCBII can undergo phosphorylation and migrate between PSI and PSII resulting in structural reorganisation of thylakoid membranes. It is proposed that this requires fission and fusion events at the interface between stroma lamellar and grana domains (Chuartzman et al., 2008).

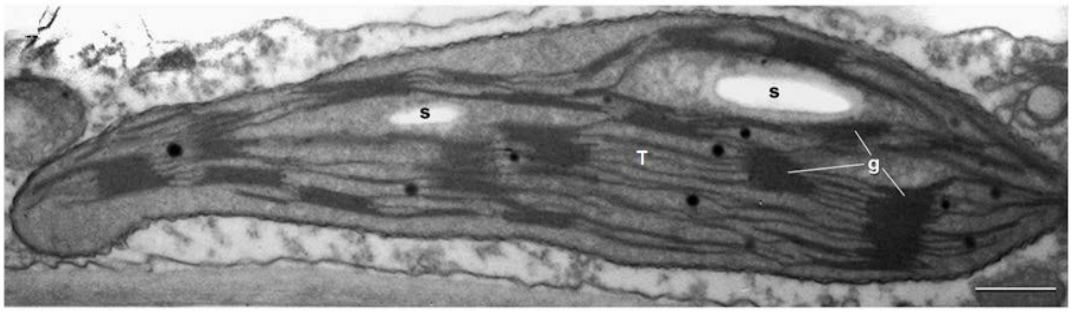

Figure1.1 Transmission electron micrograph of a single chloroplast from light-grown *Arabidopsis thaliana.* Micrograph shows typical chloroplast structure, with well-organised complex system of thylakoid membranes (T) associated in stacks (grana, g). (s) Starch grains within the stroma. Figure from Schattat et al. (2012).

1.2 Chloroplast genomes

Semiautonomous plastids originated more than 1.2 billion years ago from a free living cyanobacterium engulfed and enslaved by a host eukaryotic cell (Martin 2003). The strong resemblance found between chloroplasts and prokaryotes is in agreement with the endosymbiotic theory of the chloroplast origin. Firstly, they both have a comparable size. Secondly, chloroplasts retain their own transcriptional and translational machineries that are similar to their bacterial ancestor, and distinct from the nucleo-cytoplasmic system. Most chloroplast-encoded genes of land plants are organised in clusters that are co-transcribed as polycistronic precursor mRNAs (Barkan et al., 1988). Chloroplasts transcribe genes using the bacterial-type RNA-polymerase and possess similar sized ribosomes, with most of proteins having homologues in bacterial 70S ribosomes (Hu and Bogorad, 1990; see Chapter 1.4 for more detail). Moreover, chloroplast ribosomes are sensitive to antibiotics inhibiting bacterial ribosomes like spectinomycin, lincomycin and erythromycin (Ellis, 1970). Finally, both chloroplasts and bacteria replicate by binary fission. Reverse genetic and phylogenetic studies showed that many components of the plastid division machinery are of prokaryotic origin e.g. Filamentous Temperature Sensitive Z (FtsZ), which is a tubulin-related GTPase that assembles into a concentric ring structure (Z-ring) around the constriction zone of dividing plastids (Osteryoung et al., 1998), and other proteins regulating placement of the Z-ring such as components of the Min (Minicell) system: MinD, MinE (Colletti et al., 2000; Itoh et al., 2001), or the transmembrane protein Accumulation And Replication Of Chloroplasts 6 (ARC6), which is a homologue of cyanobacterial factor Ftn2 and functions as a positive regulator of Z ring formation (Vitha et al., 2003).

Similarly to bacteria, chloroplasts contain circular and double stranded DNA, but chloroplast genomes encode only a small number of ~120 genes (Sugiura, 1992). This is due to a massive transfer of plastid DNA to the nuclear genome that occurred in the course of evolution, and resulted in a strong reduction in plastid genome size, as compared to their bacterial ancestor (Timmis et al., 2004). Moreover, evolutionary gene transfer from organelles to the nucleus is an ongoing process and the possibility of whole plastome loss has also been discussed (Barbrook et al., 2006). It was originally proposed by von Heijne (1986) that some membrane proteins need to be synthesized *de novo* in organelles due to the presence of hydrophobic regions that could prevent these proteins being imported from the cytosol or trigger their mis-targeting to other cell compartments. However, there are examples that argue against this hypothesis including nuclear-encoded and chloroplast-targeted hydrophobic proteins of light harvesting complexes (LHCBI and LHCBII), or the synthesis of the water-soluble, large subunit of the ribulose-1,5-bisphosphate carboxylase-oxygenase (RuBisCO) enzyme in the chloroplast (Barbrook et al.,

2006). Another hypothesis that explains retention of some genes in organellar genomes, termed co-location for redox regulation (CORR), indicates that the rate of synthesis of some organellar-encoded proteins requires regulation by the redox state of their gene products, or electron carriers, with which they interact (Allen, 2003). This could provide a rapid and direct control over the redox imbalance in response to environmental changes including light intensity or carbon dioxide concentration. In support with this hypothesis is experimental evidence for changes in the transcription rate of genes encoding components of photosystem I and II (PSI and PSII) following different light treatments, or addition of specific inhibitors of chloroplast photosynthetic electron transport (Pfannschmidt et al., 1999a). Another example could be the bacterial-type, chloroplast sensor kinase (CSK) for which auto-phosphorylation is redox dependent. Knock-out of the *CSK* gene in *Arabidopsis* T-DNA insertion mutants modified the kinetics of chloroplast *psaA* expression in response to light induced changes in the redox state of plastoquinone (Puthiyaveetil et al., 2008).

Researchers have proposed distinct hypotheses for the underlying basic mechanisms of the evolutionary gene transfer (Timmis et al., 2004). Direct recombination of the organelle DNA with nuclear DNA is the dominant one, as there is evidence for transfer of almost the complete chloroplast genome to the rice nuclear genome at chromosome 10 (Masood et al., 2004), along with the insertion of single chloroplast genes containing introns (Fuentes et al., 2012). The rapid expansion in the availability of new genome sequences creates an opportunity to extend our knowledge about plastome evolution. However, it does not give precise information about the functional organization of genes at the molecular or biochemical level. Currently over 400 complete plastid genome sequences are publicly available (www.ncbi.nlm.nih.gov/genomes/ ORGANELLES/ organelles.html). Structural studies have demonstrated that the chloroplast genomes of land plants are highly conserved, displaying comparable number of genes that are similar in structure and order (Sugiura 1992; Wakasugi et al., 2001). Typically, they are organized into four basic segments: two asymmetrically localized identical copies of long inverted repeats (IR_s) separated by two others regions containing only single copies of genes termed Large and Small Single Copy regions (LSC and SSC). There is a great degree of variability in the size of chloroplast genomes of land plants, which can be determined by a few factors: the loss or variable length of the IR regions that is specific to different plant groups, variability in the intergenic region size, and the loss of genes as has been observed for grass genomes or resulted in the small genome size of parasitic plants (Palmer et al., 1987; Wu et al., 2011; Tang et al., 2004; Guisinger et al., 2010; Wolfe et al., 1992).

The coexistence of different genomes in separated plant cell compartments implies very precise coordination of gene expression. Hence, endosymbiotic gene transfer from organelles to the nucleus ensured a strict regulation of organellar processes. It is estimated that current plastid genomes encode only around 50-200 proteins (Martin 2003; Timmis et al., 2004), while the vast majority of plastid proteins are the products of nuclear genes. Open reading frames (ORFs) of the chloroplast genome can be assigned to at least four basic functional categories: structural RNA genes (e. g. *rrn* and *trn,* encoding subunits of ribosomal and transfer RNAs), genes involved in transcription and translation (like subunits of RNA polymerase, *rpo*), genes involved in photosynthesis (e.g. large subunit of RuBisCO, *rbc*L; cytochrome complex subunits, *pet*; subunits of ATP-synthase, *atp*; and subunits of NADPH-dehydrogenase, *ndh*) and those involved in other metabolic processes (like *accD* and *cysA* functioning in lipid and sulphate metabolism, respectively (Wakasugi et al., 2001). However, to build up complete protein complexes to ensure proper functioning of the organelle, subunits encoded by both chloroplast and nuclear genomes are required. It has been estimated that chloroplasts contain several thousand proteins and up to 3500 gene products are predicted to be imported from the nucleus to plastids (Wakasugi et al., 2001). This necessitates translation of protein precursors in the cytosol and further targeting into the chloroplast by complex and energy-dependent post-translational processes.

1.3 Protein import into the chloroplast

Nuclear-encoded and cytosol-synthesized precursor proteins (pre-proteins), which are necessary for chloroplast biogenesis and function, require targeting and translocation across chloroplast envelopes to reach different organelle sub-compartments. Since different membranes of the chloroplast are generally not permeable to larger molecules including proteins, the precise import machineries need to be incorporated. Most pre-proteins are characterised by the presence of a targeting signal at their N-terminus termed a transit signal, which is necessary for their sorting and routing to the chloroplast. Chloroplast transit signals vary considerably in size, ranging between ~13-146 (average 58) amino acids and they are overall positively charged, due to the high content of hydrophobic and hydroxylated residues, and lack of acidic amino acids (Zhang and Glaser, 2002). For the stroma-targeted pre-proteins three distinct regions of homology in their transit peptides were proposed: an N-terminal region of ~10-15 residues beginning with Ala and rich in Pro and Gly, a variable central region rich in Ser, Thr, positively charged Arg, Lys and lacking acidic residues, and a C-terminal region enriched in Arg and potentially forming an amphiphilic β–strand, that is a site for proteolytic cleavage (Von Heijne et

al., 1989; Zhang and Glaser, 2002). Apart from these features there is no clear similarity among primary sequences of transit signals for different chloroplast pre-proteins.

Successful organellar import requires pre-proteins to be maintained in the unfolded conformation. This is accomplished by binding of precursor proteins to different chaperonin proteins including a subset of heat shock proteins from the Hsp60, Hsp70, Hsp90 and Hsp100 (ClpC) families, which prevent pre-protein aggregation and mis-folding, and keep precursors in a high import-competent state during different stages of the translocation process (Zhang and Glaser, 2002). A well-studied example are chaperones from the Hsp70 family that have versatile and important roles during chloroplast protein import. Bioinformatic analysis predicted that 75% of chloroplast precursor transit peptides have at least one putative Hsp70 binding site, and this interaction was confirmed by *in vitro* binding assays between Hsp70 and the transit peptide of the precursor ferredoxin-$NADP^+$ reductase (FNR), or the small subunit of RuBisCO (Rial et al., 2000; Ivey et al., 2000). Biochemical studies indicated that the Hsp70 homologs localised in different chloroplast compartments including Com70 (Chloroplast Outer Membrane protein), or the stromal Hsp70 in pea (cpHsc70), co-immunoprecipitate, or are with the close association with, pre-proteins and components of the translocon machinery (Kourtz and Ko, 1997; Su and Li, 2010). Moreover, genetic studies on *Arabidopsis* T-DNA knock-out mutants of the two stromal Hsp70 proteins (*cphsc70-1* and *cphsc70-2*), showed defects in protein import assays for photosynthetic and non-photosynthetic pre-proteins (Su and Li, 2010). At the cytosolic side, Hsp70 interacts with another chaperonin protein 14-3-3 to form a hetero-oligomeric guidance complex with the chloroplast pre-proteins (May and Soll, 2000; Zhang and Glasser, 2002). Plant 14-3-3 proteins bind to a motif in a transit signal following an ATP-dependent phosphorylation within the pre-protein-specific Ser or Thr residue (May and Soll, 2000; Martin et al., 2006). Since plant mitochondria pre-proteins cannot serve as a substrate for this protein kinase, and do not interact with the plant 14-3-3 proteins, formation of the 14-3-3 guidance complex was proposed to provide the specificity mechanism for selective chloroplast protein import (May and Soll, 2000). Together these results support the essential role of Hsp70 chaperonin in protein translocation.

After decoding transit sequences, chloroplast-designated pre-proteins can be transported to six different chloroplast subcompartments: outer envelope membrane, intermembrane space, inner envelope membrane, chloroplast stroma, thylakoid membrane or thylakoid lumen (Cline and Henry, 1996). Precursor protein translocation across inner and outer envelopes is accomplished mostly with multi-protein complexes called TOC (Translocon of the Outer Envelope of Chloroplasts) and TIC (Translocon of the Inner Envelope of Chloroplasts). The main components of the TOC complex include: Toc159, Toc34 and Toc75, where numbers indicate protein

molecular mass in kDa (a detailed description can be found in the review of Jarvis and Robinson (2004)). Toc159 and Toc34 both have a GTPase domain, with a high level of homology, are anchored at the surface of the outer membrane, and thus both proteins function as GTP-regulated receptors responsible for pre-protein recognition (Kessler et al., 1994; Seedorf et al., 1995). In contrast to the other translocon components, almost half of Toc159 proteins were shown to be present in the soluble fractions of *Arabidopsis* and pea protein extracts suggesting that Toc159 could mediate targeting of pre-proteins between the cytosol and the outer membrane (Hiltbrunner et al., 2001b). Toc75 is composed of multiple transmembrane strands forming a β-barrel channel structure ~14 Å in diameter through which the precursor proteins move to cross the outer chloroplast envelope (Hinnah et al., 2002). Although the main components of the TIC complex include Tic110, Tic62, Tic55, Tic40, Tic32, Tic22 and Tic20, there is no clear agreement on their function, with the exception of its core component the Tic110 protein, which has a hydrophilic C-terminal domain facing the stroma and has been proposed to recruit stromal chaperonin proteins such as Cpn60 and Hsp93 that facilitate translocation and folding of imported proteins (Jarvis and Robinson, 2004; Nielsen et al., 1997; Jackson et al., 1998). Heins et al. (2002) proposed that Tic110 forms a pore channel for the TIC translocon, and the hydrophilic region of Tic110 in the intermembrane envelope space was additionally suggested to serve as a connection site between the Tic and Toc complexes (Lübeck et al., 1996). Although most proteins are targeted to chloroplasts via the TIC/TOC translocon complexes, there are examples suggesting possible independent import pathways (Jarvis and Robinson, 2004). These include the synthesis of proteins with a transit peptide for the endoplasmic reticulum (ER) translocon, which are further imported into chloroplasts through the endomembrane route, or the Tic32 protein that lacks a cleavable transit peptide, and for which translocation to the inner chloroplast envelope proceeds independent of protease-sensitive receptors and main TOC components (Nada and Soll, 2004; Villarejo et al., 2005).

After import into the chloroplast stroma, transit peptides of pre-proteins can be cleaved by the stromal processing peptidase (SPP; Jarvis and Robinson, 2004). A subset of these proteins are further translocated to the thylakoid membrane or the thylakoid lumen. Four independent and substrate-specific pathways are known to be involved in this import process: thylakoid lumen proteins utilise the secretory (Sec) pathway, or the twin-arginine translocation (TAT) pathway, while proteins targeted to the thylakoid membrane use the signal recognition pathway (SRP), or are inserted spontaneously without any import machinery (Jarvis and Robinson, 2004). In the TAT pathway, folded substrate proteins with the twin arginine motif in their lumenal transit peptides are imported utilizing the thylakoid proton gradient as a driving force, while the Sec

machinery accepts unfolded proteins lacking the twin arginine motif and utilizes the ATP hydrolysis and the SecAEY translocon, which is homologous to the bacterial system (Jarvis and Robinson, 2004; Schünemann, 2007). The SRP pathway is utilized mainly by proteins of the light harvesting complex, where insertion of the protein into the thylakoid membrane involves binding of SRP recognition proteins to a substrate, GTP hydrolysis, and the assistance of partner proteins such as FtsY and Alb3 (Jarvis and Robinson, 2004; Schünemann, 2007).

1.4 Chloroplast gene expression

1.4.1 Chloroplast transcription

Chloroplast gene expression is regulated by the coordinated action of two RNA polymerases: a plastid encoded polymerase (PEP) and a nuclear encoded polymerase (NEP). PEP and NEP differ in their origin, transcriptional activity and types of promoter sequence they recognize. PEP is a homologue of the *Escherichia coli* multimeric enzyme, which has four main subunits: α, β, β' and β''that are encoded in the chloroplast genome by *rpoA*, *rpoB*, *rpoC1* and *rpoC2* genes, respectively (Hajdukiewicz et al., 1997; Serino and Maliga, 1998). The gene organisation for PEP subunits is also reminiscent of the bacterial system, with *rpoB*, *rpoC1*, *rpoC2* forming a part of one operon, whereas the *rpoA* is present in a separate operon with several other genes encoding ribosomal proteins (Siguira, 1992). Additionally, PEP recognizes bacterial type σ^{70} consensus promoter sequences: a TAtaaT motif, and a TTGaca motif localized 10 and 35 nucleotides upstream of the transcription start site, respectively (Serino and Maliga, 1998). In contrast to the PEP enzyme, NEP is a single subunit, T7/T3 bacteriophage-type polymerase of around 110 kDa (Lerbs-Mache, 1993). Up to three different nuclear *RpoT* genes were found to encode NEP in *Arabidopsis* and other dicotyledonous plants: products of *RpoTp* and *RpoTm* are targeted from cytoplasm to plastids and mitochondria, respectively, while the product of *RpoTmp* is dually localised in plastids and mitochondria (Hedtke et al., 2000). In contrast, only two genes for phage-type polymerases (*RpoTp* and *RpoTm*) were found in monocotyledons (Chang et al., 1999; Ikeda and Gray, 1999; Kusumi et al., 2004). Since a series of *Arabidopsis* EMS mutants lacking functional *RpoTp* displayed severe growth inhibition and impaired chlorophyll accumulation, despite elevated expression of *RpoTmp,* and the double mutant for the *RpoTp* and *RpoTpm* genes was lethal, it was proposed that both genes are only partially redundant and have specific functions (Hricova et al., 2006). NEP does not utilise the bacterial σ^{70} type promoter, instead distinct types of conserved promoter regions recognized specifically by NEP were identified and classified: type-Ia is the most widely present and possesses a conserved YRTA motif (ATAGAAT), type-IIb has an additional GGA-box upstream of

the YRTA motif, and the type-II promoter has acore motif that lacks these two conserved sequences and was found, for example, in the promoter of the *clpP* gene in tobacco (Serino and Maliga, 1998; Liere and Maliga, 1999; Weihe and Börner, 1999).

The first evidence for the existence of a second plastid-localised polymerase activity of nuclear origin, came from a genetic study with mutants lacking chloroplast ribosomes and thus lacking active PEP, such as the *albostrians* mutant in barley, and heat-bleached rye plants (Hess et al., 1993), or the maize *iojap* mutant (Han et al., 1992), which all retained expression of selected sets of chloroplast genes. Subsequently, the tobacco Δ*rpoB* mutant lacking one of the PEP subunits was shown to maintain high mRNA levels for the chloroplast structural gene *rrn* (Alison et al., 1996). A further study by Serino and Maliga (1998) using targeted deletion of other *rpo* genes also resulted in tobacco plants with arrested development and inhibited photosynthesis, but which retained high levels of chloroplast *clpP* or *accD* mRNAs transcribed from NEP promoters. Extensive genomic and genetic analyses reveal a rather complex picture for the regulation of transcription by PEP and NEP. PEP was originally proposed to exclusively control expression of photosynthetic genes, as demonstrated by the reduced expression of photosynthetic genes in the PEP-deficient mutants described above, and due to the presence of PEP promoters upstream of photosynthetic genes (Weihe and Börner, 1999). Most of the housekeeping genes including genes for translation genes have active promoters for both PEP and NEP, with only a few examples of genes being exclusively transcribed via the NEP promoter, such as *accD,* and the *rpo* operon (Hajdukiewicz et al., 1997; Serino and Maliga 1998; Weihe and Börner, 1999). An active NEP is therefore necessary for the establishment of a fully functional PEP complex. However, more recent mapping of transcription start sites in the barley *albostrians* mutant by differential RNA sequencing revealed the presence of active NEP promoter sites for most chloroplast genes including photosynthetic genes for PSI and PSII subunits as well as *rbcL* and that these promoters were active in the tissue sectors without functional PEP (Zhelyazkova et al., 2012). Based on an early classification with the three groups of genes that possess PEP and/or NEP promoters (Hajdukiewicz et al., 1997; Weihe and Börner, 1999), a model for the interaction of plastid polymerases was proposed, in which both enzymes act sequentially at the early stages of plastid development, with initially NEP being predominantly active to provide subunits for PEP assembly and the structural components of the ribosome. Consequently, during the greening process, PEP activity increases to meet the high demand to build-up the photosynthetic machinery, while NEP activity declines. In agreement with this model, the switch between NEP and PEP activity during chloroplast development was shown *in vitro* to be controlled by feedback inhibition of RpoTp by glutamyl-tRNA, which is a precursor for protein

synthesis, but also for 5-aminolevulinic acid - the main substrate for tetrapyrrole biosynthesis (Hanaoka et al, 2005). However, not all experimental data are fully supportive for this NEP-PEP model. For example, an increased transcription rate for RNAs derived from both PEP and NEP promoters, with the little change in abundance of NEP-specific mRNAs, was observed during maize plastid development, which suggests that transcript stability and mRNA turnover could affect developmental patterns of chloroplast gene expression (Cahoon et al., 2005).

In addition to NEP, numerous nuclear-encoded components are imported into the chloroplast to control transcription by direct or in-direct regulation of PEP activity. These include: multiple sigma factors (SIG1-SIG6 in *Arabidopsis*), 12 proteins associated with PEP (PAPs) forming core polymerase complex subunits, and other proteins that co-elute with PEP forming a transcriptionally active chromosome (pTAC), which is a DNA-protein mega complex (containing around 40-60 proteins) regulating transcription, RNA processing and translation (reviewed in Pfannschmidt et al., 2015).

SIGs participate in the transcription initiation step and are required for the recognition and binding of PEP to its promoters. Plant sigma factors were classified based on phylogenetic analysis as being related to the bacterial σ^{70} type of sigma factor family, and are defined in two groups: essential and non-essential for cell growth and survival (Allison, 2000). The functions of SIGs in plant transcription have been most extensively studied in *Arabidopsis* either by biochemical studies or molecular genetic analysis of T-DNA insertion lines. The six *Arabidopsis* SIG proteins are proposed to have specific as well more general functions. Using CHIP-qPCR analysis, SIG1 target genes were identified as *rbcL*, *psaAB*, *psbBT*, *psbEFLJ* and *clpP* (Hanaoka et al., 2012). SIG3 is specifically responsible for the transcription of the *psbN* and *atpH* genes (Zghidi et al., 2007), while SIG4 transcribes *ndhF* (Favory et al., 2005). SIG5 is required for the transcription of *psbD,* and since the expression of *SIG5* is induced specifically by blue light similar to the activation of the blue light responsive *psbD* promoter, SIG5 could be a mediator of blue light signalling (Tsunoyama et al., 2002; Tsunoyama et al., 2004). Of all sigma factors, only the knock-out of *SIG2* or *SIG6* in *Arabidopsis* results in seedlings with a pale green phenotype, deficiencies in chlorophyll accumulation and photosynthesis (Woodson et al., 2013), thus both are examples of essential and general sigma factors. SIG2 was shown to control expression of tRNA genes (Kanamaru et al., 2001), while SIG6 is responsible for the expression of various photosynthetic genes during chloroplast development (Ishizaki et al., 2005).

A common feature for all PAPs is that their corresponding mutants display severe phenotypes, such as pale green, ivory or albino seedlings, disturbed chloroplast development,

reduced PEP and enhanced NEP activities, which are all similar to phenotypes of *rpo* mutants (Hajdukiewicz et al., 1997; Serino and Maliga 1998; Pfannschmidt et al., 2015). While analysis of mutants lacking PAP and pTAC proteins clearly indicates their involvement in plastid gene expression their precise function and mode of action still has to be defined.

1.4.2 Chloroplast post-transcriptional regulation

Although chloroplast genes are predominately transcribed from polycistronic units, unlike bacterial genes, plastid transcripts require several processing steps before translation. Chloroplast post-transcriptional modifications include polycistronic transcript processing including RNA splicing and editing, both of which are performed with the assistance of nuclear encoded factors and affect mature mRNA stability and translation (for a detailed review see Stern et al., 2010). The early transcript processing involves intracistronic cleavage of the gene clusters into smaller units, as well as 5´ and 3´ end trimming, which are mediated by nuclear-encoded endo- and exoribonucleases (RNases). Some of the plant RNases are homologues of bacterial enzymes and thus are expected to fulfil similar functions, however for many ribonucleases functions still need to be defined. Considerable experimental work has focused on the roles of endoribonucleases and exoribonucleases in controlling 3´ and 5´ end formation (Stern et al., 2010). One example of such an endoribonuclease is RNase E, which cleaves single-strand AU-rich regions. Knockout mutants of RNase E in *Arabidopsis* accumulate polycistronic transcript precursors, and additionally have severe growth defects due to the reduced expression of the *RPL22* transcripts leading to ribosome deficiencies (Walter et al., 2010). CSP41 is a heterodimer of two related proteins with endonucleolytic activity that binds to and cleaves RNAs at stem-loops such as the one found in the *psbA* 5´ untranslated region (UTR) of spinach (Horlitz and Klaff 2000; Stern et al., 2010). A well-studied example of an exoribonuclease is a polynucleotide phosphorylase (PNPase), which is a 3´ to 5´ processing ribonuclease involved in transcript degradation stimulated by polyadenylation at 3´ termini and blocked by stable 3´ secondary structures (Stern et al., 2010). PNPase is also important for efficient 3´ end formation, as the accumulation of transcripts with 3´ extensions in PNPase mutants was observed (Walter et al., 2002).

In contrast to the situation in bacteria, chloroplast transcripts contain introns, which have to be removed and are spliced either from a single precursor or from independent transcripts (*cis*- or *trans*-splicing, respectively) before translation (Stern et al., 2010). Chloroplast genes have two types of introns (group I and II) that are classified based on the splicing mechanisms and conserved primary and secondary structures (de Longevialle et al., 2010). Changes in the ratio

between unspliced and spliced transcripts is subject to developmental and the tissue-dependent regulation indicated by higher levels of spliced *atpF*, *petB*, *petD*, and *rpl16* pre-mRNAs in maize leaf tissues as compared to root tissue, or proplastid-enriched tissues (Barkan, 1989), and a decrease in splicing of the *ndhB* intron in tomato fruits (Kahalau and Bock, 2008). Activation of splicing does not seem to be regulated by light (Barkan, 1989), with the exception of group I introns of *psbA* where splicing is induced specifically by light in C*hlamydomonas reinhardtii* chloroplasts (Deshpande et al., 1997). Additionally, plastid mRNAs require editing steps that involve a conversion of specific cytidine (C) residues to uridine (U) through deamination or transamination. This process may produce a start codon for translation or restore the conserved amino acid sequence of the protein (Stern et al., 2010). Both, splicing and editing involve assistance of additional nuclear-encoded factors, many of which belong to the large family of pentatricopeptide repeat proteins (PPRs), or proteins containing chloroplast RNA splicing and ribosome maturation (CRM) domains (de Longevialle et al., 2010). Although the exact mechanism of protein function is still not clear, they are thought to stabilise RNA catalytic structures, promote intron folding to help splicing, or act as helicases to fix misfolded RNA structures. The high complexity of chloroplast gene expression and RNA metabolism involving many post-transcriptional steps suggests a necessity for tight regulatory control in response to developmental and environmental changes, which additionally need to be coordinated with the nuclear gene expression.

1.4.3 Chloroplast translation

Plastids have prokaryotic-type 70S ribosomes, along with plastid-encoded tRNAs, for the translation of plastid proteins. Once centrifuged in a high-salt sucrose gradient, chloroplast ribosomes dissociate into two subunits (a large 50S and a small 30S), and can be separated from the cytoplasmic 80S ribosomes (Chua et al., 1973). Similarly to other ribosomes, plastid ribosomes are composed of ribosomal RNAs (rRNAs) and proteins. Ribosomal RNAs in plastids are encoded in the chloroplast genome by a single *rrn* operon and include four molecules, which are similar in length to those from *Escherichia coli*: a 16S rRNA of the 30S subunit that has 1,491 nts in spinach, and three rRNAs (23S, 5S and 4.5S) of the 50S subunit comprised of 3,033 nts in spinach and 3,024 nts in *E. coli* (Sharma et al., 2007; Tiller and Bock, 2014). Plastid ribosomal RNAs are highly conserved across the plant species and very similar to their bacterial counterparts. For example, the 16S rRNA from tobacco shares 74% sequence identity with *E. coli*, and for the maize 23S rRNA the sequence identity with *E. coli* is 71% (Tohdoh and Sugiura, 1982; Edwards and Kössel, 1981). Although *E. coli* has only two rRNAs in its 50S subunit, the

nucleotide sequence of the additional plant 4.5S rRNA corresponds to the 3'-teminal region of the bacterial 23S rRNA (Edwards et al., 1981). In order to remain stable, each of the rRNA molecules requires association with a different set of proteins and folds into a complex three dimensional structure. Most of the plastid ribosomal proteins (PRPs) are nuclear encoded and in terms of structural organisation are similar to the *E. coli* ribosome. Based on proteomic studies in spinach, all 58 protein components of a plastid ribosome were identified including 33 and 25 proteins in the 50S and the 30S subunits, respectively (Yamaguchi et al., 2000; Yamaguchi and Subramanian, 2000). Of these, 52 have orthologs in *E. coli*, but six proteins were also identified as plastid specific proteins (PSRPs): four in the small ribosome subunit (PSRP1-4; Yamaguchi et al., 2000), and two in the large subunit (PSRP5 and PSRP6; Yamaguchi and Subramanian, 2000). Plastid ribosomes are involved in all steps of protein translation including initiation, elongation and termination. The 50S subunit is responsible mainly for the peptide bond formation, while the 30S subunit is essential for the formation of the translation pre-initiation complex by interacting with mRNA and initiation factors, and additionally provides the quality control for the codon decoding at the later step. It is, however, noticeable that a high proportion of chloroplast mRNAs lack properly positioned canonical Shine-Dalgarno elements at their 5´ UTRs, for which pairing with the 3´ termini of the 16S rRNA is essential for ribosome recruitment for translation (Ruf and Kössel, 1988). It is possible that alternative mechanisms for start codon recognition are utilized during chloroplast translation.

An additional specific feature of the plastid ribosome is that PRPs are mostly larger than their bacterial orthologues due to extensions at their N- and C-termini, although the functional significance of this is not well understood (Yamaguchi and Subramanian, 2000; Sharma et al., 2007). As a consequence, chloroplast ribosomes have an increased protein/RNA mass ratio from 1/3 to 2/3 compared to bacterial ribosomes. It has been speculated that the altered protein content and the presence of PSRPs evolved to fulfil specific functions of the chloroplast ribosome, such as stimulation of protein synthesis by light or the thylakoid-associated translation of membrane proteins. Indeed, based on cryo-electron microscopy reconstruction of the ribosome in *C. reinhardtii* it has been shown that terminal extensions of the S2 protein localise near to the mRNA exit channel and can potentially bind RNA, which was hypothesized to serve as a contact site for the mRNA 5´ UTR during plastid-specific translation initiation (Manuell et al., 2007). The large extensions of the L13, L21 and L24 proteins were shown to localise at the back of the 50S tunnel exit site and were recently hypothesised to potentially facilitate interaction with the thylakoid membrane or the protein-targeting machinery (Graf et al., 2017). In addition, some PSRPs were shown to compensate for the role of missing 16S rRNA segments and are therefore

fulfilling a rather the basic structural role (Sharma et al., 2007; Graf et al., 2017). Based on multiple studies for targeted inactivation of chloroplast PRPs, including a series of *Arabidopsis* T-DNA insertion or RNAi lines, and insertional mutagenesis in tobacco, the plant PRPs were functionally classified as either essential or non-essential (for a detailed review see Tiller and Bock, 2014). Despite the high structural similarity to the bacterial ribosome proteins, the essentiality of some PRPs is not always well conserved (Tiller and Bock, 2014). Although the nuclear encoded L11, L24, S1, S17 and S21 proteins are not essential ribosomal proteins in plants, knock out of these genes in *Arabidopsis* results in mutants with retarded growth, reduced chlorophyll accumulation, and impaired protein synthesis and photosynthetic efficiency (Pesaresi et al., 2001; Romani et al., 2012).

1.5 Chloroplast biogenesis

Like all the other types of plastids, chloroplasts emerge from small, globular proplastids that are very simple in structure, and which are localized in meristematic cells. Proplastids can be converted to chloroplasts directly or indirectly, via an etioplast intermediate stage during growth in the dark. The most unique and characteristic feature of the etioplast is the presence of the prolamellar body (PLB) containing lipids, the chlorophyll precursor protochlorophyllide *a* (Pchlide), and NADPH:protochlorophyllide oxidoreductase (POR). Within 24h light exposure the PLB disintegrates to form primary lamellar layers, and finally photosynthetically-active thylakoid membranes (Von Wettstein et al., 1995). This structural transformation occurs with Pchlide reduction to chlorophyllide by light activated POR, resulting in chlorophyll synthesis. Unlike angiosperms, gymnosperms and algae can produce photosynthetically-competent chloroplasts in the dark, as they have the additional dark-operative POR (DPOR), and rarely accumulate complexes of Pchlide with the light-dependent POR (LPOR) (Forreiter and Apel 1993). In *Arabidopsis*, POR enzymes are represented by three distinct isoforms PORA-C characterised by divergent patterns of expression depending on light and plant developmental status (Paddock et al., 2010). Light labile PORA occurs at a high level in the dark, i.e. in etiolated seedlings. In contrast, *PORC* transcripts increase only upon illumination. PORB is present in both etiolated seedlings and mature plants, but uniquely it remains under the control of circadian clock (Su et al., 2001). This differentiation in *POR* gene regulation might be used as a strategy to adapt the plant requirement for more selective chlorophyll production (Su et al., 2001). Indeed, ectopic expression of *PORA* cDNA was sufficient to rescue the small PLB, reduced greening and strong growth defect phenotypes of a *porB-1porC-1* double mutant, indicating that the function of PORs is determined by their gene expression patterns (Paddock et al., 2010).

The manner by which light controls chloroplast formation has been well characterised at the molecular level during the past years. Plants perceive light through different photoreceptors belonging to the phytochrome, cryptochrome and phototropin families (Franklin et al. 2005). A group of nuclear-localised transcription factors (TFs) acting downstream of photoreceptors is crucial for transmitting light signals, and induces a large reprogramming of the transcriptional profile in the nucleus, which ultimately leads to the developmental changes (Franklin et al. 2005). These transcription factors can act as positive and negative regulators. The involvement of light in controlling chloroplast biogenesis is supported by microarray experiments. Full transcriptome comparison between light- and dark-grown *Arabidopsis* seedlings revealed differential expression of up to one-third of the genes, and around half of these genes overlap with the genes with altered expression in response to disturbed chloroplast development (Ma et al., 2001; Ruckle et al., 2012). Phytochrome-dependent light sensing acts through a series of specific transcription factors belonging to the basic Helix-Loop-Helix (bHLH) family termed Phytochrome Interacting Factors (PIFs). PIFs contain a C-terminal domain responsible for dimerization and a DNA-binding N-terminal domain that recognizes specific G-box elements (CACGTG) in gene promoters. PIFs regulate various aspects of chloroplast development acting mainly as repressors of gene expression (Shin et al., 2007). Two PIF proteins, PIF1 and PIF3, have been shown to act additively in negative regulation of chlorophyll biosynthesis, as etiolated *pif1* and *pif3* single and double mutants are characterised by elevated levels of Pchlide and increased expression of chlorophyll biosynthetic genes (Huq et al., 2004; Shin et al., 2009; Stephenson et al., 2009). After activation by light, phytochromes can directly or indirectly, phosphorylate PIF1 and PIF3, resulting in transcription factor polyubiquitination and degradation by proteasome 26S (Al-Sady et al., 2006).

COP/DET/FUS proteins are another example of repressors of photomorphogenesis that are largely involved in the ubiquitin-mediated degradation of positive regulators of plastid development. Wild-type dark-grown seedlings remain developmentally arrested, with long hypocotyls, short roots and closed cotyledons. Several mutant alleles of *cop/det/fus* have mutations in COP9 signalosome subunits, which is part of the multi-complex 26S proteasome, and once grown in the dark all these mutants have phenotypes and gene expression profiles similar to those of light-grown seedlings termed constitutively photomoprhogenic (Schwechheimer and Deng, 2000; Ma et al., 2003). One example of a COP/DET/FUS protein is COP1, which is not a part of the COP9 signalosome, but is a ring-type ubiquitin E3 ligase that associates with the Suppressor Of Phytochrome A-105 proteins (SPA1-4) (Schwechheimer and Deng, 2000; Hoecker et al., 1999). The *cop1* mutant also has a constitutively photomorphogenic phenotype in the dark.

COP1-SPA complexes promote degradation of key transcription factors such as LONG HYPOCOTYL5 (HY5), HY5 HOMOLOG (HYH), LONG AFTER FAR-RED LIGHT1 (LAF1) and LONG HYPOCOTYL IN FAR-RED1 (HFR1; Osterlund et al., 2000b; Seo et al., 2003; Jang et al., 2005). After light exposure COP1 is depleted from the nucleus via exclusion mechanisms and photomorphogenesis proceeds.

In addition, a series of genetic studies on *Arabidopsis* seedlings displaying pale-green, chlorotic or albino phenotypes, and affected in chloroplast biogenesis, have shown they are largely impaired in the expression of nuclear-encoded chloroplast genes (Waters and Langdale 2009; Pogson and Albrecht 2011). Many of these chloroplast-localized proteins are critical components promoting chloroplast formation and assembly, which comprises of different molecular or cellular processes (Figure 1.2). Accurate signalling should be particularly important in coordination of such diverse and complex mechanisms. Thus, the impact of retrograde plastid signalling on regulation of chloroplast development has been extensively studied, with tetrapyrroles proposed as essential factors.

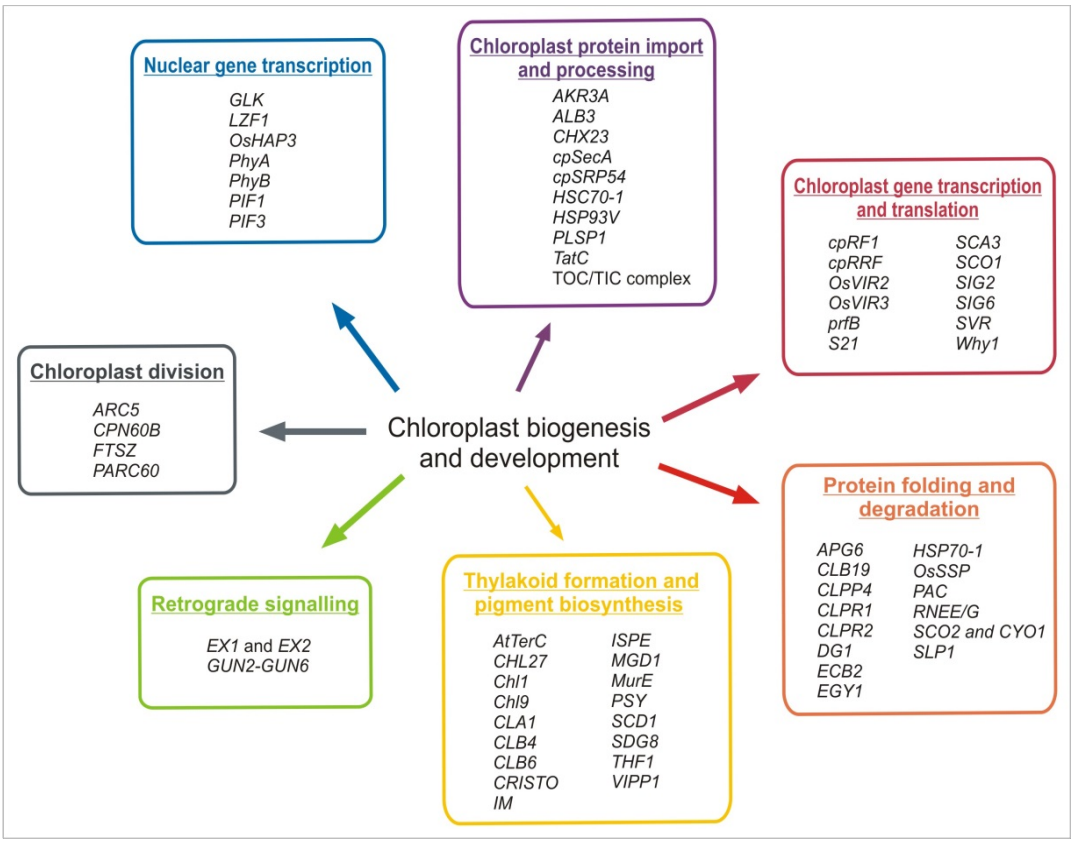

Figure 1.2 An overview of chloroplast biogenesis and development. The scheme depicts the main genes required for accurate chloroplast formation, categorised by different functional processes (figure modified from Pogson and Albrecht, 2011).

1.6 Tetrapyrrole biosynthesis in plants

The tetrapyrrole pathway is essential for many different biological processes during plant development and growth. In plants, all enzymatic steps required for tetrapyrrole synthesis are localized in plastids, although it is speculated that the last enzymatic steps of heme synthesis could additionally take place in mitochondria (Mochizuki et al., 2010). Tetrapyrrole biosynthesis leads to the production of four types of functional molecules in plants. The chlorophylls, chlorophyll *a* and chlorophyll *b*, are necessary for the absorption and transfer of light energy during photosynthesis. Secondly, heme has versatile roles as a cofactor of different proteins, including cytochromes involved in energy transfer during respiration and photosynthesis, antioxidant proteins (catalases, peroxidases), and oxygen-binding proteins. The tetrapyrrole pathways is also a source of phytochromobilin produced from heme, which is attached covalently to the phytochrome photoreceptors involved in red / far red perception. Lastly, tetrapyrrole synthesis also leads to siroheme, which is a cofactor of sulphite and nitrite reductases. Details of the enzymatic steps involved in tetrapyrrole biosynthesis are presented in Figure 1.3. An extensive review of the tetrapyrrole biosynthesis enzymatic reactions can be found in Tanaka and Tanaka (2007).

1.6.1 ALA formation

The first precursor in the tetrapyrrole biosynthetic pathway is 5-aminolevulinc acid (ALA). It is produced from glutamate via a three-step reaction. In the first step, glutamate is ligated with $tRNA^{Glu}$ by the enzyme glutamyl-tRNA synthetase (GST), which results in the formation of glutamyl-tRNA. Next, the enzyme glutamyl-tRNA reductase, also named GluTR (encoded by the *HEMA* gene family) reduces glutamyl-tRNA to form glutamate-1-semialdehyde (GSA). Finally, through a transamination exchange reaction catalysed by glutamate-1-semialdechyde aminotransferase, GSA is converted to ALA (Figure 1.3).

The most critical stage of ALA synthesis involves GluTR, as its substrate glutamyl tRNA is also used for plastid protein synthesis and GluTR therefore catalyses the first committed step of tetrapyrrole synthesis. It is thus not surprising that this enzyme is under the very tight control. In *Arabidopsis* there are 3 genes encoding this enzyme. The first 2 are differentially expressed in plant tissues, with *HEMA1* being widely expressed in green plant tissues, and *HEMA2* having a more constitutive expression profile (Kumar et al., 1996; Ujwal et al., 2002). *HEMA3* is expected to be a pseudogene (McCormac et al., 2001). Based on this, it was proposed that *HEMA2* might be important in maintaining heme synthesis in non-photosynthetic organs, while *HEMA1* is

primarily responsible for photosynthetic heme production. A recent study showed that *HEMA2* expression under the *HEMA1* promoter can functionally complement a *hema1* mutant (Apitz et al., 2014).

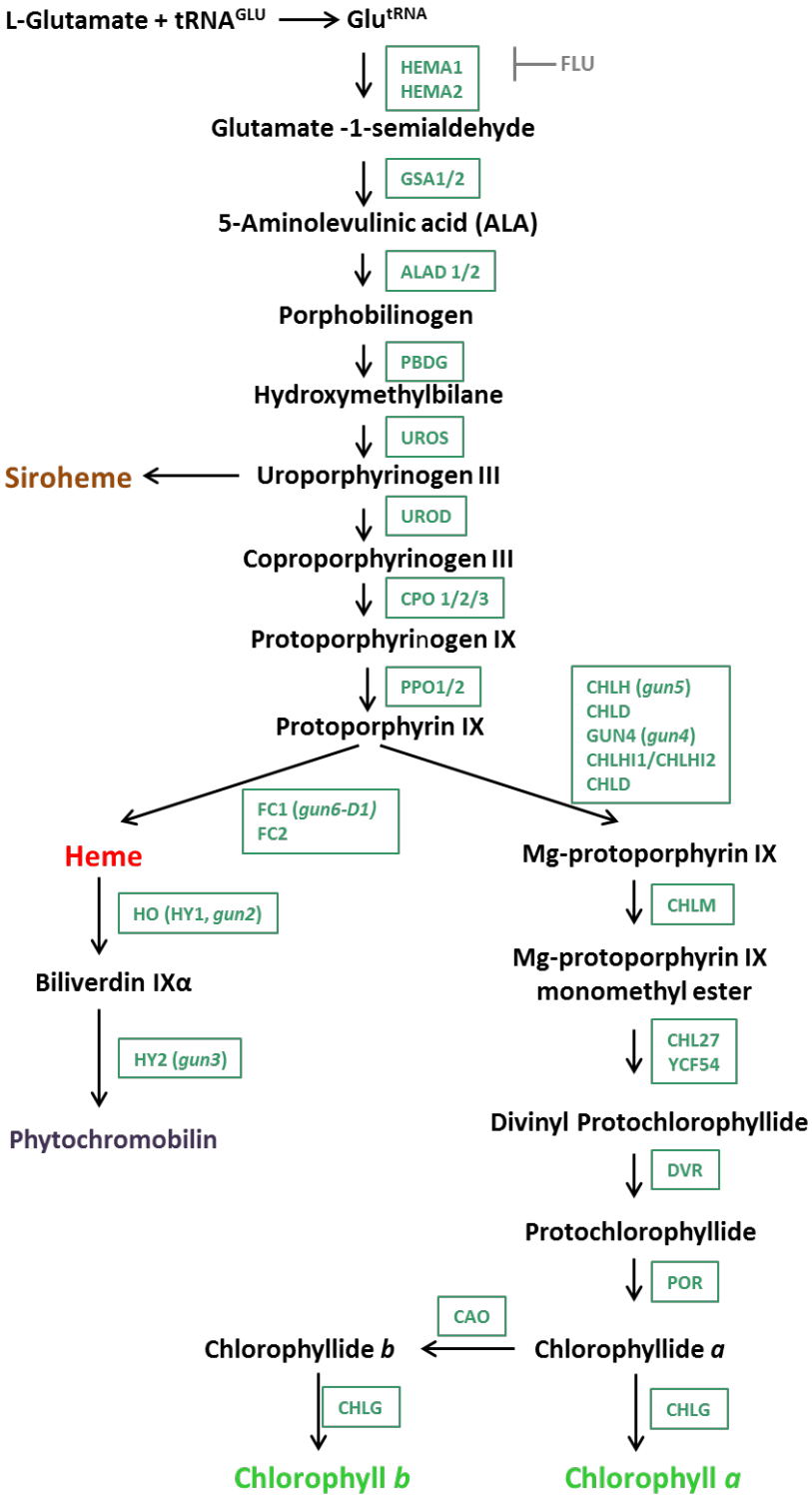

Figure 1.3 The tetrapyrrole biosynthetic pathway and main genes involved in tetrapyrrole synthesis in *Arabidopsis*. The tetrapyrrole pathway leads to the synthesis of heme, siroheme, chlorophyll and phytochromobilin (indicated in colour). The main intermediates of the pathway are indicated in black and synthesis enzymes are presented in green frame.

Thus it is the expression profile rather than the enzyme properties that convey this difference in activity. There is considerable evidence in the literature for *HEMA1* being a light regulated gene and *HEMA1* expression is known to be regulated by red, far red and blue light in a phytochrome- and cryptochrome-dependent manner (Ilag et al., 1994; McCormac et al., 2001; McCormac and Terry, 2002). The GluTR step is also subject to post-translational control that involves three main factors: FLU, a GluTR binding protein (GBP) and heme. FLU was shown to bind to the C-terminus of GluTR (encoded by *HEMA1* only) and inhibit its activity. Thus the *flu* mutant accumulates high levels of Pchlide in the dark (Meskauskiene et al., 2001). GBP is a thylakoid membrane protein that is proposed to protect GluTR from inactivation by FLU (Czarnecki et al., 2011). Finally, heme is known to be a feedback inhibitor of the pathway, possibly through direct binding to GluTR (discussed in Cornah et al., 2003). This was demonstrated through experiments using the iron chelator dipyridyl (DP) (Duggan and Gassman, 1974) and through the characterization of mutants lacking heme breakdown enzymes (Terry and Kendrick 1999; Terry et al., 2001). Heme was shown to directly inhibit recombinant GluTR activity (Pontoppidan and Kannangara, 1994), but it remains possible that other proteins may be involved.

1.6.2 Porphyrin synthesis

The first pyrrole in the tetrapyrrole pathway (porphobilinogen) is formed from two condensed molecules of ALA. This reaction is catalysed by the enzyme porphobilinogen synthase. The first closed cyclic porphyrin in the tetrapyrrole pathway is uroporphyrinogen III formed from 4 porphobillinogen molecules and rearranged by uroporphyrinogen III synthase (Tanaka and Tanaka, 2007). Importantly, uroporphyrinogen III is the first porphyrin in the tetrapyrrole pathway that can act as a photosensitiser and lead to singlet oxygen production. Uroporphyrinogen III can be methylated by uroporphyrinogen III methylase in a reaction that requires S-adenosyl-L-methionine, and after incorporation of Fe into sirohydrochlorin, siroheme is formed (Leustek et al., 1997). Alternatively, uroporphyrinogen III can be decarboxylated by uroporphyrinogen III decarboxylase, which results in coporphyrinogen III formation. Through the activity of coporphyrinogen II oxidase (CPO) it is further decarboxylated to form protoporphyrinogen IX and eventually protoporphyrin IX, which is the substrate for the main branch point in tetrapyrrole biosynthesis.

1.6.3 Chlorophyll synthesis

The first step of chlorophyll synthesis requires incorporation of Mg^{2+} into protoporphyrin IX to produce Mg-protoporphyrin IX. This step is catalysed by a magnesium chelatase enzyme

that is composed of 3 subunits: CHLI (38-40 kDa), CHLD (60-74 kDa) and CHLH (140-150 kDa) (Jensen et al., 2000). These have been well characterised and it was shown that CHLH can bind porphyrins and is the catalytic site for chelation, and that CHLI forms complexes with CHLD to activate CHLH (Willows and Beale, 1998; Jensen et al., 1999). There is also a requirement for ATP to control magnesium chelatase complex formation and binding to the substrate Proto IX (Walker and Willows, 1997; Jensen et al., 2000). The GUN4 protein is able to activate Mg-chelatase activity (Larkin et al., 2003). In the next step two enzymes: Mg-protoporphyrin IX methyltransferase and Mg-protoporphyrin IX monomethyl ester cyclase form Pchlide. This can be further reduced by protochlorophyllide oxidoreductase (POR) to chlorophyllide (Chlide) *a,* which can then be esterified by chlorophyll synthase to chlorophyll *a* or oxygenised to form chlorophyll *b* (via Chlide *b*) (Tanaka and Tanaka, 2007).

1.6.4 Heme synthesis

Protoheme (heme b) is synthesized through the incorporation of Fe^{2+} ions into protoporphyrin IX by the enzyme ferrochelatase. In *Arabidopsis* there are two genes encoding ferrochelatase: *FC1* and *FC2*, which, similarly to *HEMA* genes, differ in their expression patterns (Chow et al., 1998; Suzuki et al., 2002; Nagai et al., 2007). *FC2* was shown to be light induced and expressed mostly in photosynthetic tissues. It is therefore is proposed to be responsible primarily for the production of photosynthetic heme. In contrast, *FC1* is expressed in all tissues and may provide extra-chloroplastic heme. Additionally, both of these genes were shown to be induced by stress treatments in different tissues and under different conditions supporting their diverse roles (Singh et al., 2002; Nagai et al., 2007; Scharfenberg et al., 2015).

1.6.5 Phytochromobilin synthesis

Heme can be either incorporated into different proteins, via covalent or non-covalent linkages, or can be metabolised further through the action of heme oxygenase and phytochromobilin synthase to produce phytochromobilin (Terry et al., 1993). This molecule serves as the chromophore necessary for the functionality of the phytochrome photoreceptors, phyA-E.

1.7 Plastid retrograde signalling

As a consequence of endosymbiosis, plastids and the nucleus continue to have complex interdependencies and communication between these organelles has been of great interest to researchers for more than 30 years (Bradbeer et al., 1979). Numerous recent studies have

focused on defining the mechanisms of chloroplast-nucleus cross-talk and the precise identity of signals conveyed by these organelles. Communication between chloroplasts and the nucleus exhibits a bidirectional pattern, as both organelles generate signals that adjust the expression of numerous genes (Pogson et al., 2008; Waters and Langdale 2009; Jung and Chory 2010).

Signals termed *anterograde signalling* originate in the nucleus to coordinate plastid genome expression at the transcriptional and translational level. Plastid derived molecules that regulate nuclear gene expression are classified as *retrograde signals*. Although it is widely accepted that changes in nuclear gene expression (NGE) represent a final consequence of plastid signalling, the components of the signalling cascade events are still largely unknown. According to present knowledge retrograde control can be achieved by utilizing at least four different types of signalling pathways: signals connected with the redox state of plastoquinone pool (PQ), reactive oxygen species (ROS), signals derived by plastid synthesized proteins and by metabolites, including tetrapyrroles, products of carotene oxidation, methylerythritol cyclodiphosphate (MEcPP) and phosphoadenosine phosphate (PAP) (Xiao et al., 2012; Ramel et al., 2012; Estavillo et al., 2013; Terry and Smith 2013; Chan et al., 2016). These signals can be additionally distinguished depending on the developmental status of the chloroplast. “Operational” retrograde signalling is implicated in responses of mature chloroplasts to changes in environmental conditions. Retrograde signals active during chloroplast biogenesis are termed “biogenic control”. Another interesting aspect of organellar communication might be represented by stromules, stroma filled membranous tubules, which have been shown to provide a physical connection, not only between separate plastids, but also plastids and nucleus (Kwok and Hanson 2004). However, recent studies using novel green to red photoconvertible fluorescent protein, mEosFP fused to a plastid transit sequence in *Arabidopsis* and *Nicotiana benthamiana* did not show protein movement within 30-50 min after irradiation (Schattat et al., 2012). The significance of stromule involvement in protein exchange between plastids and their overall potential to transduce organellar information still needs to be investigated in more detail.

1.7.1 Historical overview

In 1979 Bradbeer and colleagues analysed the *albostrians* and *Saskatoon* barley mutants, characterised by disturbed plastid gene expression due to the lack of functional plastid ribosomes, and observed that plastid defects were accompanied by reduced expression and accumulation of nucleus-encoded chloroplast photosynthesis proteins, like the small subunit of RuBisCO, ferredoxin-$NADP^+$ reductase (FNR) and chloroplast coupling factor-1 (CF1) (Bradbeer et al., 1979). This investigation presented the first hypothesis and evidence for the existence of a plastid

signal that is able to govern nuclear gene expression. Over the following years, other strategies utilising inhibitors of plastid translation or carotenoid synthesis (including the most widely used lincomycin or norflurazon (NF; 4-Chloro-5-methylamino-2-α,α,α-trifluoro-m-tolyl-32H-pyridazinone), respectively) have provided a simpler way of studying chloroplast to nucleus retrograde signalling pathways in numerous of plant species (Gray et al., 2003; Strand et al., 2003; Moulin et al., 2008). Lincomycin and erythromycin inhibit synthesis of plastid proteins. Seedlings of the pea *lip1* and *Arabidopsis cop1* constitutively photomorphogenic mutants treated with these antibiotics showed reduced levels of transcripts of *Lhcb*, *RbcS, PetE,* and *AtpC* as observed by RNA gel blot hybridization (Sullivan and Gray 1999). This indicated that the plastid signalling pathways activated in the *lip1* mutant were dependent on plastid translation, but photosynthesis is not required for plastid signalling to the nucleus. NF is an herbicide that blocks phytoene desaturase, an enzyme catalysing oxidation of phytoene to ζ-carotene early in the carotenoid biosynthesis pathway (Norris et al., 1995). Excess absorbed light energy increases the probability of long lifetime triplet chlorophyll state (^{3}Chl*) formation, leading to the generation of highly reactive singlet oxygen ($^1O_2$). This, in turn, results in photobleaching and interruption of the integrity of cellular components. Carotenoids are able to quench this excess energy, forming triplet states (^{3}Car), which quickly decay with energy dissipation as heat (Mathis et al., 1979). Thus, application of NF results in photo-oxidative damage and dysfunctional chloroplasts. Treatment of seedlings with NF is probably the most extensively used approach to investigate plastid-to-nucleus signalling. Numerous studies performed on NF-treated seedlings indicated a reduction in transcripts of selected nuclear encoded photosynthetic genes (mostly *Lhcb* and *RbcS*), for example in mustard (Oelmüller and Mohr 1986), maize (Mayfield and Taylor 1984), and tobacco (Gray et al., 2003).

New insight into the field came with the concept of tetrapyrroles as intermediates of plastid-to-nucleus signalling pathways. Although, currently, it seems to be the most supported mechanism for biogenic retrograde signalling, there is no agreement between researchers on how precisely this signalling operates (Strand et al., 2003; Mochizuki et al., 2008; Moulin et al., 2008; Pogson et al., 2008; Leister 2012). The first suggestion of this hypothesis was introduced by Johanningmeier and Howell (1984) following work with the green alga *Chlamydomonas reinhardtii*. Using a series of inhibitors of chlorophyll biosynthesis, the authors analysed changes in *Lhcb* transcripts level using gel blots. No disturbance in the amount of *Lhcb* transcript was noted when chlorophyll synthesis was blocked at the earliest steps (e.g. by levulinic acid), but *Lhcb* mRNA did not accumulate after chlorophyll synthesis was blocked at latest later step resulting in specific accumulation of magnesium protoporphyrin methyl ester (Johanningmeier

and Howell 1984). These results inferred that balanced tetrapyrroles biosynthesis, with an emphasis on porphyrin intermediates, plays an important role in regulation of retrograde signalling. The hypothesis was most strongly supported by the identification of *Arabidopsis genomes uncoupled (gun)* mutants (Figure 1.3; see section 1.7.2) as five of these mutations affected components of tetrapyrrole biosynthesis (Mochizuki et al., 2001; Larkin et al., 2003; Woodson et al., 2011). Recent investigations have focused also on a possible role for ALA synthesis as a regulator of plastid signalling (Czarnecki et al., 2012). ALA is the first common precursor of the plant tetrapyrrole biosynthesis pathway, formation of which is controlled by a series of negative feedback mechanisms e.g. involving both the heme branch of the pathway and FLU (Figure 1.3; see section 1.6.1) (Goslings et al., 2004). Direct inhibition of ALA by gabaculine resulted in a *gun* phenotype in which the reduction in the transcript levels of photosynthetic marker genes (*Lhcb* and *RbcS*) after NF treatment is less severe than in untreated seedlings, whereas ALA feeding suppressed the elevated gene expression of *gun1* and *gun4* mutants (Czarnecki et al., 2012). It can be considered that feedback regulation of ALA synthesis is an important modulator of biogenic retrograde signalling traits.

1.7.2 *genomes uncoupled (gun)* mutants

In all *gun* mutants expression of photosynthesis-associated marker genes is uncoupled from the physiological state of the chloroplast. A series of *Arabidopsis* ethyl methanesulfonate (EMS) mutagenized lines were generated using a parental line containing *GUS* and *HPH* marker genes fused to an *Lhcb1.2* promoter. These lines were subjected to a screen for elevated GUS activity after NF treatment, resulting in final identification of 5 non-allelic loci, named *gun1-gun5* (Susek et al., 1993; Mochizuki et al., 2001). Four of these genes were shown to participate in tetrapyrrole biosynthesis (Figure 1.3): *GUN2*, *GUN3* and *GUN5* encode heme oxygenase, phytochromobilin synthase and the H subunit of Mg-chelatase, respectively, and *GUN4* encodes a regulator of Mg-chelatase activity (Mochizuki et al., 2001; Larkin et al., 2003). *GUN2* and *GUN3* are allelic to *hy1* and *hy2* (Mochizuki et al., 2001), respectively, and therefore lack active phytochrome photoreceptors. Light-grown *gun* mutants (and in particular *gun1*) exhibit an abnormal de-etiolated phenotype resulting in delayed or defective chlorophyll accumulation or cotyledon expansion (Mochizuki et al., 1996; Mochizuki et al., 2001). Some researchers attempted to link GUN-modulated signalling with abscisic acid (ABA)-dependent regulation. Indeed, when grown in the presence of NF, *gun2, gun4* and *gun5* retained some carotenoid pigments (neoxanthin, violaxanthin and lutein) compared to the barely detectable level seen in wild type, and exogenous application of ABA partially rescued NF-induced *Lhcb* repression in

wild-type seedlings (Voigt et al., 2010). It has also been proposed that GUN5 may have the potential to bind to ABA and therefore act as an ABA receptor (Wu et al., 2009).

GUN1 is a chloroplast-localised pentatricopeptide-repeat protein (PPR) that binds nucleic acids (Koussevitzky et al., 2007) and is unique among all GUNs. PPR proteins have tandem repeats of a 31-36 amino acid motif with RNA binding activity, are localised in mitochondria or chloroplast and have important roles in RNA metabolism including RNA processing, editing, stability and translation (Liu et al., 2013). GUN1 is one of the 5 PPR proteins that contains an additional SMR domain at the C-terminus, and is localised in the chloroplast (Liu et al., 2013). The precise role of the SMR domain is not known, although it might be responsible for the proposed interaction of GUN1 with DNA (Koussevitzky et al., 2007). In contrast to other *gun* mutants, only *gun1* rescues repression of *Lhcb1* expression after inhibition from both NF treatment as well blocked plastid gene expression either chemically using lincomycin or genetically in *sig2* or *sig6* mutants (Koussevitzky et al., 2007; Woodson et al., 2013). On the basis of microarray analyses, Strand et al. (2003) indicated that gene expression profiles differed between *gun1* and other single *gun* mutants, suggesting that *GUN1* regulates a separate signalling pathway. These results were contradicted by more precise microarray studies displaying a strong correlation between differentially expressed genes after NF treatment in *gun1* and *gun5*, with no additive effect observed in the double mutant (Koussevitzky et al., 2007). Thus, *GUN1* and *GUN5* may operate through the same signalling pathway. However, in *gun1* altered expression of photosynthesis associated genes can be observed under different conditions, while in other *guns* this response is specific to NF (Koussevitzky et al., 2007; Voigt et al., 2010). Although the precise mechanisms of GUN1 function are not known, it is proposed to regulate and coordinate distinct retrograde signals related to plastid developmental or functional status, and therefore, potentially, to act downstream of these signals (Koussevitzky et al., 2007).

It was initially proposed that one of the tetrapyrrole biosynthetic intermediates Mg-protoporphyrin (Mg-proto IX; Figure 1.3) plays a pivotal role as a signalling molecule in tetrapyrrole-dependent signalling. Strand et al. (2003) reported reduced Mg-proto IX content in *gun* mutants after NF treatment and suggested it as a main indicator of mis-regulation of photosynthetic gene expression observed after NF treatment. The observation that Mg-proto IX could be detected in the cytosol, and potentially serve as a mobile signalling molecule, supported that hypothesis (Ankele et al., 2007). However, subsequent studies, performed by independent laboratories, did not confirm a positive correlation between changes in the Mg-proto IX level (or other intermediates e.g. protoporphyrin IX [Proto IX], the monomethyl ester of Mg-Proto IX [Mg-Proto-Me]) and NF-triggered altered expression of photosynthetic genes under a range of

conditions (Mochizuki et al., 2008; Moulin et al., 2008). These results did not support Mg-proto IX as a primary signalling molecule. Interestingly, Schlicke et al. (2014), aimed to perform more specific time course analyses after manipulating steady state levels of porphyrins, by generating transgenic lines with chemically inducible gene silencing of *CHLH*, *CHLM* and *CHL27* (encoding early enzymes in the Mg branch of tetrapyrrole biosynthesis). While the lack of nuclear gene expression modulation observed within 24h of gene silencing support previous findings (Mochizuki et al., 2008; Moulin et al., 2008), the altered expression of photosynthesis and ROS marker genes, with different patterns and kinetics of expression after prolonged enzyme deactivation (Schlicke et al., 2014), suggest high complexity for tetrapyrrole-mediated retrograde signalling.

Recently a sixth gun mutant, the dominant *gun6-1D* mutant, resulting in the overexpression of ferrochelatase 1 (FC1; Figure 1.3), was discovered (Woodson et al., 2011). *gun6-1D* also presents a *gun* phenotype. On the basis of these findings authors proposed a new model for a positive plastid signal operating through a specific heme pool to promote chloroplast development. This model has been further developed by Terry and Smith (2013), suggesting heme as the primary promotive plastid signal controlling plastid development (Figure 1.4). It can be proposed that reduction or loss of this positive signal as a result of chloroplast damage triggered by unfavourable conditions (e.g. mutagenesis, chemical treatment) leads to a loss of nuclear gene expression. Whether heme can act directly to induce changes in nuclear gene expression or indirectly through additional molecular intermediates is unknown.

Numerous transcription factors have been implicated in plastid signalling, and therefore might be potentially interesting candidates for the plastid signal transduction. The discovery of PTM, a chloroplast envelope-bound plant homeodomain (PHD) transcription factor is one such example (Sun et al., 2011). PTM was proposed to operate in the same pathway as GUN1 and it could potentially be a very strong candidate for a new intermediate in plastid retrograde signalling. Another example could be the Golden 2-like transcription factors GLK1 and GLK2, which are important regulators of plastid development, and expression of which has been showed to be affected by tetrapyrrole-dependent retrograde signalling (Waters et al., 2009). Both GLKs can bind to G-box elements in promoter regions and function as transcriptional activators of hundreds of genes including the photosynthetic genes, genes for the chlorophyll biosynthesis, and SIG2 (Waters et al., 2009). Furthermore, it was recently suggested that PAPP5 (PHYTOCHROME ASSOCIATED PROTEIN PHOSPHATASE 5) can act as a negative regulator of GLKs, repressing photosynthetic gene expression (Barajas-Lopez Je et al., 2013).

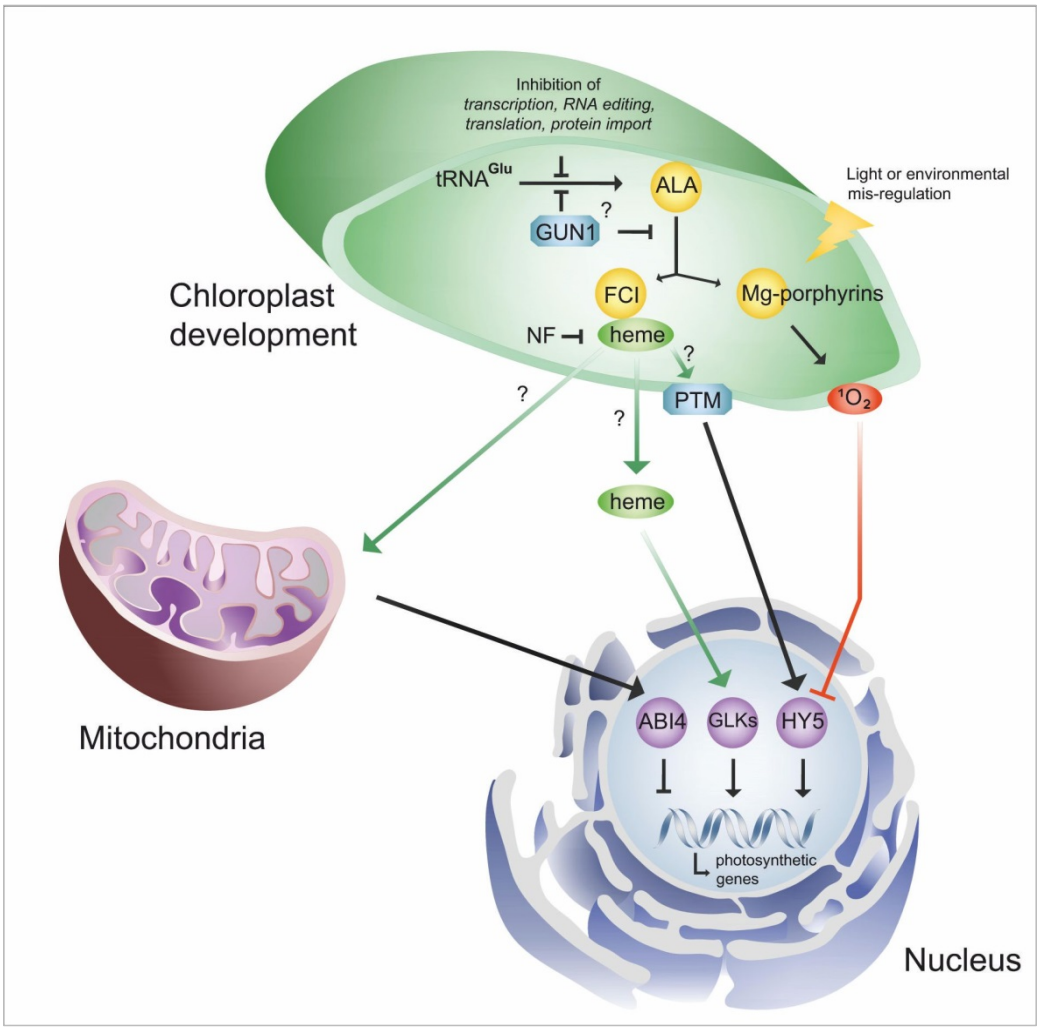

Figure 1.4 A hypothetical model for chloroplast-to-nucleus signalling during chloroplast biogenesis. In this model, there are two signalling pathways proposed. A positive heme-related signal, mediated by ferrochelatase 1 and an inhibitory light-dependent signal that is mediated by singlet oxygen. Abbreviations: $tRNA^{Glu}$, glutamic acid transfer RNA; GUN1, GENOMES UNCOUPLED 1; ALA, 5-aminolevulinic acid; FC1, ferrochelatase 1; $^1O_2$, singlet oxygen; PTM, plant homeodomain transcription factor with transmembrane domains; ABI4, ABA Insensitive 4; GLKs, Golden-like proteins; HY5, LONG HYPOCOTYL 5; NF, norflurazon. Figure modified from Terry and Smith, 2013.

PAPP5 was also identified as a Mg-Proto IX interacting protein (Barajas-Lopez Je et al., 2013). Authors proposed that it contributes to plastid signalling, due to sensing the accumulation of Mg-Proto IX. This is in disagreement with the most current hypothesis (Mochizuki et al., 2008; Woodson et al., 2011). Whether PAPP5 is sensitive to signals derived in response to plastid damage, and participates in the control of nuclear gene expression during these conditions, was not reported. Thus, its involvement in tetrapyrrole-dependent retrograde signalling remains questionable.

1.7.3 An inhibitory signal resulting from mis-regulation of chlorophyll synthesis

In addition to a positive plastid signal, a second inhibitory pathway has also been proposed to function in biogenic plastid retrograde signalling as a result of mis-regulation of

tetrapyrrole synthesis (Terry and Smith 2013). It is hypothesised that the inhibitory signal is specifically mediated by singlet oxygen ($^1O_2$; Figure 1.4). Conditions triggering overproduction of protochlorophyllide, not bound to active site of POR, can result in chloroplast damage and seedling death. A classic example is represented by the *flu* mutant that accumulates Pchlide in the dark, which ultimately leads to $^1O_2$ production when seedlings are transferred to WL (Op den Camp, 2003). Pre-treatment of plants with far red (FR) light is another example of such a situation. Seedlings exposed to FR exposure fail to green in white light (WL). This response depends selectively on the phytochrome A (phyA) mediated pathway, but is independent of the intensity of WL, as no differences in seedling greening response were noted after FR pre-irradiation followed by exposure to increased WL fluence rates (Barnes et al., 1996; McCormac and Terry 2002). The FR pre-treatment experiment resulted also in inhibition of nuclear gene expression in *Arabidopsis* seedlings, which accumulated lower levels of *HEMA1* and *Lhcb* transcripts compared to a dark pre-treated control (McCormac and Terry 2002, 2004; Page et al., 2017a). Although, preliminary findings are supportive for the existence of a second negative plastid signal, the mechanisms involved in control of this response are still unknown. Due to high $^1O_2$ toxicity, it is possible that other transcription factors are involved in mediating this response and studies on light regulation of plant developmental processes provide a possible example, HY5. In the *Arabidopsis hy5* mutant, light responses are perturbed and the mutant exhibits reduced expression of the photosynthesis-related genes *HEMA1* and *Lhcb* under distinct light qualities, including FR (McCormac and Terry 2002). The combination of chromatin immunoprecipitation together with microarray hybridization (ChIP-chip) has been used to examine the in vivo binding targets of HY5 throughout the genome. Among all of the defined HY5 targets, photosynthesis-related genes were one of the most enriched groups, and HY5 was showed experimentally not only to regulate transcription of some of this group (for example *Lhcb*, *F3H*, *RbcS* and *CHS*), but also to bind directly to the promoter of these genes conferring chlorophyll and anthocyanin accumulation during the dark-light shift (Lee et al., 2007).

1.8 The response to abiotic stresses

Mechanisms adopted by plants to develop and survive in a constantly fluctuating environment are characterized by their high diversity and plasticity. The existence of a complex and an integrated network of signalling pathways is then crucial for the ability to induce rapid and long-term changes in plant growth and development leading to further acclimation to stress conditions. Chloroplasts comprise an essential component of this massive signalling machinery, regulating a wide spectrum of responses to different environmental stimuli in both developing and

mature plants. However, it is more difficult to clearly indicate responses specific only for one type of the stress. The intricacy and multidirectional character of signalling cascade events impede their precise examination, demanding application of diverse and comprehensive approaches.

Light intensity, temperature, salt, nutrition deficiency or a lack of water are the main environmental factors that govern plant functional status. Each deviation from optimal conditions can induce physiological and molecular changes, eventually, affecting plant cellular homeostasis, growth and reproduction. Thus, plants have evolved a number of unique mechanisms, which allow them to perceive, monitor and effectively respond to both sudden and seasonal environmental changes. Strategies utilized by plants to endure abiotic stresses can be divided generally into two categories: avoidance and acquisition of tolerance (Janská et al., 2010). Those processes can vary significantly depending on the plant species and type of stress. However, all of them increase the probability of plant survival in severe environments. Avoidance can be described as delay or prevention from exposure to the negative pressure of an environmental stress stimulus. This is achieved mainly through generation of various boundaries that differ in their physical nature. For drought stress, avoidance is predominantly associated with keeping tissue water potential at the highest possible level in order to prevent dehydration. Plants can reach this by executing well conserved adaptive mechanisms, like stomata closure, reduction of absorbed light by leaf cooling or decreased transpiration due to changes in leaf area (Harb et al., 2010). Water status disturbance also lays at the basis of other abiotic stresses, thus responses triggered by different environmental perturbations have much in common. Tolerance comprises mechanisms allowing plants to sustain their functional status, despite the stress occurrence and its negative effect on the organism. Consequently, stress tolerance determines the ability of the plant to acclimatise to unfavourable conditions, an active and complex process. In the context of both drought and cold stresses, these can include reduction in cell size; modifications of membranes and cell walls; accumulation of different solutes e.g. sugars, proline, glycine betaine in order to stabilize protein conformation; membrane architecture; and water relations (Harb et al., 2010; Janská et al., 2010).

During plant acclimation to stress conditions, numerous metabolic and physiological traits are induced. Plants integrate environmental and endogenous metabolic signals through a molecular network combining multiple signal transduction pathways, which ultimately, alter changes in gene expression. Years of investigations have indicated increased expression for hundreds genes in response to abiotic stresses, like cold and drought. These include many functional proteins falling into a few different categories e.g. the Cold Responsive Genes/Late Embryogenesis Abundant proteins (COR/LEA group*)*, Anti-Freeze Proteins (AFP), chaperones,

water channel proteins and lipid protection proteins. An example of proteins protecting against dehydration during different stress conditions, mainly in cold and drought, are the highly hydrophilic dehydrins. Among different functions that have been proposed for dehydrins, like stabilisation of enzymes or the plasma membrane, they also display the capacity for metal binding (Alsheikh et al., 2003). Through this mechanism dehydrins reduce metal ion toxicity and therefore exhibit antioxidant properties. Promoter regions of COR genes contain numerous of cis-elements required for induction of gene transcription by different stresses including cold, drought, salt and heat (Nakashima et al., 2014). The best known and most common examples of these promoter elements are: DRE/CRT (Dehydration-Responsive Elements/C-repeat elements) consisting of the A/GCCGAC motif implicated in responses to drought, salt and cold stresses; ABRE (ABA-responsive element) containing a PyACGTGGC conserved sequence responsive to changes in abscisic acid content; and MYBR (C/TACNA/G) and MYCR (CANNTG), core sequences that are recognized by the specific transcription factors MYB and MYC, respectively (Yamaguchi-Shinozaki and Shinozaki 1994; Abe et al., 2003). Although complex molecular events underlying acclimatory responses in plants are not fully understood and necessitate further investigations, we know the basic sequence of events, along with the main components of the pathways. Plant responses to stress conditions begin with the perception of stress stimuli resulting in changes in the calcium signature and induction of numerous phosphatases and kinases, such as the Mitogen-Activated Map Kinases (MAPKs). Consequently, different sets of transcription factors are activated, which, as main regulators of the signalling cascade, directly or indirectly bind to cis-elements of target genes activating or repressing their expression. For cold stress the main transcriptional activators are members of the DREB1 family, also described as the CBF regulon (CBF1-3), that recognize DRE/CRT elements. Overexpression of each of the *CBF* genes in *Arabidopsis* resulted in higher accumulation of proline and sugars, and conferred increased freezing tolerance (Gilmour et al, 2004). The main upstream transcriptional regulators of the CBF regulon are Inducer of CBF Expression1 (ICE1) and High Expression of Cosmetically Responsive Genes (HOS1). ICE1, a nuclear localized and constitutively expressed transcription factor, is activated during low temperature conditions via phosphorylation, which results in activation of *CBF* genes. *HOS1* encodes a RING finger ubiquitin E3 ligase that represses ICE1 by triggering ICE1 proteolysis after 12h of cold (Chinnusamy et al., 2010). DREB2 is another transcription factor that binds to DRE/CRT promoter elements. However, it has been shown that constitutive overexpression of active DREB2A resulted mostly in increased tolerance to drought, and some of the genes that were under the regulation of DREB2A were not responsive to DREB1A (Sakuma et al., 2006). Thus DREB2 is proposed to function as a regulator that is specific to drought stress signalling. In addition, CBF4 is another transcription factor that

recognizes the DRE/CRT motif of *COR* genes and specifically ensures drought tolerance, but, in contrast to DREB2, it also requires ABA for induction of *COR* genes (Haake et al., 2002). These examples demonstrate the high complexity of molecular signalling pathways involved in responses to abiotic stresses. Although a single transcription factor is capable of adjusting the expression of many stress-related genes, it is necessary for plants to involve multiple signalling pathways in response to unfavourable conditions. Extensive cross-talk between these different signalling cascades can also be observed. This intricacy allows plants to fully evaluate the impact of stresses, leading to fast response to environmental changes and overall coordination of acclimatory processes.

For heat stress, although we do know its final consequence, which is the production of many chaperonin proteins generally termed HEAT SHOCK PROTEINS (HSP), we do not know much about how heat is sensed in plants and what the precise molecular signalling events leading to HSP production are. The large group of HSPs is usually classified in a few different families based on their molecular mass and include HSP100, HSP90, HSP70, HSP60 and small HSPs. Transcription of genes coding for HSPs is well known to be induced by heat shock transcription factors (HSFs) and these are essential for heat stress signal transduction. However, HSPs can also accumulate in response to oxidative stress (Volkow et al., 2006; Miller et al., 2006). The role of phytochromes as temperature sensors was recently proposed, providing a new mechanism in which the thermal relaxation of phytochrome from the active to the inactive state is temperature sensitive and thus phyB associates with downstream gene promoters in a temperature-dependent manner (Jung et al., 2016).

The response to abiotic stresses is the subject of intensive studies, and different approaches have been undertaken to investigate and quantify plant tolerance to environmental change. the impact of the stress treatment correlates not only with the dose of the stressor, but is also affected by many other factors, such as time of exposure to the stress, light quality and quantity, humidity, and plant developmental stage. It's obvious that a higher level of injury can be observed with extended time of stress exposure, or when stress treatment is applied to younger plants. In contrast, very high humidity or darkness can reduce the effects of abiotic stresses.

Temperature is the essential factor regulating plant yield. It has been shown that even small temperature changes can induce a transition to a new plant developmental stage (Patel and Franklin 2009), for example by influencing hormone distribution (e.g. low temperature induced gibberellin biosynthesis and promotion of germination). A decrease in temperature can also considerably reduce plant growth and development. However, depending on the origin of the

plant, they are characterised by different sensitivities to low temperatures. In species from tropical and subtropical zones, cold injuries occur after plant exposure to 10-15°C (Saltveit and Morris, 1990). In contrast, plants from the temperate climatic zone, subsequently exposed to episodes of low temperature, present higher tolerance to cold stress (e.g. for some crops the lethal temperature can have a range of -3°C to -5°C or even lower). A standard approach for drought stress imposition to seedlings is application of solutes, like mannitol and polyethylene glycol (PEG), to the growth media. This causes a reduction of water potential and therefore overall water availability for the plant. Of these two substances PEG is considered to better mimic drought stress as, in contrast to mannitol, its high molecular weight does not allow it to enter the pores of the cells and prevents plasmolysis (Verslues et al., 1998). In nature plants are primed by changes in different environmental stimuli, with both rhythmic and more random variation. If moderate stress occurs, this priming state can be maintained to further improve plant resistance to more severe conditions. However, our knowledge about the molecular or physiological components underlying these phenomena is still elusive (Shahnejat-Bushehri et al., 2012).

1.9 Role of chloroplast signals in response to abiotic stress

An increasing number of chloroplast-derived signals have been linked with transduction and coordination of stress responses. Retrograde signalling events operating in mature plants in response to environmental changes are extremely complicated and not always mechanistically understood. However, there is a general agreement about the source of the main components directing this signature. The most classic and long studied example is the role of the redox state of the photosynthetic electron transport chain (PET) in the regulation of plant stress responses. Numerous environmental conditions, including light intensity, can vary intensively, leading to a situation in which the amount of absorbed energy is in excess of the capacity for CO_2 fixation (Takahashi and Murata, 2008). This imbalance between energy absorption and its consumption through metabolic processes can result in photooxidative stress, ROS generation and photoinhibition. To avoid that, plants utilise different mechanisms to quench overexcited chlorophyll molecules, therefore maximizing excitation energy absorption and increasing free energy available for electrochemical reactions. Signals produced due to disturbance of the photosynthetic electron transfer generally include reduced and oxidised plastoquinone (PQ), stromal thioredoxin, glutathione, NADPH and ROS (Pfannschmidt et al., 2001). A standard approach for studying redox-dependent signalling (mainly the redox state of the PQ pool) is by using high light or chemicals such as DCMU (3-(3,4-dichlorophenyl)-1,1-dimethyl urea) and DBMIB (2,5-dibromo-3-methyl-6-isopropyl-p-benzoquinone), which inhibit electron transfer from

PSII to PQ and from PQ to cytochrome b6f, respectively, allowing for the manipulation of the extent of reduction/oxidation of the Q_A-Q_B of the PQ pool (Pfannschmidt et al., 2001). It is well established that redox status of the PQ poll is an important regulator of signalling between the plastid and nucleus, altering both chloroplast gene expression (Alfonso et al., 2000) and nuclear gene expression (Escoubas et al., 1995; Chang et al., 2004). The involvement of redox state–dependent signalling in governing expression of nuclear-encoded plastid proteins was also confirmed by microarray analyses (Fey et al., 2005), on the basis of which the authors additionally suggested that this signalling pathway operates independently from other established retrograde pathways. Genetic studies revealed one of the possible mediators of PQ redox state-dependent signalling, a protein kinase State Transition 7 (STN7) (Pesaresi et al., 2009). STN7 is important for phosphorylation of Light Harvesting Complex II (LHCII) during low light conditions, resulting in its movement from Photosystem II (PSII) to Photosystem I (PSI), which in turn allows for more efficient light absorption. Additionally, redox changes around the PQ pool, in relation to both genetic and metabolic components, were shown to be involved in cross-talk between signalling pathways in response to light-induced excess excitation energy (EEE) and pathogen stresses (Muhlenbock et al., 2008). Therefore, chloroplast signals play an important role in coordinating systemic acquired acclimation (SAA) and systemic acquired resistance (SAR), indicating high plasticity of the control of redox-dependent gene expression.

It is widely accepted that different environmental stresses trigger an increase in ROS generation. As ROS display high potential for the oxidation of cellular components, ROS accumulation can result in damage to lipids, nucleotides and proteins causing metabolic limitations and influencing cell integrity. The increase in ROS levels can activate programmed cell death (PCD), leading to removal of damaged cells and subsequent induction of acclimatory responses. Chloroplast-derived ROS are also implicated in the induction and coordination of signalling pathways altering nuclear gene expression, and thus they can regulate plant functional status, metabolism, and initiate different plant processes including PCD and systemic signalling (Karpinski et al., 1999; Mittler et al., 2004; Danon et al., 2005). ROS steady state levels remain under tight control of the molecular network incorporating ROS-scavenging and ROS-producing components (Mittler et al., 2004). Even though the role of ROS as a crucial part of stress-induced signalling is clear, little is known about the molecular components directly interacting with ROS or ROS-specific DNA target sequences. ROS (mainly hydrogen peroxide, H_2O_2) are proposed to activate transcription factors either by direct oxidation or indirectly e.g. by activating MAPKs, which then can phosphorylate resulting in changes in expression of ROS-responsive genes (Mittler et al., 2004).

The multidirectional character of ROS-dependent signalling events and high diversification in plant processes regulated by this signalling (including plant development, growth, metabolism and environmental stress responses) suggest a requirement for specification in ROS action. It is presumed that unique ROS signatures could be achieved in at least three different ways: ROS can function directly as signals, whereby flux exhibits specific patterns i.e. with different amplitudes, frequency and localization; by acting indirectly to activate other signalling molecules; or by the potential existence of a series of differently compartmentalised ROS signal receptors (Mittler et al., 2011). The idea of high specificity of ROS signalling seems to be supported by analysis of comparative microarray data sets, which showed differences in transcriptome signatures for individual ROS species (Gadjev et al., 2006). Among different ROS, hydrogen peroxide and singlet oxygen are most strongly linked with plastid-dependent signalling. Due to its relatively low toxicity and long half-life H_2O_2 can be presumed to play a role as a long distance signalling molecule. H_2O_2 has the potential to pass through biological membranes and studies using both spin trapping EPR spectroscopy and fluorescent microscopy (with incorporation of Amplex Red reagent) showed that around 5% of H_2O_2 produced in response to high light in the chloroplast could be detected outside the organelle (Mubarakshina et al., 2010). New direct evidence for the role of H_2O_2 as a mobile retrograde signal was provided by the use of the fluorescent biosensor HyPer2 in tobacco to visualise the HL-induced and photosynthesis-dependent H_2O_2 transport from chloroplasts to the nucleus (Exposito-Rodriguez et al., 2017). An increase in the H_2O_2 pool has been repeatedly implicated in responses to diverse abiotic stresses e.g. as a part of a general response to low temperature stress and regulator of chilling tolerance or conferring stabilisation of transcripts for stress-related proteins such as SOS1 involved in salt stress (Prasad et al., 1994; Chung et al., 2008). Additionally, chloroplast-specific H_2O_2 over-production was shown to down-regulate expression of genes connected to cold and pathogen stresses, especially genes from the CBF regulon (Maruta et al., 2012). Subtle changes in the balance between scavenging enzymes and ROS production will be crucial for signalling and oxidative damage and these two processes may not be easily separated.

In contrast to H_2O_2, singlet oxygen predominantly contributes to the response to photooxidative stress. The discovery of $^1O_2$-specific retrograde signalling brought additional questions about the mode of action. Because $^1O_2$ has a short half-life and high reactivity, its capacity for movement is limited. Some findings suggest that in fact $^1O_2$ could be more stable than originally assumed. The presence of $^1O_2$ was detected in the cytoplasm of high light (HL) exposed *Chlamydomonas reinhardtii* cells by fluorescence measurements of Dane-Py-oxylase (Fischer et al., 2007). Treatment of cell cultures with both HL and NF resulted also in a higher

degree of thylakoid lipid peroxidation and an increase in expression of the nuclear-encoded antioxidant gene *GPXH* (Fischer et al., 2007). It could be, however, questioned if $^1O_2$ appeared in the cytoplasm due to its movement from the chloroplast or it was newly synthesised as a secondary effect of $^1O_2$ action. Indeed, $^1O_2$ has been shown to specifically interact with membrane lipids, which leads to formation of fatty acid peroxides preceding any cytotoxic effect of the $^1O_2$ (Triantaphylides et al., 2008). An important example of a chloroplast-derived $^1O_2$ burst operating specifically as a redox retrograde signal is represented by the *flu* mutant (Meskauskiene et al., 2001). $^1O_2$ over-accumulation observed in the *Arabidopsis flu* mutant results in activation of some early stress-response genes (op den Camp et al., 2003). The $^1O_2$ response in *flu* was further shown to depend on two genes *EX1* and *EX2* (EXECUTER1 and EXECUTER2), which rescue the $^1O_2$ signalling phenotype of the mutant, although the precise mechanism of their action in not known (Danon et al., 2005; Kim et al., 2009). Recently, a new potential candidate as a signalling component in $^1O_2$ signalling was characterised, termed METHYLENE BLUE SENSITIVITY1 (MBS1), which is a zinc finger protein (Shao et al., 2013). In mature *Arabidopsis* plants $^1O_2$ signalling was induced using a genetic system, with a mutant (*chlorina1*) affected in chlorophyll *b* synthesis that produces $^1O_2$ due to functional loss of PSII (Ramel et al.,2013). Interestingly, transcripts changed in *chlorina1* show a partial overlap with those identified following $^1O_2$ production after a FR pre-retreatment (Page et al., 2017a) suggesting a conservation of the response to $^1O_2$ in young seedlings and plants at the rosette stage.

In addition to ROS-dependent signalling, other products of chloroplast metabolism have been implicated as signals to the nucleus during abiotic stress. An example of a metabolite directly influencing nuclear gene expression is PAP (phosphonucleotide 3'-phosphoadenosine 5'-phosphate), as increased levels in the chloroplast correlate with drought and high light stresses. PAP can move to the nucleus where it is proposed to inhibit exoribonucleases (XRNs) and alter stress-responsive gene expression (Estavillo et al., 2011). It was also shown that the chloroplast phosphatase SAL1 functions as a negative regulator of PAP levels and can prevent its action in reducing expression of stress genes such as *APX2* or *ELIP2* (Estavillo et al., 2011). A second example is one of the precursors of a plastid isoprenoid biosynthesis pathway, MEcPP (methylerythritol cyclodiphosphate), which normally is converted to HMBPP (hydroxymethylbutenyl diphosphate) in a reaction catalysed by HDS (1-hydroxy-2 methyl-2-(E)-butenyl-4-diphosphatesynthase) (Xiao et al., 2012). Only increased concentration of the MEcPP component of the isoprenoid pathway is accompanied by elevated levels of salicylic acid (SA) and increased expression of some nuclear-encoded stress responsive genes (e.g. *HPL*, *ICS1)*.

This results in higher resistance to pathogens, wounding and high light stresses. Interestingly, MEcPP-directed signalling might act independently at least from some of the other networks, since this pathway did not influence nuclear photosynthetic gene expression regulated by a GUN-dependent signalling pathway (Xiao et al., 2012). As plant responses to abiotic stresses can differ markedly and trigger changes in numerous processes at distinct levels of cell organisation, it is not surprising that plastid-to-nucleus signalling operating during stress conditions involves a wide spectrum of complex and diverse mechanisms.

1.10 Project aims

The main focus for this project is to test a newly proposed model for tetrapyrrole-dependent plastid-to-nucleus retrograde signalling and to increase our understanding of factors that control this response. In this model retrograde signalling involves two pathways: a positive FC1-derived, heme-related signal and a singlet oxygen ($^1O_2$)-mediated inhibitory signal resulting from mis-regulation of chlorophyll synthesis (Terry and Smith, 2013). This hypothesis is based on published experimental data and requires further evaluation. For the heme positive signal it was shown that FC1 (but not FC2) overexpressor lines maintain higher photosynthetic gene expression on NF (Woodson et al. 2011). Additionally, feeding ALA can also rescue gene expression on NF (Woodson et al., 2011). It is therefore proposed that flux through the heme branch of the tetrapyrrole pathway promotes expression of nuclear-encoded chloroplast genes and seedling development. Any condition that blocks chloroplast development would lead to a loss of this signal. This model is in agreement with higher gene expression observed earlier in *gun2-gun5* under NF treatment (Mochizuki et al., 2001), as each mutation can potentially lead to increased heme synthesis. GUN1 has been recently shown to interact with tetrapyrrole proteins (Tadini et al., 2016), but it precise mechanism of function in retrograde signalling is still not clear. The impact of GUN1 on tetrapyrrole-dependent signalling with respect to newly proposed pathways needs to be re-examined. Signalling pathways controlling expression of nuclear-encoded plastid genes will also be examined in this study. The ability of GUN1 to interact with plastid ribosome proteins (Tadini et al., 2016) suggests the possibility of an interaction between tetrapyrrole signalling and plastid gene expression signalling and this will be tested here.

The role of heme-dependent signal in promotion of chloroplast gene expression will be addressed by quantitative RT-PCR analyses of selected photosynthetic and tetrapyrrole gene expression after chemical treatment with 2'2-dipirydyl (DP) that is known to block heme synthesis. Additionally, the *gun* phenotype of *gun6-1D* on NF as well as new mutants that have been proposed to control retrograde signalling (*ptm*, *abi4*) will be re-examined. The effect of *gun1* on

heme-dependent signalling will be evaluated by measuring levels of Pchlide after feeding with ALA. Using quantitative RT-PCR, the *gun1* phenotype on NF and Lin will be examined after an additional block of heme synthesis with DP.

To understand the role of plastid protein synthesis in retrograde signalling the phenotype of mutants, such as *prpl11*, lacking components of the chloroplast ribosome will be examined for their effect on nuclear gene expression. The effect of *prpl11* mutations as well other plastid translation mutants on tetrapyrrole metabolism will also be determined. The effect of PRPL11 overexpression will also be tested and the lines made used in pull-down experiments to look for interacting proteins. This should provide an insight into the molecular function of PRPL11. Overall, the proposed experiments should allow for a better understanding of the role of plastid protein synthesis, and PRPL11 in particular, on tetrapyrrole metabolism and plastid-to-nucleus retrograde signalling.

The role of chlorophyll precursors in induction of $^1O_2$ inhibitory retrograde signal will be addressed by feeding ALA to dark-grown seedlings before transferring to WL. The physiological consequences of this treatment on tetrapyrrole metabolism as well as ROS production will be initially carried out to test if $^1O_2$ can be generated. The inhibitory effect of ALA feeding on photosynthetic gene expression will be studied using quantitative RT-PCR analyses. The inhibition of photosynthetic gene expression will be additionally examined in *flu* and *fc2* mutants that are known to produce $^1O_2$ after transfer to WL.

Lastly, the hypothesis will be tested that chloroplast-mediated environmental regulation of gene expression is operating in young seedlings and that this communication requires known biogenic tetrapyrrole signalling pathways. Plastid signalling microarray datasets will be examined for overlap with abiotic stresses signalling arrays. Where there is evidence for an overlap in gene expression profiles this will be tested experimentally using simultaneous stress and retrograde signalling treatments and by using mutants altered in chloroplast function. Additionally, mutants compromised in their response to abiotic stresses (selected from the array analyses) will be tested for their response to experimental conditions demonstrating retrograde signalling.

Chapter 2 Materials and methods

2.1 Plant material, growth conditions and treatments

Arabidopsis thaliana T-DNA insertion mutants were selected via the SIGNAL database (http://signal.salk.edu/cgi-bin/tdnaexpress). These and other Arabidopsis lines, including EMS-generated mutants were ordered from the Nottingham Arabidopsis Stock Centre (NASC). The T-DNA insertion homozygous lines were selected by PCR using a primer pair specific for the gene region and for the T-DNA insert. EMS substitution and T-DNA localisation were confirmed by sequencing. The additional overexpressor lines not generated in this study were produced previously in the Terry laboratory (Patrick Stephenson,2009) or were gifted from other laboratories. A summary of information for all lines used in this study is shown in Table 2.1.

Arabidopsis seeds were surfaced-sterilized prior to growth on plates. For seed sterilisation 70 % (v/v) ethanol and a sterilisation solution containing 20 % (v/v) bleach (Domestos, UK) with 0.05 % (v/v) Triton X-100 (Sigma Aldrich, UK) were used. Seeds were mixed with ethanol for 5 min at room temperature, followed by 10 min incubation in the sterilisation solution with occasionally vortexing. After bleach removal, seeds were washed 6-7 times with sterile Mili-Q water (MQ). *Arabidopsis* wild-type and mutant seeds were plated on 90 mm Petri dishes containing 25 mL agar-solidified0.5 x MS media (Murashige and Skoog 1962; Duchefa Biochemie, UK), with 1 % (w/v) agar and without sucrose (unless otherwise stated). For norflurazon (NF) and lincomycin (Lin) treatments, 0.5 x MS medium was additionally supplemented with 1 µM NF (or 50 nM for selected experiments) in dimethyl sulfoxide (DMSO, Sigma Aldrich, UK) to a final concentration of 0.02 % (v/v) or 0.5 mM lincomycin (lincomycin hydrochloride, Sigma Aldrich, UK). For dipyridyl (DP) (2,2-dipyridyl, Sigma Aldrich, UK) treatments, seedlings were transferred from solid 0.5 x MS agar medium to water supplemented with 0.05-1 mM DP. For 5-aminolevulinc acid (ALA) feeding experiments, 0.5 x MS was supplemented with 5 mM 4-morpholineethanesulfonic acid (MES, Sigma Aldrich, UK) with or without 0.05-0.2 mM ALA (Sigma Aldrich, UK). For the salt stress experiments, seedlings were grown on 0.5 x MS agar medium supplemented with or without 90 mM sodium chloride (NaCl, Sigma Aldrich, UK) or were transferred to liquid 0.5 x MS with 150 mM NaCl. Seeds were plated in small clumps (around 10-15 seeds per clump). In order to maintain a sterile environment, plates were sealed with micropore tape (3M). Before each experiment plates were incubated three days at 4°C in the dark to break dormancy and to synchronize germination.

Arabidopsis thaliana wild type (Col-0), mutant and overexpressor lines seeds were exposed to 2 h of white light (WL) to induce germination and placed in darkness (D) for 2 d at 22°C. Unless specified otherwise, after germination in the dark, seedlings were grown under continuous WL (WLc) for 3 days in standard conditions (100±10 µmol m^{-2} s^{-1}; mean temperature 22±1°C) in a WL growth cabinet (I-36 HILQ, Percival Scientific, Inc., USA). For singlet oxygen experiments, after 2 h WL incubation, seeds were left to grow in darkness at 22°C±1°C for 4 days, or after 2 days dark were transferred to a FR cabinet at 23°C for additional 2 days. To induce oxidative stress, seedlings were exposed to WLc for 2-24 h under standard light conditions. The heat shock (HS) treatment was applied by immersing sealed plates in a water bath at 44°C for 1 h under standard light conditions, or without light for selected experiments by covering plates with foil. For cold stress treatments, plates were placed in the cold room at 4°C.

Table 2.1 Mutant and overexpressor lines used in this study including original WT background and source

Mutant allele	Type of mutation	Background	Insert name	Acquired from	Reference
gun1-1	EMS	pOCA107-2	-	J. Chory	Koussevitzky et al., 2007
gun1-103	T-DNA	Col-0	SAIL_742_A11	NASC	Sun et al., 2011, this work
gun4-1	EMS	pOCA107-2	-	J. Chory	Larkin et al., 2004
gun5-1	EMS	pOCA107-2	-	J. Chory	Mochizuki et al., 2001
gun6-1D	T-DNA	pOCA107-2	-	J. Chory	Woodson et al., 2011
GUN1ox1	-	Col-0	-	D. Leister	Tadini et al., 2016
GUN1ox1	-	Col-0	-	D. Leister	Tadini et al., 2016
abi4-102	EMS	Col-0	CS3837	NASC	Laby et al., 2000
abi4-2	T-DNA	Col-0	SALK_080095	NASC	Kakizaki et al., 2009
ptm-1	T-DNA	Col-0	SALK_013123	NASC	Sun et al., 2011
sig2-2	T-DNA	Col-0	SALK_045706	B. Montgomery	Kanamaru et al., 2001
sig6-1	T-DNA	Col-0	SAIL_893_C09	T. Shiina	Ishizaki et al. 2005
prpl11-1	T-DNA	Col-0	-	D. Leister	Pesaresi et al., 2001
prpl11-3	T-DNA	Col-0	GABI_366H05	NASC	this work
prpl24-1	T-DNA	Col-0	SALK_010822	D. Leister	Romani et al., 2012
prps21-1	T-DNA	Col-0	SAIL_1173_CO3	D. Leister	Tadini et al., 2016
hsfa2-1	T-DNA	Col-0	SALK_008978	NASC	Alonso et al., 2003
cphsc70-1	T-DNA	Col-0	SALK_140810	NASC	Su and Li, 2008
cphsc70-2	T-DNA	Col-0	SALK_095715	NASC	Su and Li, 2008
chip-1	T-DNA	Col-0	SALK_048371	NASC	Zhou et al., 2014
atg5-1	T-DNA	Col-3	SAIL_129_B07	NASC	Thompson et al., 2007
atg7-2	T-DNA	Col-0	GABI_655B06	NASC	Chung et al., 2010
mpk6-3	T-DNA	Col-0	SALK_127507	NASC	Xing et al., 2009
mbs1-1	T-DNA	Col-0	SAIL_661_B05	NASC	Shao et al., 2013
ex1/ex2	T-DNA	Col-0	-	K. Apel	Lee et al., 2007
flu-1	EMS	Col-0	-	K. Apel	Meskauskiene et al., 2001
cas-1	T-DNA	Col-0	SALK_070416	T. Shiina	Nomura et al., 2012
CASox	-	Col-0	-	T. Shiina	Nomura et al., 2012
phyA-211	γ-Ray	Col-0	-	NASC	Reed et al., 1994
phyB-9	EMS	Col-0	-	NASC	Reed et al., 1993
cry1	EMS	Col-0	-	M. Ahmad	Ahmad et al., 1994

For the WL source Sylvania Luxine Plus lamps (type 39W, light colour 830) were used and set to emit light at a fluence of 100±10 µmol m^{-2} s^{-1}. For the low light experiments, neutral density filters were used to reach the desired PFD (Lee Filters, Andover, UK). Far-red light (FR) was derived from the LEDs passed through a filter that removed λ<700nm (#116, Lee Filters, Andover, UK) and gave a final fluence rate at around 10 µmol m^{-2} $s^{-1,}$ as described in Stephenson and Terry (2008). For red and blue light experiments broad-band white light was passed through red and blue filters, respectively resulting in a fluence rate of 60 µmol m^{-2} s^{-1} (red light) and 20 µmol m^{-2} s^{-1} (blue light).

2.2 Basic physiology and biochemistry

2.2.1 Pigment measurements

2.2.1.1 Chlorophyll and carotenoids

Chlorophyll and carotenoid was extracted from 20-30 whole *Arabidopsis* seedlings, which were weighed, frozen in liquid nitrogen and stored in -80°C b. Pigments were extracted with cold 80% acetone (v/v; Duchefa). Seedlings were ground in mortars and pestles on ice, and centrifuged at 16,000 x *g* for 5 min at 4°C. Supernatants from two sequential extractions were combined to a final volume of 800 µL. Absorbance was measured at 470, 647, and 663 nm using an Hitachi U-2001 spectrophotometer (Hitachi High-Tech, Japan). Results were calculated according to Lichtenthaler (1987) and, depending on the experiment, expressed in µg/g seedling fresh weight, or in ng/seedling. In order to calculate chlorophyll *a*, chlorophyll *b*, total chlorophyll and carotenoid content the following equations were used (Lichtenthaler, 1987):

Chlorophyll *a* = 12.25 A_{663} – 2.79 A_{647}

Chlorophyll *b* = 21.50 A_{647} – 5.10 A_{663}

Total chlorophyll = 7.15 A_{663} + 18.71 A_{647}

Carotenoids = (1000 A_{470} – 1.82 Chl*a* – 85.02 Chl*b*) / 198

2.2.1.2 Chlorophyll fluorescence measurements

The photosynthetic performance of PSII was assessed *in-vivo* using Imaging-PAM *M-series* and the ImagingWin software (Walz, Germany). Seedlings were grown in small clumps under standard conditions for 2 d D and 3 d WLc (100±10 µmol m^{-2} s^{-1}). After 30 min dark-adaptation the minimal fluorescence (F_o) was measured by exposure to a pulse of blue light. The

maximum fluorescence (F_m) was measured following a pulse of saturating WL and the maximum quantum yield of PSII (F_v / F_m) was calculated as the ratio (F_m-F_o / F_m).

2.2.1.3 Protochlorophyllide measurements

Protochlorophyllide (Pchlide) levels were measured from 20-30 4-d old D grown *Arabidopsis* seedlings. Seedlings were ground in liquid nitrogen, covered with foil and stored in -80°C until required. All extraction steps were performed in the dark room, under the safe green light. Seedlings were ground in mortars and pestles on ice with cold alkaline acetone solution (acetone: 0.1M NH_4OH; 9:1 (v/v)). Samples were vortexed briefly and centrifuged at 16,000 x *g* for 5 min at room temperature. Supernatants from two sequential extraction steps were collected and Pchlide levels were measured using a fluorescence spectrophotometer F-2000 (Hitachi High-Tech, Japan) following excitation at 440 nm. Emission spectra were recorded between 500 nm to 700 nm and the Pchlide emission λmax at 636 nm was measured. Final results were expressed as relative fluorescence (RFU) per seedling.

2.2.1.4 Heme detection by chemiluminescence

Total non-covalently-bound heme measurements were performed following the protocol described in Espinas et al. (2012), with small modifications. 5-d old seedlings that were grown 2 d D and 3 d WLc were used for the analyses. Cotyledon tissue was removed, weighed (approximately 4-6 mg per sample) and quickly frozen in liquid nitrogen. Tissue was stored at -80°C until required. Frozen material was ground in liquid nitrogen to a powder, extracted twice with 1 mL of acetone (acetone:1.6 M HCl (80/20, v/v) and centrifuged at 16,000 x *g* at 4°C for 15 min to remove cell debris. Cleared extracts were diluted 1:100 with sterile water. An authentic 1 mM hemin stock solution (bovine hemin chloride, Sigma Aldrich, UK) was prepared in DMSO using an excitation coefficient of ε_{mM} = 183 at 404 nm (Collier et al., 1979). To create a calibration curve, the hemin stock solution was further diluted with water in the range 50-600 pmol.

To reconstitute horse radish peroxidase (HRP), 10µL of a diluted hemin extract or a known hemin standard was mixed with 40 µL of apo-HRP enzyme (BBI Solutions) in 100 mM Tris-HCl, pH 8.4. The final enzyme concentration in each sample was 2.5 nM apo-HRP. Samples were vortexed, spun briefly and incubated for 30 min at room temperature. After transferring samples to a 96-well white polystyrene plate, 50 µL of HRP substrate (H_2O_2:luminol, 1:1; ImmobilonTM Western Chemiluminescent HRP Substrate, Merckmillipore) was added to each sample. Samples were mixed well by pipetting and incubated for 5 min. Chemiluminescence was

recorded using micro-plate reader (GloMax® 96 Microplate Luminometer, Promega) with 0.5 s integration time.

2.2.2 Measurement of 5-aminolevulinic acid synthesis

5-aminolevulinic acid (ALA) synthesis was measured according to Mauzerall and Granick (1956). 2 d D and 3 d WLc-grown whole seedlings were transferred from 0.5 x MS agar plates to 50 mM Tris-HCl, pH 7.2 supplemented with 40 mM levulinic acid (LA, Sigma Aldrich, UK) and incubated in WL for 2 h (100 µmol m^{-2} s^{-1}, 22±1°C). Seedlings were blotted dry and the fresh weight of cotyledon tissue was recorded. Tissue was frozen in liquid nitrogen and stored at -80°C until required. Frozen tissue was ground to a powder in liquid nitrogen and re-suspended in 600 µM 20 mM potassium phosphate buffer, pH 6.8. After centrifugation at 16,000 x *g* for 10 min at 4°C, 400 µL of the cleared supernatant was transferred to a new Eppendorf tube and mixed with 100 µL ethylacetoacetate (Sigma Aldrich, UK). Samples were boiled for 10 min using a thermomixer (Eppendorf) and cooled on ice for 5 min. 500 µL of modified Ehrlich's reagent (122 mM p-dimethyl aminobenzaldehyde, 75% (v/v) acetic acid 12.5% (v/v) perchloric acid, 11.5 mM $HgCl_2$) was added to each sample and mixed by vortexing. After centrifugation at 16,000 x *g* for 10 min at room temperature, absorption was recorded at 553 nm using a Hitachi U-2001 spectrophotometer (Hitachi High-Tech, Japan). The final ALA concentration in extracts was calculated based on a calibration curve for ALA (Sigma Aldrich, UK) treated the same as the test samples.

2.2.3 ROS detection by fluorescence microscopy

Singlet oxygen ($^1O_2$) and hydrogen peroxide (H_2O_2) accumulation was monitored in ALA-treated, FR pre-treated and HS-treated seedlings grown as described previously (section 2.1). For $^1O_2$ and H_2O_2 detection, Singlet Oxygen Sensor Green (SOSG, Molecular Probes, UK) and 2',7'-dichlorodihydrofluorescein diacetate (H_2DCFDA, Molecular Probes) were used, respectively. An SOSG stock solution was prepared in methanol according to the manufacturer's instruction giving a final concentration of 5 mM. For SOSG measurements, whole seedlings (10-15) were gently immersed in 300 µL 50 µM SOSG in potassium phosphate buffer, pH 7.2, in a 24-well plate (flat bottom, non-treated, clear; Falcon®, Corning). Immersion directly followed 2 d FR or 4 d D with or without 0.1 mM ALA and with or without an additional 1 h HS stress during the D period. Seedlings were vacuum treated for 20 min in D, washed briefly with liquid 0.5 x MS, blotted dry on filter paper, transferred to fresh liquid 0.5 x MS on a 24-well plate and moved to standard WLc conditions for different durations of time (0.5-4 h). Microscope slides were prepared 10-15 min before the end of the different time points in WLc to account for the time

difference needed for sample manipulation and transfer to the imaging facility. For the negative control, seedlings were vacuum treated in D, kept in liquid 0.5 x MS in D and visualised at the equivalent time points. These slides were prepared under dim green light. For H_2O_2 detection, seedlings were transferred directly on agar plates from dark or FR to WL for different durations of time. A 10 mM H_2DCFDA stock solution was prepared in DMSO. 15-20 min before the end of each time point, 10 whole seedlings were immersed in 500 µL 10 µM H_2DCFDA in 10 mM Tris-HCl, pH 7.2, in 1.5 mL Eppendorf tubes and vacuum treated for 10-15 min under dim laboratory light. Seedlings were washed in 1 mL Tris-HCl buffer, blotted dry on filter paper and analysed immediately. As a positive control, seedlings were wounded after the shift from D/FR to WL and analysed after 2 h WL exposure.

In both cases, SOSG and H_2DCFDA fluorescence was detected using a GFP filter (ex: 480/20 nm; em: 510/20 nm) on a Zeiss Axioplan 2 fluorescence microscope (10x objective; Carl Zeiss, Germany). Seedling auto-fluorescence and SOSG or H_2DCFDA background fluorescence was also monitored. Representative images from at least 5 seedlings were taken for each time point and treatment. Relative fluorescence intensity values were calculated using Image J (https://imagej.nih.gov/ij/).

2.2.4 Trypan blue staining

Trypan blue staining was used to assess cell death in seedlings subjected to singlet oxygen stress. Around ten 4 day-old seedlings exposed to WLc for 2-24 h were placed in 1.5 mL Eppendorf tubes with 1 mL of trypan blue solution [10 mL glycerol, 10 mL lactic acid, 10 mL phenol, 10 mL H_2O and 10 mg trypan blue (Sigma Aldrich, UK)] diluted with ethanol 1:2 (v/v). Samples were boiled for 3 min using a Thermomixer (Eppendorf) and left at room temperature overnight with gentle shaking. Non-specific staining was removed from seedlings by at least two incubations in chloral hydrate solution (25 g for 50 mL H_2O) for a total time of 6 h. Samples were stored in 50% (v/v) glycerol and imaged using a Nikon Eclipse E400 microscope equipped with colour camera.

2.3 Analysis of gene expression by quantitative real-time PCR (qPCR)

2.3.1 Total RNA isolation from seedlings

All tips, Eppendorfs and buffers were autoclaved for 1.5 h at 121°C before use. 100-200 mg of *Arabidopsis* young seedling tissue was harvested directly into liquid nitrogen and stored in -80°C until required. 150 µL phenol (pH 4.8, Sigma Aldrich, UK) and 500 µL ”RNA Miniprep” buffer

(100 mM NaCl, 10 mM Tris pH 7.0, 1 mM EDTA and 1 % (w/v) SDS) were added to each Eppendorf tube and samples were ground carefully in the tube with hand pestles. 250 µL chloroform (Sigma Aldrich, UK) was added and samples were vortexed thoroughly for 30 s. After vortexing, samples were centrifuged at 16,000 x *g* for 5 min at 4°C to allow phase separation. Approximately 500 µL of the upper phase was carefully transferred to a new Eppendorf, mixed with 450 µL 4M LiCl, and precipitated for around 12 h at 4°C. The precipitate was recovered by centrifugation at 16,000 x *g* for 10 min at 4°C. In order to avoid genomic DNA contamination, pellets were resuspended in 300 µL of DNase buffer (10 mM Tris HCl pH 7.5, 2.5 mM $MgCl_2$, 0.5 mM $CaCl_2$) and treated with 1 µL of DNase I (Promega, USA). Samples were incubated at 37°C for 25 min using a thermomixer (Eppendorf, UK). 500 µL phenol:chloroform:isoamyl alcohol (25:24:1, v/v/v; Thermo Fisher Scientific, USA) was added, samples were vortexed thoroughly for 30 s, and centrifuged at 16,000 x *g* for 5 min at 4°C. The upper phase was retained and mixed with 750 µL ethanol containing 5% (w/v) 3 M NaAc (pH 5.5). Samples were mixed briefly and left for 1 h at -20°C to precipitate. The RNA was collected by centrifugation for 10 min at 16,000 x *g* at 4°C. The resulting RNA pellet was allowed to air dry at room temperature for approximately 10-15 min. The final RNA pellet was resuspended in 30-60 µL TE buffer (10 mM Tris HCl (pH 8), 1 mM EDTA).

The concentration and purity of RNA samples were determined using the Nano-Drop ND-1000 spectrophotometer (Thermo Fischer Scientific, USA). The absorption ratios of 260nm/280nm and 260 nm/230 nm allowed the evaluation of protein and salt contamination. If possible, RNA was directly subjected to cDNA synthesis. RNA samples were stored at -80°C.

2.3.2 First strand cDNA synthesis

cDNA was prepared in two steps from 1 µL total RNA using the Precision nanoScript2 Reverse Transcription kit (Primerdesign, UK). Briefly, 1 µL RNA was added to a mixture of 1 µL oligo-dT primers and 1 µL of random primers and adjusted to a final volume of 10 µL with RNAse/DNAse free water. Samples were vortexed and heated to 65°C for 5 min using a peqSTAR thermal cycler (Peqlab, USA) and immediately transferred to ice for 5 min. After cooling, 10 µL of reverse transcription mix solution (5 µL nanoScript2 4x Buffer, 1µL 10mM dNTP, 3 µL RNAse/DNAse free water, 1µL nanoScript2 enzyme) was added to each sample. Samples were vortexed, centrifuged and placed in a peqSTAR thermal cycler (Peqlab, USA). cDNA synthesis was performed using the following cycle conditions: 25°C for 5 min, 42°C for 20 min and 75°C for 10 min. cDNA samples were stored in -20°C until required. For reverse transcription PCR (RT-PCR), 0.5-1 µL cDNA and 10 µM of gene specific primers were added to 1x BiomixRed solution. A primer pair for *ACTIN2* spanning an exon-exon junction was used as an additional control to

confirm the quality and integrity of synthesized cDNA. The thermal cycling conditions were as follows: 95°C for 3 min, 30 cycles of 30 s at 95°C, 30 s at 58-64°C and 60 s at 72°C followed by 10 min at 72°C.

2.3.3 Quantitative real-time PCR

Each qPCR reaction was prepared in a final volume of 10 µL. Samples consisted of: 5 µL PrecisionPLUS-SY or PecisionFAST-SY 2x MasterMix premixed with SYBRgreen (Primerdesign, UK), 0.5 µL cDNA template, 2 µL MQ water and 2.5 µL primer mix, containing 2 µM gene specific primers resuspended in MQ water. MQ water alone was used as a negative control. qPCR was performed using white plastic 96-well plates (Starlab, UK) and conducted using a Chromo4 Thermal Cycler (Bio-Rad, USA) or a Step One Plus Real Time PCR System (Thermo Fisher Scientific, USA). A summary of thermal cycling conditions is shown in Figure2.1. A melting curve was generated for each sample, to ensure no unspecific products were amplified. Each reaction was performed in two technical replicates with 3 biological replicates.

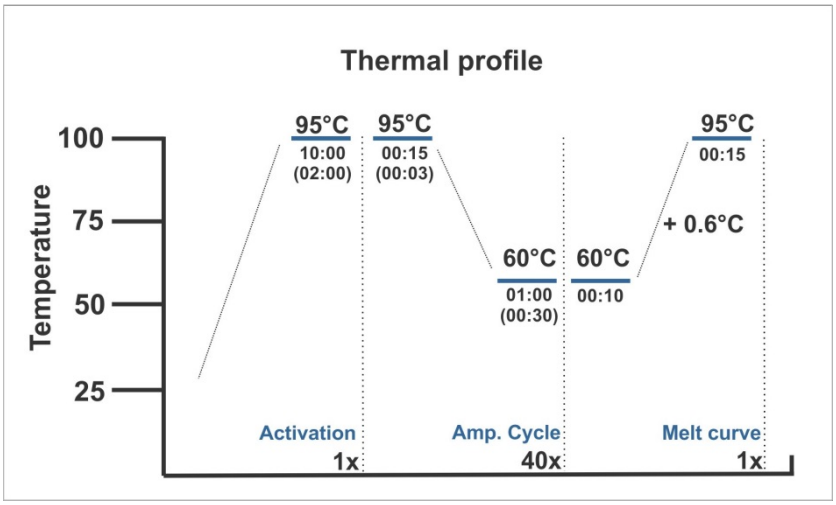

Figure 2.1 Protocol for qPCR reactions. Schematic profile illustrating the thermal cycling program used for qPCR analyses in both the Step One Plus and Chromo 4 machines. The first step is an activation at 95°C for 10 min followed by 40 cycles of 15s denaturation at 95°C, and 1 min of annealing at 60°C. Numbers in parenthesis correspond to time intervals of each temperature step used in the fast thermal cycling program. For melt curve generation, fluorescence was read after every 0.6°C increase in temperature.

All of the genes analysed, and their corresponding primers, are listed in Table 2.2. The melting temperature (T_m) of each primer was close to 56°C, and primers generated amplicons between 70-200 bp. If possible, primers were designed to flank introns or span exon-exon junctions. All primers were tested for secondary structures with NetPrimer (Primer Biosoft International, USA) and MFEprimer-2.0 (http://mfeprimer.com/). To ensure primer specificity, primer sequences were checked against the *Arabidopsis* genome sequence (www.ncbi.nlm.nih.gov/tools/primer-blast).

Threshold adjustment was performed using Opticon Monitor 3.1 software (for Chromo4; Bio-Rad) or StepOnePlus™Software v2.3 (for Step One Plus Real Time PCR System; Thermo Fisher Scientific, USA). Data were exported to Excel and C(t) values used to calculate relative gene expression. Results were presented, as gene expression relative to the reference gene, and normalized to the untreated WT control (Col-0), using the following equation:

$$ratio = \frac{(Efficiency_{target})^{\Delta C(t)target\ (control-sample)}}{(Efficiency_{reference})^{\Delta c(t)reference(control-sample)}}$$

Primer efficiencies were assessed by standard qPCR analysis of serially diluted control cDNA under the same conditions described above, with C(t) values plotted against $\log_2$ cDNA concentration. Using the slope of the amplification curve, efficiencies for the primer pairs were evaluated with the equation: Efficiency = $(2^{(-1/slope)})$.

Table 2.2 List of primer pairs used in all qPCR analyses. Primer names with corresponding sequences, melting temperatures (T_m) and product size are presented.

Primer name	Primer sequence 5'-3'	T_m [°C]	Product size [bp]	PE[1]
qHEMA1_F	GCTTCTTCTGATTCTGCGTC	55.0	128	2.02
qHEMA1_R	GCTGTGTGAATACTAAGTCCAATC	55.7		
qCHLH_F	CATTGCTGACACTACAACTGC	54.0	145	1.87
qCHLH_R	CTTCTCTATCTCACGAACTCCTTC	56.5		
qGUN1_F	GCTACTAAACATACGCTCCATTG	56.9	115	2.26
qGUN1_R	TCGTCTTAGTGCTCCGTCTC	55.1		
qGUN4_F	CAATCTCACTTCGGACCAAC	55.0	121	2.00
qGUN4_R	TTGAAACGGCAGATACGG	54.9		
qFC1_F	CCTGAAACTCTTAACGATGTTC	53.9	164	1.99
qFC1_R	CCACCAATAGCAGCATACC	53.6		
qFC2_F	GCAGAGATGGAAGAATGTGTTG	57.3	139	2.16
qFC2_R	CAGTAATGGCTTCTTCAGTGTATG	56.7		
qNPQ4_F	AAGGTTGAGAAGCCGAAGAG	56.3	100	2.25
qNPQ4_R	CAACACGACCAACGAATAGC	56.5		
qPSBQ-1_F	AAACCCAAGGATGAGAAGAAGT	56.6	82	2.25
qPSBQ-1_R	TCGCCGCATAATCCAGAT	56.9		
qCP12-2_F	GACAAGAAGAAGGCTGATGGTT	57.8	76	2.12
qCP12-2_R	TACGGCACTCGTTGGTCTC	56.4		
qLHCB1.2_F	GAGTGAGAGACATGAGGAGAAAG	54.9	60	2.15
qLHCB1.2_R	ACATCTGAAAGTCTCAAACCATC	55.3		
qLHCB2.1_F	CTCCGCAAGGTTGGTGTATC	59.2	142	1.89
qLHCB2.1_R	CGGTTAGGTAGGACGGTGTAT	59.3		
qAOX1a_F	CCTACCGATTTGTTCTTCCAG	56.8	147	1.85
qAOX1a_R	AGCCTTAATCCATCCTCCAC	55.7		
qUPOX1_F	AGAGGGTGAAGGATGATAACG	55.9	122	1.91
qUPOX1_R	GCTCCCGAATATCTTGTCCA	58.9		
qNDA1_F	TGCTCCAAACTTGATGCTGA	57.3	67	1.92
qNDA1_R	ATGTGCTAGACCCCTCAGTTA	54.1		
qNDA2_F	GGTCGATACAAAGCCCTAGTC	55.9	77	1.93
qNDA2_R	CAGCTCACGAAACCAGTCAT	55.6		
qNDB2_F	ATCGGCTCTATCTCAGGTTG	54.3	139	1.82
qNDB2_R	CCTAATGGGACCTTCTGGAC	55.9		
qGLK1_F	CGGTGACTTATGACGGTGAC	55.8	138	1.87
qGLK1_R	CGAATCTCCTGTGTAGCTCTG	55.0		
qGLK2_F	CATCAGCAACCACTCTATCCA	55.8	192	1.81
qGLK2_R	CGGTTTCAGTCCCAAAGGAA	59.9		
qADF2_F	CGATTTCGACTTTGTCACTGC	58.3	95	1.77
qADF2_R	TCATCTTGTCTCTCACTTTGGC	57.0		

qYLS8_F	AAGGACAAGCAGGAGTTCATT	57.4	93	2.09
qYLS8_R	AGTAATCTTTTGGAGCAATCACC	56.9		
qPRF1_F	AGGTGAACAAGGAGCTGTGAT	56.1	95	1.91
qPRF1_R	CATCGTAGAAGCCAAAGACCA	57.9		
qACTIN_F	GGTAACATTGTGCTCAGTGGTG	57.9	201	1.75
qACTIN_R	CTCGGCCTTGGAGATCCACATC	65.4		
qpsbA_F	ATTGCTGCTCCTCCAGTAGAT	55.8	181	1.92
qpsbA_R	CATAAGGACCGCCGTTGTAT	57.8		
qpsbB_F	TTATTCCGAGCGGGTTCA	57.1	158	1.93
qpsbB_R	ATTCCGTCTCCGTCTACCAA	56.9		
qrpoB_F	GGCGTATTTGTCCCATTGA	56.4	102	1.99
qrpoB_R	GACTTTCTAACGACCCCCAA	56.7		
qclpP_F	ATTTGTGCGACCCGATGTA	56.8	161	1.92
qclpP_R	CTCCCGTTTGTGCCTCATA	56.6		
qnad2_F	GGAGGAGCAGTTGATTTAGC	54.2	118	1.98
qnad2_R	GCATAGTCATTCCAGGTCCA	55.4		
qcox1_F	TGGGTTGGCTTGGATTACT	55.2	79	1.99
qcox1_F	TGGGCAATAGTTAGGAGAGG	54.6		
qCOR15A_F	GTTGATCTACGCCGCTAAAG	55.6	113	2.07
qCOR15A_R	CACCATCTGCTAATGCCTCTT	57.1		
qRD29B_F	TGATGAGTATGACGAGCAAGAC	55.3	85	2.04
qRD29B_R	TTTACCCGTTACACCACCTC	55.0		
qKIN1_F	CCACATCTCTTCTCATCATCACT	55.8	100	2.03
qKIN1_R	AAGGCATTCTTGTTGGTCTCTG	58.7		
qCBF1_F	ATGTTTGGGATGCCGACTT	57.5	99	2.00
qCBF1_R	ATCTCCTTCGCCGTCATAAT	56.4		
qAPX2_F	AGATGTGTTTGGTCGGATGG	57.7	93	1.86
qAPX2_R	CCTGAACGCTCCTTGTGG	56.7		
qHSP17.4_F	GTTTCGGTTGCCAGAGAATG	57.9	100	1.86
qHSP17.4_R	CGGCTTACTCTCCTGAACTTT	55.9		
qHSFA2_F	TTCAGCAGTTTGCGGTTATG	57.3	77	2.09
qHSFA2_R	AGTAAGCCTCCGTTTCCTCC	57.7		
RD29B_F	TGATGAGTATGACGAGCAAGAC	55.3	85	2.04
RD29B_R	TTTACCCGTTACACCACCTC	55.0		
qFER1F	CTCTGTCTCCTAAGCCACTACT	52.7	126	1.86
qFER1R	TGTTGTTTGTGTCCACCGTAG	56.6		
qAPX1_F	TGACAAAGCACTATTGGACGA	56.6	73	1.98
qAPX1_R	AAAGGCATCTTCATCAGCAG	55.3		
qCAT2_F	ATTTCATGCACAGGGACGA	56.5	87	2.02
qCAT2_R	CAGGCGGAGTTGGATACTTC	57.2		
qBAP1F	CGAACAGGTTCTGGGCATG	59.3	137	1.89
qBAP1R	CCACACTTATCACCAAACTCATC	56.5		
qNOD_F	GCTGTTGGGGTTTGTTTTCT	56.8	94	2.13
qNOD_R	GTCGAAGTCGCATTTGTCAG	56.3		
qLTI30_F	GGTCACATCAAACTGGGACTA	55.7	97	1.93
qLTI30_F	AGTTGCTCTTTAATCTTTTCTGCT	58.3		
qERF6F	GTGGTTGAGAAAGTGCTAAAGAC	55.7	100	2.45
qERF6R	CCGTCAAATCCCAGTCATCTAT	58.3		
qPORA_F	GTTCGGTGTTTCACTTTCGG	57.9	74	1.92
qPORA_R	TCTGTTCCCTCTTGCATCTCA	57.9		
qPORB_F	CCACTACGATAGTTTTCTTCAGC	56.0	124	1.93
qPORB_R	AGCATTCAACTTCGCATCTTTG	59.9		
qPRPL11_F	TCATTCCTGTTGAAATCACTGTC	56.8	64	1.72
qPRPL11_R	GGCGGGGTCTTGAGAATAA	57.5		
qPRPL11_Fw	CGCTTGGTTCTAAGGGAGTT	56.4	105	1.80
qPRPL11_Rw	CGAAGACAGTGATTTCAACAGG	57.5		
qGFP_F	GAGGACCATCTCTTTCAAGGAC	57.0	163	2.01
qGFP_R	GTTGTGGGAGTTGTAGTTGTATTC	55.4		

[1]primer efficiency

2.4 Genomic PCR and High-fidelity PCR

For mutant genotyping, DNA was extracted from a small section of *Arabidopsis* leave tissue (5x5 mm) using DNAMITE, a DNA extraction kit (Microzone, UK) according to the

manufacturer's instructions. The DNA pellet was resuspended in 30 µL of sterile MQ water and1 µL was used for each PCR reaction. For all lines tested, genomic PCR (gPCR) analysis was performed with Biomix PCR Mastermix (Bioline, MA, USA), in a total reaction volume of 10 µL containing 2 µL of 2x PCR Mastermix with Taq polymerase and 0.5 µM of each primer. PCR reactions were carried out using a peqSTAR thermal cycler (Peqlab, USA) with the following cycling conditions: 95°C for 3 min, 30-38 cycles of 30 s at 95°C, 30 s at 58°C and 60 s at 72°C followed by 10 min at 72°C.

Phusion High-Fidelity DNA Polymerase (NEB, UK) was used for construction of overexpression plasmids. The gene of interest was amplified from 1 µL WT *Arabidopsis* cDNA, synthesized as described in section 2.5.2. The PCR reaction was carried out in a total volume of 25 µL according to manufacturer's specifications and contained: 5 µL of 5x Phusion GC Buffer, 0.5 µM of each primer, 200 µM of dNTPs and 1 unit of Phusion HF DNA Polymerase. For Gateway cloning, a 2-step High fidelity PCR reaction was performed. In the first step, a gene specific primer pair was used and the cycling conditions were as follows: 98°C for 3 min, 10 cycles of 30 s at 98°C, 30 s at 52°C and 30 s at 72°C followed by 21 cycles of 10 s at 98°C, 30 s at 70°C and 30 s at 72°C finishing with 10 min at 72°C. The second step was performed under the same reaction conditions, but using 5 µL of the previous reaction as a template, and 0.5 µM of each universal attB adapter primer. For gPCR and High fidelity PCR, the annealing temperature was set 2-3°C below the lowest primer T_m in a pair. Primer pairs used for different PCR reactions are shown in Table 2.3. PCR products were loaded on a 1% (w/v) agarose TAE (40 mM Tris, 20 mM acetic acid, 1 mM EDTA) gel, with 3 µL of Gel Red (Biotium, USA) or SYBR safe (Thermo Fisher Scientific, USA) for DNA detection. 3-5 µL of a 1kb DNA ladder, Gene Ruler PLUS (Thermo Fisher Scientific, USA), was used to estimate product size. Gels were run for 1 h at 110 volts using a Powerpac (Thermo Fisher Scientific, USA) in 1% TAE buffer and were visualized under UV light.

Table 2.3 List of primer pairs used for all PCR reactions, except qPCR (primers listed separately in Table 2.2)

Primer name	Primer sequence 5'-3'	Use
SALK_LBb1.3	ATTTTGCCGATTTCGGAAC	gPCR
SAIL_LB	GTGTACCAAACAACGCTTTACAGC	gPCR
GK_LB	CCCATTTGGACGTGAATGTAGACA	gPCR
GUN1-103_F	ATGTTTAGTAGCCACGCATGG	gPCR
GUN1-103_R	TTGATCGATGGGTACTCGAAG	gPCR
ABI4-2_F	TGAATGCCTTGGAGTGTTTTC	gPCR
ABI4-2_R	GTGTTGGAATTGTCCCATCTG	gPCR
abi4-102seq_F	GATTCCACCACCGACTCATC	sequencing
abi4-102seq_R	ACGGAGGAGGAAGAGGAAGA	sequencing
ATG5-1_F	ATTTGCTATTTGTTTGGCACG	gPCR
ATG5-1_R	TACCGTTCATGACAGAGGTCC	gPCR

rtATG5-1_F	ATTTGCTATTTGTTTGGCACG	RT-PCR
rtATG5-1_R	TACCGTTCATGACAGAGGTCC	RT-PCR
HSFA2_F	AAGGTTCCGAACCAAGAAAAC	gPCR
HSFA2_R	TCCTTCCACGTTACTTCAAGC	gPCR
cpHSc70-1_F	CAAGCTGTTGTTAATCCCGAG	gPCR
cpHSc70-1_R	GAAGCCAGATGCTTGTGAAAG	gPCR
rtcpHSc70-1_F	GGGCAGATTGCGAAGAGGCA	RT-PCR
rtcpHSc70-1_R	TCCCAGTCACCTTCCTCACGA	RT-PCR
CHIP-1_F	GGAAACTTGTGAGGCTGCTC	gPCR
CHIP-1_R	GCCACTGCCTCTTTGATAGC	gPCR
rtCHIP-1_F	CGGAGCGGTTAAAGGAAGACG	RT-PCR
rtCHIP-1_R	CCACTGCCTCTTTGATAGCCA	RT-PCR
PRPL11-3_F	TCCAACCAACGTTCTTGTAGG	gPCR
PRPL11-3_R	CGAAGACAGTGATTTCAACAGG	gPCR
rtPRPL11-3_F	CATCCCAACTCCAAACTCTCAC	RT-PCR
rtPRPL11-3_R	CAAGAATCGGAGGGTCAATGTC	RT-PCR
attB1	GGGGACAAGTTTGTACAAAAAAGCAGGCT	molecular cloning
attB2	GGG GAC CACTTTGTACAAGAAAGCTGGGT	molecular cloning
PRPL11_GWF	TTGTACAAAAAAGCAGGCTTCATGGCGTCTTCTTCTCTATC	molecular cloning
PRPL11_GWR1	TTGTACAAGAAAGCTGGGTGTTACAATAAAACTGCTTTCTTTTTG	molecular cloning
PRPL11_GWR2	TTGTACAAGAAAGCTGGGTGCAATAAAACTGCTTTCTTTTTG	molecular cloning
M13_F	TGTAAAACGACGGCCAGT	sequencing
M13_R	CAGGAAACAGCTATGAC	sequencing
35S_F	ACGCACAATCCCACTATCCTTC	gPCR
PRPL11_R	TTTTCCCGCCTCTAAAGCAA	gPCR

2.5 Gene cloning and transformation

The Gateway™ (Invitrogen, CA, USA) reaction strategy was employed to produce binary vectors for protein expression of PRPL11-GFP and PRPL11-TAP in *Arabidopsis* plants. For the entry vector construction, the coding sequence of *PRPL11* (Plastid Ribosomal Protein L11) was amplified from cDNA, as described in section 2.6, using High Fidelity DNA polymerase (NEB, UK). Primer pairs were designed to contain fragments of the universal attB adapter primer sequences prior to the start of the gene specific sequence (see Table 2.3). Primers for cloning the gene of interest into a vector with a C-terminal tag were designed without a stop codon. The correct size of the PCR fragment was confirmed by gel electrophoresis, and DNA was purified from the 1% agarose TAE gel using the QIAquick gel extraction kit (QIAgen, UK) exactly following manufacturer's instructions. The purified DNA fragment was cloned into the entry vector (pDonor207, Invitrogen, USA) using BP ClonaseII™ enzyme reaction mix (Invitrogen, USA) according to manufacturer's instructions: 50 fmol of PCR product and 150 ng of pDonor207 were combined with TE buffer, pH 8 (10 mM Tris, 1mM EDTA) and 2 µL enzyme mix in a 10 µL final reaction volume, centrifuged briefly and incubated overnight at 25°C. Proteinase K (1 µL) was added and the reaction mix incubated at 37°C for 10 min to terminate the reaction. 2 µL of reaction mix was added to 50 µL One Shot® DH5α chemically-competent *E. coli* cells, mixed gently and incubated on ice for 30 min. A heat shock was applied by immersing bacterial cells in

a water bath for 45 s at 42°C. Cells were transferred back to ice for 2 min, mixed with 250 µL SOC medium (0.5% (w/v) yeast extract, 2% (w/v) Tryptone, 10 mM NaCl, 2.5 mM KCl, 10 mM $MgCl_2$, 10 mM $MgSO_4$ and 20 mM glucose) and shaken at 37°C for 1 h. Cells were spread on fresh Lysogeny broth (LB) agar plates supplemented with 50 µg/mL kanamycin (Sigma Aldrich, UK) and incubated at 37°C overnight. Selected clones were cultured at 37°C in 5 mL LB broth with 50 µg/µL kanamycin overnight and plasmid DNA was extracted using a GeneJET Plasmid Miniprep Kit (Thermo Fisher Scientific, USA) following manufacturer's instructions. The correct DNA sequence of the insert was confirmed by sequencing plasmid DNA with M13 forward/reverse primers (Table 2.3).

The cloned *PRPL11* DNA fragment was further transferred to the 35S overexpression vectors ImpGWB (kindly provided by T. Nakagawa, Japan) with C-terminal GFP (pGWB505) and TAP (pGWB529) tags using LR ClonaseII™ enzyme mix (Invitrogen, USA). The LR reaction was conducted according to the manufacturer. Briefly, 100 ng of entry vector was mixed with 100 ng of destination vector and TE buffer (pH 8) to a final volume of 9 µL, 1 µL LR ClonaseII™ enzyme was added and the reaction mix incubated at 25°C overnight. The reaction was terminated by incubation for 10 min at 37°C, with 1 µL Proteinase K. 50 µL of DH5α chemically-competent *E. coli* cells were transformed with 1 µL of the LR reaction mix using the same heat shock conditions described above. Cells were spread on fresh LB agar plates containing 100 µg/mL spectinomycin (Sigma Aldrich, UK) and incubated overnight. Plasmid DNA from successful transformations was extracted using a GeneJET Plasmid Miniprep Kit (Thermo Fisher Scientific, USA) following manufacturer's instruction.

2.6 *Arabidopsis* transformation

Approximately 6-7 week-old *Arabidopsis* plants grown under standard 16/8 h photoperiodic conditions (100 µmol m^{-2} s^{-1}, 24/22°C) were used for transformation. First, 2 µL plasmid DNA was mixed gently with chemically-competent *Agrobacterium tumefaciens* strain GV3101 and flash-frozen in liquid nitrogen. Bacteria were then incubated at 37°C for 5 min, mixed with 1mL LB broth and incubated for an additional 2.5 h at 28°C with shaking at 200 rpm. Cells were collected by rapid centrifugation, re-suspended in 100 µL LB broth, plated on fresh LB agar with 30 µg/mL gentamycin, 100 µg/mL spectinomycin and 25 µg/mL rifampicin and incubated at 30°C for 3 d. Single colonies from each plate were dipped in 10 mL 2YT broth (1% (w/v) yeast extract, 1.6% (w/v) tryptone, 0.5 mM NaCl, pH 7.0) with 30 µg/mL gentamycin, 100 µg/mL spectinomycin and 25 µg/mL rifampicin and incubated at 30°C for an additional 2 d. Half of the bacterial culture was used for DNA extraction and the other half was used to inoculate 200

mL 2YT broth with 30 µg/mL gentamycin, 100 µg/mL spectinomycin and 25 µg/mL rifampicin. The culture was shaken for 16 h at 28°C at 200 rpm. Absorbance of the cell suspension was monitored at 600 nm and once absorbance was in the range 0.6-1.0, cells were harvested by centrifugation at 2,000 x *g* for 15 min and re-suspended in 400 mL sterile MQ water, with 5 % (w/v) sucrose and 144 µL Silwett L77 (van Meeuwen Chemicals, The Netherlands). The aerial part of the flowering *Arabidopsis* plants was dipped in the *Agrobacterium* suspension for 20 s with gentle agitation. Flower buds were separated and whole plants were wrapped in plastic transparent bags to increase humidity. Plants were returned to the growth room and left with the light turned off for 1 d. Seeds were collected when dry in the normal way.

2.7 Selection of *Arabidopsis* transformants

For the selection on hygromycin-resistant plants, seeds from transformed plants were sterilised as described in section 2.1, and plated on 1% (w/v) agar supplanted with 0.5 x MS salts, with 40 µg/mL hygromycin B (Thermo Fisher Scientific, USA). Plates were incubated for 3 days at 4°C, exposed to WLc (100±10 µmol m^{-2} s^{-1}, 22±1°C) for 6 h to induce germination and transferred to D for 4 d at 22°C. Plates were returned to WLc 24 h (22±1°C) to induce seedling greening. Positive transformants with long hypocotyls and a segregation ratio (long hypocotyl/short hypocotyl) of 75% were transferred to soil and left to grow under 16/8 h photoperiodic light (23/18°C) and self-fertilise. To increase seedling survival, pots were initially covered for 1 week with cling film to increase humidity. Seeds collected from T3 plants were plated on 1% (w/v) agar supplemented with 0.5 x MSand 40 µg/mL hygromycin and grown as described above. After 24 h WLc, lines showing 100% resistance (long hypocotyl phenotype) were selected for further analysis.

2.8 Protein extraction and immuno-blot analysis

Arabidopsis seedlings were grown on 1 % (w/v) agar plates containing 0.5 x MS for 2 d D and 3 d WLc (100 µmol m^{-2} s^{-1}, 22°C). 100 mg cotyledon tissue was extracted with 500 µL 2x Laemmli buffer (0.125 M Tris-HCl, pH 6.8, 4 % (w/v) SDS, 20 % (v/v) glycerol and 5 % (v/v) 2-mercaptoethanol) with (chemiluminescence detection) or without (fluorescence detection) bromophenol blue. The sample was denatured at 99°C for 5 min using a thermomixer (Eppendorf) and centrifuged for 5 min at 16,000 x *g* at 4°C.

Proteins were separated on 4 % stacking and 12 % resolving SDS-PAGE gels (with the exception of CHLH detection, when proteins were separated on an 8 % resolving gel) using standard Tris/Glycine running buffer (25 mM Tris, 192 mM glycine, 0.1 % (w/v) SDS, 150V for 60-

80 min). Proteins were blotted overnight at 4°C at 30 V, or for selected experiments for 1 h at 100 V, to a 0.22 µm nitrocellulose membrane from Licor (926-31092, UK), or 0.45 µm PVDF membrane from Immobilion (IPVH00010). A wet transfer system was used, with transfer buffer containing: 20 % (v/v) methanol, 25 mM Tris and 192 mM glycine. Blots were stained with Ponceau S solution (0.1 % (w/v/) Ponceau S in 5 % (v/v) acetic acid), washed briefly with TBS (50 mM Tris-Cl, pH 7.6; 150 mM NaCl), and blocked with 5% (w/v) powdered skimmed milk (Marvel) in TBS for 1 h at RT with agitation.

Blots were incubated in the primary antibody in 5 % (w/v) powdered milk in TBS-T (TBS + 0.1% Tween) for 1 h at RT or overnight at 4°C. Blots were rinsed, washed six times for 5 min in TBS-T at RT with agitation and incubated in a secondary antibody in 5 % (w/v) powdered milk in TBS-T for 45 min at RT (IgG HRP) or for up to 1 h at RT (IRDye800CW) with agitation. Details of all antibodies used in this work are summarised in Table 2.4. Blots were washed six times for 5 min in TBS-T at RT with agitation and three times for 2 min with TBS to remove residual Tween. For fluorescence detection, blots were excited at 700 nm and 800 nm, with scanning intensity 3 and 5, respectively, using an Odyssey infra-red blot scanner (Odyssey® Classic, Licor). For chemiluminescent detection of an HRP-conjugated secondary antibody, an ECL Western Blotting Substrate (Thermo Fisher Scientific, USA) was used according to the manufacturer's instructions. Exposure time was 2-5 min depending on the antibody used. Relative band density for blots was determined from scanned blots using Image J.

Table 2.4 Antibodies used in western blot analyses including antibody dilution and method of detection

Target protein	Source	Code	Host	Protein size	Dilution	Detection method
LHCA1	Agrisera	AS01 005	Rabbit	26 kDa	1:5000	Ch
LHCB1	Agrisera	AS01 004	Rabbit	28 kDa	1:5000	Ch
LHCB2	Agrisera	AS01 003	Rabbit	28 kDa	1:6000	Ch
PsaC	Agrisera	AS10 939	Rabbit	10-17 kDa	1:1000	Ch
PsbQ	Agrisera	AS06 142	Rabbit	16 kDa	1:2000	Ch
PsbR	Agrisera	AS05 059	Rabbit	10 kDa	1:5000	Ch
GluTR	Agrisera	AS10 689	Rabbit	58 kDa	1:5000	F
HO1	Agrisera	Sample	Rabbit	32.7 kDA	1:2000	F
CHLI	-	-	Rabbit	46 kDa	1:5000	F
CHLH	-	-	Rabbit	153 kDa	1:1000	F
PORA	Dr W.T. Griffiths	University of Bristol	Rabbit	43.8 kDa	1:5000	F
eGFP	Agrisera	AS13 2700	Rabbit	27 kDa	1:3000	F
TAP	Fisher	CAB1001	Rabbit	20 kDa	1:1000	F
IgG HRP	Sigma Aldrich	A9169	Goat anti rabbit	-	1:10000	-
IgG IRDye800CW	Licor	925-32213	Donkey anti rabbit	-	1:20000	-

Abbreviations: Ch, chemiluminescence; F, fluorescence

2.9 TAP-tag protein purification for pull-down analysis

Protein purification was performed following the protocol described in Geraca and Moazed (2015), with modifications. 3 g of 7 d old green cotyledon tissue from seedlings grown 2 d D + 5 d WLc was frozen in liquid nitrogen, ground on ice with a pre-cooled mortar and pestle to a fine powder and mixed with 10.5 mL lysis buffer [10 % (v/v) glycerol, 50 mM HEPES-KOH pH 7.5, 100 mM KCl, 2 mM EDTA, 0.1 % (v/v) NP-40, 10 mM NaF, 0.25 mM Na_3VO_4, 50 mM β-glycerolphosphate, 2 mM DTT and 1 x EDTA-free protease inhibitor cocktail (cOmplete, Roche, UK)]. Samples were transferred to 2 mL Eppendorf tubes and incubated on ice for 30 min with occasional vortexing and centrifuged for 5 min at 4°C at 12,000 x *g*. Supernatants were transferred to new Eppendorf tubes on ice, and pellets were re-extracted with a total volume of 3 mL of low turgor lysis buffer (50 mM HEPES-KOH pH 7.5, 100 mM KCl, 2 mM EDTA, 0.1 % (v/v) NP-40, 2 mM DTT and 1 x EDTA-free protease inhibitor cocktail). After additional 30 min incubation on ice, extracts were cleared by centrifugation for 5 min at 4°C at 12,000 x *g*, the glycerol concentration was adjusted to 5% of the final volume and supernatants from both extraction steps were combined. Total protein lysate was then centrifuged for 30 min at 100,000 x *g* at 4°C. 1 mL of a 50% (v/v) slurry of IgG-Sephaorse beads (500 µL of packed beads, GE Healthcare, UK) was equilibrated before incubation with the sample, by washing 3 times with a 5-bead volume of low turgor lysis buffer. Beads were centrifuged at 500 x *g*at 4°C between washes. Protein supernatants were combines with the washed beads in a 15 mL Falcon tube and left on a rotating platform overnight at 4°C. The sample was transferred to centrifuge columns (5 mL, Thermo Fisher Scientific, USA), and the settled beads were washed 5 times with 3 mL of washing buffer (10 mM HEPES-KOH pH 8.0, 150 mM NaCl, 0.1 % (v/v) NP-40). The target protein was eluted by TEV cleavage. Columns were washed twice with 1.5 mL TEV buffer (10 mM HEPES-KOH pH 8.0, 150 mM NaCl, 0.5 mM EDTA, 0.1 % (v/v) NP-40, and 1 mM DTT). 0.5 mL of TEV buffer with 50 U TEV enzyme (AcTEV Protease, Thermo Fisher Scientific, USA) was added to each column. Columns were incubated on a rotating platform overnight at 4°C. The TEV eluate sample was collected in 1.5 mL Eppendorf tubes by centrifugation at 500 x *g* for 2 min at 4°C. Columns were washed with additional 1 ml of TEV buffer and the $CaCl_2$ concentration in the sample was adjusted to a final concentration of 3 mM using 1M $CaCl_2$. The sample was mixed 1:1 with 2x calmodulin-binding buffer (CAM-B:20 mM HEPES-KOH pH 8.0, 300 mM NaCl, 2 mM Mg Acetate, 2 mM Imidazole, 0.2 % (v/v) NP-40, 4 mM CaCl2, 20 mM β-mercaptoethanol) in a 15 mL Falcon tube, and added to 1 ml of a 50% slurry of calmodulin Sepharose 4Bbeads (500 µL of packed beads, GE Healthcare) that had been equilibrated by washing 3 times in a 5-bead volume of 1 x CAM-B buffer with centrifugation at 500 x *g* between washes. The binding reaction was

carried out for 5 h at 4°C on a rotating platform. Beads were poured to a new column and washed 5 times with 3 mL of 1 x CAM-B buffer. Proteins were eluted from the column twice with 160 µL calmodulin-elution buffer (CAM-E: 50 mM ammonium bicarbonate pH 8.0, 10 mM EGTA) and once with 160 µL CAM-E with 25 mM EGTA.

2.10 Transcriptome data analysis

Microarray data for the meta-analysis were pre-processed using FlexArray version 1.6 (Genome Quebec), an open source, and Bioconductor, which is R based software. If available, the raw Affymetrix data files (CEL files) of microarray data were downloaded from public resources: Gene Expression Omnibus and Array Express (https://www.ncbi.nlm.nih.gov/geo/). The RMA algorithm was applied to normalize array intensities from all experiments analysed. Only transcripts that had a detection call of 'present' (P, with detection p-value ≤ 0.06; assessed by the Affymetrix detection call algorithm) in at least two biological replicates in WT under the control conditions were chosen for further comparison between different arrays. A log fold-change cut-off of 1 was used to identify genes differentially regulated, either by the selected treatment or mutation. Details of all microarray experiments chosen for different analyses in this study are presented in Table 2.5. For the FR array analysis, the enrichment of known GO terms was performed for the selected cohort of genes using the ATCOECIS resource (http://bioinformatics.psb.ugent.be/ATCOECIS/). Only terms with a fold enrichment >1.5 and p-value <0.05 were considered to be significant. WT *Arabidopsis* NF and FR pre-treatment-regulated transcriptomes, as well as the *flu*-dependent transcriptome, were categorized into different functional classes using Classification Super Viewer Tool (bar.utoronto.ca), with MapMan incorporation as a classification source. Values were normalised to the frequency of the gene group on the Arabidopsis ATH1 microarray chip. Cellular localization of selected cohorts of genes was assessed using TAIR GO annotation. To create profiles for tetrapyrrole biosynthesis gene expression under different abiotic stresses the *Arabidopsis* eFP Browser (bar.utoronto.ca) was used, using an array experiment performed on young seedlings (Zeller et al., 2009).

Table 2.5 Summary of microarray experiments used in this study including description of experimental procedure.

Experiment	Material	Platform	Rep[1]	Norm	Data[2]	Ref[3]
Abiotic stresses						
Drought	96 h growth on PEG-infused media; seedlings, 7 d	ATH1	3	RMA	GSE35258	A
Salt	4d growth on 100mM NaCl plates; seedlings, 10 d	Arab4	2	-	GSE40940	B
Heat	20 min or 1h of heat at 40°C, seedlings, 11 d	ATH1	3	RMA	E-MEXP-2760	C
Cold	1 h, 24 h or 7 days at 4°C, seedlings, 10 d	ATH1	2	RMA	GSE5534	-
NF/Lin retrograde signalling						
NF (in huse data)	growth on 5 µM NF supplemented media; seedlings, 5 d	ATHI	2	RMA	GSE5726	D
NF - Aluru	spraying with 5 µM NF for 7d; rosette, 3 weeks	ATH1	3	MAS5	paper *[3]	E
NF - Woodson	growth on 5 µM NF supplemented media; seedlings, 2 d	ATH1	3	RMA	paper *	F
Lin - Woodson	growth on 0.5 mM Lin supplemented media; seedlings, 2 d	ATH2	3	RMA	paper *	F
Singlet oxygen related						
FR pre-treatment	1d D+ 2 d FR + 1 d WLc; seedlings, 4 d	ATH1	2	RMA	GSE6169	G
flu - op den Camp	2 h after dark to WL shift (*flu* versus WT); rosette, 4 weeks	ATHI	1	RMA	GSE10812	H
flu -Woodson	120 min after WL exposure; *flu* versus wild type, seedlings 4 d	ATHI	2	RMA	GSE10812	I
fc2-1	120 min after WL exposure; f*c2-1* versus wild type, seedlings 4 d	ATH1	2	RMA	GSE71764	I
cas	*cas* versus wild type, seedlings 2 week	Arab4	2	LOESS	paper *	J
ß-CC	4 h 50 µl ß-CC; rosette, 4 weeks	CATMAv5	3	LOESS	paper *	K

[1]Abbreviations: Rep, replicates; Norm, method used for normalisation; ATH1, GeneChip® Arabidopsis ATH1 Genome Array (Affymetrix); CATMA, Complete Arabidopsis Transcriptome MicroArray; Arab4, Arabidopsisv4 2 colour microarray (Agilent Technologies); NF, norflurazon; Lin, lincomycin; FR, far red; *flu*, fluorescent in blue light, *fc2-1*, ferrochelatase 2; *cas*, calcium sensing receptor; β-CC, β-cyclocitral.

[2]reference number for series accession numbers in GEO or Array Express database used to download CEL files.
*indicates there were no raw CEL files available for the selected experiment and data processed by the researcher were used. If possible cross-platform comparison was avoided.

[3]tested array experiments were published in: A- Bhaskara et al., 2012; B-Wang et al., 2013; C-Suzuki et al., 2011, D-Moulin et al., 2008; E- Aluru et al., 2009; F-Woodons et al., 2013; G- Page et al., 2017a; H- op den Camp, 2003, I-Woodson et al., 2015; J- Nomura et al., 2012; K-Ramel et al., 2012;

Chapter 3 Retrograde regulation of photosynthetic gene expression

3.1 Introduction

It was clearly demonstrated that treatments causing chloroplast disruption result in the loss of nuclear gene expression (Sullivan and Gray 1999; Gray et al., 2003). The establishment of a ferrochelatase 1 overexpressor (*gun6-1D*) as having a *gun* phenotype on NF (Woodson et al., 2011), combined with the evidence that Mg-proto does not function as a retrograde signal (Moulin et al., 2008; Mochizuki et al., 2008), both strongly support a role for heme derived from FC1 as a retrograde signal. However, results on plastid retrograde signalling that have emerged from different laboratories within the past few years present inconsistent, and to some extent, conflicting findings.

Until quite recently most models for plastid retrograde signalling assumed the existence of the single negative signal derived from damaged chloroplasts. More recently, a new model for plastid retrograde signalling has been proposed, whereby heme or its products function as a positive signal that promotes photosynthetic gene expression during plastid development in optimal growth conditions (Woodson et al., 2011; Terry and Smith, 2013). Once chloroplast development is blocked, this positive signal is lost. This can be accompanied by the over-accumulation of chlorophyll intermediates that, due to their photosensitizing activity, are expected to result in reactive oxygen species production under white light conditions (Vinti et al., 2000; Woodson et al., 2011). A burst of $^1O_2$ can potentially serve as a source of a secondary inhibitory signal (Terry and Smith, 2013; Page et al., 2017a). Changes in both of these signals could account for the repression of photosynthetic gene expression after chloroplast damage. The hypothesized model appears to be simple and testable. However, relatively little independent support for these models has been published to date. First, the severity of treatments used to block plastid signalling makes results complicated to interpret. Furthermore, the environmental impact on plastid biogenesis can have a subtle effect. Consequently, it has not yet been demonstrated how relevant this model would be in young seedlings with developing chloroplasts that are responding to natural environmental variations including diverse abiotic stresses.

Our current knowledge on retrograde signalling comes not only from chemical treatments and the subsequent mutant screen for *gun* mutants, but also from other genetic mutations that affect different processes in chloroplast development. These include inhibition of protein import in the *ppi* mutant (Kakizaki et al., 2009), reduced chloroplast transcription in *sig* mutants (Woodson et al., 2013), or a block in chloroplast translation in *prps1* (Tadini et al., 2016). Although, often described as an example of separate retrograde signalling pathways, they might

potentially be integrated into one, tetrapyrrole-dependent signalling pathway. An important example comes from the sigma factor proteins (SIG) that control the function of the plastid-encoded RNA polymerase. Mutation in two of them, *sig2-2* and *sig6-1*, results in a seedling pale green phenotype and a strong perturbation of the tetrapyrrole pathway including reduced levels of $tRNA^{Glu}$, ALA-synthesis capacity and lower heme content (Woodson et al., 2013). As a consequence, nuclear gene expression is reduced. The report that overexpression of *SIG2* or *SIG6* results in a *gun*-phenotype on herbicide NF-treated seedlings, as well as the observation that introduction of the *gun5* or *gun1* mutations into a *sig2* background can rescue heme levels and nuclear gene expression in the *sig2* mutant (Woodson et al., 2013), is also supportive of a role for heme as a positive retrograde signal.

So far there is no information in the literature on how FC1 activity can regulate photosynthetic gene expression in plants at the mechanistic level, but it has been proposed that this regulation can be direct through heme or its products or possibly involve different heme binding proteins and transcription factors. The recently discovered chloroplast envelope-bound plant homeodomain (PHD) transcription factor (PTM) might be a strong candidate for transduction of plastid retrograde signals to the nucleus (Sun et al., 2011). Once exposed to conditions triggering photooxidative changes, PTM is proposed to undergo proteolytic cleavage. This releases its N-terminal domain, which can relocate to the nucleus and regulate gene expression. Both single and double *gun1* and *ptm* mutants were shown to rescue expression of nuclear-encoded photosynthetic genes to a similar level when plastid development was impaired by NF or Lin treatments (Sun et al., 2011), suggesting that PTM operates in the same pathway as GUN1. Moreover, after migration to the nucleus PTM has been reported to regulate *ABI4* gene expression by direct binding to its promoter (Sun et al., 2011). This is a potentially important result as it was previously proposed that ABI4 acts as a cytosolic negative regulator, downstream of GUN1, competing with light-induced transcription factors for specific DNA-binding sites in target nuclear gene promoters (Koussevitzky et al., 2007). Since the first report of Koussevitzky et al. (2007) describing the *abi4-102* mutant as having a *gun* mutant phenotype, ABI4 has been strongly implicated in retrograde signalling. Further investigations by other groups using different mutant alleles in the *ABI4* gene (Sun et al., 2011; Guo et al., 2016) also defined them as *gun* mutants on NF and Lin, although the level of rescue of PhANG expression compared to known *gun* mutants differed from study to study. Interestingly, Giraud et al., (2009) reported that ABI4 controls *AOX1a* accumulation when mitochondrial performance is blocked, suggesting ABI4 might be an important integrator of plastid and mitochondrial signalling.

In the current study a genetic and a pharmacological approach was undertaken to extend our understanding of mechanisms regulating tetrapyrrole-dependent retrograde signalling, with the focus on testing the hypothesis that heme or its products act positively in regulation of photosynthetic gene expression during chloroplast biogenesis. Additionally, various mutants previously shown to exhibit a *gun*-like phenotype will be examined under different sets of standardised conditions that block photosynthetic gene expression to determine their effect on the promotive plastid retrograde signalling pathway.

3.2 Results

3.2.1 Expression profiles of the *HEMA1* and *LHCB2.1* genes on NF after transfer to WL

To gain a better understanding of the association between *gun* signalling and the regulation of nuclear gene expression during chloroplast development, the expression of the *LHCB2.1* and *HEMA1* genes was investigated after different lengths of continuous WL (WLc) exposure and in the presence or absence of 1µM norflurazon (NF). *LHCB2.1* and *HEMA1* were selected as they represent genes fundamental for chloroplast biogenesis during de-etiolation and are well established control marker genes for plastid retrograde signalling (McCormac and Terry, 2004). Investigating gene expression after different times of WL exposure should provide information on the response to different degrees of plastid damage. The expression of *LHCB2.1* and *HEMA1* was examined in wild type and two *gun* mutants, *gun1-1* and *gun5-1*, after 2 days growth in darkness and after transfer to WLc for 1 up to 3 days (Figure 3.1).

Expression of both *LHCB2.1* and *HEMA1* is known to be light-regulated (McCormac et al., 2001), and as expected under the control conditions used in this study expression of the two nuclear encoded genes increased strongly within 1 day after transfer to WLc. However, while *LHCB2.1* expression reached a plateau after this time, *HEMA1* expression declined over the next 2 days of WLc (Figure 3.1). In addition, light induction of *LHCB2.1* and *HEMA1* was altered by GUN1, and partially by GUN5. At all analysed time points after WLc exposure, *HEMA1* was more strongly up-regulated in both *gun* mutants while *LHCB2.1* was repressed in *gun1-1* mutant as compared to wild type. This result is in agreement with the strong link between light and retrograde signalling in regulation of the chloroplast development (Ruckle et al., 2007). Light-induction of *LHCB2.1* and *HEMA1* genes was inhibited on NF early, and could be detected within 1 day after WLc exposure in wild type, relative to control conditions. It was not enhanced further with increased time of WLc exposure, presumably due to the high concentration of NF used in the

experiment. Interestingly, *HEMA1* repression on NF in wild type was observed only for the first 2 days of WLc exposure and had recovered back to control level by day 3 (Figure 3.1). The necessity to maintain a higher expression of some tetrapyrrole-related genes under conditions that block plastid development is not surprising, since *HEMA1* encodes glutamyl-tRNA reductase, the rate limiting step in tetrapyrrole synthesis, and is still required for cellular heme synthesis.

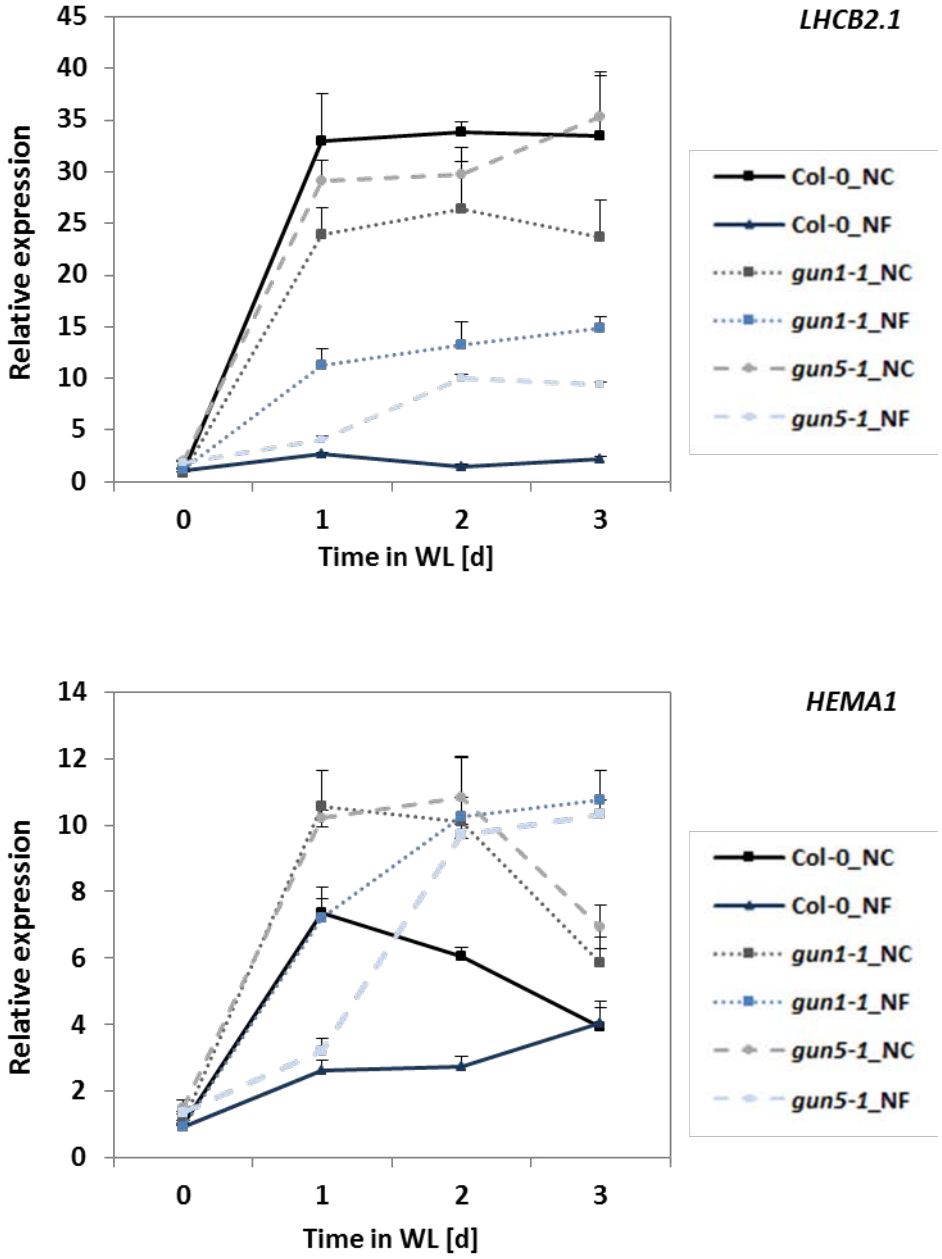

Figure 3.1 Time course of *HEMA1* and *LHCB2.1* gene expression in Col-0, *gun1-1* and *gun5-1* mutants grown on norflurazon (NF). Seedlings grown on 1% agar with ½ MS medium supplemented with (NF) or without (NC) 1 µM NF and without sucrose, under the following conditions: 2 d dark followed by a transfer to WLc (100 µmol m^{-2} s^{-1}) for 1, 2 and 3 d. Gene expression was measured by quantitative RT-PCR analysis relative to 2 d dark-grown WT (Col-0; Col-0_NC) and normalised to *YELLOW LEAF SPECIFIC GENE 8* (*YLS8,* At5g08290*)*. Data shown are means +SEM of three independent biological replicates.

Under the NF-treatment conditions tested in this experiment both *gun5-1* and *gun1-1* mutants displayed a clear and strong *gun* phenotype, but their ability to rescue gene expression on NF differed depending on the time of growth in WLc. The *gun1-1* mutant was less affected by a NF-induced block of plastid signalling compared to *gun5-1*, which was most clearly seen after 1 d of WLc exposure (Figure 3.1). Such a strong phenotype of *gun1-1* observed relatively early after a block of plastid development reveals its dominant role in retrograde signalling. A positive correlation between length of WLc exposure and strength of the gene expression rescue was observed in both *gun* mutants tested. After 3 d WLc on NF both *gun* mutants had reached a stable, higher level of *LHCB2.1* and *HEMA1* expression relative to the wild type and mutant response at earlier time points. For *HEMA1*, the expression on NF-treated *gun1-1* and *gun5-1* was even higher than in mutant seedlings grown under the control conditions (Figure 3.1). Since the degree of *gun* mutant rescue was most pronounced after 3 d WLc, this time point was chosen for future experiments as it would permit the detection of weaker *gun* phenotypes that might be masked at early time points.

3.2.2 Verification of the *gun* phenotype in the *gun6-1D* mutant

To test the robustness of the *gun* phenotype of the *gun6-1D* mutant, its ability to rescue gene expression on NF was examined using the growth conditions chosen in the previous experiment. In addition to 3 d WLc exposure, gene expression was also assessed after 4 d WLc growth to ascertain whether the *gun* phenotype is stronger at this time point. As a positive control the *gun5-1* mutant was included (Figure 3.2). After 2 d D and 3 d WLc both *gun5-1* and *gun6-1D* mutants were able to significantly rescue *HEMA1* and *GUN4* expression from the inhibitory effect of NF relative to Col-0 confirming that *gun6-1D* shows a *gun* mutant phenotype. Longer exposure to WLc did not enhance the ability of *gun5-1* or *gun6-1D* to rescue gene expression on NF. On the contrary, *gun6-1D* did not show a significant *gun* phenotype after 4 d WLc (Figure 3.2A).

Many experiments using NF treatments in the literature have been performed in the presence of sucrose, thus its potential impact on the promotion of the *gun* phenotype was examined. Expression of *HEMA1* and *GUN4* was investigated by qPCR following the previous protocol with 2 d germination in the D and 4 d of WLc growth, with an additional supplementation with 1% sucrose (Figure 3.2B). A strong inhibition of gene expression on NF was observed in the presence of sucrose and this was rescued by both *gun5-1* and *gun6-1D* to a greater extent than seen in the absence of sucrose (Figure 3.2A and B). Indeed, in contrast to the experiment without sucrose (Figure 3.2A), both *gun* mutants tested displayed a statistically significant rescue of *HEMA1* and *GUN4* expression after treatment with NF and sucrose at 4 d WLc. Independent of

sucrose, *gun5-1* had a stronger phenotype on NF compared to *gun6-1D*, with an almost complete rescue of *HEMA1* expression. Although, these results are in agreement with the latest hypothesis for the regulatory role of heme in retrograde signalling, the moderate *gun*-phenotype of *gun6-1D* suggests mechanisms other than FC1-dependent heme synthesis can potentially contribute to the control of plastid-to-nucleus retrograde signalling.

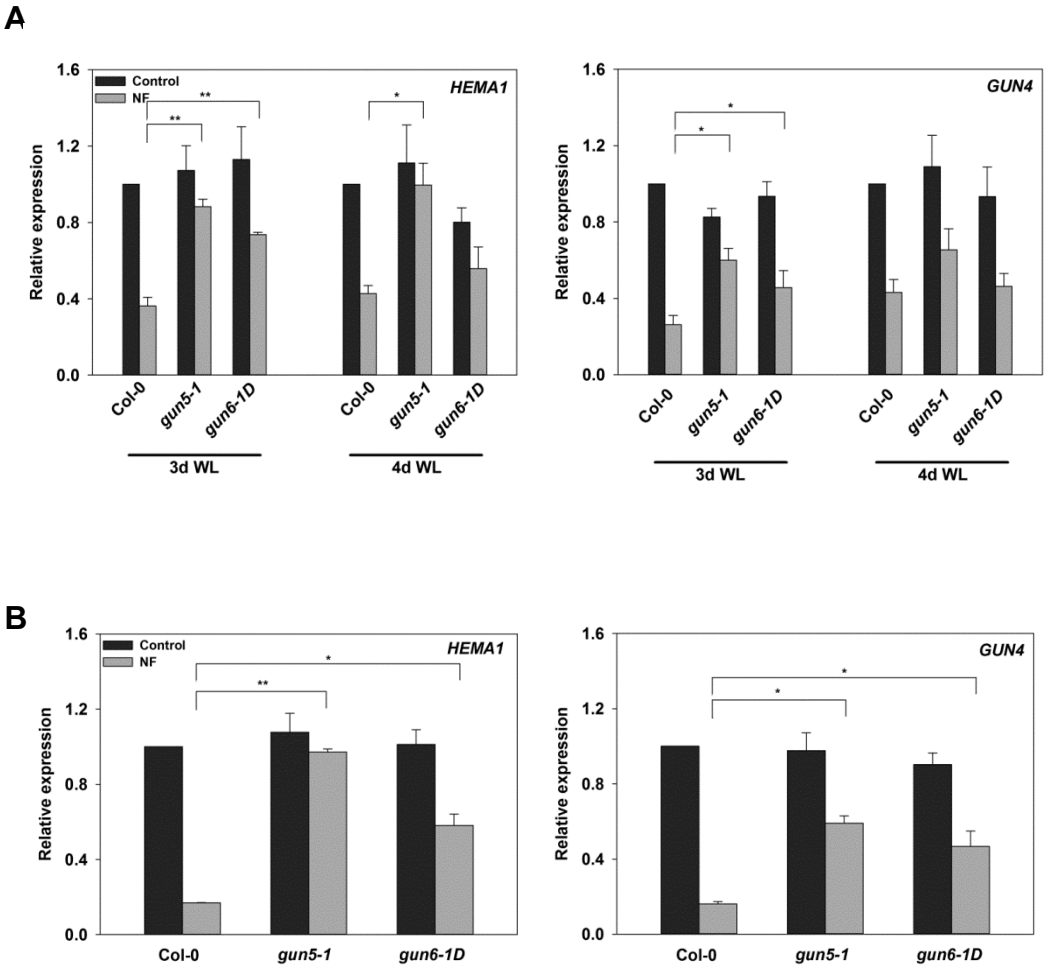

Figure 3.2 Expression of *HEMA1* and *GUN4* in *gun6-D1* after norflurazon (NF) treatment. WT (Col-0), *gun5-1* and *gun6-D1* seedlings were grown on 1% agar supplemented with½ MS in the presence or absence of 1 µM NF and without (A) or with (B) 1% sucrose under the following conditions: 2 d D, followed by 3 d and 4 d WLc (A) or 2 d D and 4 d WLc (B). Gene expression was measured by quantitative RT-PCR analysis relative to Col-0 grown without NF and normalised to *ACTIN DEPOLYMERIZING FACTOR 2* (*ADF2,* At3g46000*)*. Data shown are means +SEM of three biological replicates. Asterisks denote significant difference vs Col-0 for the same treatment (control or NF), Student's *t* test (* $p < 0.05$, ** $p < 0.01$).

3.2.3 The effect of altering tetrapyrrole synthesis on retrograde signalling

The chemical NF treatments employed to study retrograde signalling (Koussevitzky et al., 2007; Moulin et al., 2008) are sometimes criticized because of the difficulty in distinguishing

between primary effects on signalling and secondary effects on chloroplast function. To test further the role of FC1-derived heme or its products as a retrograde signal, a set of mutants and overexpressor lines for different genes in the tetrapyrrole pathway that are predicted to reduce heme levels were screened for their phenotypes on low NF conditions. These included mutants in the two ferrochelatase genes, *fc1-1* and *fc2-1* as well as a *GUN4* overexpressing line that promotes Mg-chelatase synthesis and may have reduced flux through the heme branch of the pathway (Stephenson, 2009). In contrast to *gun6-1D,* genotypes with reduced heme levels are hypothesized to exhibit a hypersensitive phenotype for the repression of photosynthetic gene expression on NF. Additionally, any differences should be more pronounced under less severe NF conditions. To test this, seedlings were grown for 2 days in the dark and 3 days in WLc on medium supplemented with low NF concentration (50 nM) under the standard light intensity. As shown in Figure 3.3, under these conditions wild type showed a moderate repression of photosynthetic gene expression for *LHCB2.1* and *GUN4,* with the small effect on *CHLH* expression, and a slight up-regulation of *HEMA1*.

The expression of all four genes was significantly higher in *gun1-1* seedlings on NF in comparison to wild type indicating that conditions applied were effective in blocking retrograde signalling. However, both *fc1-1* and the *GUN4* overexpressor line had a wild-type phenotype on NF for all analysed genes. Interestingly, the *fc2-1*mutant displayed a weak *gun* phenotype on low NF and maintained a higher expression level of *GUN4*, *HEMA1* and *CHLH*, but not *LHCB2.1* in comparison to wild type, similarly to *gun1-1*. All the lines tested, can potentially accumulate elevated levels of porphyrins that can lead to an additional photooxidative stress. Thus, the expression of *BAP1*, a gene specific to singlet oxygen stress, was also monitored (see Chapter 4 for further information on this response) Figure 3.3 shows that NF treatment resulted in more than 4-fold up regulation of the *BAP1* expression in wild type, which indicated induction of singlet oxygen stress under the conditions tested. However, there was no clear correlation between elevated *BAP1* and sensitivity to repression of photosynthetic gene on NF. All lines tested had a similar level of *BAP1* induction as the wild type after 5 days of NF treatment.

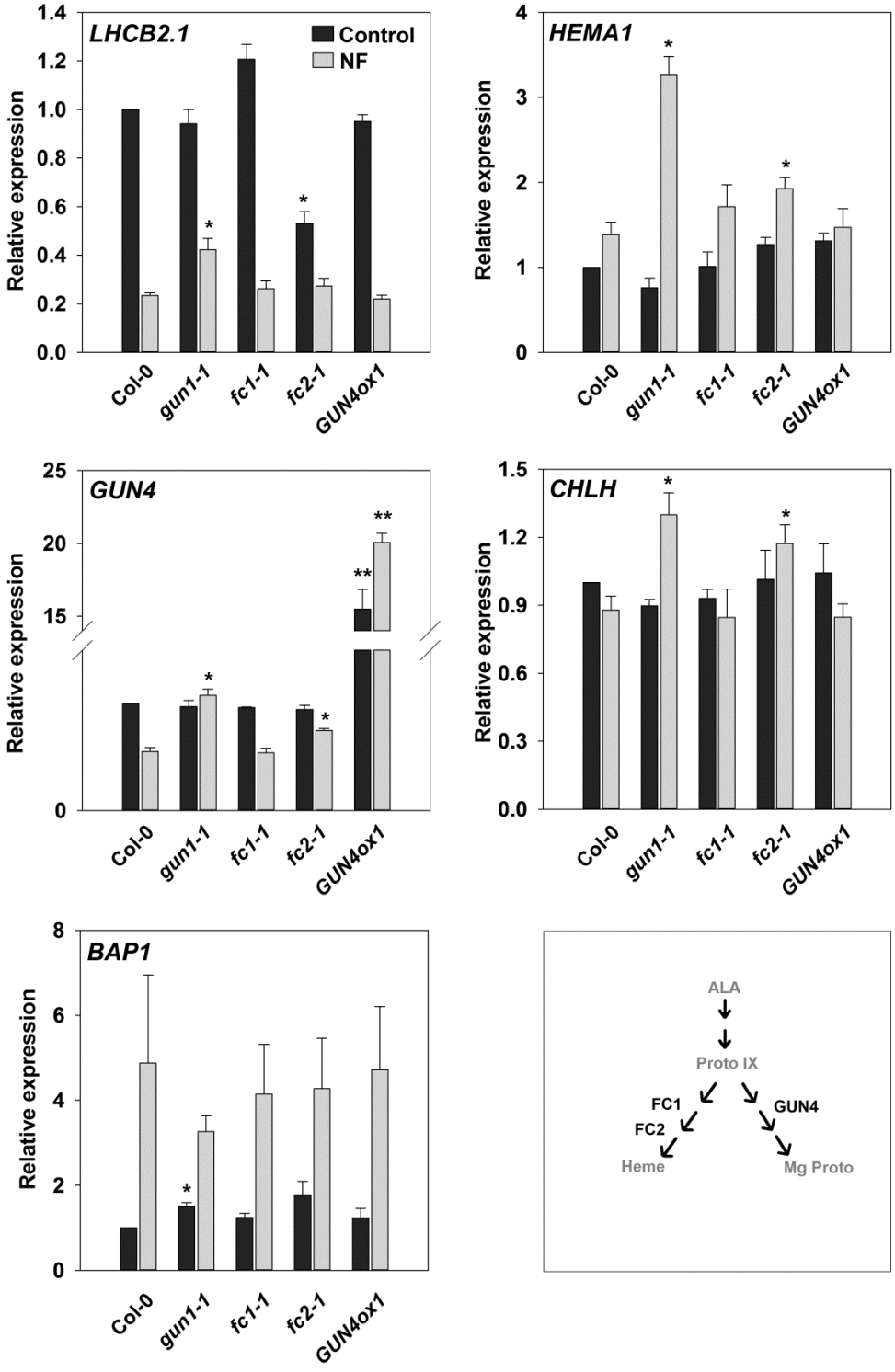

Figure 3.3 Expression of selected nuclear genes in genotypes that are predicted to alter heme synthesis under low norflurazon (NF) conditions. WT (Col-0), *fc1-1, fc2-1* and two *GUN4* overexpressor lines were grown on 1% agar with ½ MS and 1% sucrose, in the presence or absence of 50 nM NF under the following conditions: 2 d in dark, followed by 3 d WLc growth. The *gun1-1* mutant was included as positive control (known to rescue gene expression on NF). Gene expression was normalised relative to Col-0 grown without NF and relative to *YELLOW LEAF SPECIFIC GENE 8* (*YLS8*, At5g08290). Data shown are means +SEM of three biological replicates. Asterisks denote significant difference vs Col-0 for the same treatment (control or NF), Student's *t* test (*p <0.05, **p < 0.01).

3.2.4 The effect of heme synthesis inhibition on nuclear gene expression

In order to test the role of heme in promoting photosynthetic gene expression, the effect of treating seedlings with the chemical compound 2,2'-dipyridyl (DP) that directly blocks heme synthesis was examined. DP chelates Fe^{2+} and blocks ferrochelatase activity (Duggan and Gassman, 1974). If FC1-dependent heme synthesis is required to promote nuclear gene expression, we would expect to see an inhibition of gene expression after DP treatment.

A new experimental system was developed in which 2 days dark and 3 days WLc grown seedlings were immersed in water supplemented with 1 mM DP for 1-24 h under standard light conditions. Figure 3.4 shows that exposing wild type seedlings to a short DP treatment resulted in a strong repression of nuclear-encoded, photosynthesis-related and tetrapyrrole biosynthesis genes. Moreover, significant transcriptional changes were detected rapidly, within the first 2 h after immersion, with the strongest effect on *HEMA1* repression (more than 4-fold down regulated). A clear and strong repression (more than 2-fold down-regulated) of *GUN4*, *FC2* and *LHCB2.1* was detected after6 h incubation with DP. This trend was enhanced with prolonged time of DP treatment, with 24 h incubation resulting in an extremely strong down-regulation of gene expression. Based on these results, a 6 h time point was chosen for further analyses, as possibly representing early consequences of disrupted plastid retrograde signalling. In contrast to the other genes analysed, *FC1* was induced by DP treatment, with immersion in DP for 6-24 h resulting in a moderate, 2- to 3-fold up-regulation of *FC1* (Figure 3.4). Interestingly, this is similar to the observed increase in *FC1* expression when *Arabidopsis* seedlings were grown on NF (Figure 3.13; Moulin et al., 2008). Collectively, these results demonstrate that DP treatment results in a similar effect on the expression of photosynthesis-related and tetrapyrrole-related genes as a NF treatment suggesting that DP may also block plastid retrograde signalling. It is also worth noting that *GST* gene expression (a marker gene for general oxidative responses) was induced by DP treatment indicating that DP also results in a perturbation of redox homeostasis that could potentially affect the expression of these photosynthesis- and tetrapyrrole-related genes.

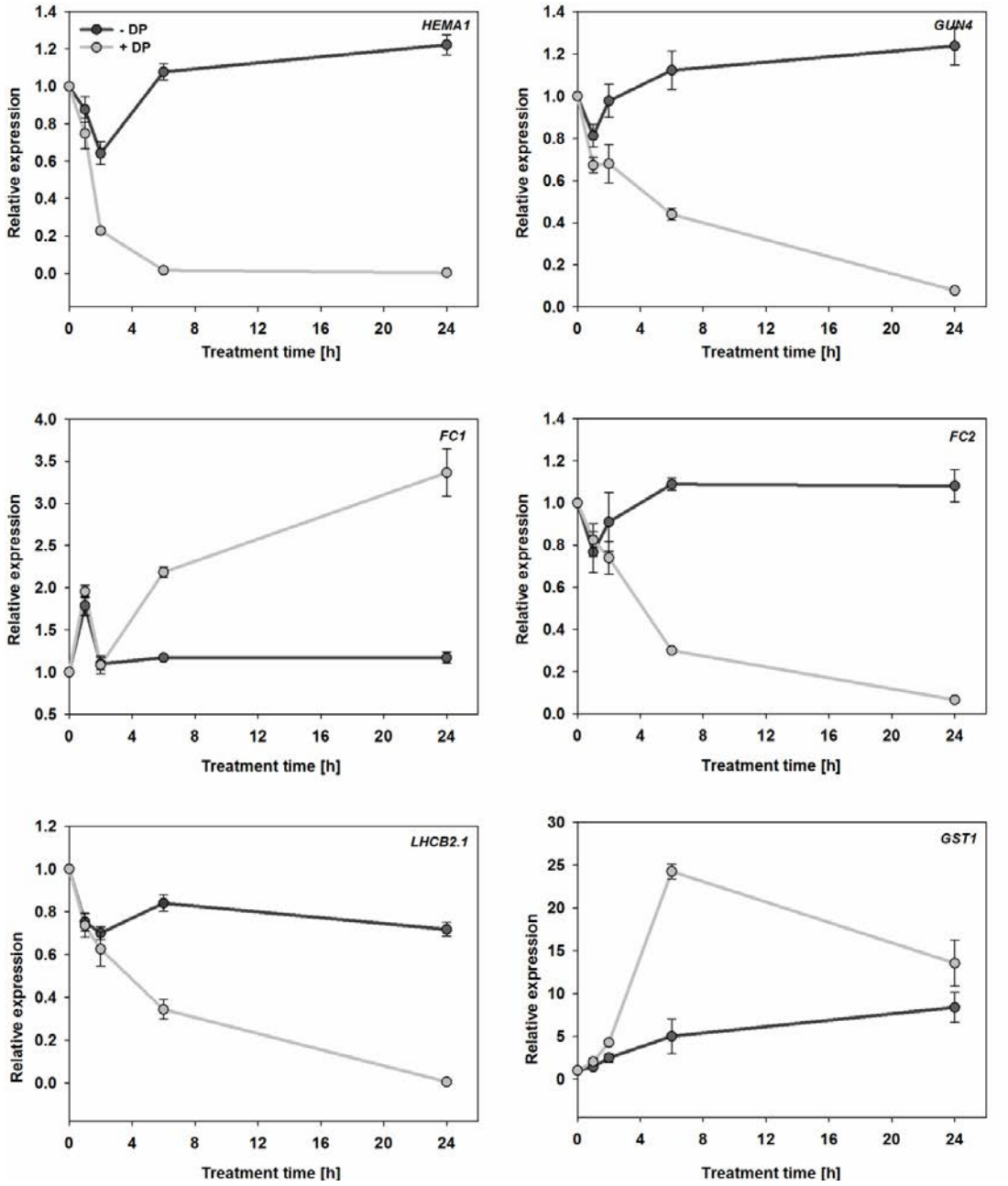

Figure 3.4 Time course for the effect of 2,2'-Dipyridyl (DP) on nuclear gene expression. WT (Col-0) seedlings were grown on 1% agar medium with ½ MS, under the following conditions: 2 d dark growth and 3 d standard WLc (100 µmol m^{-2} s^{-1}). For the last 1, 2, 6 and 24 h of WLc growth, seedlings were immersed in water with or without 1 mM 2,2'-Dipyridyl. Control plants were immersed in water with ethanol. Gene expression was normalized relative to 5 d old seedlings growing on a plate and relative to *YELLOW LEAF SPECIFIC GENE 8* (*YLS8,* At5g08290). Data shown are means ±SEM of three independent biological replicates.

The initial experiment with DP was performed under WL and might result in photo-oxidative damage. DP also inhibits the Mg-proto IX monomethyl ester cyclase reaction (Duggan and Gassman, 1974) and it is possible that repression of nuclear gene expression resulted from the production of $^1O_2$ in WL. To avoid this possibility, the analysis was repeated to compare the effect of DP treatment administered in darkness or WL. Wild type seedlings grown 2 days in the dark and 3 days in WLc were immersed in different DP concentrations for 6 h, in the dark or WL and expression of photosynthesis- and tetrapyrrole-related genes measured. As shown in Figure 3.5 the profiles were very similar between seedlings immersed in DP under these two conditions, supporting the conclusion that DP-induced transcriptional changes were due to the alteration in heme synthesis. This was consistent for all analysed DP concentrations and for most analysed genes. Only for *HEMA1,* and to some extent *GUN4*, was repression reduced less in the dark compared to the light, and this was true over a wide range of DP concentrations (0.1 to 1 mM). However, it should be noted that even in darkness, *HEMA1* was still strongly down-regulated (more than a 7–fold repression).

Treatment for 6 h with a DP concentration as low as 0.01-0.02 mM was sufficient to significantly down-regulate the expression of most analysed photosynthesis and tetrapyrrole genes to at least 2-fold, irrespective of the light conditions, with little further effect on gene expression seen at 1 mM (Figure 3.5). However, the potential influence of additional oxidative perturbation in down-regulation of tetrapyrrole and photosynthetic gene expression cannot be completely excluded, as *GST1* expression was still induced in seedlings treated with DP in the dark (Figure 3.5).

The input of light signalling is important for observation of retrograde signalling during chloroplast development (Larkin and Ruckle, 2008). In order to separate light signalling from other effects of light, such as on photo-oxidative stress, the experiment was repeated using dark-grown wild type seedlings and seedlings lacking the light-signalling PIF proteins (*pifQ* mutant) and thus showing constitutive induction of chloroplast development in the dark including an elevation of tetrapyrrole transcripts (Stephenson et al., 2009; Leivar et al., 2009). 4 d-old dark grown Col-0 and *pifQ* seedlings were treated with DP for 6 h with a concentration range of 0.05-1 mM (Figure 3.6). The qPCR analysis of gene expression confirmed that there was an up-regulation of *HEMA1*, *GUN4* and *LHCB2.1* in *pifQ* of between 2.5-10–fold compared to wild type. However, no induction of *FC1* and *FC2* transcripts was detected in dark-grown *pifQ* seedlings.

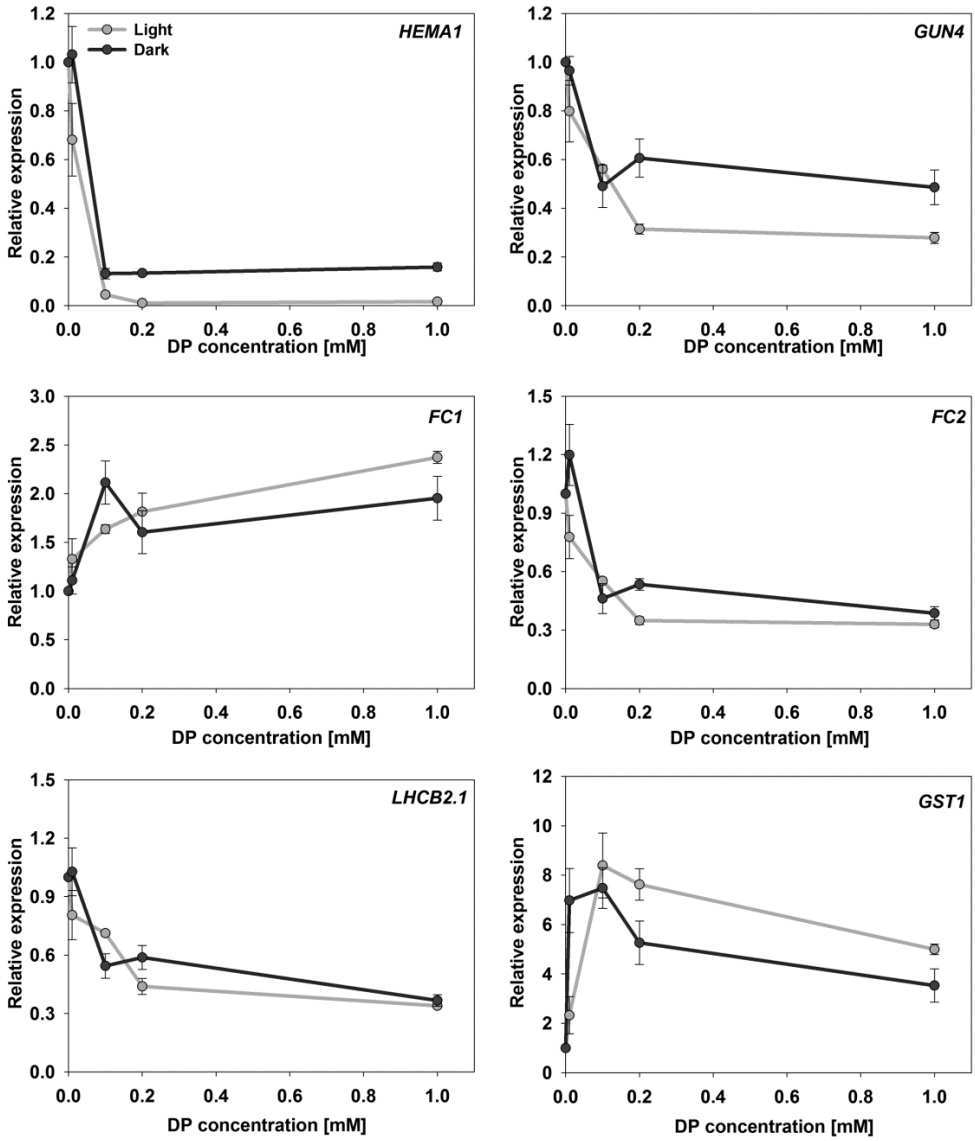

Figure 3.5 Expression analyses of selected photosynthetic, tetrapyrrole and stress-responsive genes in seedlings treated with 2,2'-Dipyridyl (DP) in the dark or light. WT (Col-0) seedlings were grown on 1% agar with ½ MS for 2 d in the dark and 3 d WLc (100 µmol m^{-2} s^{-1}). For the last 6 h of WLc growth seedlings were transferred to water supplemented with different DP concentrations (0.01, 0.1, 0.2 and 1 mM) or with 0.17% ethanol (mock). Seedlings were left in darkens or under the constant white light for 6 h. Expression is relative to mock treated Col-0 in dark or light and normalised to *YELLOW LEAF SPECIFIC GENE 8* (*YLS8*, At5g08290). Data shown are means ± SEM of three independent biological replicates.

Treatment of the *pifQ* mutant with 0.1 and1 mM DP in darkness strongly reduced elevated *HEMA1*, *GUN4* and *LHCB2.1* expression. In contrast to WLc grown wild type seedlings, no significant down-regulation (*GUN4*, *LHCB2.1*) or very moderate repression (1.5-2 - fold for *HEMA1*, *FC2*) of gene expression was observed in 4d dark grown wild type treated with DP, even upon high 1 mM concentration (Figure 3.5, Figure 3.6). In addition, there was very little increase of *GST1* or *FC1* expression under these conditions. This result is consistent with the necessity for light induction of photosynthetic and tetrapyrrole genes to see the repressive effects of disturbed tetrapyrrole metabolism and with the hypothesis that heme synthesis is required for this positive retrograde signal.

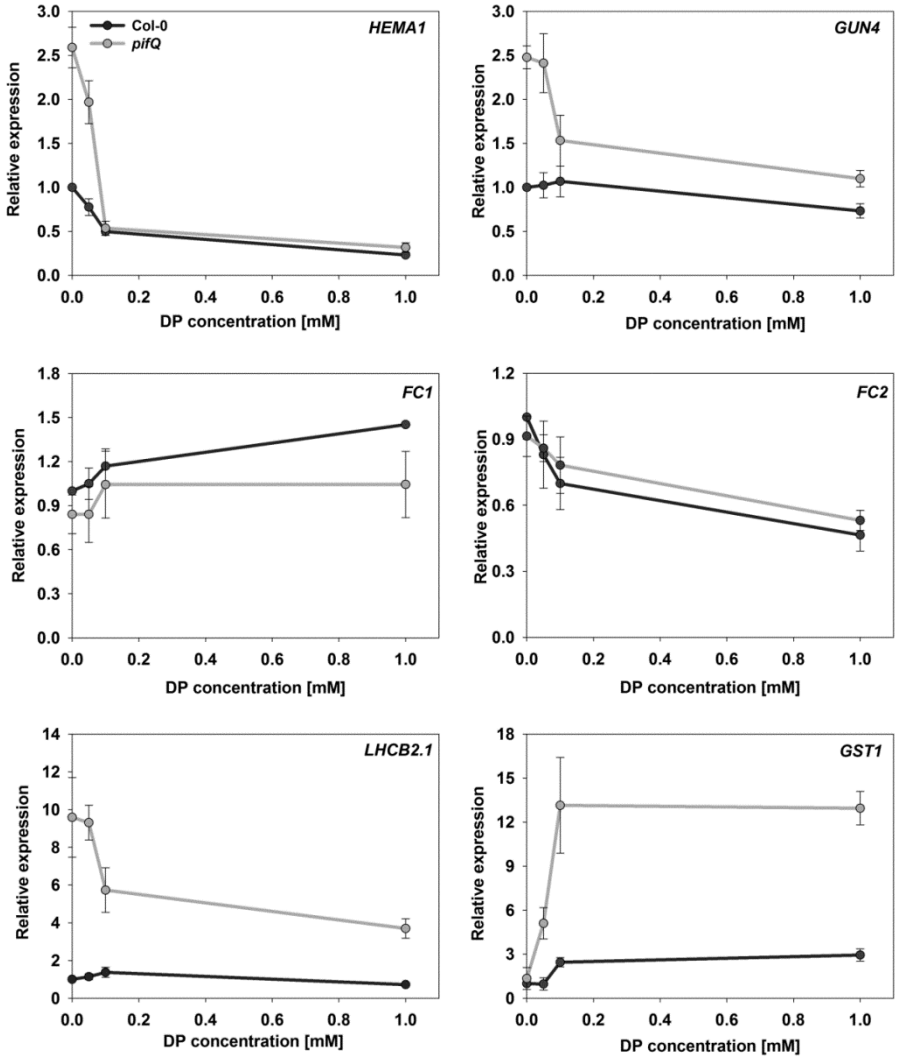

Figure 3.6 Expression analyses of selected photosynthetic, tetrapyrrole and stress responsive genes in dark-grown *pifQ* mutant seedlings treated with 2,2'-Dipyridyl. WT (Col-0) and *pifQ* seedlings were grown on 1% agar with½ MS for 4 d in the dark. For the last 6 h of growth in darkness seedlings were transferred to water supplemented with different DP concentrations (0.05, 0.1 and 1 mM) or with 0.17% ethanol (mock). Seedlings were left in dark in optimal conditions for 6 h. Expression is relative to mock treated Col-0 in dark and normalised to *YELLOW LEAF SPECIFIC GENE 8* (*YLS8*, At5g08290). Data shown are means ± SEM of three independent biological replicates.

3.2.5 The role of the sigma factors SIG2 and SIG6 in tetrapyrrole synthesis and retrograde signalling

Another class of mutants that have been implicated in altering tetrapyrrole synthesis and retrograde signalling are the *sig* mutants, *sig2* and *sig6* (Woodson et al., 2013). It has been shown previously that overexpression of *SIG2* and *SIG6* results in a *gun* phenotype, and that *sig2-2,* but not *sig6-1*, accumulated significantly less heme. The explanation for this is that these sigma factors are required the synthesis of the $tRNA^{Glu}$, glutamyl tRNA reductase substrate (Woodson et al., 2013). In order to examine if lower heme levels in *sig2-2* can contribute to the enhanced repression of photosynthetic gene expression after block of plastid signalling, *sig2-2*, along with *sig6-1* and two *gun* mutant controls *gun1-1* and *gun5-1* were grown for 2 days in dark and 3 days in WLc on low NF concentration as described in Figure 3.3. The same as in previous experiment treatment with low NF concentration resulted in a moderate repression of *LHCB2.1* and *GUN4* and almost 2-fold induction of *HEMA1* in wild type (Figure 3.7B) supporting that the plastid signalling was affected by the treatment. Surprisingly, both *sig* mutants had an elevated *HEMA1* expression (4-fold up to 6-fold induction) under the control conditions relative to the wild type plants. This phenotype was not further affected by the NF treatment (Figure 3.7B). Moreover, *sig2-2* and *sig6-1* rescued significantly *LHCB2.1* and *GUN4* expression on low NF to the level as strong (*GUN4*), or stronger (*LHCB2.1*) to control *gun* mutants: *gun1-1* and *gun5-1*.

Although both sets of mutants rescued from the inhibitory response on low NF, they were characterised by a different phenotype (Figure 3.7A). Similarly to wild type, *gun1-1* and *gun5-1* were mostly albino with only a few seedlings turning green, when grown under the low NF condition. On the contrary, *sig2-2* and *sig6-1* retained ability to turn green on NF, with *sig6-1* having a stronger phenotype. To summarize, reduced total heme levels in *sig2-2* do not contribute to the more severe responsiveness to block of plastid signalling. The phenotype of *sig2-2* and *sig6-1* on low NF suggest that increased flux through the tetrapyrrole pathway (indicated by an elevated *HEMA1* expression) is the reason for the rescue of photosynthetic gene repression. This result is still supportive for the important regulatory role of FC1 in retrograde signalling.

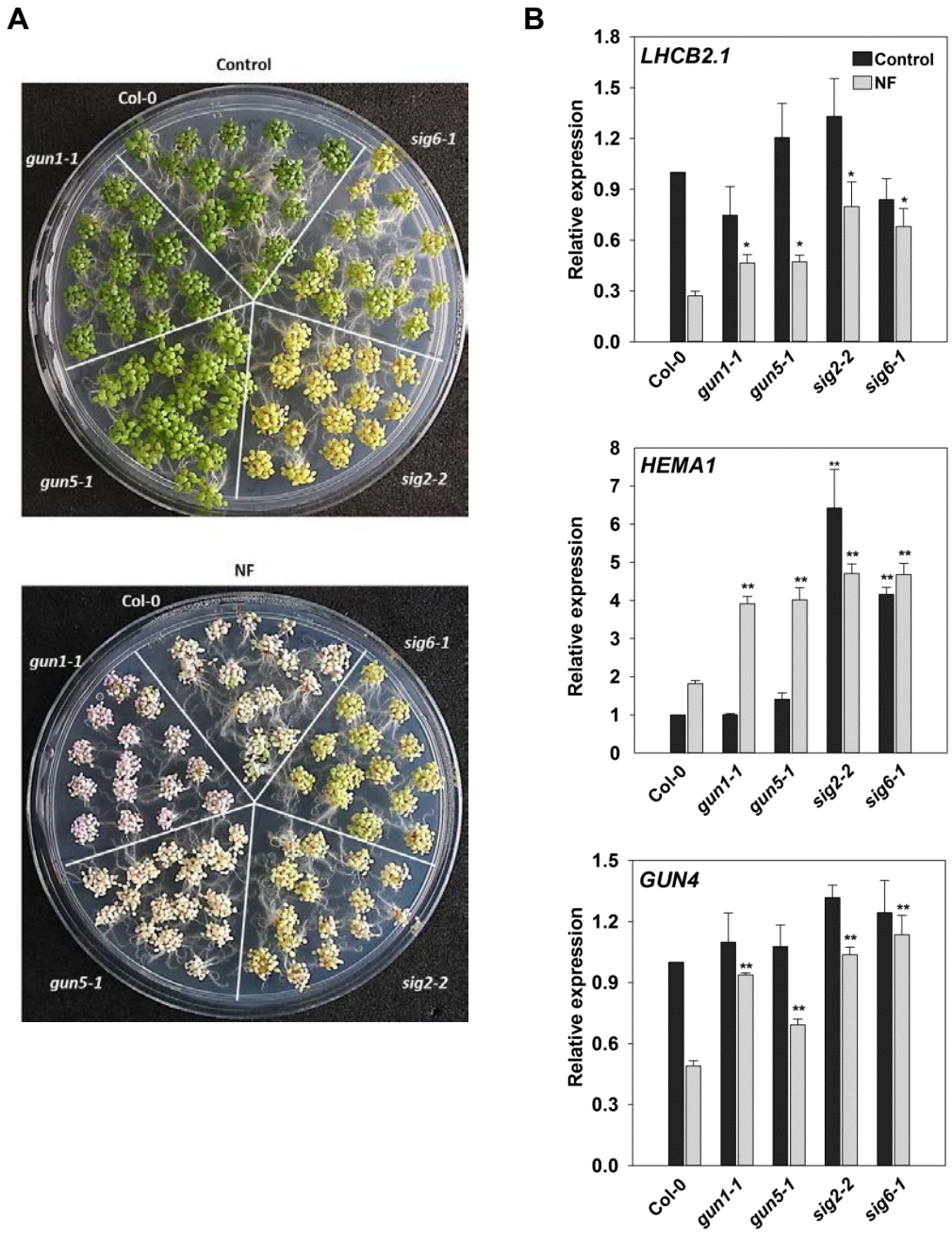

Figure 3.7 Analyses of *sig2-2* and *sig6-1* phenotype under the low NF conditions. WT (Col-0) *gun1-1*, *gun5-1*, *sig2-2* and *sig6-1* seedlings were grown on 1% agar with ½ MS supplemented with 1% sucrose and, in the presence or absence of 50 nM NF, under the following conditions: 2 d in dark followed by 3 d WLc growth. (A) Seedlings phenotype under the control and NF conditions (B) qPCR analyses of selected nuclear-encoded genes. All data were normalised relative to Col-0 grown without NF (control) and relative to *YELLOW LEAF SPECIFIC GENE 8* (*YLS8*, At5g08290). Data shown are means +SEM of three biological replicates. Asterisks denote significant difference vs Col-0 for the same treatment (control or NF), Student's *t* test (*p < 0.05, **p < 0.01).

To analyse the physiological role of SIG2 and SIG6 in the distribution of the tetrapyrrole pathway metabolites and to possibly explain mutant phenotype on NF observed in Figure 3.7, a series of feeding experiments with the precursor of tetrapyrrole synthesis, 5-aminolevulinic acid (ALA), were performed. Both *sig2-1* and *sig6-1* have been implicated with the regulation of plant light responses, and *sig2-2* has been characterised before as having a long hypocotyl phenotype under the FR (Oh and Montgomery, 2013). To confirm that it is due to chromophore deficiency, hypocotyl length measurements for the dark and FR grown seedlings were performed, with additional feeding with 0.1mM ALA that should increase tetrapyrrole synthesis and therefore flux through the heme branch. The *sig6-1* mutant was used as an additional control. In agreement with the previous finding, the hypocotyl length of *sig2-2* under the FR was 2-fold higher than in wild type. Surprisingly, the hypocotyl length of *sig6-1* was also higher than in FR grown control (1.5-fold; Figure 3.8A and B). Supplementation of both mutants with ALA was able to rescue the hypocotyl response to FR consistent with the mutant phenotype was due to chromophore deficiency. Under these conditions two mutants had only slightly longer hypocotyls than wild type (Figure 3.8B). In contrast to the effect on hypocotyl length ALA feeding was unable to fully rescue Pchlide levels in *sig2-2* and *sig6-1* although the amount of Pchlide in the mutants did increase. This suggests that the two mutants must be defective also in later steps of chlorophyll biosynthesis branch of the tetrapyrrole pathway. Feeding *sig2-2* and *sig6-1* mutants with ALA in darkness resulted in a 3-5-fold increase in protochlorophyllide levels, but this was still less than in wild type (Figure 3.8C). The difference between wild type and two *sig* mutants was even more pronounced under the FR conditions, when after ALA supplementation, Pchlide levels in the mutants were almost half that of wild type.

The effect of FR on the hypocotyl length of *sig6-1* was different to that observed by Oh and Montgomery (2013). The original experiment performed by this group was in presence of 1% sucrose in the growth media thus its potential impact on the long hypocotyl phenotype of *sig6-1* was investigated. Sucrose supplementation inhibited the response to FR, as observed by a general increase in hypocotyl length in the FR-grown wild type and other mutants (i.e. an almost 2-fold increase in wild type on sucrose relative to without sucrose; Figure 3.9). Nevertheless, the longer hypocotyl phenotype of *sig2-2* and *sig6-1* mutants in FR relative to wild type was still clearly observed (Figure 3.9). Sucrose cannot account for this difference between the results here and Oh and Montgomery (2013).

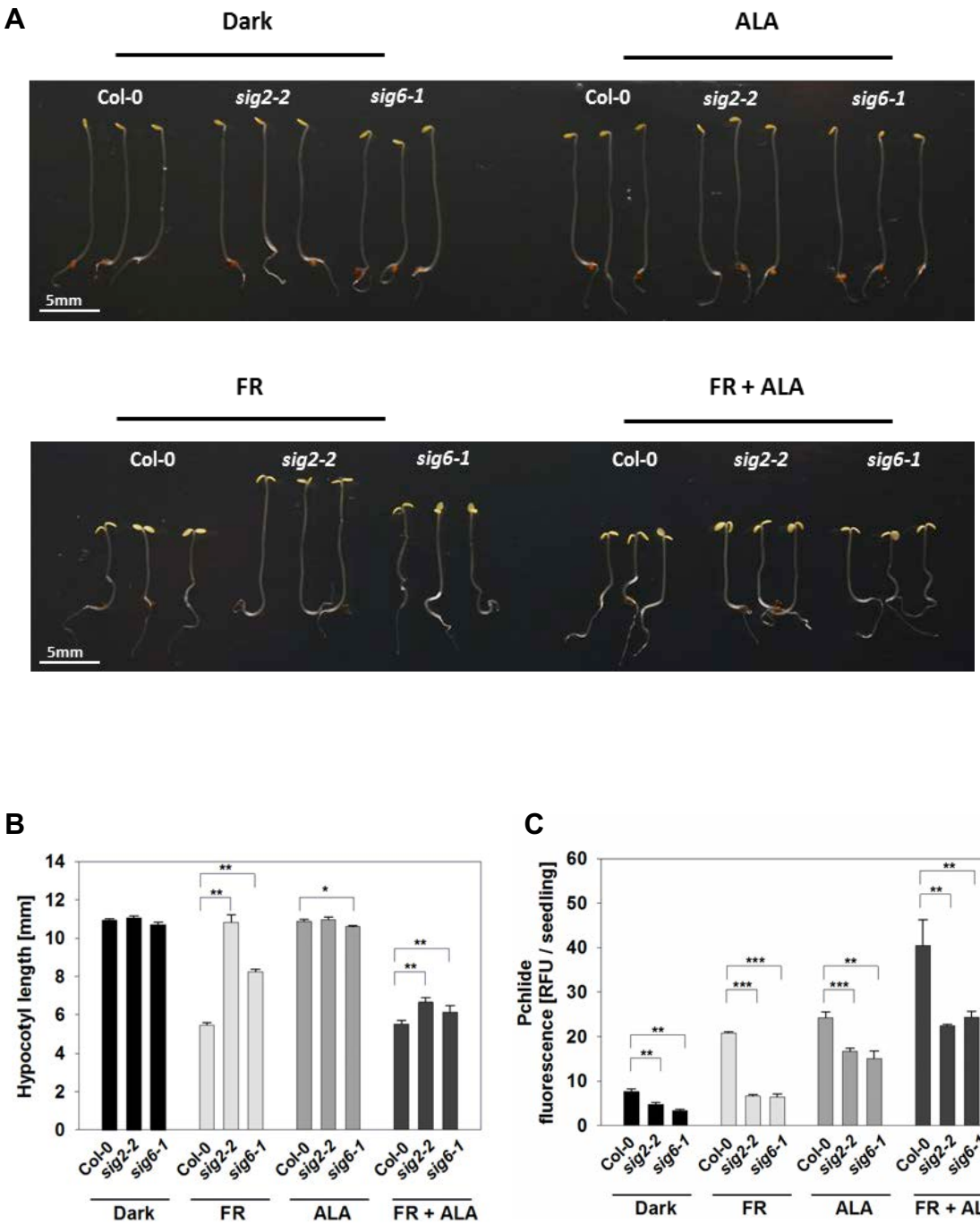

Figure 3.8 Both*sig2-2* and *sig6-1* are affected in FR sensing. Seedlings were grown on ½ MS medium supplemented with 5 mM MES, with 1% agar (pH 5.6) and with or without 0.1 mM ALA, without sucrose, at 22°C for 4 d in dark (Dark and ALA) or 2 d in dark followed by 2 d FR exposure (FR and FR + ALA). (A) The phenotype of seedlings grown under dark and FR conditions ± ALA. Scale bar indicate 5 mm. (B) Hypocotyl length. 20 seedlings were analysed for each replicate. (C) Pchlide measurements. 30 seedlings were harvested for each biological replicate. All experiments were performed in 3 independent biological replicates. Data shown are means + SD. Asterisks denote a significant difference vs. Col-0 for the same treatment (Dark, FR, ALA or FR + ALA), Tukey HSD test for hypocotyl length analysis (*$p < 0.05$, **$p < 0.01$), Student's *t*-test for Pchlide measurements (*$p < 0.05$, **$p < 0.01$, ***$p < 0.001$).

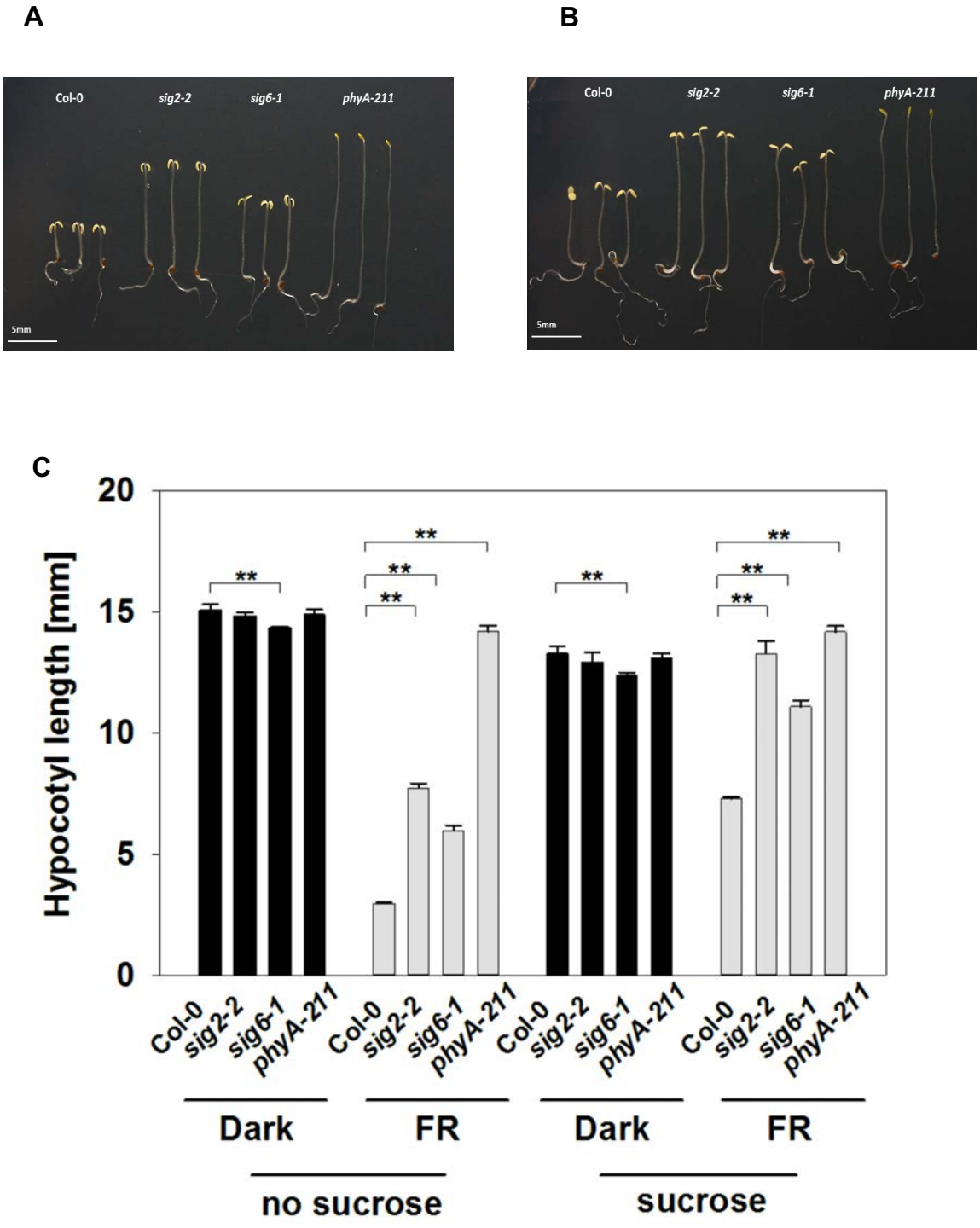

Figure 3.9 The effect of sucrose on the response of *sig2-2* and *sig6-1* to FR light. Hypocotyl length was assessed in seedlings grown on 1% agar with½ MS supplemented without (A) or with (B) sucrose, at 22°C for 1 d in dark and 4 d in FR. (A) The phenotype of seedlings grown under the FR with or without sucrose. Scale bar indicate 5 mm. (B) For hypocotyl measurements 20 seedlings were analysed for each replicate. All experiments were performed in 3 independent biological replicates. Data shown are means + SD. Asterisks denote a significant difference vs. Col-0 for the same treatment (Dark or FR, + or - sucrose), Tukey HSD test (*$p < 0.05$, **$p < 0.01$).

3.2.6 Regulation of the tetrapyrrole biosynthesis pathway by GUN1

GUN1 has been strongly implicated in the control of transduction of different plastid retrograde signals and is frequently referred to as an integrator of these different retrograde signals (Koussevitzky et al., 2007). However, it has been proposed that it could function as a repressor of tetrapyrrole synthesis such that *gun1* mutants promote or protect a heme-related signal (Terry and Smith 2013). This hypothesis is supported by the recent observation that GUN1 has the ability to bind to selected tetrapyrrole pathway proteins (Tadini et al., 2016). To test this hypothesis, the interaction between GUN1 and tetrapyrrole metabolism was investigated.

Firstly, a new allele of *gun1* mutant was isolated from the SAIL T-DNA collection. The homozygous line (SAIL_742_A11) was selected by PCR screening, with primer pairs binding specifically to the *GUN1* gene and to the T-DNA insert as indicated in Figures 3.10A and 3.10C. The RT-PCR reaction confirmed that no *GUN1* transcript could be detected in a selected homozygous line (Figure 3.10D). Sequencing showed the insertion of the T-DNA in the second exon of the *GUN1* gene. This line has been reported before by Sun et al. (2011), but they did not give it an allele number, naming it only as *gun1.* Therefore, were named it here as *gun1-103* (see also Page et al., 2017b). The two *GUN1* overexpressor lines used in this study were a gift from Prof. Dario Leister (LMU) and have been described previously (Tadini et al., 2016; see Figure 3.13 for confirmation of elevated *GUN1* gene expression in these lines).

Pchlide accumulation after feeding with ALA in the dark and ALA synthesis rate under the WLc conditions were determined in the *gun1* mutants and GUN1 overexpressor lines to test whether GUN1 affects tetrapyrrole metabolism. Previously, *gun1* mutants were shown to have a very moderate increase in Pchlide in dark-grown seedlings and similar results were observed here (Figure 3.11A insert). Under these conditions one of the GUN1ox lines showed a reduction of Pchlide. When mutant and transgenic seedlings were fed ALA all lines accumulated more Pchlide as expected but the degree of accumulation varied considerably. Under conditions where the flux through tetrapyrrole pathway was increased by feeding with a high concentration of the ALA (0.2 mM) both *gun1* mutant alleles accumulated statistically significantly more protochlorophyllide (p-values 0.003 and 0.024) and both *GUN1* overexpressor lines had significantly less protochlorophyllide than the WT (p-value 0.003 and 0.044; Figure 3.11A). This indicates that GUN1 represses the accumulation of Pchlide.

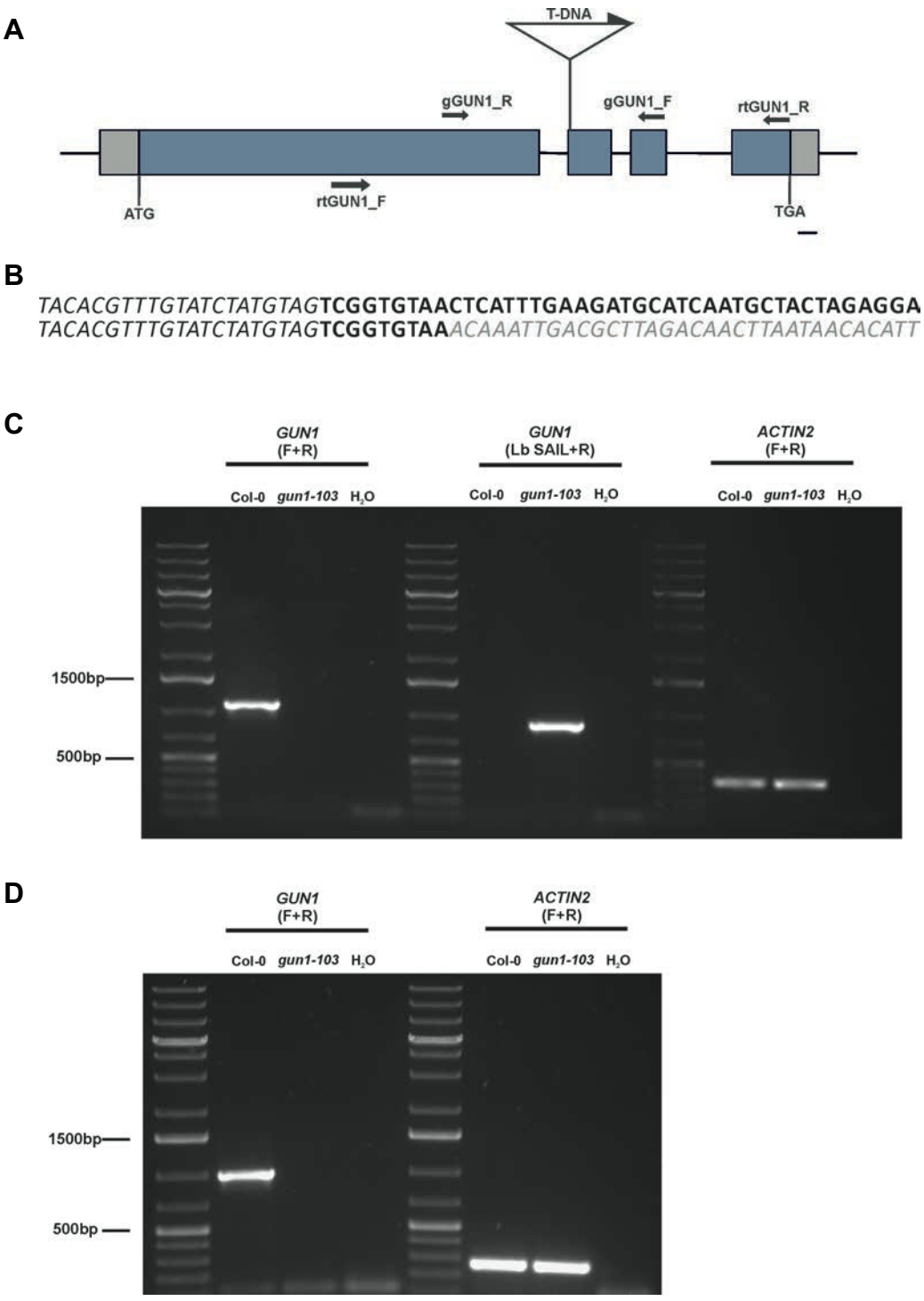

Figure 3.10 Analysis of the T-DNA insertion allele *gun1-103*. (A) Schematic diagram depicting the *gun1-103* T-DNA insertion site at the *GUN1* gene. Blue boxes represent exons, grey boxes represent UTR regions, and black lines represent introns. PCR and RT-PCR primers used for genotyping are indicated by black arrows (B) Sequence analysis of the T-DNA insertion in *gun1-103* mutant. T-DNA insert fragment is marked in grey italics, the intron in black italics and the exon in black bold letters. (C) Confirmation of the T-DNA insertion by PCR amplification. Genomic DNA from Col-0 and *gun1-103* plants was amplified using gene specific primers (gGUN1_F + gGUN1_R) and a left border specific primer (Lb SAIL + gGUN1_R). (D) RT-PCR analysis of the disrupted *GUN1* gene in *gun1-103* using primers binding to the first and fourth exon. *ACTIN2* transcripts were used as a control (C and D).

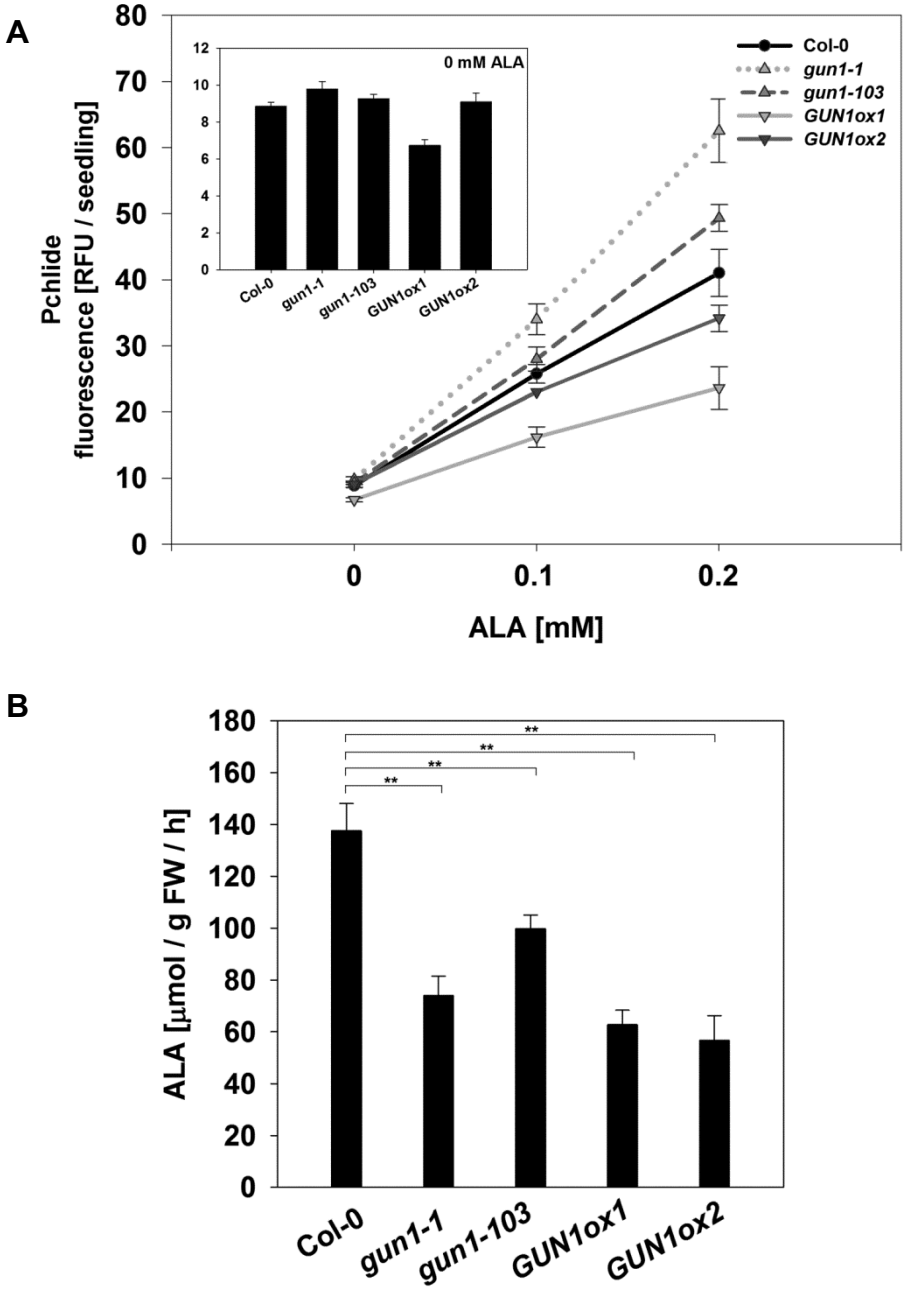

Figure 3.11 Analysis of tetrapyrrole metabolism in *gun1* mutants and GUN1 overexpressor lines. (A) Pchlide accumulation in *gun1-1*, *gun1-103*, *GUN1ox1* and *GUN1ox2* grown 4 days in the dark on 1% agar with ½ MS supplemented with 5 mM MES, (pH 5.6) and with or without 0.1-0.2 mM ALA. Data shown are means +/- SD of three independent biological replicates. 30 seedlings were analysed for each replicate. Inset: bar chart showing Pchlide in the absence of ALA with data from the main figure. (B) ALA synthesis rate in seedlings grown on 1% agar with½ MS (pH 5.6) under the following conditions: 2 d D and 3 d WLc (100 µmol m^{-2} s^{-1}). For the last 2 h of WLc treatment whole seedlings were transferred to 50 mM Tris-HCl supplemented with 40 mM levulinic acid (pH 7.2). Data shown are mean + SD of three independent biological replicates. Asterisks denote a significant difference vs. WT (Col-0), Student's *t*-test (*p < 0.05, **p < 0.01).

To determine the cause of the reduced Pchlide we measured the rate of ALA synthesis, the rate-limiting step for tetrapyrrole synthesis in seedlings. To do this, seedlings grown for 2 days dark and 3 days WLc grown were treated with the ALA dehydratase inhibitor, levulinic acid (LA) for 2 h (Figure 3.11B). Surprisingly, both *gun1* mutants and GUN1oxlines accumulated significantly less ALA compared to the wild type, although the GUN1ox lines showed a stronger response.

To test whether the reduced ALA synthesis rate in *gun1* and GUN1ox lines resulted from changes in GluTR abundance, protein levels of this enzyme were analysed by western blotting in seedlings grown under the control conditions as described above, and additionally after 6 h of transfer to 40 mM LA. As shown in figure 3.12A no difference in GluTR accumulation between wild type and mutants or GUN1ox lines were seen suggesting that the reduced Pchlide phenotype (Figure 3.11B) was not due to an effect of GUN1 on the levels of this rate-limiting enzyme. While these results together are difficult to explain is a simple model, they clearly demonstrate that GUN1 affects tetrapyrrole metabolism.

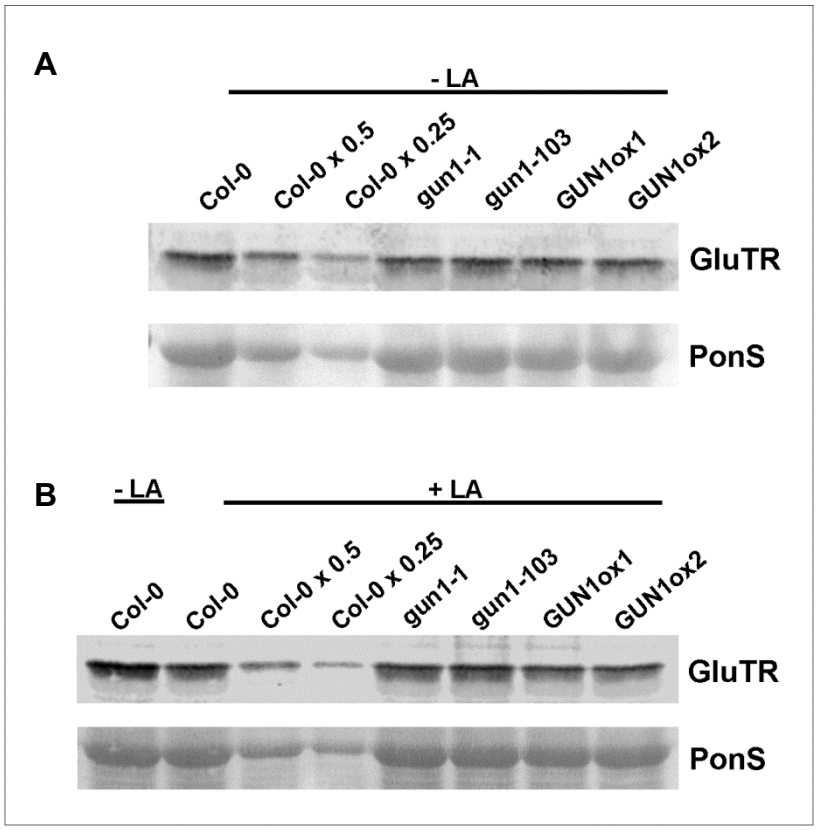

Figure 3.12 Western blot analysis of GluTR protein levels in *gun1* mutants and GUN1ox lines treated with levulinic acid (LA). WT (Col-0), *gun1-1*, *gun1-103,* GUN1ox1 and GUN1ox2 seedlings were grown on 1% agar with ½ MS under the following conditions: 2 d dark, 3 d WLc (100 µmol m^{-2} s^{-1}). For the last 6 h of WLc growth seedlings were transferred to liquid 50 mM Tris-HCl supplemented with 40 mM levulinic acid (pH 7.2; +LA). Control plants were harvested directly from ½ MS agar plates before LA treatment (-LA). Protein loading is indicated by PonceauS staining. Representative blots from 2 independent biological replicates are shown, with similar results in both replicates.

It was next examined if there is a role of GUN1 in the tetrapyrrole-dependent promotion of photosynthetic gene expression, and to what extent the known *gun* phenotype of *gun1* mutants is tetrapyrrole dependent. In order to test this, heme synthesis was blocked by DP in control and NF-treated *gun1* mutant and GUN1ox seedlings. As shown in Figure 3.13, both *gun1* mutant alleles maintained significantly higher tetrapyrrole and photosynthetic gene expression levels than WT after NF treatment, as expected. This rescue of nuclear gene expression was severely reduced by DP treatment with the effect more pronounced for tetrapyrrole biosynthesis genes like *HEMA1* and *GUN4,* than for photosynthetic genes like *LHCB2.1* and a Calvin cycle gene*CP12-2*. In the absence of NF, *gun1* mutants had slightly elevated expression of tetrapyrrole and photosynthesis genes after DP treatment. The *GUN1* overexpressor lines did not show a strong hypersensitive phenotype, however moderate, but significant enhanced repression of *HEMA1* and *LHCB2.1* was detected in these lines treated with NF and all four genes showed a small, but significant reduction in expression after NF and DP treatment for the GUN1ox1 line (Figure 3.13). Interestingly, DP and NF treatments had an additive effect on up-regulation of *FC1* expression. The strong up-regulation of *FC1* on NF and DP might be an indication of increased cellular stress. Taken together, these experiments show that the lack of GUN1 can promote flux through the tetrapyrrole pathway and this could account, at least partially, for the ability of the *gun1* mutant to rescue nuclear gene expression under the conditions that block plastid development.

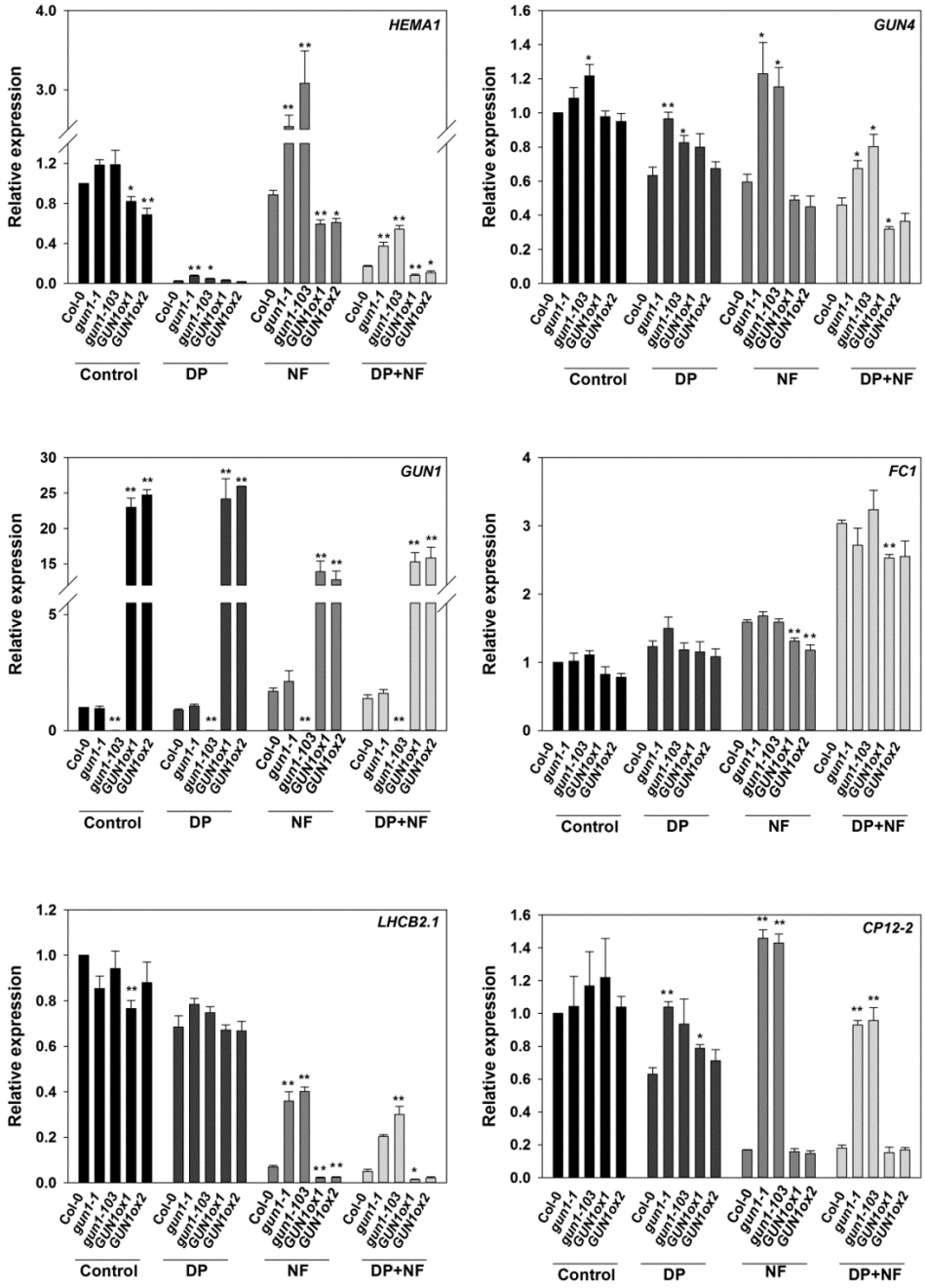

Figure 3.13 Regulation of nuclear gene expression in *gun1* mutants and GUN1ox lines treated with norflurazon (NF) and 2,2'-Dipyridyl (DP). WT (Col-0), *gun1-1*, *gun1-103,* GUN1ox1 and GUN1ox2 seedlings were grown on 1% agar with½ MS and with or without 1 µM NF under the following conditions: 2 d dark, 3 d WLc (100 µmol m^{-2} s^{-1}). For the last 6 h of WLc growth seedlings were transferred to water supplemented with: 1 µM NF (+NF), with 0.1mM DP (+DP) or with both 1 µM NF and 0.1 mM DP (DP+NF) or to control conditions (ethanol and DMSO at 0.02% each). Expression is relative to control treated Col-0 and normalised to *YELLOW LEAF SPECIFIC GENE 8* (*YLS8*, At5g08290). Data shown are means +SEM of three independent biological replicates. Asterisks denote a significant difference vs. Col-0 for the same treatment (control, +DP, +NF or DP+NF), Student's *t*-test (*p < 0.05, **p < 0.01).

3.2.7 Seedlings lacking ABI4 or PTM do not show a *gun* phenotype

ABI4 and PTM have both been implicated as central players in retrograde signalling (Koussevitzky et al., 2007; Sun et al., 2011). To test their roles further they were examined for their response to NF and LIN.

Two different mutant alleles of *ABI4* were obtained from the NASC collection. Sequencing confirmed the presence of a single point mutation in *abi4-102* (CS3837) that caused a substitution of G to A at codon 80 and resulted in a premature stop codon (Figure 3.14A, C). A homozygous insertion line of the *abi4* allele, *abi4-2*, was selected from the heterozygous SALK_080095 line by PCR using a combination of primers specific for the *ABI4* gene and to the SALK T-DNA insert (Figure 3.14A, D). The presence of the T-DNA insert 41 nucleotides from the start codon in exon of the *ABI4* gene was additionally confirmed by sequencing (Figure 3.14B).

The two *abi4* alleles along with the *ptm* mutant and two *gun1* mutant alleles were first screened for their ability to rescue nuclear gene expression on NF. A quantitative RT-PCR analysis of gene expression after seedling growth for 2 days in the dark and 3 days in WLc, in the presence of 1% sucrose and 1 μM NF revealed none of the *abi4* mutant alleles tested had a *gun* phenotype for any of the 5 genes tested (Figure 3.15). The NF conditions used resulted in a very strong repression of the photosynthetic genes *LHCB1.2* and *LHCB2.1,* and a more moderate repression of tetrapyrrole genes in WT seedlings. Of the two *abi4* alleles, *abi4-102* displayed a WT level of gene expression on NF for all analysed genes, but for *abi4-2* many genes including *LHCB1.2*, *LHCB2.1*, *HEMA1* and *GUN4* were down-regulated significantly on NF as compared to wild type although the response was small (Figure 3.15). Furthermore, under these conditions the two alleles of *gun1*, *gun1-1* and *gun1-103*, displayed a very strong *gun* phenotype, with almost complete rescue of *CHLH*, *GUN4* and *LHCB2.1* expression and 2- to 3-fold up regulation of *HEMA1,* relative to Col-0.

Additionally, the response of the *ptm* mutant was also examined. No clear rescue of gene expression under NF was found in the *ptm* mutant. The *HEMA1* and *LHCB2.1* transcripts were significantly higher in *ptm* than in control wild type (Figure 3.15), but the response was very weak compared to *gun1* controls, which showed complete rescue under these conditions, and not apparent for the other genes tested.

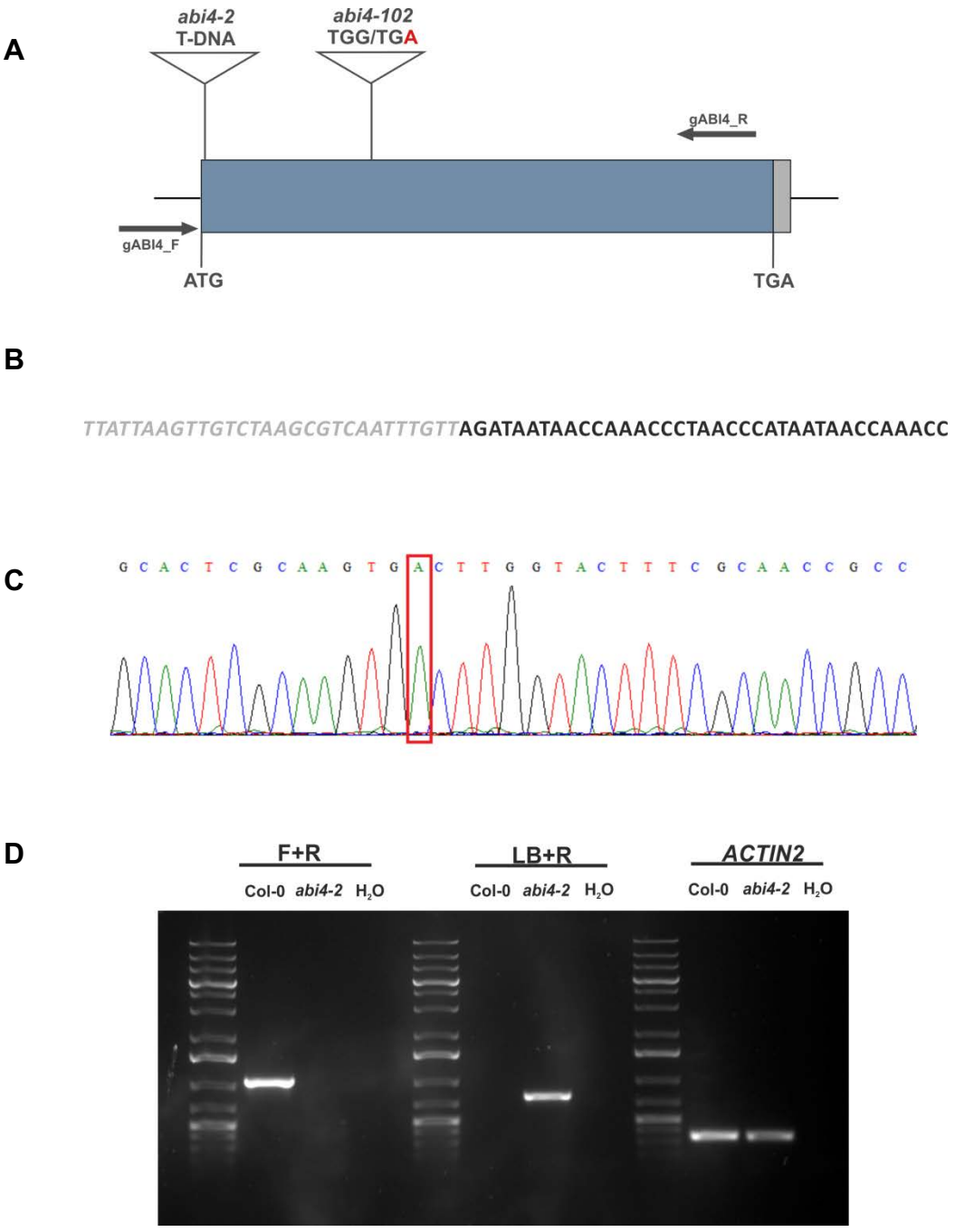

Figure 3.14 Analysis of the *abi4-102* and *abi4-2* mutant alleles. (A) Schematic diagram depicting the *abi4-102* and *abi4-2* mutation sites in the *ABI4* gene. Blue boxes represent exons, grey boxes represent UTR regions. PCR primers used for genotyping are indicated by grey arrows. (B) Sequence analysis of the T-DNA insertion in the *abi4-2* mutant. The T-DNA insert fragment is marked in grey italics and the exon in black and bold. (C) Sequence analysis showing the G/A substitution in *abi4-102* (D) Confirmation of the T-DNA insertion in *abi4-2* by PCR amplification. Genomic DNA from Col-0 and *abi4-2* plants was amplified using gene specific primers (F+R) and a left border specific primer (LB + R). *ACTIN2* transcript was used as a control.

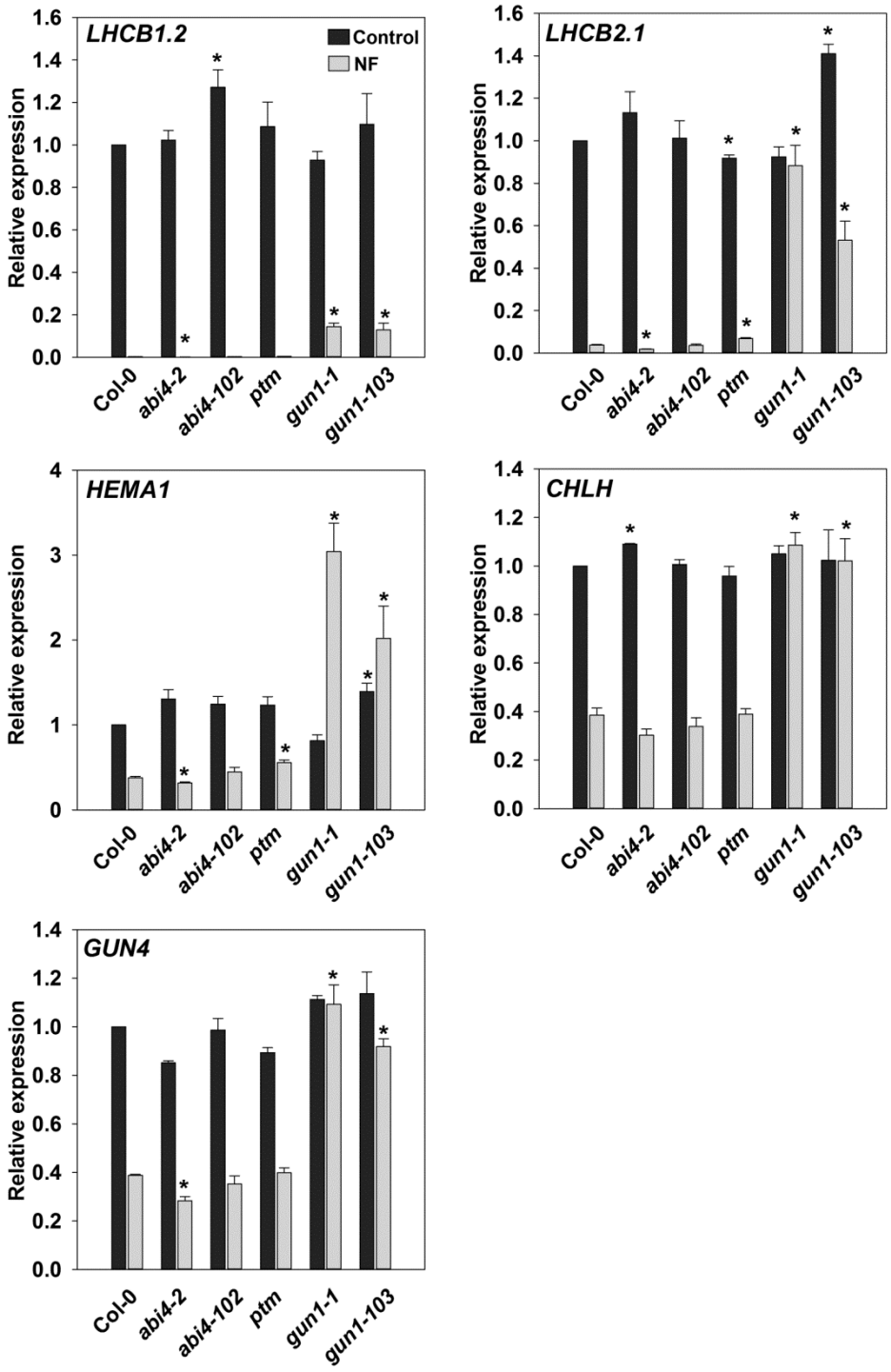

Figure 3.15 The *abi4-2*, *abi4-102* and *ptm* mutants do not show a *gun* phenotype on Norflurazon (NF). 1% agar with ½ MS supplemented with 1% sucrose and with (light grey bars) or without (dark grey bars) 1 µM NF under the following conditions: 2 d dark, 3 d WLc (100 µmol m^{-2} s^{-1}). Two alleles of *genomes uncoupled 1* (*gun1-1* and *gun1-103*) mutants were included (known to rescue gene expression on NF). Expression is relative to WT (Col-0) without NF (control) and normalised to *YELLOW LEAF SPECIFIC GENE 8* (*YLS8*, At5g08290). Data shown are means + SEM of three independent biological replicates. Asterisks denote a significant difference vs. Col-0 for the same treatment (Control or +NF), Student's *t*-test (*p<0.05).

ABI4 was reported to operate downstream of GUN1 and *abi4* mutants have been characterised previously as having a *gun* phenotype after lincomycin (Lin) treatment. The two *abi4* alleles of obtained for this study were tested for a *gun* phenotype on Lin in darkness using a real-time PCR and normalising the data against two reference genes *ACTIN2* and *YLS8*. As shown in Figure 3.16 both *abi4* alleles failed to show a convincing rescue of gene expression on Lin, independent of the reference gene used. Only for the *LHCB2.1* transcript, was there a small but statistically significant rescue of expression detected (when normalised to *ACTIN2*) in *abi4-2* as compared to wild type (7% difference in gene expression on Lin). When *YLS8* was used as a reference gene, a small, statistically significant increase in expression was seen in both *abi4* alleles for *CHLH* and *GUN4* expression, but not for the other genes tested. In all cases where any *abi4* response was observed rescue by *gun1-103* was complete (Figure 3.16A and B) and therefore this phenotype is supportive for *abi4* having a *gun* mutant phenotype.

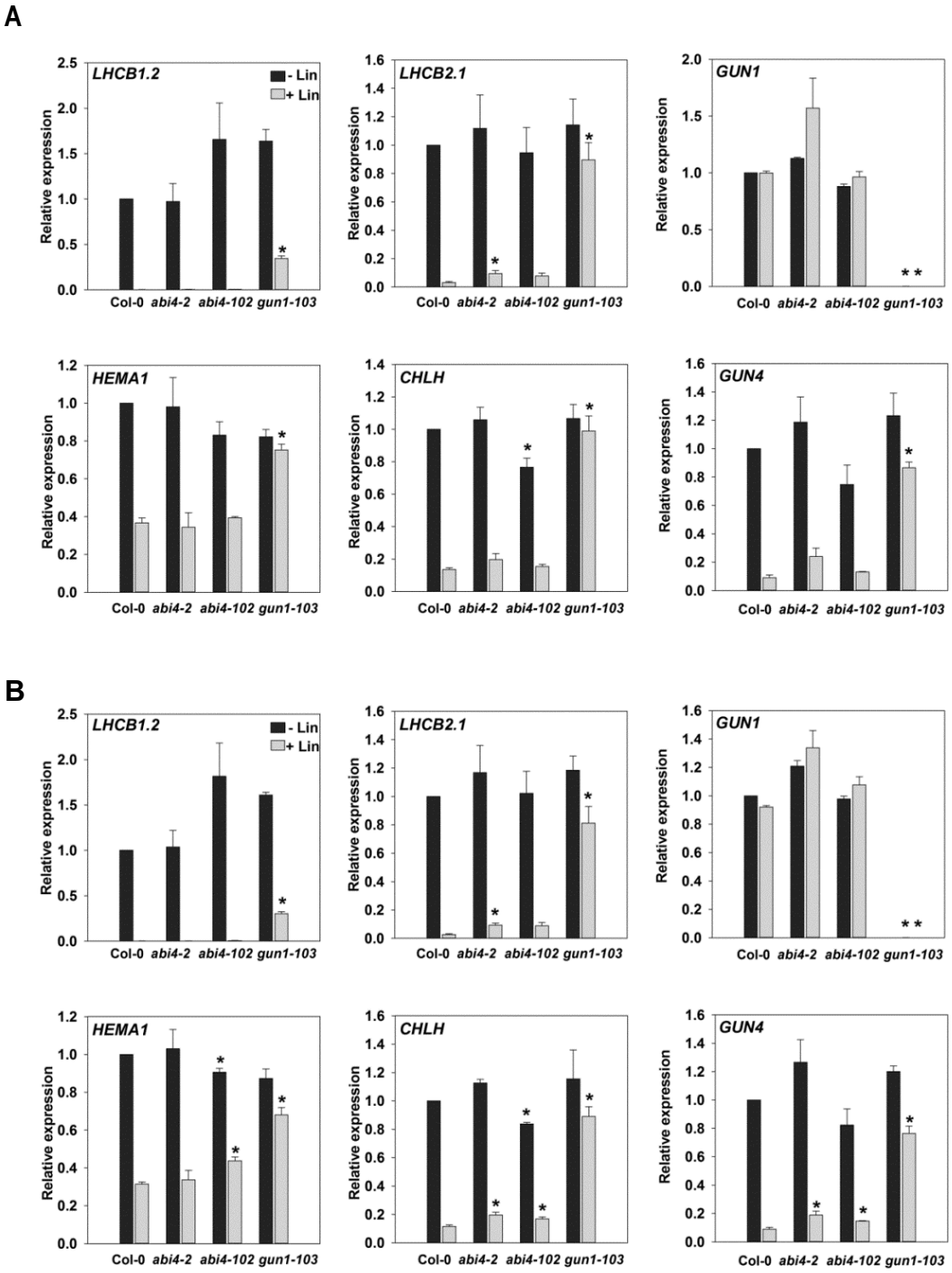

Figure 3.16 The *abi4-2 and abi4-102* mutants do not show a clear *gun* phenotype on lincomycin (Lin). Seedlings were grown on ½ Linsmaier and Skoog medium supplemented with 2% sucrose and 0.8% agar (pH 5.8) with (light grey bars) or without (dark grey bars) 0.5 mM Lin in dark for 5 d. For (A) and (B), *genomes uncoupled 1* (*gun1-103*) mutant was included as a control. Expression is relative to Col-0 -Lin and normalised to (A) *ACTIN2* (*ACT2*, At3g18780) used in Sun et al. (2011), and relative to (B) *YELLOW LEAF SPECIFIC GENE 8* (*YLS8*, At5g08290). Data shown are means +SEM of three independent biological replicates. Asterisks denote a significant difference vs. WT (Col-0) for the same treatment (-Lin or + Lin), Student's *t*-test (*p<0.05, **p < 0.0).

The *ptm* mutant has also been reported to result in elevated gene expression after Lin treatment (Sun et al., 2011). To test this, the effect of Lin was examined under two different treatment conditions: one following the exact conditions described in Sun et al. (2011), in which seedlings were grown in darkness in the presence of 0.5 mM Lin (Figure 3.17A); and a second, in which seedlings were grown on 0.5 mM Lin in darkness for 2 days before being transferred to WLc for 3 days (Figure 3.17B). For both Lin treatments there was no significant difference in transcript level for the two photosynthetic genes (*LHCB1.2* and *LHCB2.1*) and three tetrapyrrole-related genes tested in *ptm* compared to wild type (Figure 3.17A and B). To support the significance of the real-time PCR analyses, two different reference genes were tested for the data normalisation: *ACTIN2,* used by Sun et al. (Figure 3.17), and *YLS*8 (Figure 3.18). Lack of the rescue phenotype on Lin in *ptm* was observed, when the data were normalised relative to the second reference gene (Figure 3.18). Under the same conditions, there was a strong and significant rescue of expression for all genes tested (even up to complete rescue of *HEMA1*, *GUN4* and *CHLH*) in the two *gun1* mutant alleles, irrespective of the treatment and the reference gene used (Figure 3.17 and 3.18). It is worth noting that while under the WLc both *gun1* mutants had essentially the same level of gene expression rescue on Lin (Figure 3.17B, 3.18B), but that for seedlings treated with LIN in the dark, *gun1-103* maintained a higher level of photosynthetic and tetrapyrrole gene expression than *gun1-1.* Collectively, the data obtained here strongly suggest that both ABI4 and PTM are unlikely to be key elements regulating tetrapyrrole-dependent or OGE-dependent plastid-to-nucleus retrograde signalling.

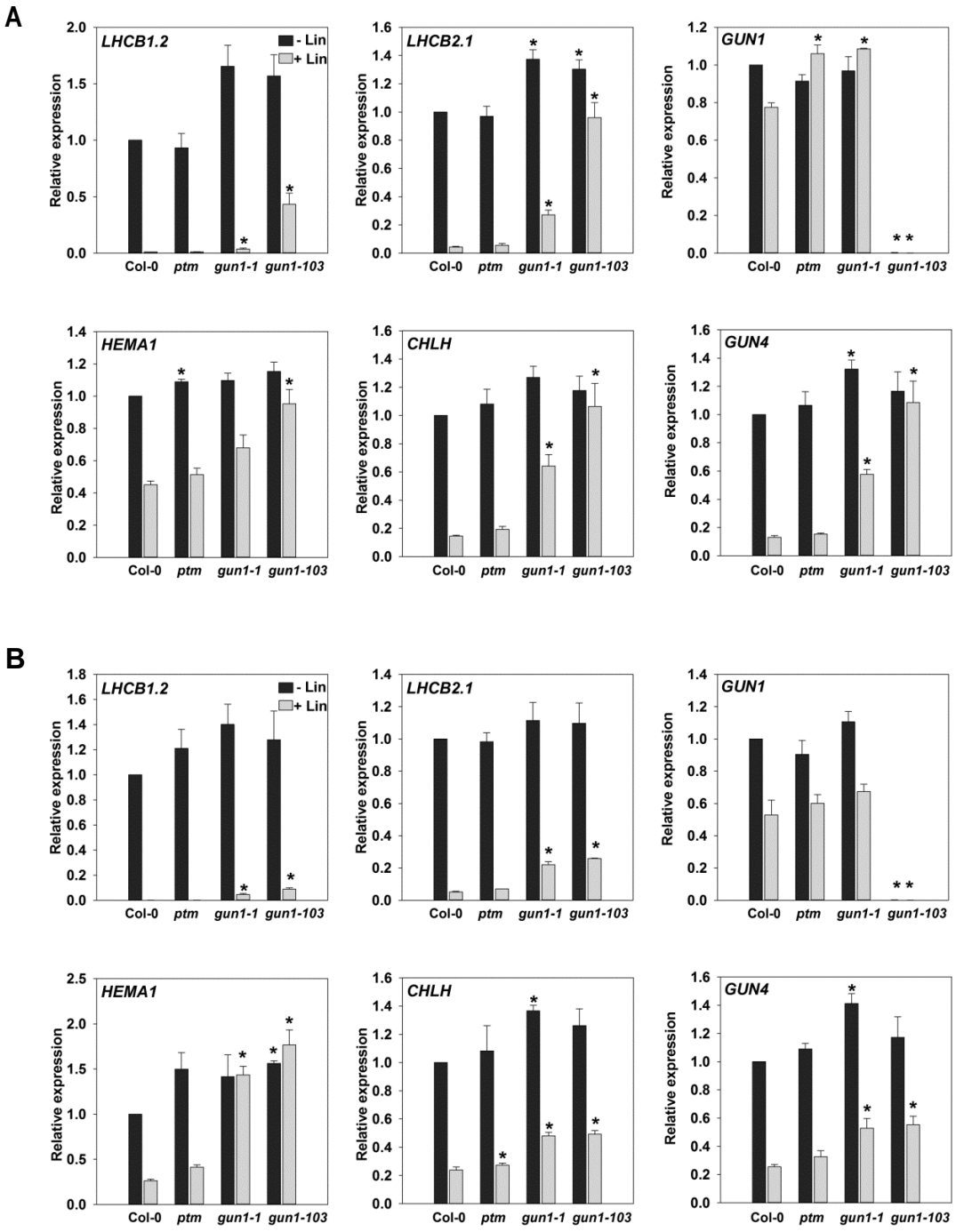

Figure 3.17 The *ptm* mutant does not show a *gun* phenotype on lincomycin (Lin). Seedlings were grown on ½ Linsmaier and Skoog medium supplemented with 2% sucrose and 0.8% agar (pH 5.8) with (light grey bars) or without (dark grey bars) 0.5 mM Lin in dark for 5 d (A), or (B) on 1% agar with ½ MS supplemented with 1% sucrose and with (dark grey bars) or without (light grey bars) 0.5 mM Lin under the following conditions: 2 d dark, 3 d WLc (100 µmol m^{-2} s^{-1}). For (A) and (B), two alleles of *genomes uncoupled 1* (*gun1-1* and *gun1-103*) mutants were included as positive control (known to rescue gene expression on Lin). Expression is relative to WT -Lin and normalised to *ACTIN2* (*ACT2*, At3g18780) used in Sun et al. (2011). Data shown are means +SEM of three independent biological replicates. Asterisks denote a significant difference vs. WT (Col-0) for the same treatment (- Lin or + Lin), Student's *t*-test (*p<0.05, **p < 0.01).

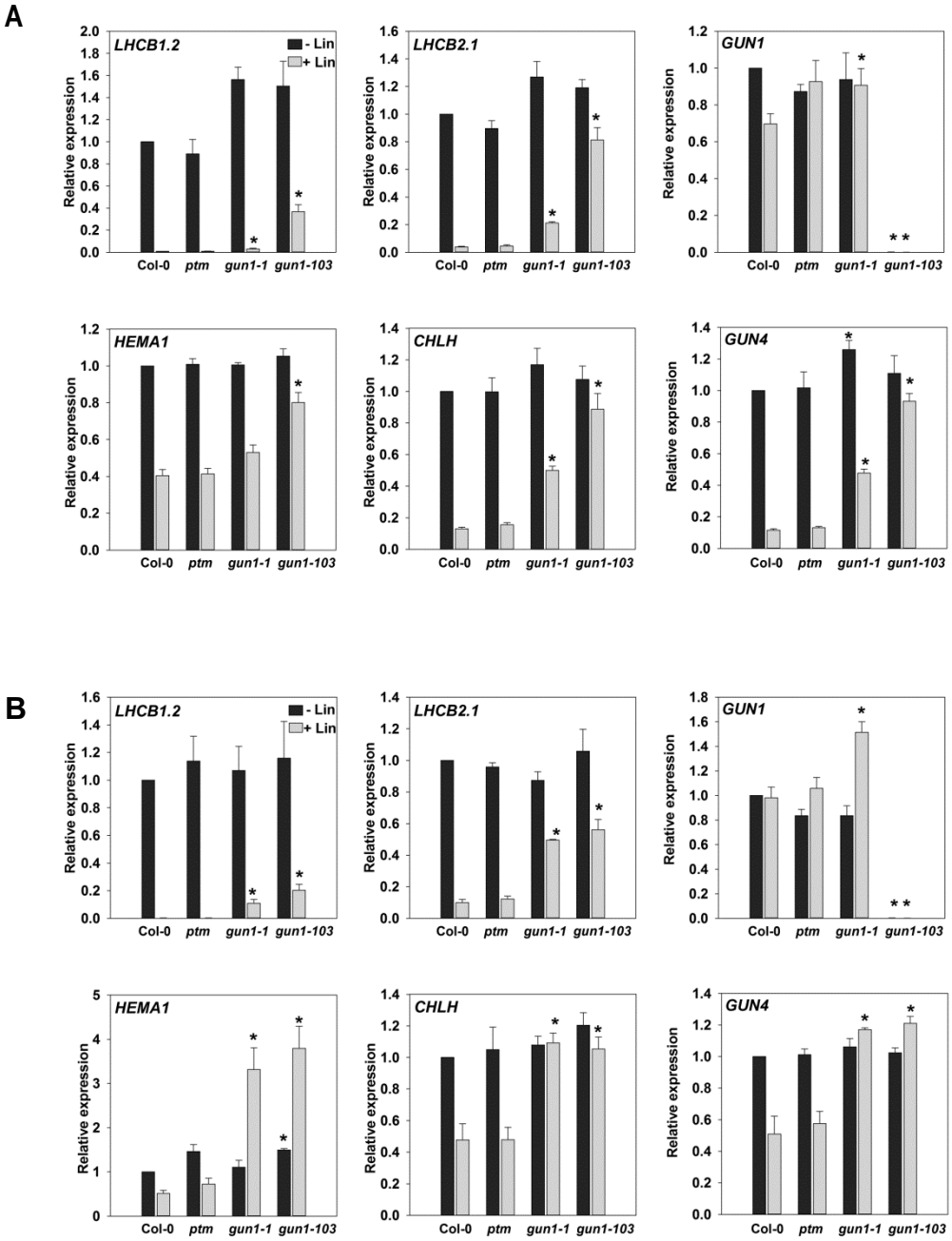

Figure 3.18 The *ptm* mutant does not show a gun phenotype on lincomycin (Lin). Seedlings were grown on ½ Linsmaier and Skoog (LS) medium supplemented with 2% sucrose and 0.8% agar (pH 5.8) with (light grey bars) or without (dark grey bars) 0.5 mM Lin in dark for 5 d (A), or (B) on 1% agar with ½ MS supplemented with 1% sucrose and with (light grey bars) or without (dark grey bars) 0.5 mM Lin under the following conditions: 2 d dark, 3 d WLc (100 µmol m^{-2} s^{-1}). For (A) and (B), two alleles of genomes uncoupled 1 (*gun1-1* and *gun1-103*) mutants were included as positive control (known to rescue gene expression on Lin). Expression is relative to WT (Col-0) -Lin and normalised to *YELLOW LEAF SPECIFIC GENE 8* (*YLS8*, At5g08290). Data shown are means +SEM of three independent biological replicates. Asterisks denote a significant difference vs. WT (Col-0) for the same treatment (-Lin or + Lin), Student's *t*-test (*p<0.05, **p < 0.01).

3.3 Discussion

At the beginning of this work the most accepted hypothesis for plastid-to-nucleus retrograde signalling suggested that FC1 activity, and thus possibly a FC1-derived heme pool or heme product, acts as a positive plastid signal that controls photosynthetic gene expression in developing chloroplasts (Woodson et al., 2011; Terry and Smith, 2013). The precise understanding of the nature of this signal and how it can move from plastid to nucleus are still not clear, but defining the *abi4-102* and *ptm* mutants as having a *gun* phenotype on NF and Lin (Koussevitzky et al., 2007; Sun et al., 2011) has led to the suggestion that they are major regulators of biogenic retrograde signalling. These findings were re-examined in this work and the results obtained only partially support the proposed hypotheses and it is necessary to re-evaluate the existing plastid retrograde signalling model (Figure 3.19).

3.3.1 Heme synthesis is required for the production of a positive retrograde signal

Under the NF conditions used in this study the dominant *gun6-1D* mutant, with the increased *FC1* expression, had a clear and significant *gun* phenotype (Figure 3.2). The ability of *gun6-1D* to maintain higher nuclear gene expression was also apparent under other NF treatments, using different growth media, light conditions and sucrose concentrations (Page et al., 2017b). This is the first independent confirmation of the *gun6-1D* phenotype since the original publication of Woodson et al. (2011). The fact that the *gun6-1D* phenotype on NF is so robust strongly supports the promotive regulatory role of FC1-derived heme in retrograde signalling. It is noticeable, however, that the rescue of gene expression on NF in *gun6-1D* was weaker than for mutant in Mg-chelatase subunit, *gun5-1* (Figure 3.2; Page et al., 2017b). The time course for gene expression on NF in Figure 3.1 shows that various *gun* mutants can differ in their ability to maintain higher gene expression with time, and this could be one explanation for the observed difference. The *gun5* mutant is blocked in Mg-porphyrin synthesis and is proposed to redirect flux towards the heme branch of the tetrapyrrole pathway. Indeed, the *gun5* mutation was shown to be sufficient to partially restore heme levels in *sig2-2* (Woodson et al., 2013). If the current hypothesis of a FC1-activity dependent signal is correct, then it might be expected that the *gun6-1D* mutant phenotype would be stronger than *gun5,* as it affects the enzyme directly responsible for the heme synthesis. One possibility is that substrate availability is the key factor in the amount of FC1-dependent heme synthesis and thus overexpression of FC1 is insufficient for a very strong response. Another possibility is that the *gun* phenotype of *gun5* on NF is only partially dependent on promotion of the heme branch. Since the mutant is also blocked in porphyrin synthesis, it is possible that an inhibitory retrograde signalling pathway resulting from $^1O_2$ production (described in more detail in Chapter 5) is also inhibited in this mutant. This might be

too simplistic an explanation, as analysis of genotypes that promote porphyrin accumulation (and potentially reduce heme synthesis) did not show a hypersensitive response on NF (Figure 3.3). A clear separation between positive and negative tetrapyrrole signals might be difficult to measure.

The *fc2-1* mutant had a weak *gun* phenotype under low NF condition (Figure 3.3). This result is fully in agreement with the elevated photosynthetic gene expression seen in the *fc2* mutant treated with NF and 1 mM ALA (Woodson et al., 2011). In addition, as *fc2-1* accumulates more Proto-IX, that could serve as a substrate for FC1 and promote FC1-dependent heme synthesis (Woodson et al., 2011, Woodson et al., 2015). Woodson et al. (2011) showed that under the same ALA treatment *fc1-1* had increased repression of photosynthetic genes, which was not seen in this work under low concentrations of NF. Since *fc1-1* is not a null mutant, it might have a more subtle phenotype, which was not seen in low NF (Figure 3.3), in contrast to the more severe conditions (6 d growth on NF and ALA) used by Woodson et al. (2011). GUN4 is an enzyme that binds to the porphyrins Proto-IX and Mg-Proto to stimulate Mg-chelatase activity (Larkin et al., 2003; Davison et al., 2005). However, the gene expression analysis did not confirm this finding (Figure 3.3), possibly because the retrograde signal was already completely lost.

Unexpectedly, both *sig2-2* and *sig6-1* were shown in this work to display a *gun* phenotype on low concentrations of NF (Figure 3.7), a result that was opposite to an earlier report of Woodson et al. (2013), showing that these mutants repress photosynthetic gene expression under control conditions. One of the differences between this study and that of Woodson et al. (2013) is the age of the seedlings, with 5 d-old and 2 d-old seedlings being analysed, respectively. As shown in Figure 3.1, *LHCB2.1* and *HEMA1* expression changes drastically within the first days of WLc exposure. It is possible that the *sig* phenotype is dependent on the length of the light treatment, or with 6 *SIG* genes, there might be different requirement for particular SIG factors at the different stages of seedlings growth. The *sig2-2* and *sig6-1* phenotype is not necessarily in disagreement with a heme-related retrograde signal, as both mutants were shown here to overexpress *HEMA1* under both control conditions and after NF treatment. This would increase the flux through tetrapyrrole pathway, including the promotion of heme synthesis.

The *gun6-1D* is a dominant mutation that results only in a moderate *FC1* overexpression. Other strong *FC1* overexpressor lines were generated by Woodson et al. (2011), and were also shown to display a *gun* phenotype on NF supporting its role in retrograde signalling. It might be interesting to know if there is a positive correlation between the level of *FC1* overexpression, the level of heme synthesized, and the rescue of photosynthetic gene expression on NF, however this was not reported by the authors. One of the complexities in the interpretation of the

retrograde signalling phenotype of FC1 overexpressor lines is that heme is a negative regulator of the tetrapyrrole pathway (Terry and Kendrick, 1999), and perhaps because of that negative feedback inhibition, it is not possible to observe stronger rescue of gene expression in *gun6-1D*. To address this possibility, a chemical approach was used in which heme synthesis was blocked with the Fe^{2+} chelator 2,2'-dipyridyl (DP) (Figures 3.4 and 3.5). Consistent with the hypothesis of a heme-dependent signal (Terry and Smith, 2013), inhibition of heme synthesis resulted in a strong down-regulation of photosynthetic and tetrapyrrole gene expression, suggesting that retrograde signalling was blocked. There are many examples of studies in plants using DP to block tetrapyrrole synthesis (e.g. Duggan and Gassman, 1974; Johanningmeier and Howell, 1984; Franklin et al., 2003; Zhang et al., 2006; Woodson et al., 2011). However, although there is evidence that DP is a specific chelator of Fe^{2+} (Lindoy and Livingstone 1967), it cannot be completely ruled out that the inhibitory effect of the DP on photosynthetic gene expression is at least partially independent of an effect on heme. It might result from broad cellular stress due to ion chelation or the effect on iron-sulfur proteins that are crucial for photosynthesis (Dos Santos et al., 2004) including chlorophyll biosynthesis (Xu et al., 2017). It is well established for example that DP also blocks the chlorophyll branch of the pathway (Duggan and Gassman, 1974) at the same step as Fe-S cluster biosynthesis mutants (Xu et al., 2017). However, not all genes tested in this study were inhibited. The *FC1* gene, which was shown earlier to be up-regulated by NF (Moulin et al., 2008), was also up-regulated after DP treatment, suggesting that the DP treatment did not cause such high levels of stress that gene expression was generally inhibited. Indeed, the DP treatment used was optimised to reduce unspecific effects by using the smallest possible DP dose and a short treatment time (6 h), in contrast to earlier studies. Interestingly, a recent study reported that another inhibitor of the tetrapyrrole pathway, LA, could repress *LHCB1* expression in a *gun5*-dependent manner (Pattanayak and Tripathy, 2016), consistent with the results described here. It would be interesting to test LA and other tetrapyrrole inhibitors using the experimental system optimised in this work. In summary, the data discussed so far are collectively consistent with the proposal for a positive retrograde signal dependent on FC1 activity that promotes photosynthetic gene expression during chloroplast development.

3.3.2 ABI4 and PTM are not required for biogenic retrograde signalling

Rigorous examination of the *ptm* and *abi4* mutants on NF and Lin (Figures 3.15, 3.17 and 3.18), showed that *ptm* and *abi4* had in general WT level of photosynthetic and gene repression, independent of the different genes and treatments tested. These results were clearly in disagreement with Sun et al. (2011), and are not supportive for *ptm* as a *gun* mutant controlling plastid retrograde signalling (see also Page et al., 2017b). One difference between this study and

that of Sun et al. (2011), is that these authors performed most of their analyses using RNA gel blot assays. However, some of their Lin experiments were analysed also by quantitative RT-PCR with the primer pair binding to the *LHCB2.1* gene, which is analysed routinely in this study. In addition, great lengths were taken to match the conditions used by Sun et al. (2011) including using the same reference gene (*ACT2*). Although a very weak rescue of *ptm* on NF was detected for selected genes it was not seen under other NF conditions and on Lin (Figure 3.17; Page et al., 2017b). If PTM is involved in retrograde signalling then the *ptm* mutant should show a much more robust phenotype and therefore the data presented here (and in Page et al., 2017b) do not support a role for PTM in retrograde signalling.

Two different *abi4* mutant alleles were also tested for their response to NF and Lin (Figures 3.15 and 3.16), but neither showed a consistent rescue of nuclear gene expression. There is an extensive literature on the *abi4* mutant phenotype in the context of the retrograde signalling (Koussevitzky et al., 2007; Miller et al., 2007; Kakizaki et al., 2009; Zhang et al., 2013; Xu et al., 2016). Interestingly, not all researchers have been able to confirm the *gun* phenotype of *abi4* mutants (Cottage and Gray, 2011; Kerchev et al., 2011), thus the role for ABI4 in plastid retrograde signalling is open to question. Table 3.1 summarizes all NF or Lin experiments performed to investigate *abi4* rescue of photosynthetic or mitochondrial gene expression. Use of different growth conditions and methods of gene expression analysis, as well as testing for different genes, may be able to account for some of the inconsistencies. One of the alleles tested here was the EMS mutant *abi4-102*, which was also examined by Koussevitzky et al. (2007) and was the first description of a *gun* phenotype for *abi4*. Interestingly, the authors also showed that *abi4* is epistatic to *gun5*, which might additionally strengthen its role in tetrapyrrole retrograde signalling.

The original study of Koussevitzky et al. (2007), showed that *abi4-102* rescue of *LHCB1* expression on Lin was weaker than *gun1,* but still had higher *LHCB1* expression than Col-0. One major difference in this report compared to the current study was the use of RNA gel blots to evaluate gene expression. More careful evaluation of the original Lin treatment data presented in Koussevitzky et al. (2007), shows that the total RNA loading control for *abi4* is higher than for Col-0, and this might partially account for the weak *gun* phenotype reported in this study. The second *abi4* allele tested here has never been evaluated for its *gun* phenotype before. Many of the experiments using *abi4* mutants have used the deletion mutant, *abi4-1.* This allele appears to have a clear elevated gene expression on NF and Lin compared to WT (see Table 3.1).

Table 3.1 Summary of retrograde signalling-related studies using *abi4* mutants

Allele tested	Treatment	Methods used	Phenotype	Source
abi4-102*	Seedlings grown on ½ LS medium with 1-2% sucrose, supplemented with or without 5µM NF (for 8 days) or 220µg/ml Lin (for 6 days) under WLc (100µmol*m^{-2}*s^{-1})	mRNA gel blot for *LHCB1* mRNA accumulation	A clear *gun*-like phenotype on both NF and Lin in *abi4*, but moderate degree of phenotype as compared to *gun1* rescue.	Koussevitzky et al, 2007, Science
abi4-1* and *abi4-102	Plants were grown under a 16/8h photoperiod, 100µmol*m^{-2}*s^{-1}, in MS media to a growth stage 1.04 and treated for 3h with 40µM rotenone .	qRT-PCR for *AOX1a*	Both *abi4* mutants were insensitive to increased *AOX1a* mRNA induced by rotenone supporting role in mitochondrial retrograde signalling.	Giraud et al, 2009, Plant Phys.
abi4-103* ***(sis5-3)***	Seedlings grown for 7 days on ½ MS medium with 2% sucrose, supplemented with or without 0.5mM Lin.	RT-PCR for *CA1* mRNA accumulation	No *gun*-like phenotype on lincomycin in *abi4* in contrast to strong phenotype in *gun1*.	Cottage and Gray, 2011, Plant Signalling & Behaviour
abi4 **(one of the *sis5* mutants but not specified)**	Seedlings grown for 5 days in 16/8h photoperiod (100µmol*m^{-2}*s^{-1}) on ½ MS medium with 0.5g/L MES, with 2% sucrose, supplemented with or without 5µM NF, or with or without 0.5mM Lin.	qRT-PCR for *LHCB1.1*	No *gun*-like phenotype on NF and Lin in *abi4* in contrast to a clear rescue phenotype in *gun1*.	Kerchev et al, 2011, The Plant Cell
abi4-1 **	Seedlings grown on ½ LS medium with 2% sucrose, 0.8% agarose, supplemented with or without 5µM NF (4d D + 3d WL under a 14/10h photoperiod, 100µmol*m^{-2}*s^{-1}) or 220µg/ml Lin (4-6d in dark).	*LHCB2.1/LHCB2.2* expression determined by mRNA gel blot and qRT-PCR	A clear *gun*-like phenotype on both NF and Lin in *abi4*; similar (Lin) or moderate (NF) degree of phenotype as compared to strong rescue in *gun1*.	Sun et al, 2011, Nature
abi4-1	Seedlings grown on ½ MS medium supplemented with or without 5µM NF or 0.5mM Lin for 4d D + 3d WL under a 14/10h photoperiod (100µmol*m^{-2}*s^{-1}).	qRT-PCR for *LHCB1.2*	A clear *gun*-like phenotype on both NF and Lin in *abi4*, with moderate/weak degree of rescue of gene expression.	Guo et al, 2016, Nature

* Original allele identified by Laby et al., 2000; **Allele information Söderman et al. 2004

With many different alleles harbouring different type of mutations it is possible that some differences for the observed presence or absence of the *gun* phenotype are simply allele specific. The situation might be even more complicated taking into account that as a transcription factor ABI4 has a lot of different biological functions in mature plants (Wind et al., 2013). Intriguingly, some alleles of the *abi4* mutant were initially identified as being insensitive to sugar (termed as *sis* mutants; Laby et al., 2000). Table 3.1 shows that all studies with *abi4* performed so far on NF or Lin were performed in the presence of sucrose (including this work). Since sucrose also affects the induction of light responsive genes it is possible that part of the *abi4* phenotype on NF or Lin is due to these effects. Additional testing of *abi4* mutants for gene expression rescue in the absence of sucrose should also be undertaken. To strengthen findings presented in this work, it would also be important to analyse additional alleles. The *abi4-1* allele and another, new unpublished allele of *abi4* have been provided by Dr Mochizuki (Kyoto University) and will be examined in the near future.

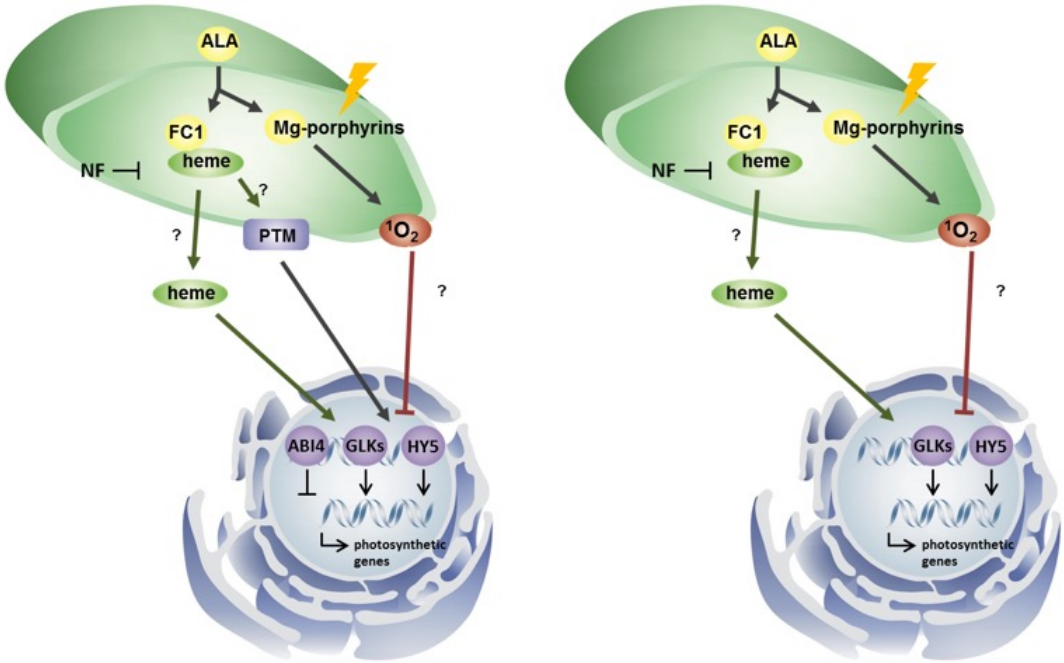

Figure 3.19 A hypothetical model for chloroplast-to-nucleus signalling during chloroplast biogenesis. (A) A model for plastid retrograde signalling at the outset of this project. In this model there are two signalling pathways proposed. A positive heme-related signal, mediated by ferrochelatase 1 (FC1) and an inhibitory light-dependent signal that is mediated by singlet oxygen ($^1O_2$) and the down-stream molecular factors PTM, ABA Insensitive 4 (ABI4), Golden-like proteins (GLKs) and Long Hypocotyl 5 (HY5). Figure modified from Terry and Smith, 2013. (B) A new model for plastid signalling pathways based on data from this Chapter and excluding the role of PTM and ABI4.

3.3.3 GUN1 affects tetrapyrrole synthesis

It was originally shown that the *gun1* mutant, but not other *gun* mutants, can rescue gene expression on both NF and Lin (Koussevitzky et al., 2007). Based on this finding it is often proposed that GUN1 is a down-stream integrator of different retrograde signals within the chloroplast. However, the precise molecular function of GUN1 remains unknown. Physiological and molecular analyses in this section provide new evidence for the role of GUN1 as a negative regulator of tetrapyrrole signalling during seedling development, which is consistent with the *gun1* phenotype described so far in the literature. The importance of GUN1 in tetrapyrrole signalling is reflected in the early work of Koussevitzky et al. (2007), who showed that out of 370 genes rescued on NF, 329 were shared by *gun1* and *gun5*. The role of GUN1 as a negative regulator of seedling development can be proposed based on the higher Pchlide levels accumulated in *gun1* mutants and the opposite phenotype seen in GUN1ox lines after ALA feeding (Figure 3.11). This observation is supported by the *gun1* hypersensitive phenotype to the FR treatment (McCormac and Terry, 2004). The higher accumulation of Pchlide in *gun1-1* after ALA feeding is also in agreement with the photo-bleaching observed for *gun1* during transfer to WL and its

hypersensitive phenotype to high light conditions (Mochizuki et al., 1996; Ruckle et al., 2007). Accumulation of more Pchlide in dark-grown *gun1* seedlings fed with ALA could promote a heme-dependent positive signal. Inhibition of *gun1*-mediated rescue of gene expression on NF by DP demonstrated in this work is supportive for this hypothesis (Figure 3.13). The recent discovery of that theGUN1 may interact with tetrapyrrole biosynthesis enzymes, including FC1 (Tadini et al., 2016) is very interesting in this context and suggest this could be a very fruitful area for further study.

Chapter 4 The role of plastid ribosomal protein L11 (PRPL11) in plastid to nucleus retrograde signalling

4.1 Introduction

The genetic screen for the mutations rescuing gene expression on NF led to the discovery of major components regulating plastid retrograde signalling and provided strong evidence for the important role of tetrapyrrole metabolism in regulation of the nuclear gene expression (Susek et al., 1995; Mochizuki et al., 2001, Woodson et al., 2011; described in detail in Chapter 1). Besides these metabolite-mediated signalling pathways, there is also increasing evidence in the literature that organellar gene expression (OGE) and chloroplast protein synthesis are important components of the retrograde signalling pathway.

There are many examples in the literature for the inhibition of photosynthesis-related nuclear gene expression after the block of chloroplast gene expression and chloroplast translation. This has been shown by chemical approaches, using prokaryote-specific antibiotics, such as Lin and chloramphenicol, which inhibit plastid protein synthesis. Treatment with these inhibitors results in reduced expression of photosynthetic genes, and has been shown for example in pea (Adamska, 1995; Sullivan and Gray, 1999), tobacco (Gray et al., 2003), and mustard seedlings (Oelmüller et al., 1986). Similar evidence is provided by genetic studies testing mutants with impaired plastid ribosomes, including the early work of Bradbeer et al. (1979), on the barley *albostrians* mutant (described in Chapter 1.7.1), which was followed up by Hess et al. (1994). Another example, that was described earlier, is that of the plastid sigma factor mutants *sig2-2* and *sig6-1* that have disturbed function of the plastid-encoded RNA polymerase and show reduced expression of photosynthetic genes (Woodson et al., 2013). In the *ppi* mutant, the atToc159 protein that functions as a receptor in plastid protein import machinery is lost, which results in a severe albino phenotype and lower expression of photosynthesis-related nuclear genes (Kakizaki et al., 2009). It was later demonstrated that lincomycin treatment and the *ppi* mutation both result in defects in RNA editing that may underlie another mechanism controlling OGE-dependent retrograde signalling (Kakizaki et al., 2012). Finally, a synergistic effect on the repression of photosynthetic gene expression was observed in mature *Arabidopsis* plants with impaired plastid and mitochondrial translation (Pesaresi et al., 2006). Only the double mutant of plastid and mitochondrial ribosomal protein L11 (*prpl11/mrpl11*) displayed an enhanced down-regulation of nuclear encoded chloroplast genes, in contrast to the very subtle phenotype of the respective single mutants (Pesaresi et al., 2006).

Among all *gun* mutants, only *gun1* was shown to rescue nuclear gene expression from the inhibitory effects of impaired OGE including lincomycin treatment (Koussevitzky et al., 2007) and mutations in *sig2-1* or *ppi1* (Woodson et al., 2013, Kakizaki et al., 2009). More recently, work of Sun et al. (2016) and Tadini et al. (2016) provided new evidence that disruption of plastid translation by mutation in ribosomal proteins and proteins involved in processing plastid transcripts plays a role in regulation of photosynthetic gene expression during plastid development. These authors showed that NF- and lincomycin-treated seedlings of two mutants, *prps-1* (plastid ribosomal protein small subunit) and *mterf4* (mitochondrial transcription termination factor 4), displayed a weak *gun* phenotype (Sun et al., 2016; Tadini et al., 2016). GUN1 could be the crucial component integrating plastid translation with retrograde signalling. Both the mTERF4 and PRPS1 proteins have been demonstrated to indirectly or directly interact with GUN1 (Sun et al., 2016; Tadini et al., 2016). GUN1 has been proposed to function down-stream of retrograde signalling and integrate different types of plastid signals. Interestingly, GUN1 has been shown to bind directly, not only to PRPS1, but also to FC1 and CHLD (Tadini et al., 2016). This suggests that plastid translation can be potentially integrated with the tetrapyrrole-dependent retrograde signalling and is possibly consistent with the current hypothesis for positive (heme dependent) and negative ($^1O_2$-dependent) retrograde signalling pathways (Terry and Smith, 2013).

The phenotype of *gun* mutants has been extensively studied and clearly defined through experiments from many research groups. The role of recently discovered, genetic components controlling plastid gene expression and therefore organellar communication still needs to be investigated in more detail. The current study was undertaken to elucidate the role of one of the plastid ribosome proteins, PRPL11, in control of retrograde signalling to the nucleus. This will be achieved through molecular and biochemical analysis of *prpl11* mutants, the generation of PRPL11 overexpressor lines, and characterization of other mutants for plastid ribosome proteins. The hypothesis will be tested that plastid ribosome proteins can impact on the tetrapyrrole pathway and integrate OGE signalling with tetrapyrrole-dependent retrograde signalling.

4.2 Results

4.2.1 The role of PRPL11 and MRPL11 in regulation of nuclear gene expression

The intriguing phenotype of *prpl11/mrpl11* double mutant described originally by Pesaresi et al. (2006), suggested there might be some requirement for mitochondrial function to co-regulate chloroplast retrograde signalling. To test the possibility of potential involvement of the plastid and mitochondrial ribosomal L11 proteins in retrograde signalling, single and double mutants were examined for their phenotype under standardised NF conditions. Under the control condition of 2 d D and 3 d WLc, expression of the photosynthetic genes *LHCB2.1* and *PSBQ-1* was not strongly affected in the single *prpl11-1* and *mrpl11-1* mutants, but repression of *LHCB2.1* was observed in the double mutant (Figure 4.1), consistent with the phenotype of mature *Arabidopsis* mutants (Pesaresi et al., 2006). Surprisingly, under the same control conditions the expression of the tetrapyrrole biosynthesis genes *HEMA1*, *CHLH* and *FC2,* and one photosynthetic gene, *CP12-2* (used previously as a marker gene in retrograde signalling; Woodson et al., 2011) was elevated in the single *prpl11-1* mutant (Figure 4.1). A similar response was seen in the double *prpl11-1/mrpl11-1* mutant, but was not observed in *mrpl11-1* (Figure 4.1). The increased gene expression phenotype of *prpl11-1* and *prpl11-1/mrpl11-1* mutants was still apparent on NF (Figure 4.1). After treatment with 1 μM NF the *prpl11-1* mutant also showed a small, but significant, rescue of *LHCB2.1* and *PSBQ-1* relative to the wild type, which indicates that *prpl11* has a *gun*-like phenotype on NF. Collectively, these results suggest the PRPL11 protein could be involved in regulation of tetrapyrrole-dependent plastid retrograde signalling and this was investigated further.

Before further examination of the role of PRPL11 in retrograde signalling, a second allele of *PRPL11* was obtained from the GABI-Kat collection. A homozygous insertion line of the new *prpl11*allele was selected from the heterozygous GK_366H05 lines by PCR using a combination of primers specific for the *PRPL11* gene and the GK T-DNA insert (Figure 4.2 A, D). This line has not been reported before. Therefore, we named it *prprl11-3*, as the *prpl11-1* and *prpl11-2* alleles were already described (Pesaresi et al., 2001; Ma et al., 2015). Mutants in *prpl11* have a pale green seedling phenotype, and this was observed for both alleles, with *prpl11-3* showing a less severe phenotype compared to *prpl11-1* (Figure 4.2B). The presence of the T-DNA insert 3 nucleotides from the start of the 5´ UTR region of the *PRPL11* gene was additionally confirmed by sequencing (Figure 4.2C). The down-regulation of *PRL11* transcript was detected by RT-PCR (Figure 4.2E), and there was a strong inhibition of *PRPL11* expression in both *prpl11-1* and *prpl11-3* when tested by quantitative PCR (Figure 4.2F).

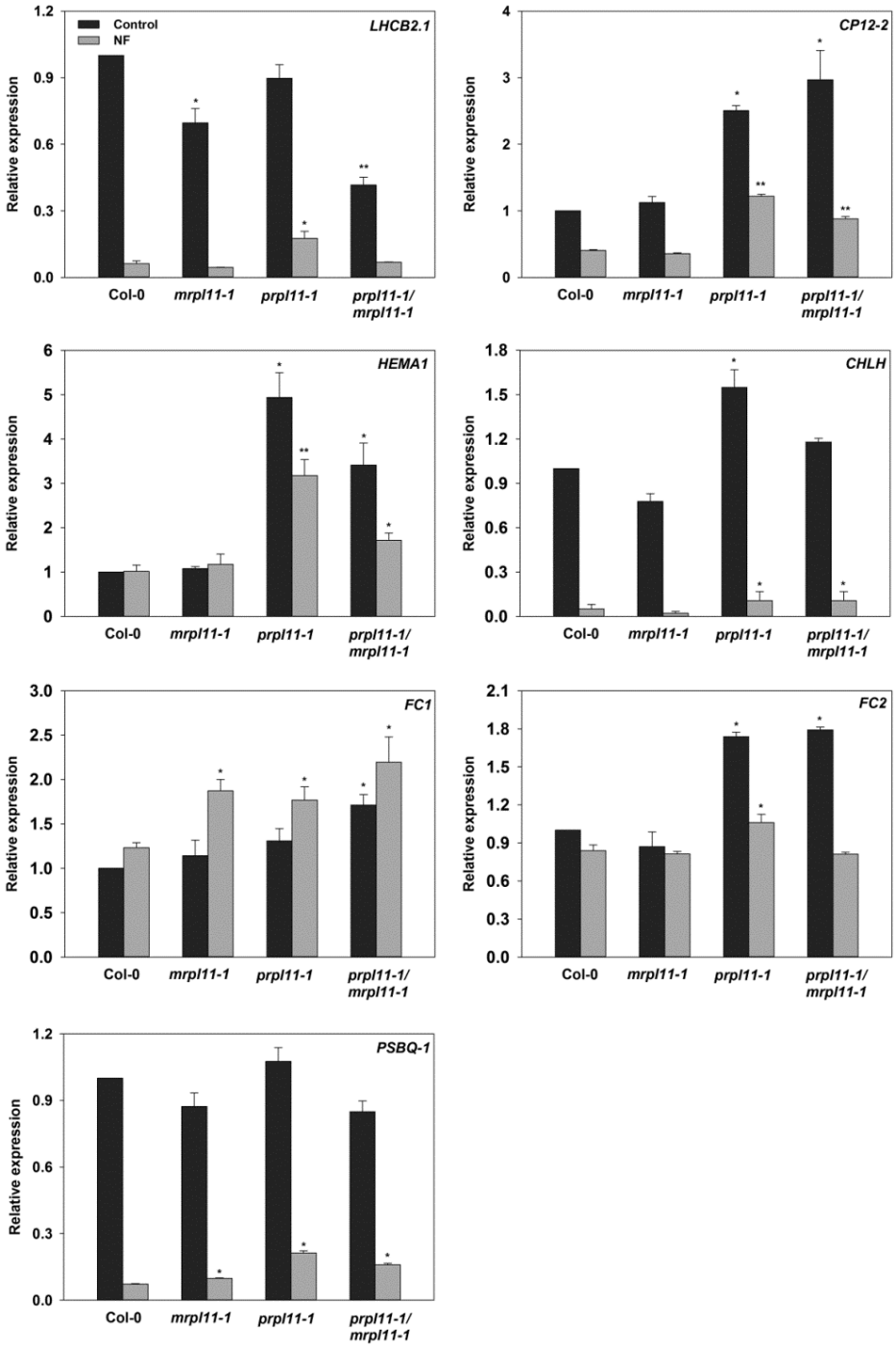

Figure 4.1 Regulation of nuclear gene expression in *prpl11-1, mrpl11-1* and double *prpl11-1*/*ml11-1* mutants treated with norflurazon (NF). WT (Col-0), *prpl11-1, mrpl11-1* and double *prpl11-1/mrpl11-1* seedlings were grown on 1% agar medium, with ½ MS (pH 5.6) and with or without 1 µM NF under the following conditions: 2 d D, 3 d WLc (100 µmol m^{-2} s^{-1}). Expression is relative to control Col-0 samples and normalised to *YELLOW LEAF SPECIFIC GENE 8* (*YLS8*, At5g08290). Data shown are means +SEM of three independent biological replicates. Asterisks denote a significant difference vs. Col-0 for the same treatment, Student's *t*-test (*$p < 0.05$, **$p < 0.01$).

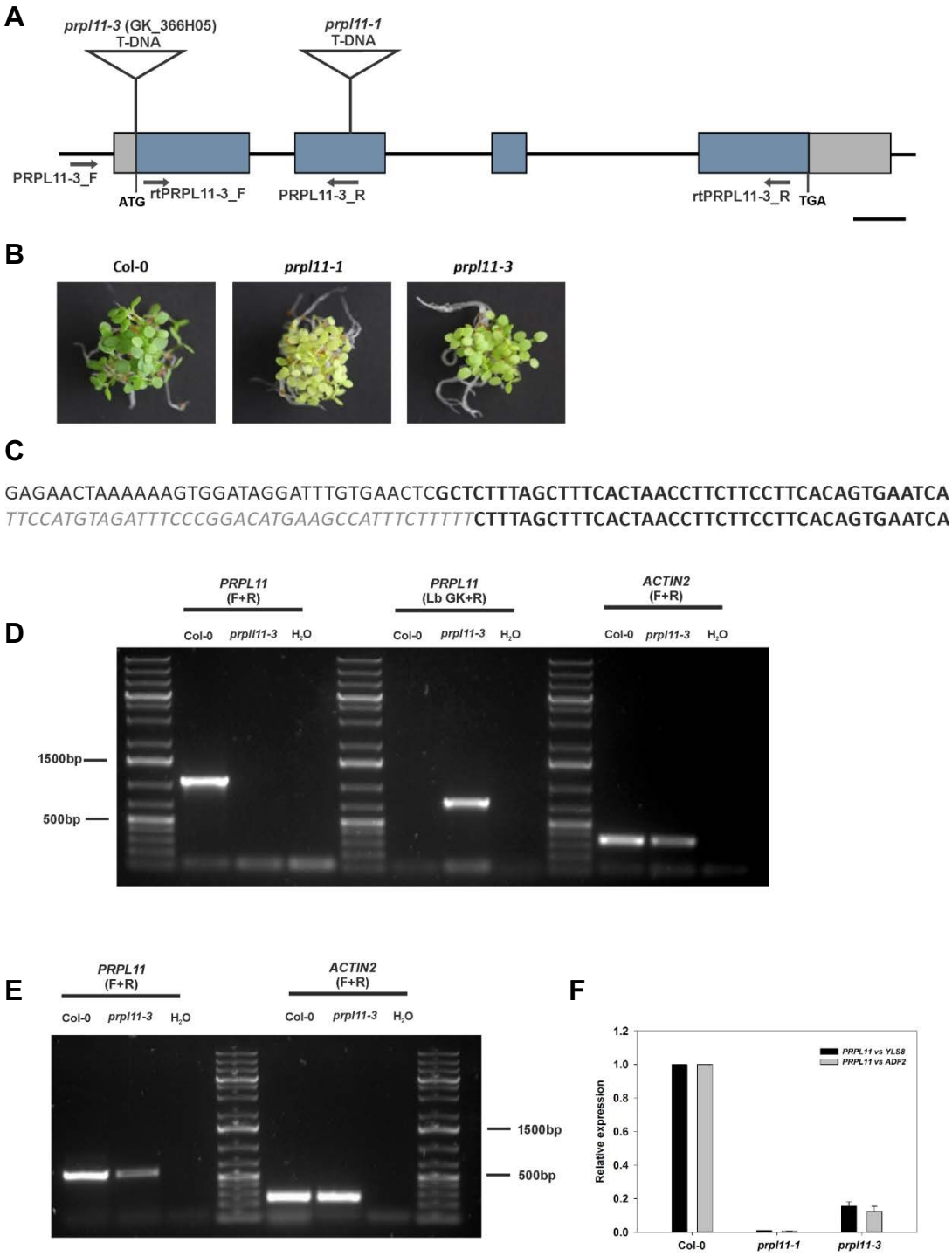

Figure 4.2 Analysis of the new T-DNA insertion allele *prpl11-3*. (A) Schematic diagram depicting the *prpl11-1* and *prpl11-3* T-DNA insertion sites at the *PRPL11* locus. Blue boxes represent exons, grey boxes represent UTR regions, and black lines represent introns. PCR and RT-PCR primers used for genotyping are indicated by black arrows. Scale bar represents 100 bp. T-DNA insertions and primer pairs are not drawn to scale. (B) Visible phenotype of the *prpl11-1* and *prpl11-3* seedlings grown for 2 d D and 3 d WLc on 1% agar, with ½ MS (pH 5.6). (C) Sequence analysis of the T-DNA insertion in *prpl11-3* mutant. T-DNA insert fragment is marked in grey italic, 5´UTR end in black bold, and the region upstream of it in black italic. (D) Confirmation of the T-DNA insertion by PCR amplification. Genomic DNA from Col-0 and *prpl11-3* plants was amplified using gene specific primers (F+R) and left border specific primer (LbGK + R). (E) RT-PCR analysis of *PRPL11* transcripts in *prpl11-3* using primers binding the first and second exon, shown in A. *ACTIN2* was used as a control. (F) qPCR analysis of *PRPL11* expression in Col-0, *prpl11-1* and *prpl11-3* mutants. Expression is normalised relative to WT (Col-0) and to *YELLOW LEAF SPECIFIC GENE 8* (*YLS8*, At5g08290). *ACTIN2* was used as a control. Data shown are mean + SEM of 3 biological replicates.

The two *prpl11* alleles, along with two *gun* mutants (*gun1-1* and *gun5-1*), were screened for their ability to rescue gene expression under the same NF conditions as before. As shown in Figure 4.3, both *prpl11* mutant alleles displayed a similar *gun*-like phenotype for *HEMA1* and *CP12-2* expression on NF. For *prpl11-1,* the two other genes tested, *LHCB2.1* and *CHLH,* were up-regulated significantly on NF compared to Col-0, but this was not observed for *prpl11-3*, supporting previous observations that *prpl11-1* is a stronger allele then *prpl11-3*. Under these conditions both control lines *gun1-1* and *gun5-1* showed a strong *gun* phenotype, with significant elevation of *LHCB2.1* expression, complete rescue of *CP12-2*, *CHLH* and up-regulation of *HEMA1* relative to wild type. Importantly, both *prpl11* alleles displayed significantly increased expression of *HEMA1* and *CP12-2* under the control conditions as seen previously. The gene expression phenotype of *prpl11-1* was therefore conserved across both *prpl11* alleles.

As described earlier, among all *gun* mutants only *gun1* can rescue photosynthetic gene expression on Lin. The *prpl11-1* and *prpl11-3* mutants, along with *gun1-1* and *gun5-1,* were screened for their ability to rescue gene expression on Lin, in order to examine whether the *gun*-like phenotype of the *prprl11* mutant is similar to *gun1* or the other *gun* mutants that can only rescue after NF treatment. The growth conditions for this experiment were the same as for the NF treatment, with the exception that the growth media was supplemented with 0.5 mM Lin. Consistent with the two earlier experiments, a significant up-regulation of *HEMA1, CHLH* and *CP12-2* was detected in both *prpl11* alleles when seedlings were grown under the control conditions of 2 d D and 3 d WLc without Lin (Figure 4.4). The trend for elevated tetrapyrrole gene expression was also apparent in *gun5-1* mutant, and to a lesser extent in the *gun1-1* mutant under control conditions. However, in contrast to the result after NF, Lin treatment resulted in a complete loss of the elevated nuclear gene expression phenotype of both *prprl11* alleles. These two mutants and *gun5-1* showed a wild type level of *LHCB2.1*, *CP12-2, HEMA1* and *CHLH* expression after Lin treatment (Figure 4.4). In agreement with literature reports (*e.g.* Koussevitzky et al., 2007), only *gun1-1* was able to maintain a higher expression of all 4 genes tested on Lin, as compared to the wild type (Figure 4.4). This suggests that the *gun*-like phenotype of *prprl11* mutants is at least partially different from *gun1*.

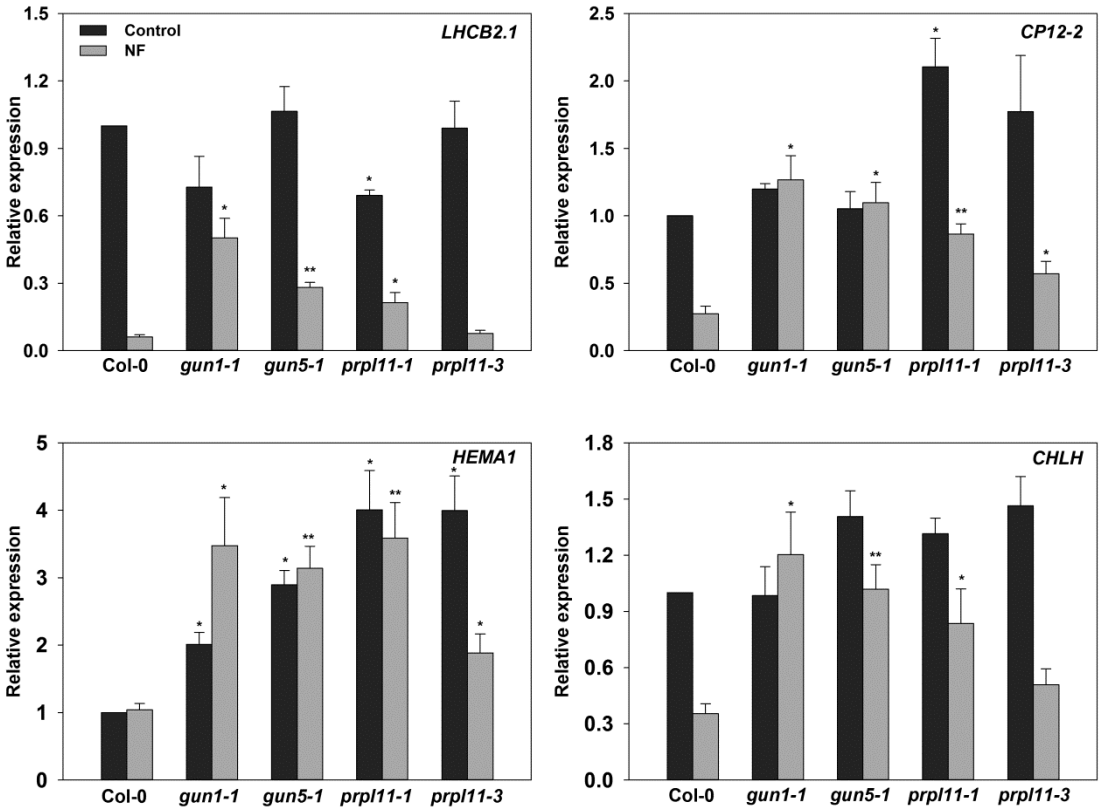

Figure 4.3 Regulation of nuclear gene expression in *prpl11-1* and *prpl11-3* mutants treated with norflurazon (NF). WT (Col-0), *gun1-1*, *gun5-1*, *prpl11-1* and *prpl11-3* seedlings were grown on 1% agar medium, with ½ MS (pH 5.6) and with or without 1 µM NF under the following conditions: 2 d D, 3 d WLc (100 µmol m^{-2} s^{-1}). The *gun1-1* and *gun5-1* mutants were included as controls for rescue of gene expression on NF. Expression is relative to Col-0 in the absence of NF and normalised to *YELLOW LEAF SPECIFIC GENE 8* (*YLS8*, At5g08290). Data shown are means +SEM of three independent biological replicates. Asterisks denote a significant difference vs. Col-0 for the same treatment (Control / NF), Student's *t*-test (*p < 0.05, **p < 0.01).

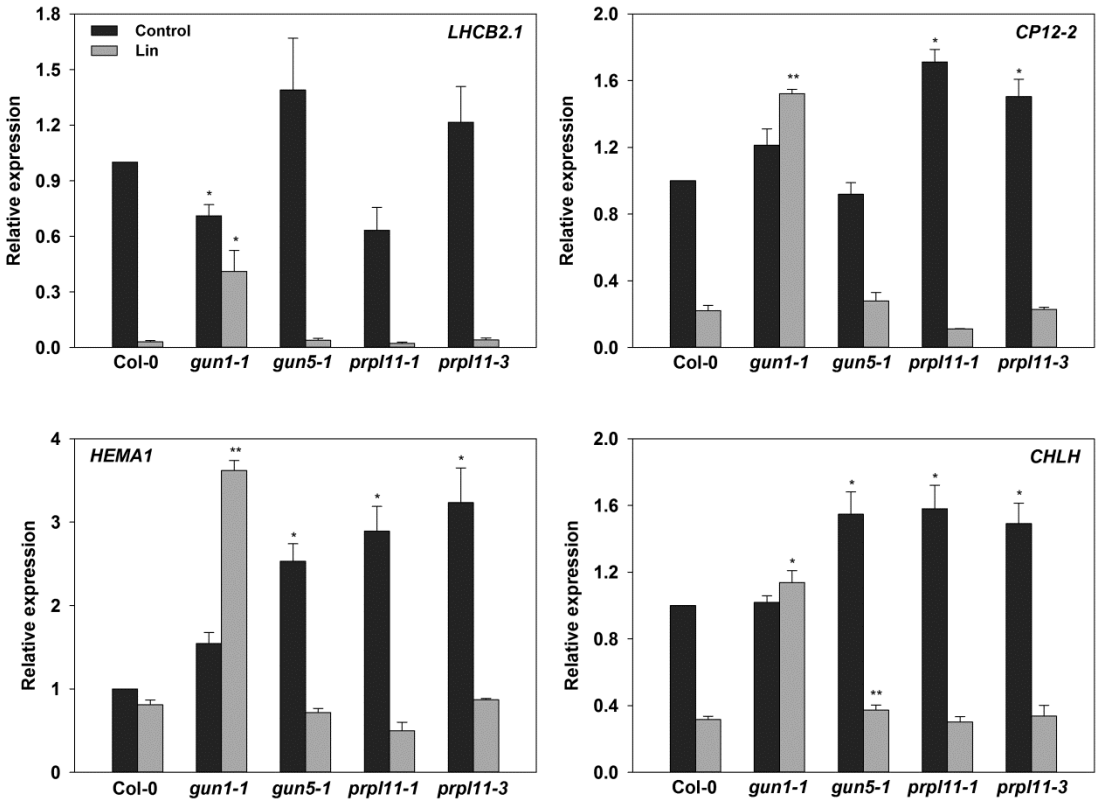

Figure 4.4 Regulation of nuclear gene expression in *prpl11-1* and *prpl11-3* mutants treated with lincomycin (Lin). WT (Col-0), *gun1-1*, *gun5-1*, *prpl11-1* and *prpl11-3* seedlings were grown on 1% agar medium, with ½ MS (pH 5.6) and with or without 0.5 mM µM Lin under the following conditions: 2 d D, 3 d WLc (100 µmol m^{-2} s^{-1}). The *gun1-1* (known to rescue gene expression on Lin) and *gun5-1* (unable to rescue gene expression on Lin) mutants were included as controls. Expression is relative to Col-0 in the absence of Lin and normalised to *YELLOW LEAF SPECIFIC GENE 8* (*YLS8*, At5g08290). Data shown are means +SEM of three independent biological replicates. Asterisks denote a significant difference vs. Col-0 for the same treatment (Control / Lin), Student's *t*-test (*$p < 0.05$, **$p < 0.01$).

To gain more understanding on the role of PRPL11 in regulation of nuclear-encoded chloroplast genes, the expression of *HEMA1*, *LHCB2.1* and *CP12-2* was studied in wild type, *prpl11-1* and *gun1-1*after 2 days growth in dark and transfer to WLc for 1-3 d (Figure 4.5). After the first day of transfer to WLc, light induction of *HEMA1*, *LHCB2.1* and *CP12-2* expression was reduced in the *prpl11-1* mutant compared to wild type and *gun1-1* (Figure 4.5). However, after 2 d WLc exposure this phenotype was reversed and expression of *HEMA1* and *CP12-2* was strongly elevated in *prpl11-1* mutant. This trend continued 3 d after WLc exposure resulting in a more than 2-fold up regulation of *HEMA1* expression in *prpl11-1* relative to Col-0. PRPL11 control over nuclear gene expression therefore depends on the time of WLc exposure. The time course of gene expression in seedlings grown on NF was consistent with previous experiments (see Figures 4.1 and 4.3). The characteristic phenotype of *prpl11-1* with enhanced expression of *HEMA1* and *CP12-2* was still apparent 2-3 days after transfer to WLc on NF (Figure 4.5), supporting the conclusion that *prprl11-1* displays a *gun*–like phenotype. However, in contrast to *gun1-1*, which showed a strong rescue of *LHCB2.1* expression on NF relative to wild type, *prpl11-1* rescue of *LHCB2.1* was very weak and detected only after 3 days after transfer to WLc (Figure 4.5).

To test whether the *prpl11* phenotype could be seen in the absence of light, seedlings were grown in the dark for 5d and gene expression measured (Figure 4.6). Under these conditions both *prpl11* alleles had a wild type level of gene expression for both photosynthetic and tetrapyrrole genes (Figure 4.6), demonstrating that the *prpl11* phenotype is light dependent. In this experiment, the expression of two *GLK* transcription factors was additionally measured as they have been proposed to coordinate light responses and retrograde signalling, as well as regulate tetrapyrrole biosynthesis gene expression (Martin et al., 2016, Waters et al., 2009). These genes were mostly unaffected in *prpl11* mutants with only a slight inhibition of dark *GLK2* expression in the *prpl11-1* allele only. *GLK1* did show a moderate up-regulation in *gun1-1* and *gun5-1*, although this wasn't significant at the 5% level. *LHCB2.1* was also elevated, especially in *gun1-1* in the dark.

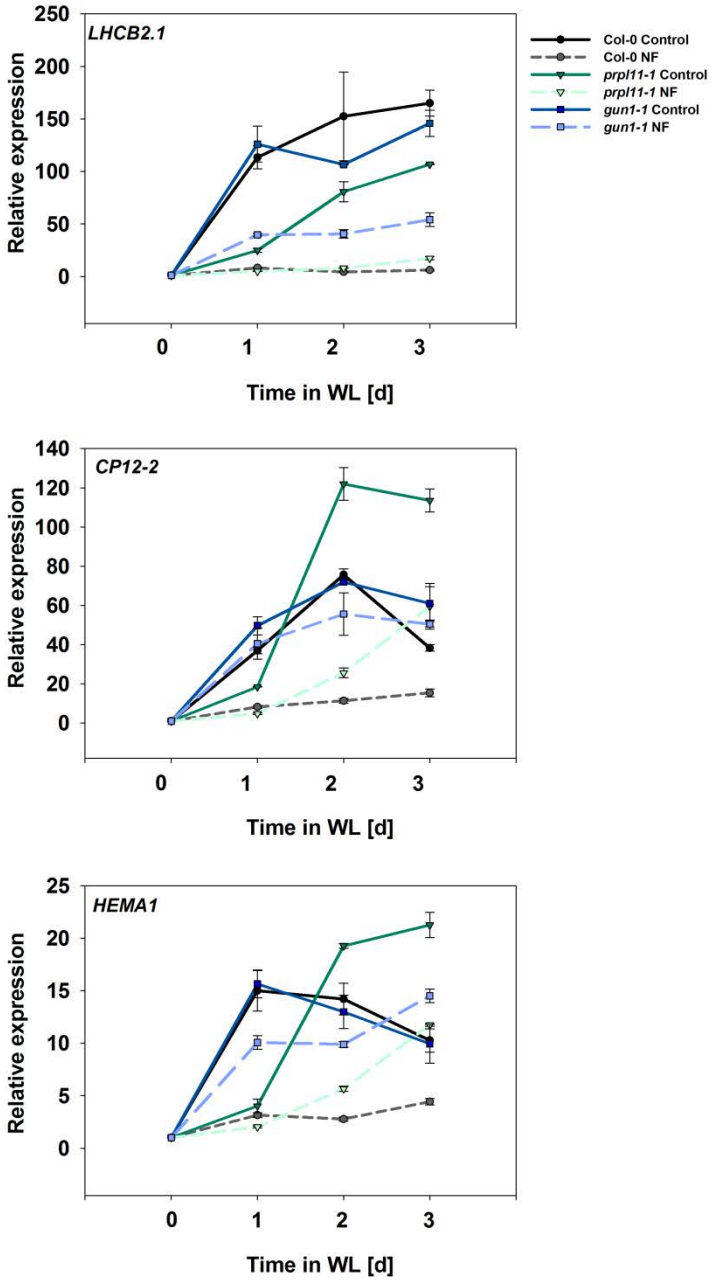

Figure 4.5 Time course of *LHCB2.1, CP12-2* and *HEMA1* gene expression in WT (Col-0), *gun1-1* and *prpl11-1* mutants grown on norflurazon (NF). Seedlings grown on 1% agar with ½ MS medium supplemented with or without 1 µM NF and without sucrose, under the following conditions: 2 d dark followed by a transfer to WLc (100 µmol m^{-2} s^{-1}) for 1, 2 and 3 d. Gene expression was measured by quantitative RT-PCR analysis and is shown relative to 2 d dark-grown Col-0 and normalised to *YELLOW LEAF SPECIFIC GENE 8* (*YLS8,* At5g08290*)*. Data shown are means ±SEM of three independent biological replicates.

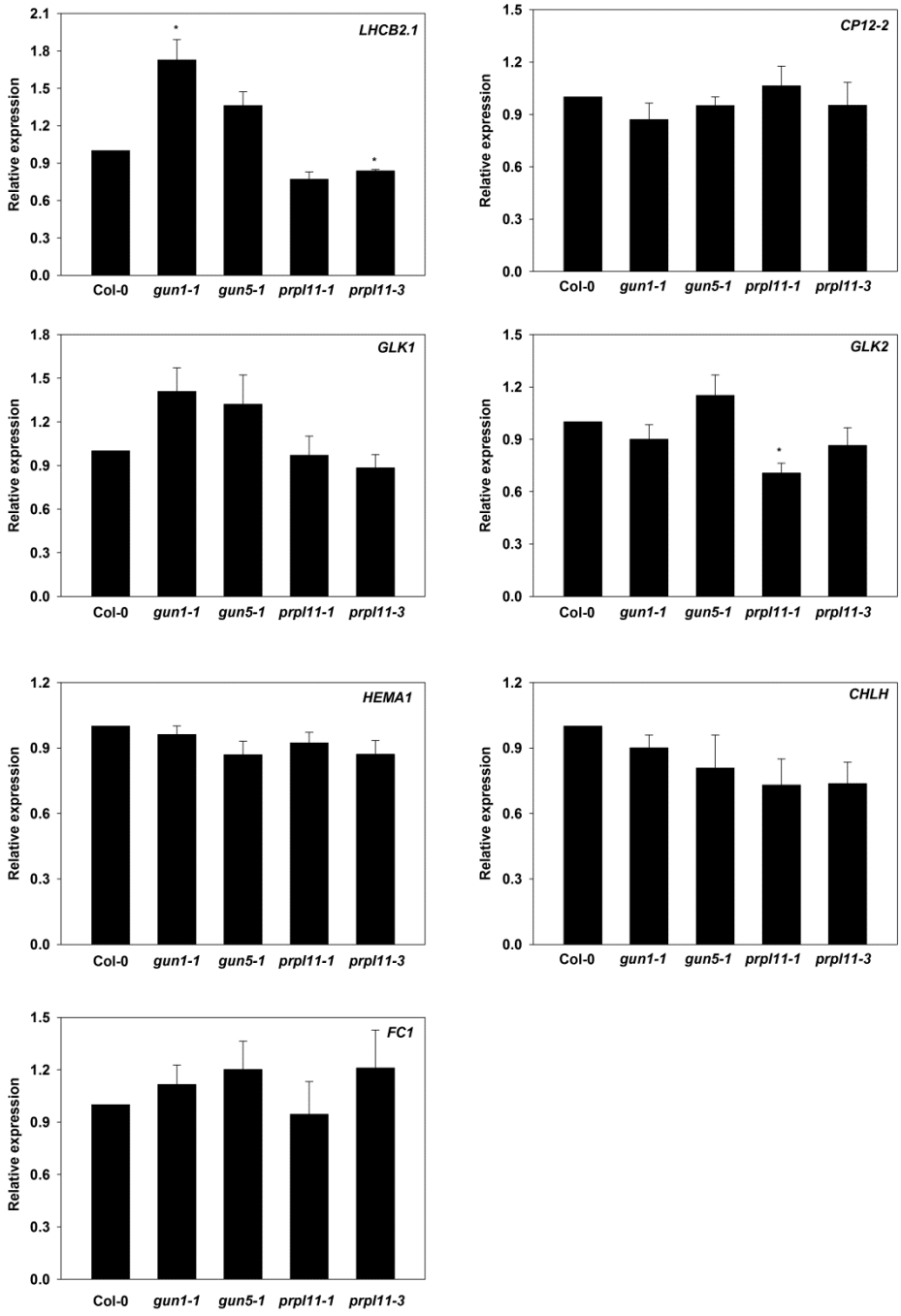

Figure 4.6 Nuclear gene expression in dark-grown *prpl11* mutants. WT (Col-0), *gun1-1*, *gun5-1*, *prpl11-1* and *prpl11-3* seedlings were grown on 1% agar medium, with ½ MS (pH 5.6) without sucrose for 5 d in the dark. Expression is relative to Col-0 and normalised to *YELLOW LEAF SPECIFIC GENE 8* (*YLS8*, At5g08290). Data shown are means +SEM of three independent biological replicates. Asterisks denote a significant difference vs. Col-0, Student's *t*-test (*p < 0.05).

In the next step it was important to examine the specificity of the *prprl11* gene expression phenotype. Firstly, the expression of nuclear-encoded mitochondrial genes was examined in the single *prpl11-1*, *mrpl11-1* and the double *prpl11-1/mrpl11-1* mutants grown under the same control conditions of 2 d D and 3 d WLc used earlier (Figure 4.7A). The quantitative RT-PCR analysis of gene expression showed significant up-regulation of some nuclear-encoded mitochondrial transcripts, including *NDA2*, *NDB2* and *UPOX1,* in the mitochondrial translation mutant *mrprl1-1.* However, this response was not specific to the mitochondrial disruption, as expression of *UPOX1* was also enhanced in *prpl11-1,* as were *NDA1* and *APOX1a* that were not significantly elevated in *mrprl1-1* (Figure 4.7A). In the double mutant *NDA1*, *NDB2*, *APOX1a* and *UPOX1* were all up regulated, but with no additive effect. The PEP-, NEP-dependent transcripts plastid transcripts and mitochondrial transcripts were then analysed in these mutants under the same growth conditions (Figure 4.7B). The general trend was that mitochondrial transcripts *cox1* and *nad2* were up regulated in the *mrpl11-1* mutant and NEP-dependent transcripts (*clpP* and *rpoB*) were more than 2-3-fold up-regulated in *prprl11-1* and *prpl11-1/mrpl11-1*. The phenotype observed in single mutants was not further changed in the double *prpl11-1/mrpl11-1* mutant (Figure 4.7B).

PRPL11 is a part of a large protein complex in the chloroplast ribosome. To further assess its specificity, the expression of nuclear-encoded chloroplast genes was measured in two additional mutants: one lacking the large ribosome subunit L24 (*prpl24-1*) and another small ribosome subunit S21 (*prps21-1*). As shown in Figure 4.8, significantly elevated expression of *HEMA1* and *CP12-2* was measured in both *prpl24-1* and *prps21-1* mutants as compared to their representative wild types under the control conditions. Although the expression of these genes in both mutants was strongly down-regulated on NF, it was still higher relative to the NF-treated wild types. The gene expression phenotypes of *prpl24-1* and *prps21-1* mutants are therefore similar to the *prpl11-1* mutant, but not as strong.

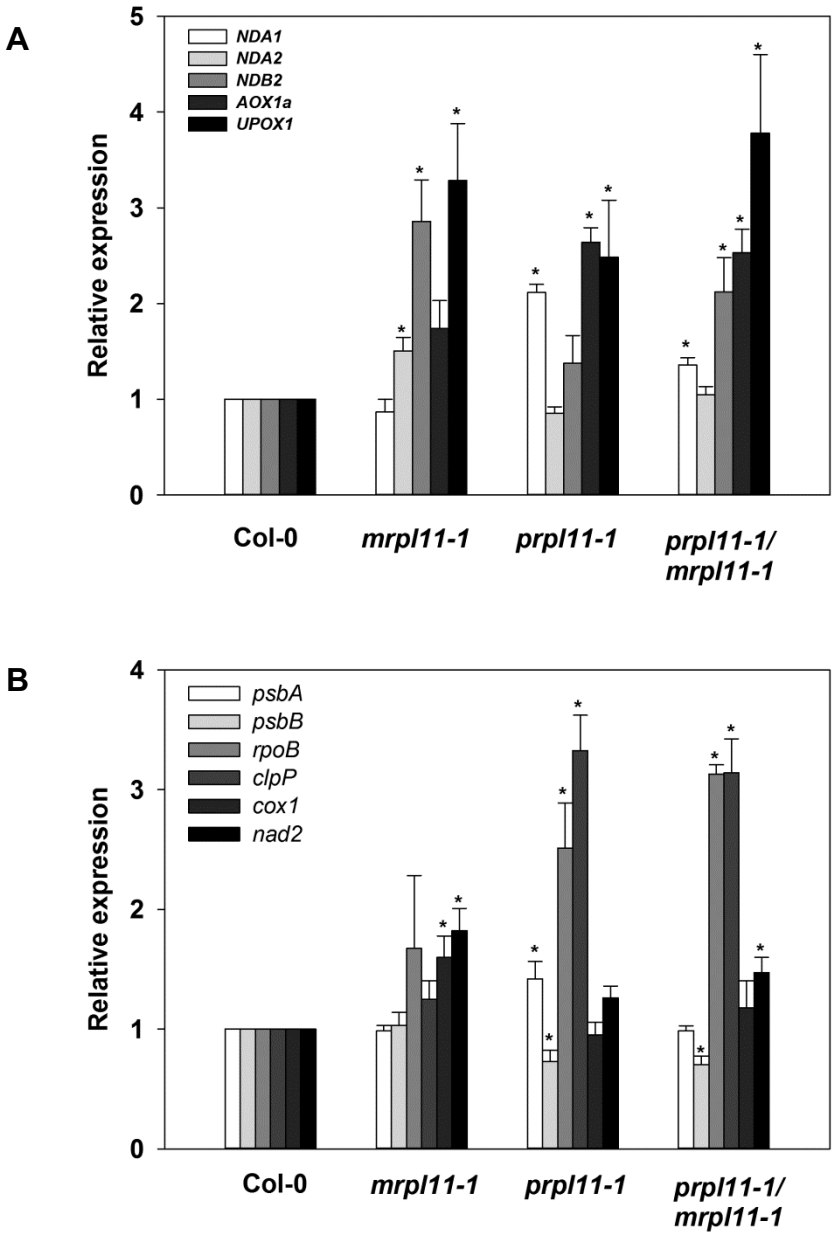

Figure 4.7 Regulation of nuclear- and organelle-encoded gene expression in *prpl11-1, mrpl11-1* and *prpl11-1/mrpl11-1* mutants. WT (Col-0), *prpl11-1, mrpl11-1* and *prpl11-1/mrpl11-1* seedlings were grown on 1% agar medium, with ½ MS (pH 5.6) without sucrose under the following conditions: 2 d D, 3 d WLc (100 µmol m^{-2} s^{-1}). (A) Nuclear-encoded mitochondrial genes. (B) Chloroplast- (NEP–dependent *rpoB*, *clpP*; PEP-dependent *psbA*, *psbB*) and mitochondria-encoded (*cox1*, *nad2*) genes. Expression is shown relative to Col-0 and normalised to *YELLOW LEAF SPECIFIC GENE 8* (*YLS8*, At5g08290). Data shown are means +SEM of three independent biological replicates. Asterisks denote a significant difference vs. Col-0. Student's *t*-test (*$p < 0.05$).

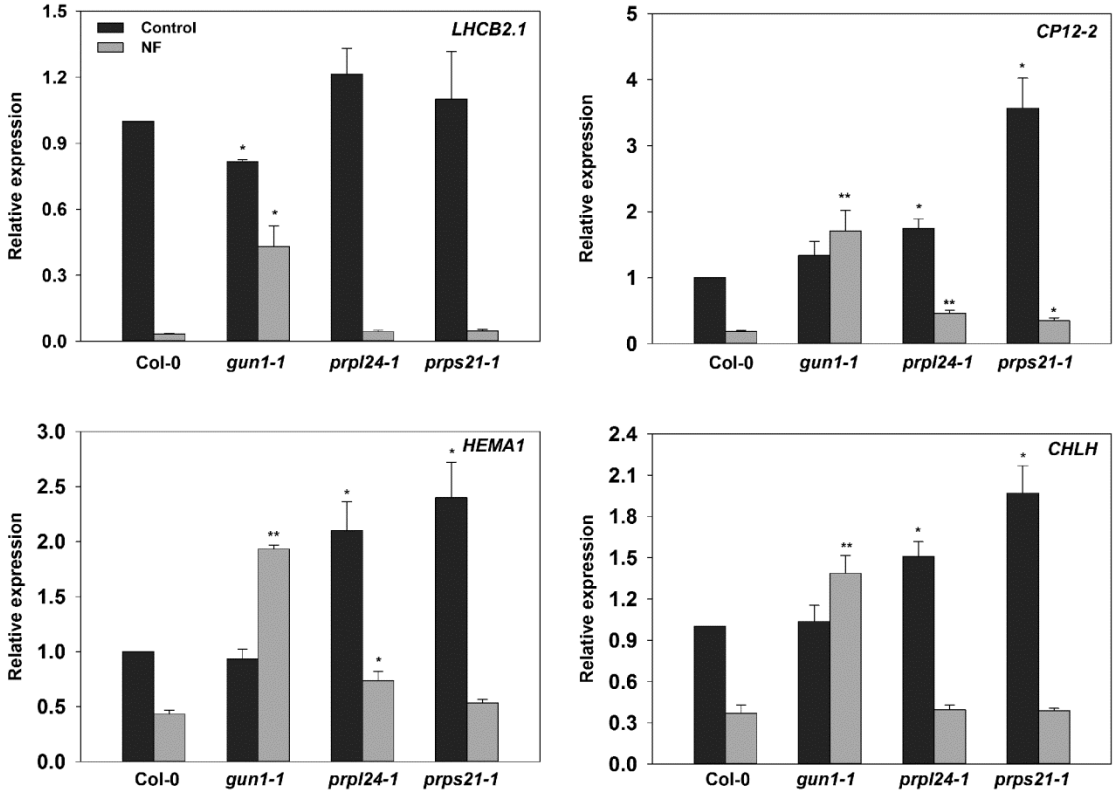

Figure 4.8 Regulation of nuclear gene expression in *prpl24-1* and *prps21-1* mutants treated with norflurazon (NF). WT (Col-0), *prpl24-1* and *prps21-1* seedlings were grown on 1% agar medium, with ½ MS (pH 5.6) and with or without 1 µM NF under the following conditions: 2 d D, 3 d WLc (100 µmol m^{-2} s^{-1}). Expression is shown relative to wild type under control conditions and normalised to *YELLOW LEAF SPECIFIC GENE 8* (*YLS8*, At5g08290). Data shown are means +SEM of three independent biological replicates. Asterisks denote a significant difference vs. Col-0 for the same treatment (Control / NF), Student's *t*-test (*p < 0.05, **p < 0.01).

4.2.2 PRPL11 alters tetrapyrrole metabolism

The *prprl11* mutant displays an elevated expression of some photosynthetic and tetrapyrrole genes suggesting a potential involvement in retrograde signalling. One current hypothesis for this signal is that it is mediated via an increase in FC1 activity (Woodosn et al., 2011; see Chapter 3). To examine this in more detail, the PRPL11 impact on tetrapyrrole metabolism was next examined. As shown in Figure 4.9A (left panel) both alleles of dark-grown *prprl11* mutant seedlings had 2 up to 4 time less Pchlide than wild type. To test whether this was due to an inhibition of early steps in the tetrapyrrole pathway synthesis or due to the defects at later stages, seedlings were fed with ALA in the dark. Figure 4.9A (left) shows that seedlings of both *prpll11* alleles still accumulated less Pchlide, even after treatment with a high ALA concentration of 0.2 mM, which actually exacerbated the difference between mutants and wild type. This suggests *prpl11* is affected in downstream steps of protochlorophyllide biosynthesis.

Mutants in two other plastid ribosomal proteins, *prpl24-1* and *prps21-1,* had the same phenotype for Pchlide accumulation after ALA feeding (Figure 4.9A, right).

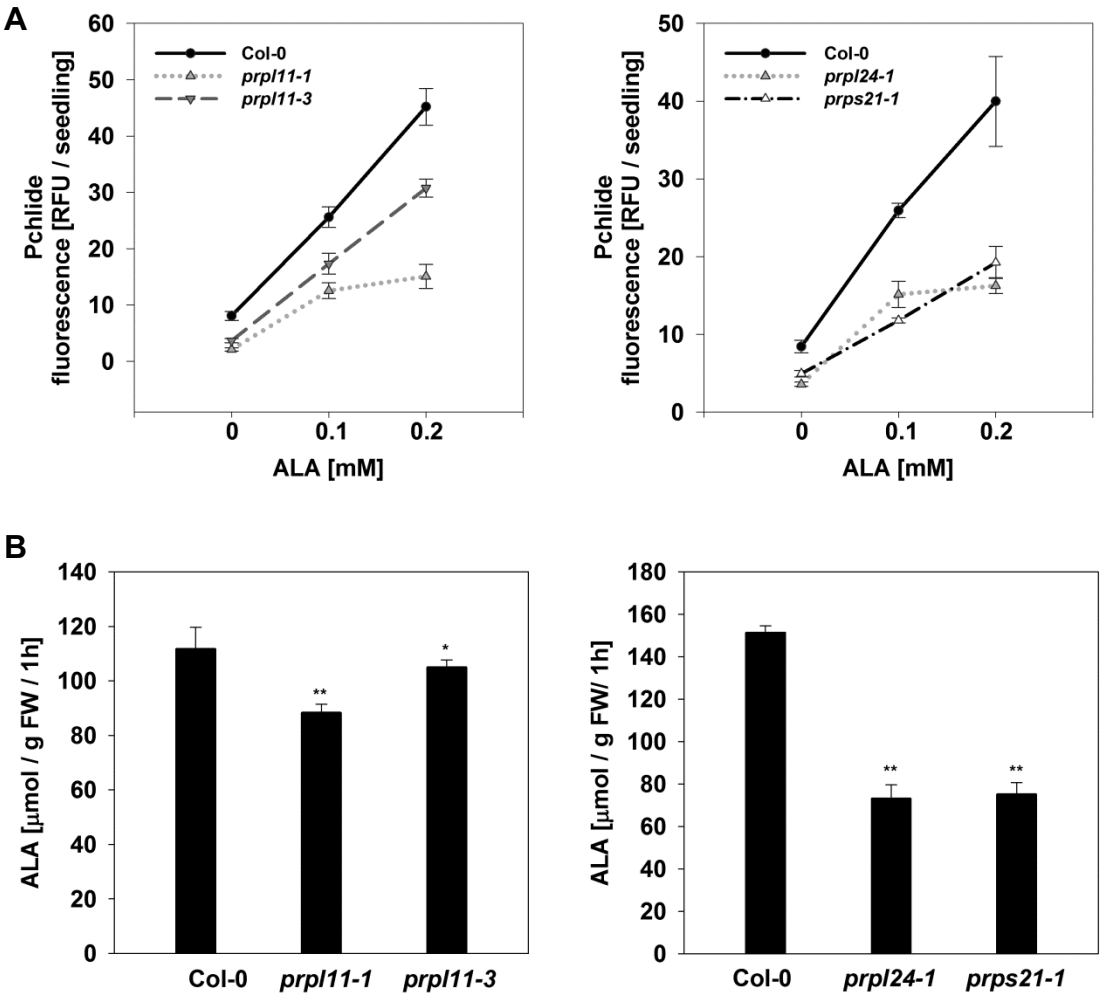

Figure 4.9 Analysis of tetrapyrrole metabolism in *prpl11-1, prpl11-3* and other plastid translation mutants. (A) Protochlorophyllide (Pchlide) analysis for WT (Col-0), *prpl11-1, prpl11-3, prpl24-1*and *prps21-1* seedlings grown 4 days in the dark on 1% agar medium with ½ MS (pH 5.6), supplemented with 5 mM MES, and with or without 0.1-0.2 mM ALA. Data shown are means ± SD of three independent biological replicates. 30 seedlings were analysed for each replicate. (B) ALA synthesis rate in Col-0, *prpl11-1, prpl11-3, prpl24-1*and *prps21-1* seedlings grown on 1% agar medium, with ½ MS (pH 5.6) under the following conditions: 2 d dark and 3 d WLc (100 µmol m^{-2} s^{-1}). For the last 2 h of WLc treatment whole seedlings were transferred to 50 mM Tris-HCl supplemented with 40 mM levulinic acid (pH 7.2). Data shown are mean + SD of three independent biological replicates. Asterisks denote a significant difference vs. Col-0, Student's *t*-test (*p < 0.05, **p < 0.01).

One possible reason for the reduced Pchlide in *prpl11* is that flux through the tetrapyrrole pathway is redirected to the heme branch. To test this possibility, the rate of ALA synthesis was measured in *prprl11* mutant lines as well in *prpl24-1* and *prps21-1* (Figure 4.9B). Using growth

conditions of 2 d D and 3 d WLc followed by 2 h of treatment with ALA dehydratase inhibitor, LA, all analysed genotypes accumulated significantly less ALA as compared to the wild type. Since ALA feeding cannot rescue Pchlide levels, one explanation for this result is that increased flux through the heme branch of the pathway is causing feedback inhibition of ALA synthesis (Terry and Kendrick, 1999). To test this, it would be necessary to measure this heme pool, but this is not currently feasible. Instead, total heme content was measured in light-grown seedlings (Figure 4.10). For both *prpl11* alleles the total heme content was significantly lower relative to the wild type (Figure 4.10) and this is consistent with the reduced size of the photosynthetic apparatus in these plants (Pesaresi et al., 2006).

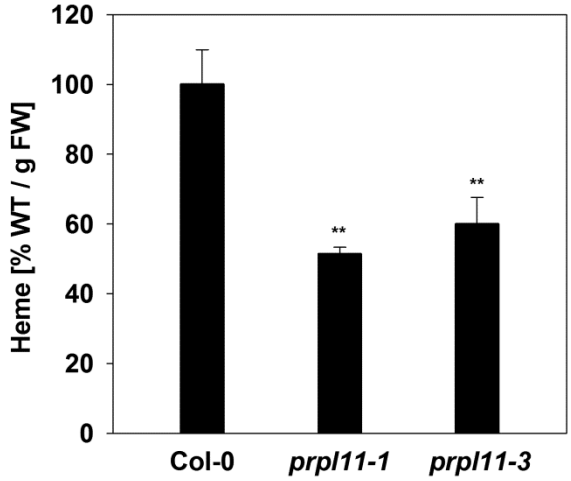

Figure 4.10 Analysis of total heme levels in *prpl11-1* and *prpl11-3* mutants. WT (Col-0), *prpl11-1*, and *prpl11-3* seedlings grown on 1% agar medium, with ½ MS (pH 5.6), without sucrose, under the following conditions: 2 d dark and 3 d WLc (100 µmol m^{-2} s^{-1}). Data shown are means +SD of three independent biological replicates. Asterisks denote a significant difference vs. Col-0, Student's *t*-test (**$p < 0.01$).

To test further the hypothesis that increased heme levels was the cause of the increased gene expression phenotype in *prpl11* mutants, heme synthesis was blocked by treatment with 2,2'-dipyridyl (DP). As shown in Figure 4.11, in both *prpl11* mutant alleles *HEMA1* expression was up-regulated almost 3-fold under the control conditions of 2 d D and 3 d WLc, and was severely reduced by DP treatment with even the lowest DP concentration showing a strong effect. Similar results were seen for *LHCB2.1*. Interestingly, *FC1* expression, which is usually enhanced during conditions that block plastid signalling, was more up regulated in *prprl11* mutants than in wild type after treatment with higher concentrations of DP (Figure 4.11). In this experiment the heme oxygenase mutant, *hy1 (gun2)*, was included. This mutant is deficient in heme degradation and was predicted to be more resistant to the effects of DP. Such a response was seen for *HEMA1* but not for *LHCB2.1* (Figure 4.11).

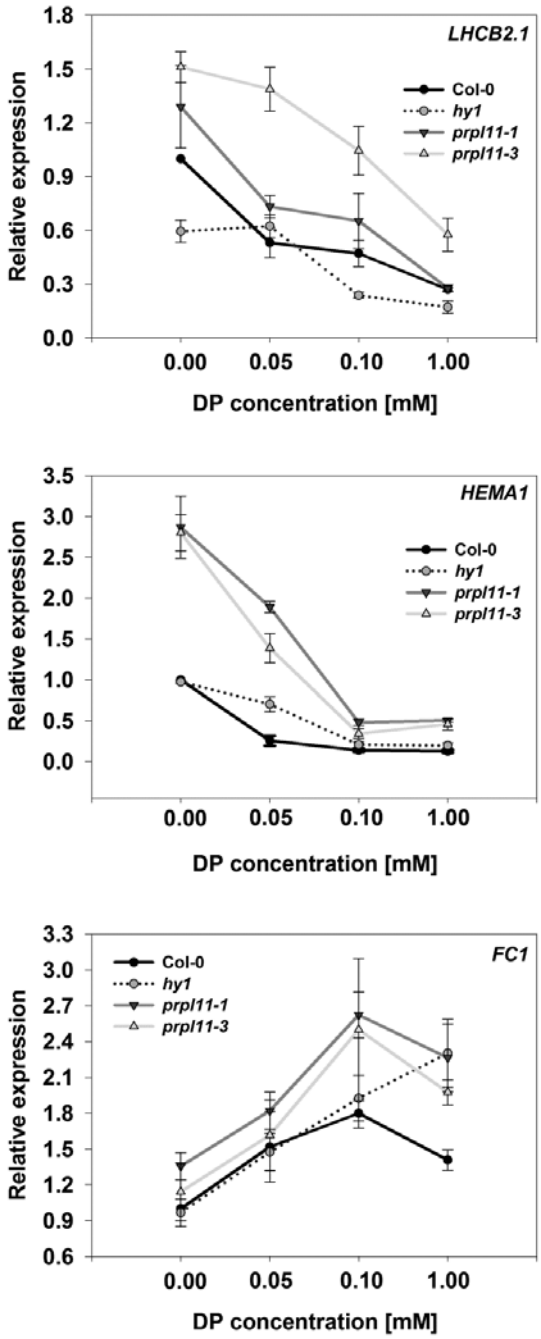

Figure 4.11 Regulation of nuclear gene expression in *prpl11-1* and *prpl11-3* mutants treated with 2,2'-Dipyridyl (DP). WT (Col-0), *prpl11-1, prpl11-3* and *hy1* seedlings were grown on 1% agar medium, with ½ MS (pH 5.6) and under the following conditions: 2 d dark, 3 d WLc (100 µmol m^{-2} s^{-1}). For the last 6 h of WLc growth seedlings were transferred to water supplemented with 0.1 mM DP (DP) or to control conditions (water with ethanol at 0.02%). Expression is shown relative to Col-0 in the absence of DP and normalised to *YELLOW LEAF SPECIFIC GENE 8* (*YLS8*, At5g08290). Data shown are means ±SEM of three independent biological replicates.

The plastid ribosome protein mutants clearly affect tetrapyrrole metabolism and it was therefore of interest to test whether they are also impaired in light sensing. The hypocotyl length was measured in the dark, far-red, red, blue and low WL grown seedlings of wild type, both *prpl11* alleles, *prpl24-1* and *prps21-1* as well control lines (Figures 4.12 and 4.13). Analysis showed that all plastid translation mutants are hypersensitive to red, blue and WL light, with a shorter hypocotyl length than the wild type. The length of the hypocotyl in all 4 mutant alleles was similar to WT level under far red and in the dark, with the exception of *prpl24-1* that had a slightly shorter hypocotyl length in the dark (Figures 4.12 and 4.13).

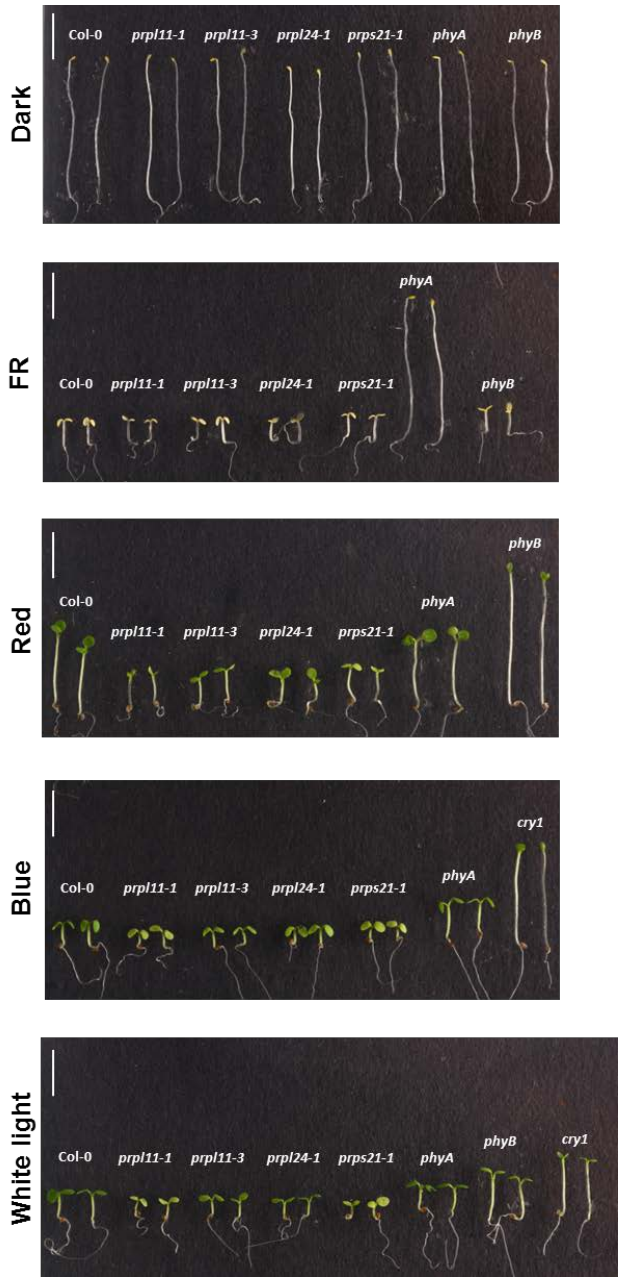

Figure 4.12 *Arabidopsis* plastid translation mutants are affected in light sensing. Seedlings were grown on 1% agar medium, with ½ MS (pH 5.6), without sucrose, at 22°C under the following conditions: 1 d dark pre-treatment and 5 d dark, far-red (FR, 10 µmol m^{-2} s^{-1}), red (60 µmol m^{-2} s^{-1}), blue (20 µmol m^{-2} s^{-1}) and low while light (20 µmol m^{-2} s^{-1}). Representative photographs showing phenotype of seedlings are displayed. Scale bar represents 5 mm.

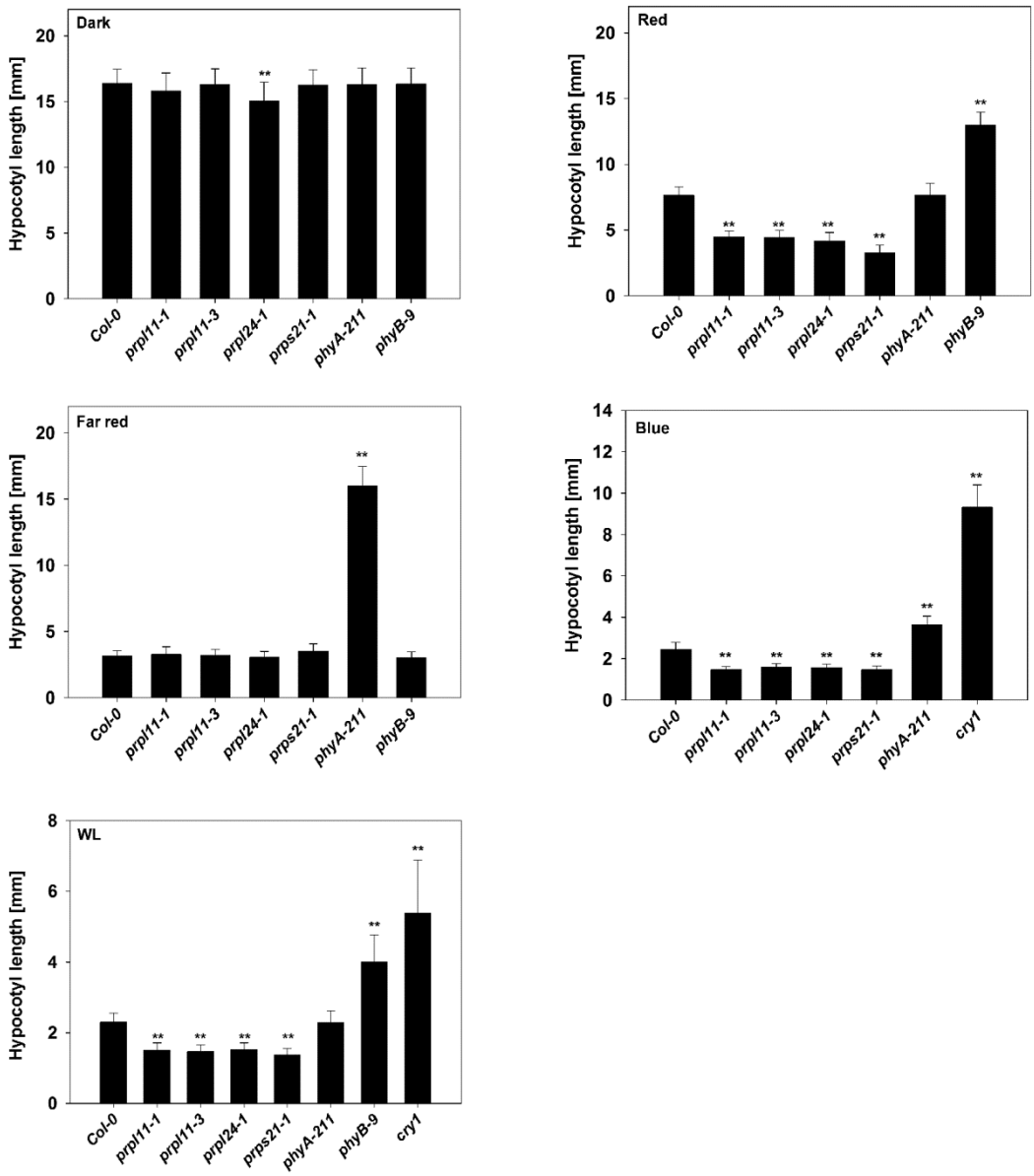

Figure 4.13 Hypocotyl length of various p**lastid translation under different light conditions**. Seedlings were grown on 1% agar medium, with ½ MS (pH 5.6), without sucrose, at 22°C under the following conditions: 1 d dark pre-treatment and 5 d dark, far-red (10 µmol m^{-2} s^{-1}), red (60 µmol m^{-2} s^{-1}), blue (20 µmol m^{-2} s^{-1}) and low while light (WL, 20 µmol m^{-2} s^{-1}). Data shown are means + SD from 3 independent experiments with 20 seedlings analysed for each replicate. Asterisks denote a significant difference vs. WT (Col-0) for the same treatment (Dark, Far red, Red, Blue, WL), Tukey HSD test (*$p < 0.05$, **$p < 0.01$).

4.2.3 Construction of PRPL11 overexpressing lines

To further define the molecular role of PRPL11 in tetrapyrrole-dependent retrograde signalling and to explain the specific gene expression phenotype, the functional mechanism of PRPL11 was examined in more detail. A series of 35S::PRPL11-GFP and 35S::PRPL11-TAP lines (herein named 35S::PL11-GFP/TAP) were generated in both WT and *prpl11-1* mutant backgrounds to look for proteins that can bind PRPL11. Homozygote transformants were selected in the T3 generation and expression of the transgenes was evaluated by quantitative RT-PCR using a *PRPL11* specific qPCR primer pair (Figure 4.14). Analysis showed that all lines generated in the WT background, had a WT level of *PRPL11* expression or slightly lower and this was true for both the 35S::PL11-GFPand 35S::PL11-TAPlines. This was coupled with a *prpl11*-like phenotype in seedlings of many of these lines, seen as reduced greening (data not included), strongly suggesting that silencing was occurring. In contrast, most of the lines generated in the *prpl11-1* genetic background showed a clear and considerable increase in *PRPL11* expression, and this was observed for both 35S::PL11-GFPand 35S::PL11-TAPlines (Figure 4.14). Two lines *prpl11*35S::PL11-GFP3.2 and *prpl11*35S::PL11-GFP10.1 showed the highest increase in *PRPL11* expression (a more than 10-15 fold increase) when normalised to both *YLS8* and *ADF2* reference genes (Figure 4.14A). Other lines had a moderate or close to WT level of *PRPL11* expression including *prpl11*35S::PL11-GFP5.5, *prpl11*35S::PL11-GFP4.4, *prpl11*35S::PL11-TAP6.3 and *prpl11*35S::PL11-TAP9.6 (Figure 4.14 A, B). One line *prpl11*35S::PL11-TAP3.6 showed a low level of expression, which was only slightly higher than in the *prpl11-1* mutant control. The expression of *GFP* was additionally evaluated in control lines lacking the *PRPL11* genes. These lines showed a massive increase in *GFP* expression in all 6 lines tested compared to control Col-0 (Figure 4.14C).

Both genetic constructs, *35S::PRPL11-GFP* and *35S::PRPL11-TAP,* were able to complement the pale green *prprl11-1* phenotype, as seen by full rescue of greening in 2 d D and 3 d WLc grown *prpl11*35S::PL11-GFP3.2, *prpl11*35S::PL11-GFP4.4, *prpl11*35S::PL11-GFP10.1 and *prpl11*35S::PL11-TAP6.3, and a moderate increase in greening in lines *prpl11*35S::PL11-GFP5.5 and *prpl11*35S::PL11-TAP9.6 (Figure 4.15A). The rescue of the *prpl11-1* phenotype in *PRPL11* overexpressing lines was also reflected in a substantial increase in the Fv/Fm ratio depicted as a heat map in Figure 4.15B. This parameter recovered to almost WT level, with the exception of the *prpl11*35S::PL11-GFP5.5, *prpl11*35S::PL11-TAP3.6 and *prpl11*35S::PL11-TAP9.6 lines, in which a moderate or no increase in Fv/Fm was observed. Overall, these results demonstrate that the 35S::PL11-GFPand 35S::PL11-TAPconstructs are expressed and functional in a *prpl11-1* background.

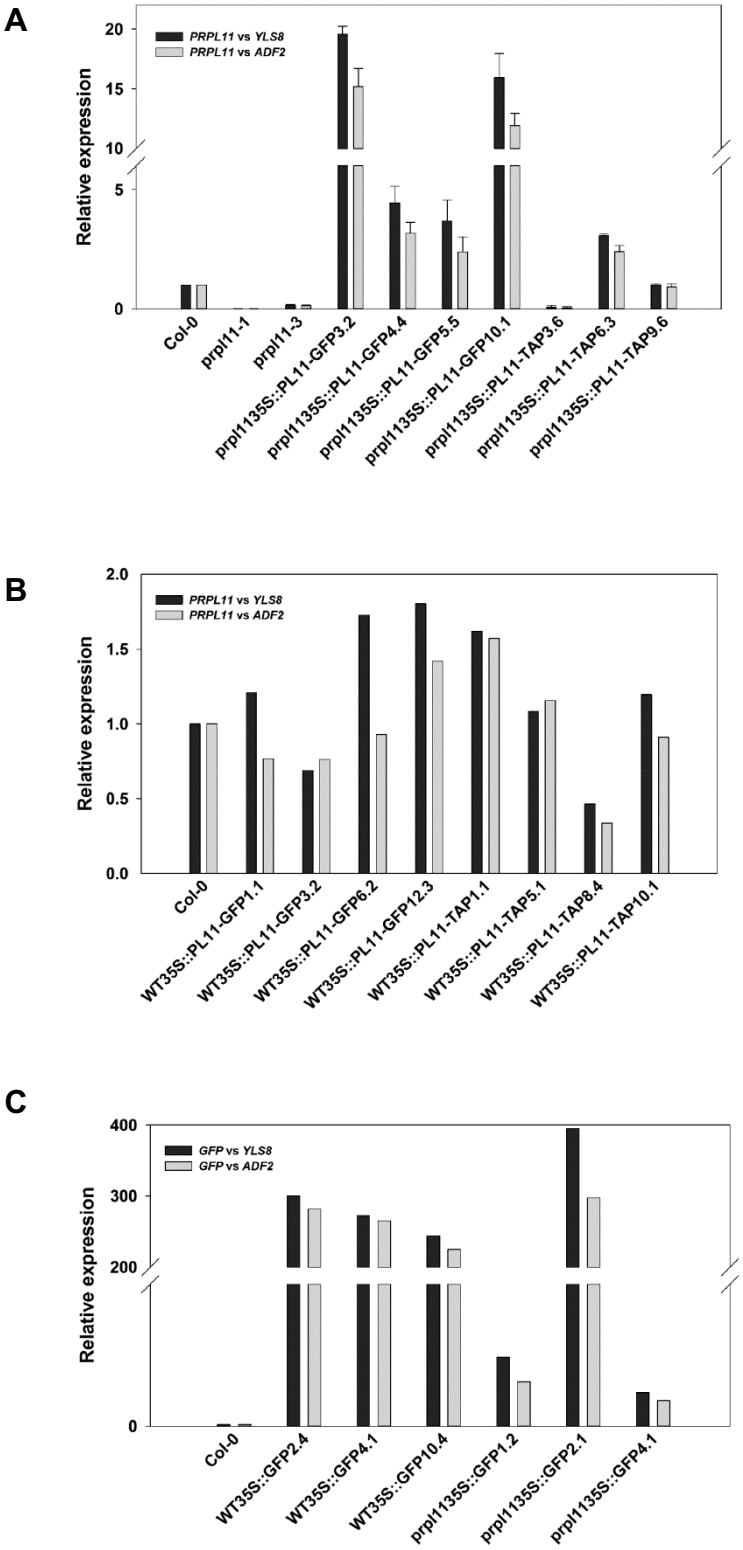

Figure 4.14 Confirmation of the presence of the 35S::*PRPL11*-GFP, 35S::*PRPL11*-TAP and 35S::GFP constructs in transgenic *Arabidopsis thaliana* seedlings. WT (Col-0), *prpl11-1*, *prpl11-3* and series of transgenic lines in Col-0 (WT) and *prprl11-1* (*prpl11*) backgrounds were grown on 1% agar medium, with ½ MS (pH 5.6) and under the following conditions: 2 d dark, 3 d WLc (100 µmol m^{-2} s^{-1}). (A and B) Expression of *PRPL11* in mutant and transgenic lines analysed using quantitative RT-PCR. (C) Expression of *GFP* in transgenic empty vector control lines analysed using quantitative RT-PCR. Expression is relative to control Col-0 and normalised to *YELLOW LEAF SPECIFIC GENE 8* (*YLS8*, At5g08290) and to *ACTIN DEPOLYMERIZING FACTOR 2* (*ADF2,* At3g46000). Results shown are from a single experiment.

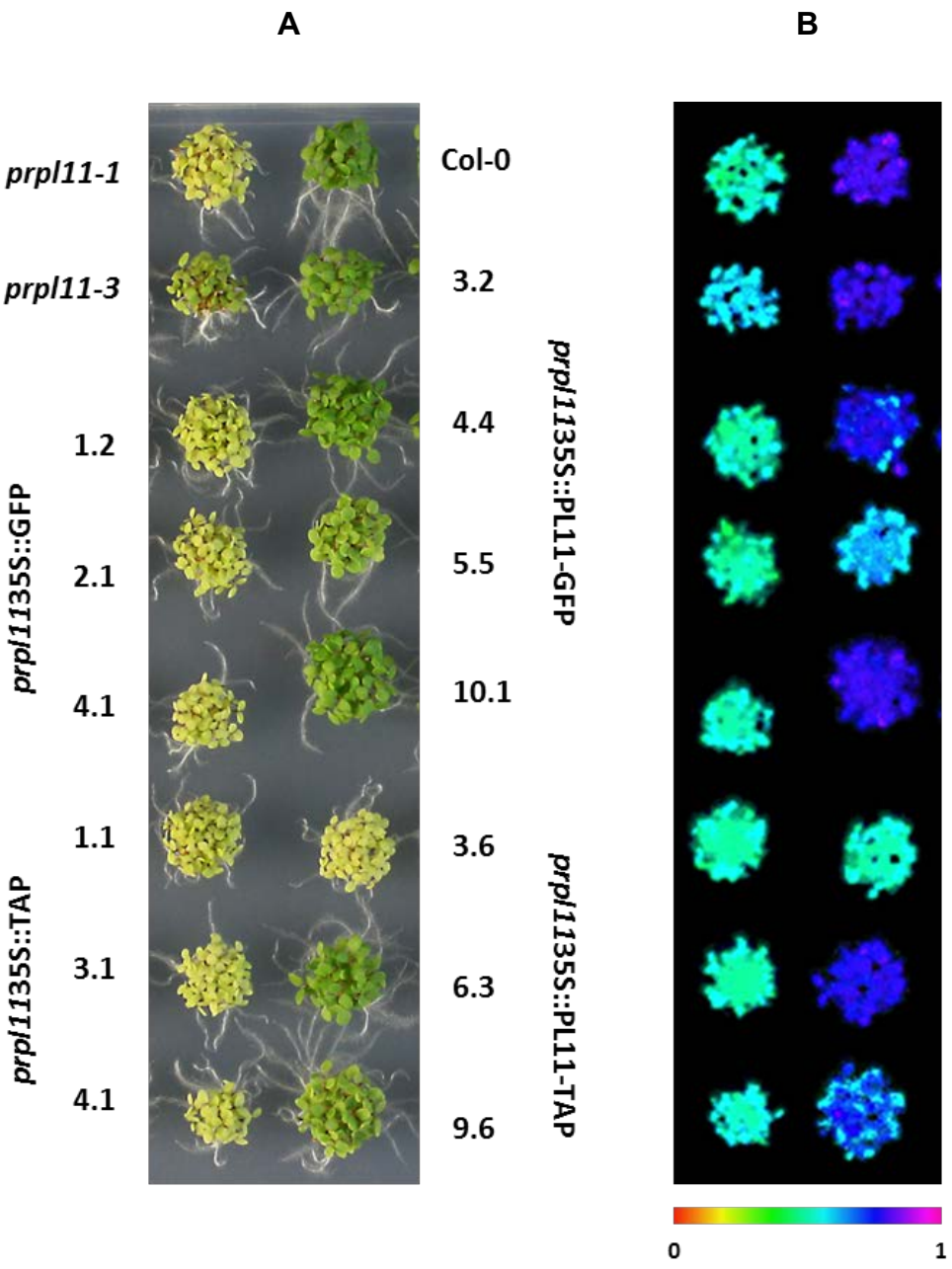

Figure 4.15 Phenotypes of *prpl11-1* and *prpl11-3* mutants and complemented PRPL11 overexpression transgenic lines with GFP and TAP tags. Seedlings of WT (Col-0), *prpl11-1* and *prpl11-3* mutants, *prpl11*35S::PL11-GFP and *prpl11*35S::PL11-TAP transgenic lines and control empty vector lines in the *prpl11-1* background were grown on 1% agar medium, with ½ MS (pH 5.6) under the following conditions: 2 d dark, 3 d WLc (100 µmol m^{-2} s^{-1}). (A) Visible phenotype of 5-d old seedlings. (B) Representative photographs from Imaging-PAM measurements for Fv/Fm values of PSII depicted as a heat map. The colour scale is marked below ranging from 0 (red) to 1 (violet).

Since there was no PRPL11 antibody available, the presence of the chimeric proteins PRPL11-GFP and PRPL11-TAP in the selected PRPL11ox lines was confirmed by immunoblot analysis with GFP and TAP antibodies using the same growth conditions as before (Figure 4.16). All three *prpl11*35S::PL11-GFP10.1 and both *prpl11*35S::PL11-TAP6.3 selected showed a band of the expected molecular mass for the respective chimeric proteins with no band present in WT seedlings. The additional lower molecular bands apparent in the *prpl11*35S::PL11-GFP3.2, *prpl11*35S::PL11-GFP10.1 and *prpl11*35S::PL11-TAP6.3 lanes may indicate protein cleavage.

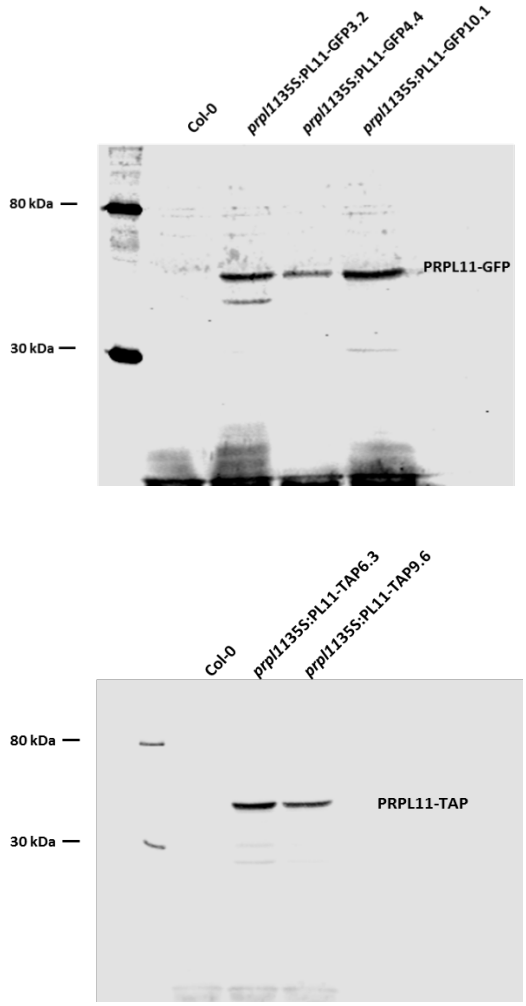

Figure 4.16 Western blot analysis of fusion proteins PRPL11-GFP and PRPL11-TAP in *prpl11*35S:PL11-GFP and *prpl11*35S:PL11-TAP transgenic lines. WT (Col-0), *prpl11*35S:PL11-GFP3.2, *prpl11*35S:PL11-GFP4.4, *prpl11*PL11-GFP10.1, *prpl11*35S:PL11-TAP6.3, *prpl11*35S:PL11-GFP9.6 seedlings were grown on 1% agar medium, with ½ MS (pH 5.6) under the following conditions: 2 d dark, 3 d WLc (100 µmol m^{-2} s^{-1}). Immuno-blot detection on total protein extracts was performed with antibodies against GFP (top) and TAP (bottom).

To investigate further the consequence of *PRPL11* overexpression, an immuno-blot analysis was performed on total protein extracts from *prpl11* mutants and PRPL11-GFPox lines to evaluate the protein composition of the photosynthetic machinery (Figure 4.17). Consistent with previous reports (Pesaresi et al., 2006), both *prpl11* mutants had reduced levels of all photosynthetic proteins analysed between 30-80% of WT level. This included proteins belonging to the light harvesting complex (LHCA1, LHCB1, LHCB2), PSI core (PsaC) and PSII core (PsbQ, PsbR). In all 3 tested PRPL11ox lines this repression was rescued to at least the WT level and for two proteins, PsbQ and PsbR, a slightly higher level was detected compared to wild type (Figure 4.17).

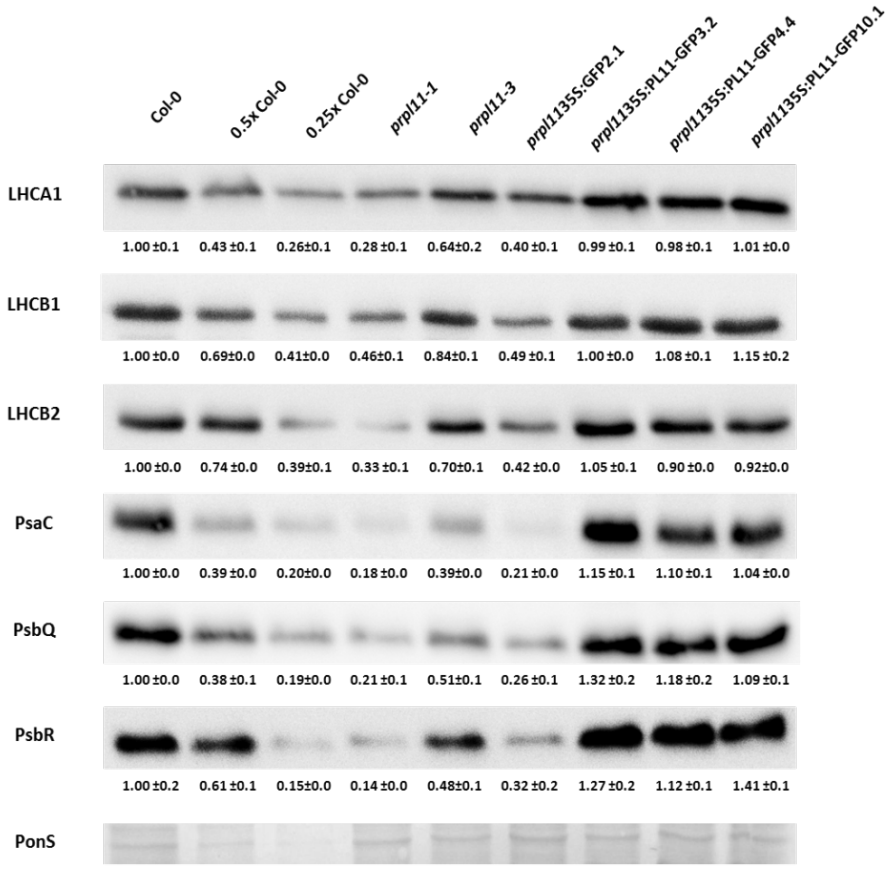

Figure 4.17 Western blot analysis of selected LHC, photosystem I and II (PSI, PSII) protein levels in *prpl111* mutants and *prpl11*35S:PL11-GFP transgenic lines. WT (Col-0), *prpl11-1*, *prpl11-3, prpl11*35S::GFP2.1, *prpl11*35S::PL11-GFP3.2*, prpl11*35S::PL11-GFP4.4 and *prpl11*35S::PL11-GFP10.1 seedlings were grown on 1% agar medium, with ½ MS (pH 5.6) under the following conditions: 2 d dark, 3 d WLc (100 µmol m^{-2} s^{-1}). Representative blots from 3 independent biological replicates are shown, with average band signal intensity (± SEM) from all three replicates shown. 0.5x Col-0 and 0.25x Col-0 indicates serial dilution of total protein extract from wild type seedlings. Protein loading is indicated by PonceauS staining (PonS). Signal intensities from each blot were calculated with ImageJ.

4.2.4 Identification of putative PRPL11 interacting proteins

In order to identify putative PRPL11 interacting proteins, a pull-down assay was carried out using the *prpl11*35S::PL11-TAP6.3 overexpressor line. This line was chosen as it does not strongly overexpress *PRPL11*, while it clearly complements *prpl11* phenotype. The pull down analysis was performed on 2 d D and 5 d WLc grown seedlings to maintain the growth conditions similar to those used earlier in this study. To avoid potential protein cleavage, additional proteinase inhibitors were included during protein extraction and purification (see Chapter 2 for details). PRPL11 protein was purified using the TAP-tag purification protocol and putative interacting proteins were identified using nano liquid chromatography coupled to tandem mass spectrometry (nano LC-MS/MS). Table 4.1 shows the list of the 130 top proteins (by no. of peptides) out of 2384 proteins found to co-immunoprecipitate with PRPL11 in two independent experiments. Among them there was a strong enrichment for protease system proteins like ClpC1, ClpC2, chloroplast-localised heat shock proteins (e.g. HSP90-5), proteins involved in regulation of translation, and proteins for different subunits of the plastid ribosome including PRPS1, PRPL24. Interestingly, a few proteins for different enzymatic steps in the tetrapyrrole synthesis pathway were also identified as potentially interacting with PRPL11. These included all of the proteins that comprise Mg-chelatase, CHLD, CHLI1, CHLI2, and CHLH, later steps of the chlorophyll synthesis branch CHLM, PORC (not included in the table), as well proteins involved between ALA and Proto IX synthesis (HEMEC, HEME2).

This result is supportive of an interaction of PRPL11 with the tetrapyrrole pathway and may point to a mechanism for its regulation of retrograde signalling. It is interesting to note that many genes for tetrapyrrole biosynthesis are also co-expressed with *PRPL11* (Figure 4.18). This cohort of genes does not include the most highly regulated components of the pathway, but there is apartial overlap with possible PRPL11 interacting partners, including *CHLD*, *CHLI2*, *HEME2*, *HEMC* and *PORC*.

Table 4.1 Proteins identified in co-immunoprecipitates of PRPL11-TAP by nano LC-MS/MS. The top 130 proteins by peptide no. are shown. Data represents the mean from two independent experiments. Highlighted in grey are proteins belonging to the tetrapyrrole biosynthetic pathway. The PRPL11 protein is marked in red.

Accession	Description	No of Peptides	Coverage
Q9FI56	Chaperone protein ClpC1	41.0	52.9
Q9SIF2	Heat shock protein 90-5	34.0	52.4
F4JF64	Clp ATPase	32.5	49.2
Q9SXJ7	Chaperone protein ClpC2	32.5	47.6
P55737	Heat shock protein 90-2	31.5	46.1
P51818	Heat shock protein 90-3	31.0	47.0
F4K6B6	Heat shock protein 81-2	30.5	43.3
P10896	Ribulose bisphosphate carboxylase/oxygenase activase	29.5	71.3
F4IVZ7	Rubisco activase	28.5	70.7
P19366	ATP synthase subunit beta	27.5	73.3
Q9ASR1	Elongation factor 2	26.0	44.0
O03986	Heat shock protein 90-4	25.0	38.2
P21240	Chaperonin 60 subunit beta 1	24.5	47.6
Q8S9L5	Trigger factor-like protein TIG	24.5	42.5
Q9FFC7	Alanine--tRNA ligase, chloroplastic/mitochondrial	24.0	33.9
A0A1P8BCC6	Probable alanine--tRNA ligase	24.0	33.1
Q9LJE4	Chaperonin 60 subunit beta 2	23.5	46.9
O03042	Ribulose bisphosphate carboxylase large chain	23.0	54.9
Q9LF37	Chaperone protein ClpB3	22.5	30.6
Q9SZD6	Elongation factor Ts	22.0	32.4
P17745	Elongation factor Tu	21.5	57.2
P21238	Chaperonin 60 subunit alpha 1	21.5	53.5
O50008	5-methyltetrahydropteroyltriglutamate	21.5	38.4
P54609	Cell division control protein 48 homolog	20.5	31.5
Q9LRR9	Peroxisomal (S)-2-hydroxy-acid oxidase GLO1	20.0	72.1
Q0WLB5	Clathrin heavy chain	19.5	15.5
Q56WK6	Patellin-1	19.5	40.4
Q2V3V9	Aldolase-type TIM barrel family protein	19.0	67.2
Q9SYI0	Protein translocase subunit SECA1	19.0	26.5
A0A1P8B485	Protein translocase subunit SecA	19.0	26.4
P29513	Tubulin beta-5 chain	18.5	49.1
P56757	ATP synthase subunit alpha, chloroplastic	18.5	47.3
Q9LRS0	Peroxisomal (S)-2-hydroxy-acid oxidase GLO2	18.5	65.3
Q9SI75	Elongation factor G	18.5	31.2
P25856	Glyceraldehyde-3-phosphate dehydrogenase GAPA1	18.5	51.4
Q9SJE1	Magnesium-chelatase subunit ChlD	18.5	26.8
O23654	V-type proton ATPase catalytic subunit A	18.5	39.2
Q0WNJ6	Clathrin heavy chain 1	18.5	14.8
Q9ASR0	Tubulin beta-3 chain	18.0	47.7
P29511	Tubulin alpha-6 chain	18.0	57.0
P25858	Glyceraldehyde-3-phosphate dehydrogenase GAPC1	18.0	66.7
A8MS37	Aldolase-type TIM barrel family protein	18.0	64.0
B3H4B8	Aldolase-type TIM barrel family protein	18.0	63.0
Q9LD57	Phosphoglycerate kinase 1	18.0	51.2
P25857	Glyceraldehyde-3-phosphate dehydrogenase GAPB	18.0	44.4
F4JG57	Albino or Glassy Yellow 1	18.0	24.7
Q42472	Glutamate decarboxylase 2	17.5	46.0
B9DGT7	Tubulin alpha-2 chain	17.5	55.4
Q9LSB4	TSA1-like protein	17.5	33.0
P25697	Phosphoribulokinase, chloroplastic	17.0	57.8
Q9FX54	Glyceraldehyde-3-phosphate dehydrogenase GAPC2	17.0	65.5
P29515	Tubulin beta-7 chain	17.0	43.2
P24636	Tubulin beta-4 chain	16.5	47.5
Q96292	Actin-2	16.5	59.9
Q96293	Actin-8	16.5	59.9
F4JFV6	Aldolase-type TIM barrel family protein	16.5	59.1
Q05758	Ketol-acid reductoisomerase	16.5	38.5
B9DHQ0	Tubulin alpha-5 chain	16.5	49.2
Q9LPW0	Glyceraldehyde-3-phosphate dehydrogenase GAPA2	16.5	47.4
A0A1P8APR6	Glyceraldehyde-3-phosphate dehydrogenase	16.5	42.9
F4HQD4	Heat shock 70 kDa protein	16.5	24.5
P29516	Tubulin beta-8 chain	16.0	41.3
P29197	Chaperonin CPN60	16.0	34.7
P41376	Eukaryotic initiation factor 4A-1	16.0	51.1
Q9S7C0	Heat shock 70 kDa protein 14	16.0	24.7
Q9LR30	Glutamate--glyoxylate aminotransferase 1	16.0	45.6
Q9LD43	Acetyl-coenzyme A carboxylase carboxyl transferase subunit alpha	16.0	30.2
Q9SAC6	Alpha-glucan water dikinase 1,	16.0	19.2
P29517	Tubulin beta-9	15.5	43.1
P29514	Tubulin beta-6 chain	15.5	36.9
F4JEL4	Eukaryotic translation initiation factor 4A1	15.5	49.9
A0A1I9LSZ7	Eukaryotic translation initiation factor 4A1	15.5	49.4

A8MRZ7	Eukaryotic translation initiation factor 4A1	15.5	48.3
P53492	Actin-7	15.5	54.5
Q43127	Glutamine synthetase, chloroplastic/mitochondrial	15.5	47.4
Q9LUT2	S-adenosylmethionine synthase 4	15.5	47.5
P16127	Magnesium-chelatase subunit ChlI-1	15.5	42.1
Q9LX99	Kinesin-like protein KIN-14A	15.5	19.1
P22953	Probable mediator of RNA polymerase II transcription subunit 37e	15.5	38.2
F4JEL5	Eukaryotic translation initiation factor 4A1	15.0	47.8
O04983	Biotin carboxylase	15.0	38.5
F4J8V9	Actin 2	14.5	54.2
P41377	Eukaryotic initiation factor 4A-2	14.5	45.4
Q9FVT2	Probable elongation factor 1-gamma 2	14.5	43.9
P52410	3-oxoacyl-[acyl-carrier-protein] synthase I	14.5	46.1
Q43316	Porphobilinogen deaminase	14.5	31.5
F4HQD5	Heat shock protein 70 (Hsp 70) family protein	14.5	25.8
O65719	Heat shock 70 kDa protein 3	14.5	33.7
F4KCE5	Heat shock cognate protein 70-1	14.5	42.8
A8MR05	Magnesium-chelatase subunit chlH	14.0	14.4
Q9FNB0	Magnesium-chelatase subunit ChlH	14.0	13.2
F4JYE0	Acetyl Co-enzyme a carboxylase biotin carboxylase subunit	14.0	34.6
F4I3L1	Phosphoglycerate kinase	14.0	43.8
P50318	Phosphoglycerate kinase 2	14.0	37.1
Q9LZF6	Cell division control protein 48 homolog E	14.0	20.8
P17562	S-adenosylmethionine synthase	14.0	45.2
A0A1I9LQE4	DNA topoisomerase-like protein	14.0	33.7
Q94A40	Coatomer subunit alpha-1	14.0	24.9
P12411	Tubulin beta-1 chain	13.5	31.8
F4HV96	Eif4a-2	13.5	42.0
A0A1I9LQB3	Carbonic anhydrase	13.5	67.6
F4KHF4	3-ketoacyl-acyl carrier protein synthase I	13.5	38.7
P27140	Beta carbonic anhydrase 1	13.5	50.6
B9DFF8	Tubulin alpha chain	13.0	47.2
Q9LY66	50S ribosomal protein L1	13.0	40.0
F4HQT1	Glyceraldehyde-3-phosphate dehydrogenase	12.5	52.7
F4HNZ6	Glyceraldehyde 3-phosphate dehydrogenase A subunit 2	12.5	44.2
F4IVR2	Heat shock protein 60-2	12.5	28.1
Q8L7B5	Chaperonin CPN60-like 1	12.5	27.9
Q42601	Carbamoyl-phosphate synthase large chain	12.0	15.1
F4JYE1	Acetyl Co-enzyme a carboxylase biotin carboxylase subunit	11.5	34.0
P0DH99	Elongation factor 1-alpha 1	11.0	32.1
C0Z361	Chaperonin 60 subunit beta 3	11.0	20.9
P53496	Actin-11	11.0	41.2
A8MQE0	P-loop containing nucleoside triphosphate hydrolases superfamily protein	11.0	36.1
F4HS63	P-loop containing nucleoside triphosphate hydrolases superfamily protein	11.0	29.2
Q944I4	D-glycerate 3-kinase	11.0	28.8
P0CJ46	Actin-1	11.0	41.2
Q9ZT91	Elongation factor Tu, mitochondrial	11.0	31.5
O22886	Uroporphyrinogen decarboxylase 2	10.5	42.5
P57751	UTP--glucose-1-phosphate uridylyltransferase 1	10.5	29.4
F4HUA0	GTP binding Elongation factor Tu family protein	10.0	32.3
Q9MAP3	50S ribosomal protein L11	9.5	48.6
P23686	S-adenosylmethionine synthase	9.5	40.5
P42643	14-3-3-like protein GF14	9.0	43.4
Q8VZH2	Aminopeptidase M1	9.0	13.4
Q94B60	ATP-dependent Clp protease proteolytic subunit 4	9.0	40.6
Q9SJT9	Coatomer subunit alpha-2	8.5	15.5
F4KGV2	G-box regulating factor 6	8.0	40.0

A

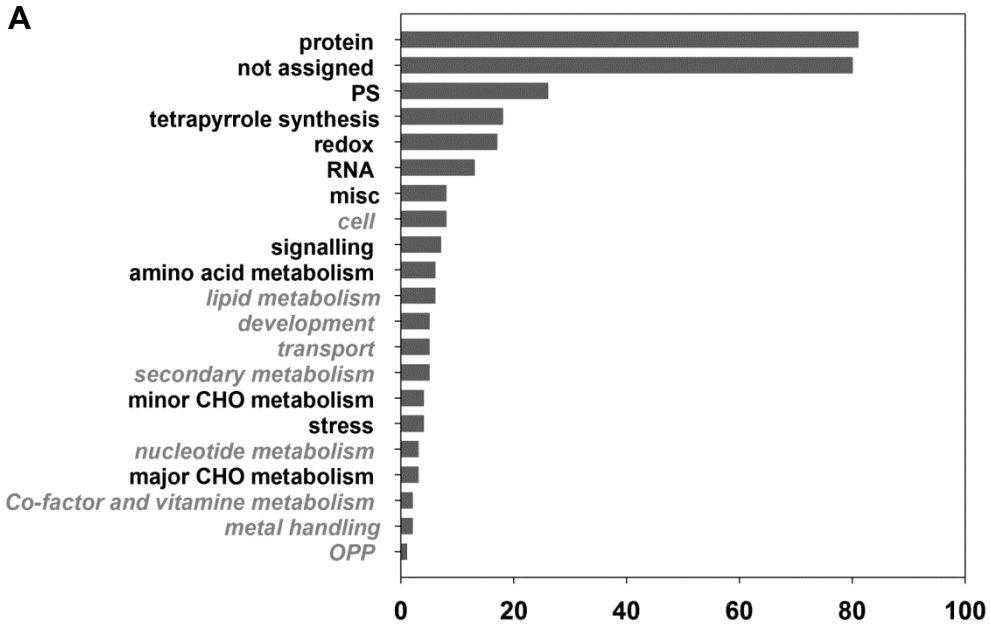

B

ID	Tetrapyrrole synthesis subcategory	Symbol	Annotation
At3g25660	[19.1] glu-tRNA synthetase	-	Amidase family protein
At1g48520	[19.1] glu-tRNA synthetase	GATB	GLU-ADT subunit B
At5g45930	[19.10] magnesium chelatase	CHLI2	Magnesium chelatase i2
At1g08520	[19.10] magnesium chelatase	ALB1, CHLD	CHLD subunit of the Mg-chelatase enzyme
At4g18480	[19.10] magnesium chelatase	CH-42, CHL11	CHLORINA 42, LOST1
At5g18660	[19.13] divinyl chlorophyllide-a 8-vinyl-reductase	PCB2	NAD(P)-binding Rossmann-fold superfamily protein
At1g03630	[19.14] protochlorophyllide reductase	POR C	Protochlorophyllide oxidoreductase C
At3g51820	[19.15] chlorophyll synthase	CHLG, PDE325	Pigment defectiveE 325
At2g26550	[19.21] heme oxygenase	HO2	Heme oxygenase 2
At3g48730	[19.3] GSA	GSA2	Glutamate-1-semialdehyde 2,1-aminomutase 2
At1g69740	[19.4] ALA dehydratase	HEMB1	Aldolase superfamily protein
At3g14110	[19.40] tetrapyrrole synthesis.regulation	FLU	Fluorescent in blue light
At5g08280	[19.5] porphobilinogen deaminase	HEMC, RUG1	Hydroxymethylbilane synthase
At2g26540	[19.6] uroporphyrinogen III synthase	DUF3, HEMD, UROS	Uroporphyrinogen-III synthase family protein
At2g40490	[19.7] uroporphyrinogen decarboxylase	HEME2	Uroporphyrinogen decarboxylase
At3g14930	[19.7] uroporphyrinogen decarboxylase	HEME1	Uroporphyrinogen decarboxylase
At1g03475	[19.8] coproporphyrinogen III oxidase	HEMF1, LIN2	Coproporphyrinogen III oxidase
At4g01690	[19.9] protoporphyrin IX oxidase	PPOX	Protoporphyrinogen oxidase

Figure 4.18 Bioinformatics analysis of genes co-expressed with *PRPL11*. (A) Gene ontology (GO) term enrichment for the set of 200 genes co-expressed with *PRPL11* that were selected using trans-factor and cis-element prediction database, ATTED-II. GO terms were based on Mapman bins, and number of genes that fall into each GO category are plotted. GO terms with significant p-values (< 0.05) of the hypergeometric distribution are highlighted in bold. (B) Summary table depicting all genes involved in tetrapyrrole biosynthesis that were found to be co-expressed with *PRPL11*.

Although pull-down analysis suggesting PRPL11 interaction with Mg-chelatase is preliminary, further immune-blot analyses on seedlings grown 2 d and 3 d WLc showed that knock out of PRPL11 affects the abundance of some tetrapyrrole synthesis proteins (Figure 4.19). The accumulation of GluTR and CHLH was higher in both *prpl11* mutant alleles lines compared to wild type and declined to the wild type level, when *PRPL11* was overexpressed. Also HO1 appeared to accumulate to a higher level in *prprl11* mutant lines. In contrast, there was no difference in CHLI accumulation between wild type, *prprl11* mutants and PRPL11ox lines (Figure 4.19).

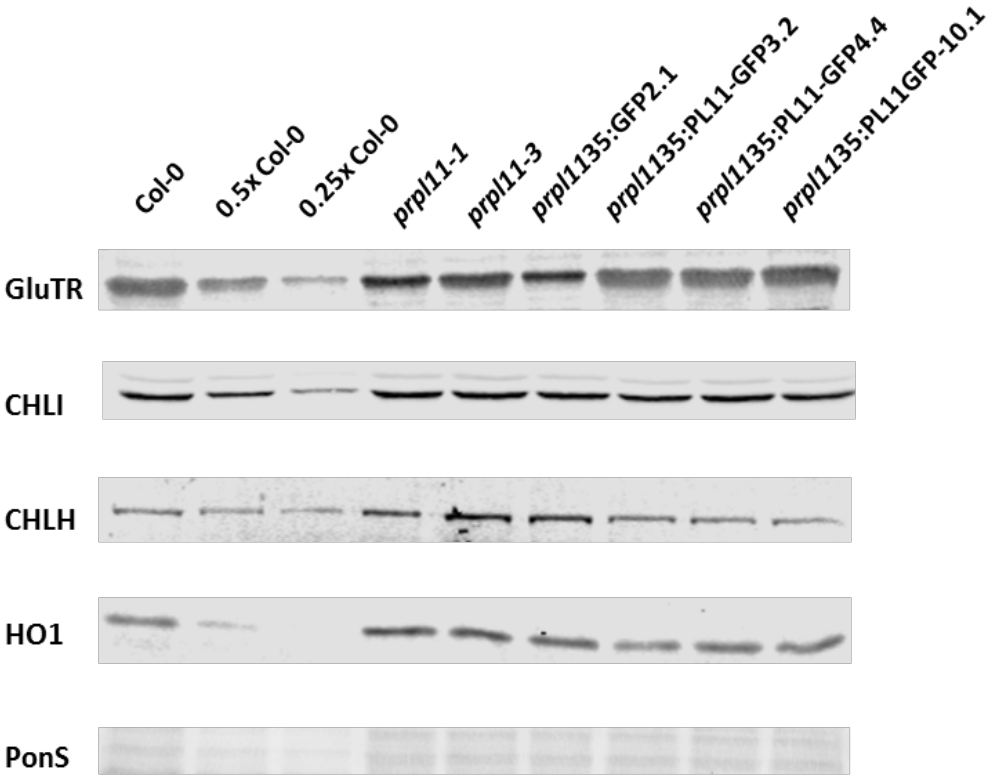

Figure 4.19 Western blot analysis of selected tetrapyrrole biosynthesis pathway proteins in *prpl11* mutants and *prpl11*35S::PL11-GFP transgenic lines. WT (Col-0), *prpl11-1*, *prpl11-3, prpl11*35S::GFP2.1, *prpl11*35S::PL11-GFP3.2*, prpl11*35S::PL11-GFP4.4 and *prpl11*35S::PL11-GFP10.1 seedlings were grown on 1% agar medium, with ½ MS (pH 5.6) under the following conditions: 2 d dark, 3 d WLc (100 µmol m^{-2} s^{-1}). Representative blots from 3 independent biological replicates are shown. 0.5x Col-0 and 0.25x Col-0 indicates serial dilution of total protein extracts from wild type. Protein loading is indicated by PonceauS staining (PonS).

4.2.5 Interaction of plastid translation-dependent signalling with tetrapyrrole signalling

Results presented in this chapter indicate that PRPL11 might provide a link between plastid translation and tetrapyrrole-dependent retrograde signalling. Another such an example could be GUN1, which is supported by the recent observation that GUN1 can bind both plastid ribosome and tetrapyrrole pathway proteins (Tadini et al., 2016), as well by its role in inhibition of Pchlide accumulation shown in this work (Figure 3.11A). Based on results presented by Tadini et al. (2016), it could be speculated that the *gun* phenotype of *gun1* observed in the literature under the conditions that block plastid translation is due to its role in redirecting tetrapyrrole precursor metabolites and promotion of positive tetrapyrrole signalling pathway.

To further test this hypothesis heme synthesis was blocked with DP in control and Lin treated wild type seedlings and two *gun1* mutant alleles using the same conditions as in previous experiments in this section (for details see also the legend for Figure 4.20). Figure 4.20 shows that very strong rescue of *LHCB2.1*, *HEMA1*, *CHLH* and *GUN4* expression after Lin treatment seen in both *gun1* alleles was severely inhibited by additional DP treatment. This effect was more pronounced for the tetrapyrrole genes than *LHCB2.1*. It suggests that *gun1* phenotype on Lin might be at least partially dependent on tetrapyrrole metabolism. Interestingly, while there was no additive effect of DP and Lin on the repression of *LHCB2.1*, *HEMA1*, *CHLH* and *GUN4* in wild type, the *FC1* induction was much more elevated after this double treatment in all analysed lines.

To further test the interaction between plastid translation and tetrapyrrole synthesis, the effect of Lin treatment on Pchlide accumulation was examined. Measurements of Pchlide content in dark-grown seedlings showed its accumulation was strongly reduced when plastid translation was inhibited by Lin treatment, and this was only partially rescued by ALA feeding (Figure 4.21A). Thus the reduced Pchlide in Lin treated seedlings was presumably due to inhibition of later steps in tetrapyrrole synthesis. Pchlide accumulation was also substantially inhibited in wild type and the *flu* mutant either in the dark or after Pchlide accumulation had been promoted by FR light treatment (Figure 4.21B). Since no components of the tetrapyrrole pathway are known to require a component synthesized on plastid ribosomes, the ability of Lin to strongly affect tetrapyrrole synthesis suggests a regulatory effect that could support an interaction between tetrapyrrole-dependent signalling and plastid translation-dependent retrograde signalling.

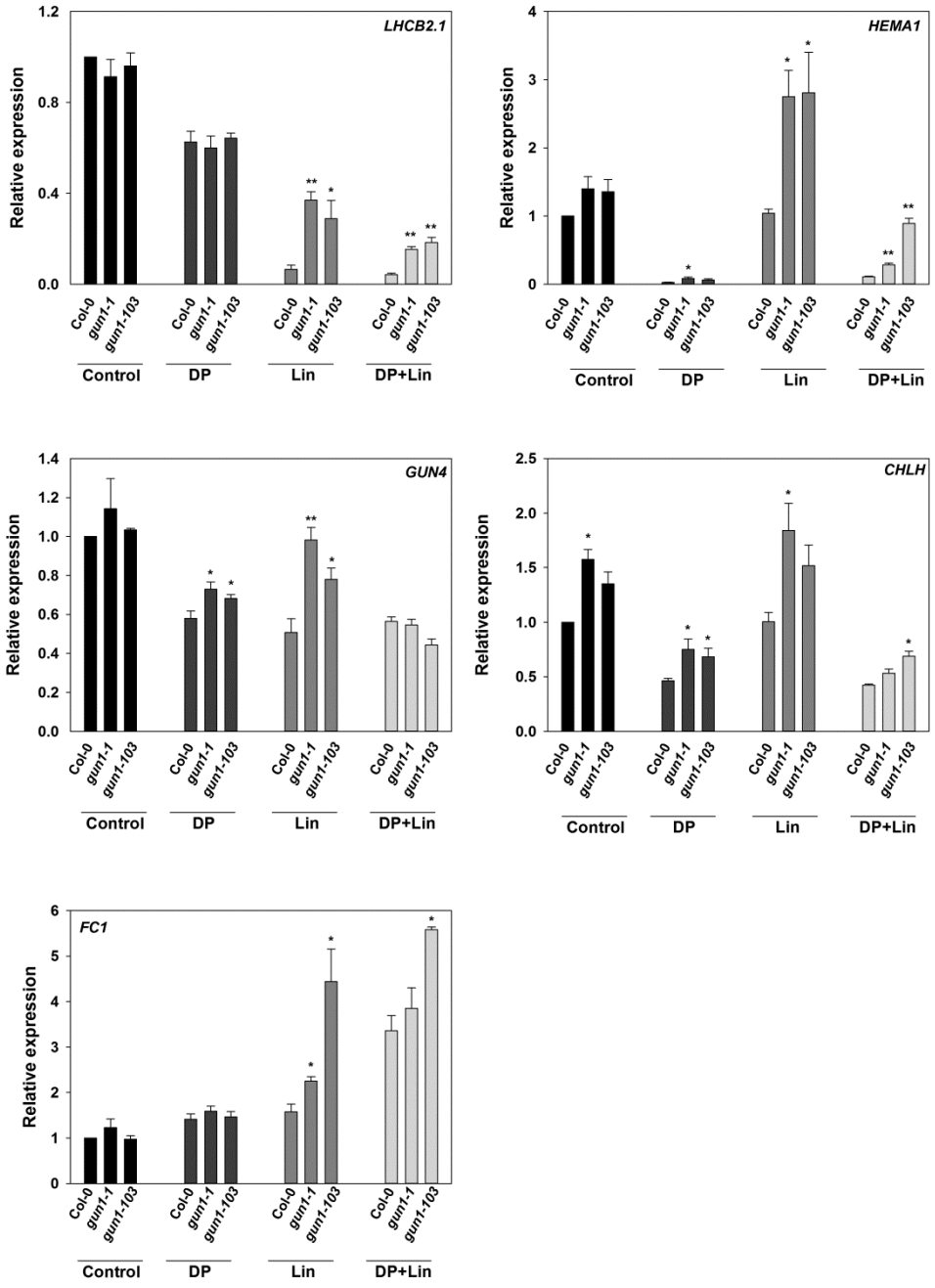

Figure 4.20 Regulation of nuclear gene expression in *gun1* mutants treated with lincomycin (Lin) and 2,2'-Dipyridyl (DP). WT (Col-0), *gun1-1* and *gun1-103* seedlings were grown on 1% agar medium, with ½ MS (pH 5.6) and with or without 0.5 mM Lin under the following conditions: 2 d dark, 3 d WLc (100 µmol m^{-2} s^{-1}). For the last 6 h of WLc growth seedlings were transferred to water supplemented with 0.5 mM Lin (+Lin), with 0.1 mM DP (+DP) or with both 0.5 mM Lin and 0.1 mM DP (DP+Lin) or to control conditions (0.02% ethanol). Expression is shown relative to Col-0 control samples and normalised to *YELLOW LEAF SPECIFIC GENE 8* (*YLS8*, At5g08290). Data shown are means +SEM of three independent biological replicates. Asterisks denote a significant difference vs. Col-0 for the same treatment (control, +DP, +Lin or DP+NF), Student's *t*-test (*p < 0.05, **p < 0.01)

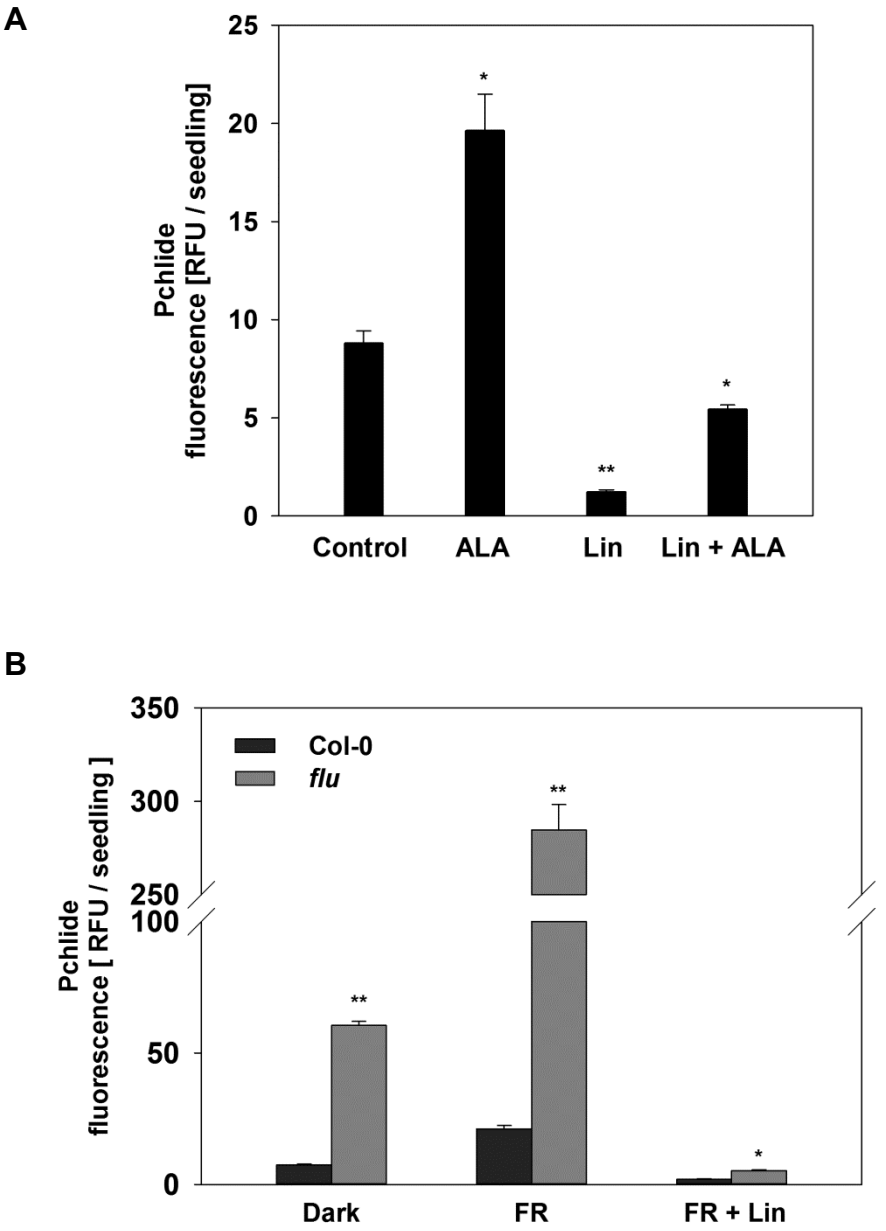

Figure 4.21 Effect of lincomycin (Lin) on protochlorophyllide (Pchlide) accumulation in wild type and the *flu* mutant. WT (Col-0) and *flu* mutant seedlings were grown on 1% agar with ½ MS medium supplemented with (A) or without (B) 5 mM MES, without sucrose and with or without 0.5 mM Lin for 4 d in dark. (A) The effect of Lin on Pchlide accumulation without and with 0.1 mM ALA. Asterisks denote significant difference vs untreated control Col-0, Student's *t* test (*p < 0.05, **p < 0.01). (B) The effect of Lin on Pchlide accumulation in Col-0 and *flu* mutant seedlings grown in 4d D (Dark) or 2 d D and 2 d FR (FR). Data shown are means + SD of three independent biological replicates. 30-40 seedlings were harvested for each biological replicate. Asterisks denote significant difference vs Col-0 for the same treatment (Dark, FR, FR+Lin), Student's *t* test (*p < 0.05, **p < 0.01).

4.3 Discussion

4.3.1 Loss of PRPL11 promotes nuclear gene expression

The aim of this Chapter was to determinate the role of plastid translation in tetrapyrrole-dependent retrograde signalling. The double mutant for *Arabidopsis* ribosome L11 proteins, *prpl11*/*mrpl11* had been shown previously to have reduced expression of photosynthetic genes (Pesaresi et al., 2006). It could be hypothesized that a deficiency in translation in both organelles is causing a retrograde signalling response. Indeed, consistent with Pesaresi et al. (2006), we could detect an additive effect of the *prpl11*/*mrpl11* mutations on *LHCB2.1* expression in seedlings under the control conditions (Figure 4.1), although not for other genes tested. In mitochondria heme is an essential component of the respiratory chain, and according to the most current hypothesis FC1-derived heme-dependent signal can promote photosynthetic gene expression. It is therefore possible that a promotive heme-dependent signal requires both chloroplast and mitochondrial function. On NF, the single *prpl11* mutant exhibited elevated nuclear gene expression compared to WT and this was also true for some transcripts under control conditions without NF. However, the single *mrpl11* mutant had a similar response to WT for *LHCB2.1* transcript accumulation, and the double *prpl11*/*mrprl11* mutant did not show an additive response (Figure 4.1). Thus no evidence for coordinative plastid and mitochondria action on regulation of photosynthetic gene expression in seedlings.

Many treatments and mutations have been used to block plastid transcription, translation or protein targeting, but they all resulted in a reduction or loss of nuclear gene expression (described in detail in section 4.1). This positions the *prpl11-1* mutant phenotype in a very interesting context, with WLc grown *prpl11-1* displaying higher expression of selected tetrapyrrole and photosynthetic genes (Figure 4.1, 4.3 and 4.5). This phenotype was most robust for the expression of the tetrapyrrole genes *HEMA1* and *CHLH* and a photosynthetic gene, *CP12-2* (Figure 4.1 and 4.5). It is not surprising that among different genes, *HEMA1* and *CHLH* were strongly affected in *prpl11-1*, as they belong to the small group of the most highly regulated tetrapyrrole genes (Matsumoto et al., 2004; Stephenson and Terry, 2008). On the other hand, there is little evidence in the literature for increased expression of these genes under the conditions that block chloroplast development. One example is rice mutant *al1,* which lacks plastid ribosomal protein L12, and also shows higher expression of *HEMA1,* but no other tetrapyrrole genes (Zhao et al., 2016). The *Arabidopsis* mutant *hos1*, which lacks the HOOKLESS1 protein that functions downstream of PIF and ethylene signalling is affected in chlorophyll synthesis, but shows up-regulation of *HEMA1* and *CHLH* (Jeong et al., 2016).

Elevated *HEMA1* and *CHLH* expression was also seen in two other rice mutants, *grc1* and *ylc2,* that are blocked in two rice heme oxygenase genes (*osHO1* and *osHO2;* Li et al., 2013*;* Li et al., 2014). The last 2 examples are very interesting, as they are blocked in heme metabolism and thus are expected to promote a positive heme-dependent signal similarly to *Arabidopsisgun2 (hy1)*, which lacks HO1 activity (Mochizuki et al., 2001). In the current study the *hy1* mutant did not show elevated *HEMA1* expression or rescue of gene expression on DP (Figure 4.11). It is, however, possible that this phenotype is dependent on the length of WL exposure and it was not visible under the conditions tested. A dependency on the length of the WL treatment was seen for elevated *HEMA1* expression in *prpl11* (Figure 4.5) and it would be interesting to also examine a time course for *HEMA1* expression for *hy1*.

One important question relates to the specificity of the elevated gene expression phenotype seen in *prprl11* mutants. An up-regulation of *HEMA1* and *CP12-2* was also seen in two other mutants for large and small subunit plastid proteins (*prpl24-1* and *prps17-1*). Also *sig2-2* and *sig6-2* seem to have a similar phenotype under WLc (Figure 3.7; see also discussion in Chapter 3). It is possible that the elevated gene expression was a more general consequence of disturbed chloroplast translation or, alternatively, that mutation in other plastid ribosome proteins inhibited PRPL11 protein function affecting gene expression phenotype indirectly. The precise mechanism of PRPL11 function is difficult to clearly define, as plastid ribosome protein mutants have complex phenotypes. Inhibition of ribosome activity can be expected to result in many secondary effects, with additional cellular stress resulting from the accumulation of precursor rRNA and blocked plastid RNA polymerase (PEP) and PEP-mRNA processing. Indeed, since the PEP complex is chloroplast encoded, inhibition of chloroplast translation will impact on the rate of RNA synthesis (Gray et al., 2003). This could possibly account for why an up-regulation of *HEMA1* expression was also observed in the *sig2-2* and *sig6-1* mutants.

Analyses of mitochondrial gene expression in *prpl11* and *mrpl11* mutants did not show an absolute specificity for defects in each organelle (Figure 4.7A). Intriguingly, the *AOX1a* and *UPOX1* transcripts were up regulated in *prpl11* suggesting that the mutant could suffer from mild oxidative stress under control conditions. Additional analysis of ROS production should be performed to test this, but if true, it is possible that the *prpl11* elevated gene expression phenotype is partially dependent on ROS production. The oxidative perturbation in the mutant could also possibly account for the elevated *CP12-2* expression, as CP12 might function in redox regulation of metabolism (Marii et al., 2009). It can be argued that elevated *HEMA1* expression is a compensation mechanism in response to stress resulting from disturbed chlorophyll synthesis, as *HEMA1* encodes the limiting step for tetrapyrrole synthesis. This possibility cannot be

excluded, but not every mutation that results in an inhibition of greening will give such a phenotype as seen for example for the *fc2-1* mutant, which has a WT level of *HEMA1* expression in WLc (Figure 3.3). It would be interesting to test if elevated gene expression can be affected by light intensity, which could also provide some insight into whether the response is related to oxidative disruption. Another important aspect of the elevated gene expression in *prprl11* is that this phenotype is enhanced with prolonged exposure to WLc (Figure 4.5). This is not necessary surprising, and may reflect increasing necessity for plastid ribosomal proteins within the first days of WLc growth when the photosynthetic apparatus requires assembly. This result is also in agreement with the strong link between plastid signalling and light signalling (Ruckle et al., 2007; Oh and Montgomery, 2013; Martin et al., 2016).

4.3.2 PRPL11 affects tetrapyrrole metabolism

Mutants of *prprl11* are affected in greening and have reduced photosynthetic efficiency and were shown here to accumulate less Pchlide, have reduced ALA synthesis, and accumulate less heme (Figures 4.9 and 4.10). This phenotype is the same as that described for *sig2-2* and *sig6-1* (Woodson et al., 2013). However, feeding ALA to seedlings in D does not restore Pchlide levels, thus in contrast to what have been proposed for *sig* mutants, it can be expected that PRPL11 controls a step in the tetrapyrrole pathway beyond ALA synthesis. This may be a role in redirecting tetrapyrroles between the two branches to heme and Mg-porphyrins. Reduced ALA synthesis rates in *prpl11* support this finding as more heme can potentially block this step through feedback inhibition, as described earlier. The reduced total heme concentration in the mutant might seem in disagreement with these findings, but since heme is a cofactor of photosynthetic proteins, and in *prpl11* accumulation of photosynthetic proteins is clearly disturbed (Figure 4.17), it is not surprising that the total heme pool was reduced in the *prpl11* mutant. The detection of free regulatory pool could give more reliable information about what is happening, but such a pool is currently very difficult to measure and awaits the development of improved methodology. Another experiment that is supportive for a role for PRPL11 in redirecting tetrapyrroles to the heme branch is the fact that elevated *HEMA1* expression can be blocked by DP treatment (Figure 4.11). If the mutant phenotype was completely independent, then we might not expect to see any difference in gene expression on DP.

4.3.3 PRPL11 may interact with Mg-chelatase

Among the proteins that co-immunoprecipitate with PRPL11, there were a lot of chaperonin proteins, but also an enrichment of tetrapyrrole proteins, with all the Mg-chelatase subunits represented. These are still preliminary data that will need to be further confirmed using a yeast-two hybrid system and bimolecular fluorescence complementation (BiFC). Nevertheless, if PRPL11 indeed can directly impact on the Mg-chelatase branch this would provide a mechanism for the observed phenotype with PRPL11 acting as a positive regulator of Mg-porphyrin synthesis. In support of the pull-down result is the observation that PRPL11 is co-expressed with tetrapyrrole genes (Figure 4.18). This result was obtained probably in part because PRPL11 is a light-induced gene (Genevestigator^{TM}), as are most tetrapyrrole synthesis genes. Interestingly, among the top proteins found in the pull-down analyses were some that have also been shown to bind GUN1 including e.g. ClpC1, ClpC2, and the ATP synthase beta subunit (Tadini et al., 2016). It could be proposed that perhaps PRPL11 (and maybe other ribosomal proteins) interact with Mg-chelatase as another example of post-translational feedback control over the tetrapyrrole biosynthesis pathway. This has already been shown for ClpC1 and ClpS1 (Nishimura et al., 2013; Apitz et al., 2016). Interestingly PRPL11 has been characterised recently as a methylprotein (Alban et al., 2014; Mazzoleni et al., 2015), suggesting it is post-translationally regulated itself. In summary, based on the data for PRPL11 presented here, as well as the interaction of GUN1 with PRPL11 and other plastid translation proteins described by Tadini et al. (2016), it can be speculated that plastid translation dependent signalling and tetrapyrrole signalling are closely linked. The observation that *gun1* rescue of gene expression on Lin can be abolished by DP is also in agreement with this hypothesis.

Chapter 5 The role of singlet oxygen in retrograde signalling

5.1 Introduction

In plants, light is required not only as the source of energy for photosynthesis, but also the information that triggers transition from skotomorphogenic to photomorphogenic development, in a process termed de-etiolation (Josse and Halliday, 2008). When grown in the dark seedlings are characterised by long hypocotyls, small cotyledons folded in a hook structure, and undifferentiated plastids. Upon light sensing, a transcriptional reprograming is induced that activates a series of developmental changes including inhibition of hypocotyl elongation, hook opening, leaf differentiation and chloroplast formation that all lead to an acquisition of autotrophic growth (Josse and Halliday, 2008; Waters and Langdale, 2009). The tetrapyrrole biosynthetic pathway is of primary importance during seedling development as it provides a source of phytochromobilin for light perception (via phytochromes), and the heme and chlorophylls that are fundamental components of the photosynthetic apparatus (for more detail see section 1.6).

Each condition that disturbs flux through the tetrapyrrole pathway can result in an accumulation of tetrapyrrole precursors within the chloroplast, many of which can potentially be toxic to cellular components and block seedling photomorphogenesis. Knock-out of the protochlorophyllide oxidoreductase *PORA* gene encoding the enzyme reducing protochlorophyllide (Pchlide) to chlorophyllide (Childe), which ultimately forms chlorophyll, was shown to result in a severe seedling growth arrest (Paddock et al., 2012). It is well established that chlorophyll precursors like free Pchlide lead to the $^1O_2$ production after excitation by light (op den Camp et al., 2003). Different ROS species produced within chloroplast are also important source of signalling molecules that control gene expression (described in more detail in section 1.7; for review see Pfannschmidt et al., 2003). One of the very first examples of a chloroplast-derived $^1O_2$ burst operating specifically as a redox retrograde signal is represented by the fluorescence (*flu)* mutant. FLU is a chloroplast membrane protein that functions as a negative regulator of chlorophyll biosynthesis (Meskauskiene et al., 2001). The *flu* mutant, generated in an EMS-mutagenesis screen is not able to restrict Pchlide accumulation in the dark and bleaches after exposure to WL (Meskauskiene et al., 2001). $^1O_2$ production was observed in the *flu* mutant, and this resulted in activation of some early stress-response genes, and lead to an acceleration of cell death (op den Camp et al., 2003; Danon et al., 2005). Subsequent genetic screens revealed that inactivation of two genes *EX1* and *EX2* (EXECUTER1 and EXECUTER2) blocks the $^1O_2$-mediated signalling cascade in *flu* (Wagner et al., 2004; Danon et al., 2005). Establishment of this EX-directed retrograde signalling is required for proper plastid differentiation,

and additionally incorporates ABA (Kim et al., 2009). Thus, EX-triggered and $^1O_2$-dependent stress response may constitute an important signalling pathway for biogenic retrograde plastid signalling.

New evidence for the role of Pchlide-derived $^1O_2$ in regulation of nuclear gene expression during early stages of seedling development comes from the molecular study of seedlings transferred to WL after pre-treatment with far red (FR) light (McCormac and Terry, 2002, 2004; Page et al., 2017a). Seedlings kept in darkness followed by FR exposure fail to green in WL. Plastids of *A. thaliana* seedlings receiving this treatment are unable to form PLBs, and instead accumulate aberrant vesicles (Barnes et al., 1996). This response depends on PhyA) activity (Barnes et al., 1996) that induces early steps in the tetrapyrrole pathway, but not the activity of the POR enzyme (Griffiths, 1991). This leads, consequently, to an accumulation of Pchlide during the FR treatment. Analyses of the transcriptome of seedlings transferred from FR to WL indicate induction of $^1O_2$-specific genes in wild type, but not in the *gun5* mutant (Page et al., 2017a), which supports the role of porphyrins in induction of singlet oxygen signalling. Induction of $^1O_2$ by FR pre-treatment is coupled with inhibition of photosynthetic gene expression in *Arabidopsis* seedlings, as shown by reduced accumulation of *HEMA1* and *LHCB* transcripts after WL exposure (McCormac and Terry 2002, 2004; Page et al., 2017a). Based on these findings it can be proposed that the chlorophyll branch of the tetrapyrrole pathway could generate a new negative plastid retrograde signalling pathway, although the genetic components involved in this response still need to be elucidated. More recently, Woodson et al. (2015), characterised induction of a different $^1O_2$ signalling pathway resulting from the accumulation of protoporphyrin IX (Proto IX) in dark grown *fc2* mutants that results in ubiquitin-mediated chloroplast degradation. The E3 ligase, PLANT U-BOX 4 (PUB4) identified by these researchers in a genetic screen for suppression of the *fc2* phenotype, is proposed to play an important role in stress acclimation (Woodson et al., 2015).

SOLDAT10 is another example of a gene for which mutation suppresses acceleration of cell death due to $^1O_2$ over-accumulation and is therefore implicated in influencing retrograde signalling (Meskauskiene et al., 2009). In this case it was proposed that proper plastid protein synthesis, which maintains chloroplast homeostasis, controls $^1O_2$–dependent organellar communication (Meskauskiene et al., 2009). In addition, β-cyclocitral, a product of carotenoid oxidation was shown to selectively influence the expression of many $^1O_2$ responsive genes, and it was therefore suggested to play a role in high light stress responsive retrograde signalling pathways (Ramel et al., 2012). Whether β-cyclocitral can act directly as a signalling molecule or interact with other molecules needs to be determined. So far investigations on $^1O_2$-dependent

signalling have revealed a high level of complexity and possible diversification of models operating to adjust nuclear gene expression.

The increasing amount of evidence discussed above suggests that $^1O_2$ can block photosynthetic gene expression and chloroplast biogenesis to regulate plant photomorphogenesis. However, linking, mechanistically, $^1O_2$ signalling and seedling development remains challenging and this information is still lacking. The aim of this study is to increase our general understanding of mechanisms of $^1O_2$ signalling during seedling development. This will be undertaken using a chemical approach, where the $^1O_2$ response will be induced in a controlled system by feeding the tetrapyrrole precursor ALA. Analysis will focus on testing the recently proposed hypothesis for the role of $^1O_2$ as an inhibitory signal in tetrapyrrole-dependent retrograde signalling to the nucleus (Terry and Smith 2013). This will be achieved by dissecting the effect of chemical treatments and mutations, known to be involved in induction of $^1O_2$, on the inhibition of key photosynthetic and tetrapyrrole genes. The possible integration of different $^1O_2$ responses will also be assessed.

5.2 Results

5.2.1 Induction of singlet oxygen signalling with ALA treatment

To understand better the role of tetrapyrrole-derived $^1O_2$ in regulation of seedling development a new experimental system was examined in which *Arabidopsis* seedlings were grown on ½ MS agar plates, with the tetrapyrrole precursor ALA for 4 d in D. This was designed to increase accumulation of phototoxic tetrapyrrole precursors from the chlorophyll synthesis branch in a controlled manner. Indeed, Figure 5.1A confirms that Col-0 seedlings treated with ALA accumulated an elevated level of Pchlide (and possibly other porphyrins) in the dark compared to non-treated seedlings. Each 0.05 mM increase in the ALA concentration resulted in an almost 2-fold increase in Pchlide content. This indicates ALA applied exogenously can actively impact on tetrapyrrole pathway metabolism and can be potentially a useful strategy to manipulate singlet oxygen-dependent photooxidative stress in young seedlings. To test this further, chlorophyll levels and seedling phenotype were evaluated in 4 d D grown and ALA-treated seedlings after transfer to standard WLc for 24 h (Figure 5.1). A significant, negative correlation ($r = 0.82$) between chlorophyll levels synthesized in WL and ALA concentration applied to D-grown seedlings was observed. Figures 5.1A and 5.1B show that 0.1 mM ALA was sufficient to induce severe photooxidative damage, seen as a block of the ability of seedlings to turn green after transfer to WLc. Feeding with ALA concentrations of 0.15 mM and above completely blocked seedling greening (Figure 5.1B).

To test whether increased ALA levels in seedlings might have deleterious effects independent of light we examined the phenotype of dark-grown seedlings and also measured hypocotyl length. As shown in Figure 5.1C, 0.2 mM ALA significantly blocked seedling growth in darkness, although other aspects of the etiolated phenotype appeared unaltered. To assess specificity for induction of $^1O_2$ signatures, ALA concentrations above 0.15 mM should be avoided in future experiments.

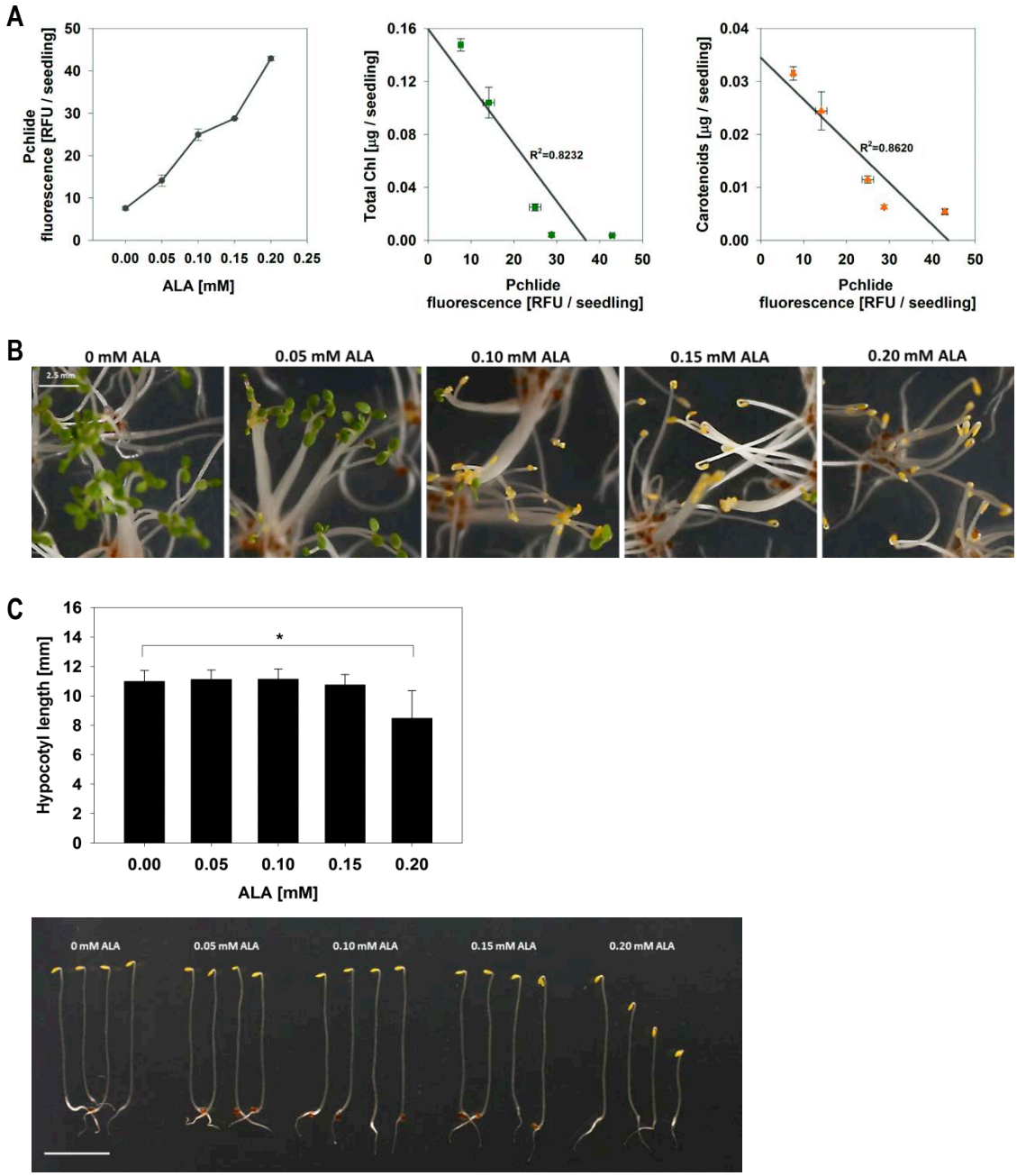

Figure 5.1 Treatment with 5-aminolevulinic acid (ALA) in darkness blocks seedling de-etiolation in light. WT (Col-0) seedlings were grown on 1% agar with ½ MS medium supplemented with 5 mM MES, without sucrose, and with 0-0.2 mM ALA under the following conditions: 4 d D followed by a transfer to WLc (100 µmol m^{-2} s^{-1}) for 1 d. (A) Pchlide and correlation between Pchlide and chlorophyll or carotenoids levels in ALA treated D grown and WLc transferred seedlings, respectively. 30 seedlings were harvested for each biological replicate. Data are means ± SD of three biological replicates. (B) Phenotypes of Col-0 seedlings fed with ALA and transferred to WLc for 24 h. Scale bar indicates 2.5 mm (C) Hypocotyl measurements (top panel) and phenotype (lower panel) of 4d D dark-grown seedlings fed with ALA. 20 seedlings were analysed for each replicate and treatment. Scale bar indicates 5 mm. Asterisks denote significant difference vs Col-0 grown without ALA (Tukey HSD test, *p < 0.05).

It was shown previously that transferring FR pre-treated seedling to WL can block induction of photosynthetic gene expression (McCormac and Terry, 2004; Page et al., 2017a). To ascertain whether the same response was seen after ALA treatment, the expression of selected nuclear-encoded photosynthetic and tetrapyrrole genes was studied in wild type seedlings fed with ALA as described above and transferred to WLc (Figure 5.2). Changes in gene expression were monitored 2 h after transfer to WLc in an attempt to target more closely a response that is direct consequence of singlet oxygen production, and not a secondary effect of oxidative damage. Figure 5.2 shows that feeding dark-grown seedlings with ALA reduced light induction of *LHCB2.1,* and two tetrapyrrole genes, *HEMA1* and *GUN4*. This repression was observed very strongly (5-7-fold down regulation) after treatment with 0.1 mM ALA and was only slightly enhanced with higher ALA concentrations. Thus, 0.1 mM ALA was chosen to be used in future experiments. The repression of photosynthetic gene expression was matched by the induction of *BAP1* expression, a marker gene specific to the singlet oxygen response (op den Camp et al., 2003). This result supports the role of singlet oxygen as a signal controlling photosynthetic gene expression. Interestingly, ALA treatment also activated general stress signalling, as represented by the accumulation of heat shock transcription factor *HSFA2* (Figure 5.2). While the expression of photosynthetic gene expression in light was correlated negatively with Pchlide levels accumulated in dark after ALA feeding (Figure 5.3), the regulation of ROS and stress responsive gene expression was more complex. For example, *BAP1* expression was up-regulated to a similar level after treatment with all ALA concentrations tested (Figure 5.2 and 5.3). This suggests that *BAP1* might be exclusively responsive to the $^1O_2$ and $^1O_2$-dependent signatures can be detected even with small changes in Pchlide levels.

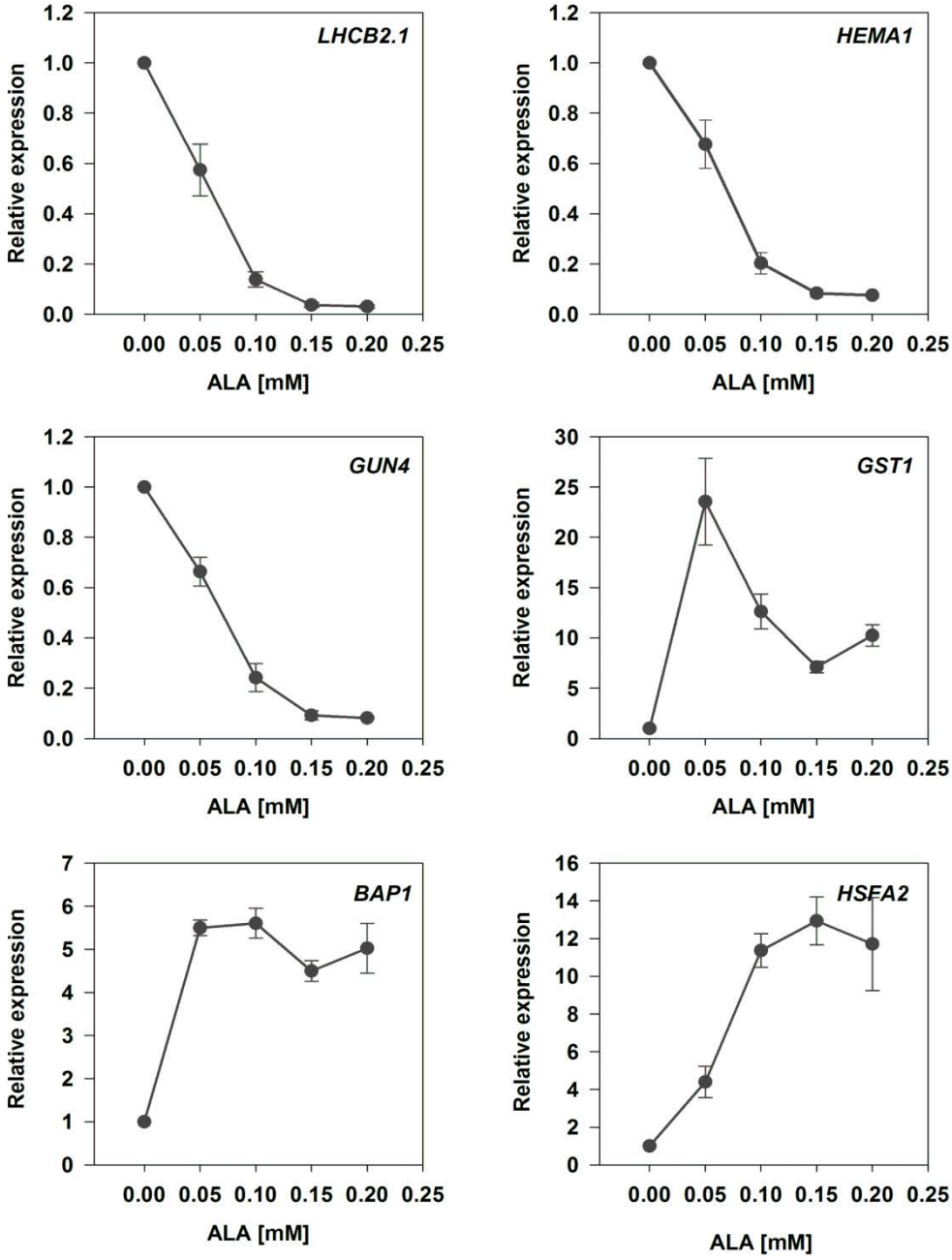

Figure 5.2 Expression of selected photosynthetic, tetrapyrrole, ROS and stress-related marker genes in wild type seedlings after ALA treatment. WT (Col-0) seedlings were grown on 1% agar with ½ MS medium supplemented with 5 mM MES, without sucrose, and with or without different ALA concentration: 0-0.2 mM ALA, under the following conditions: 4 d in D and 2 h in WLc (100 µmol m^{-2} s^{-1}). Gene expression was measured 2 h after WL exposure by quantitative RT-PCR analysis relative to Col-0 grown without ALA, and normalised to *ACTIN DEPOLYMERIZING FACTOR 2* (*ADF2,* At3g46000*)*. Data shown are means +/-SEM of three biological replicates.

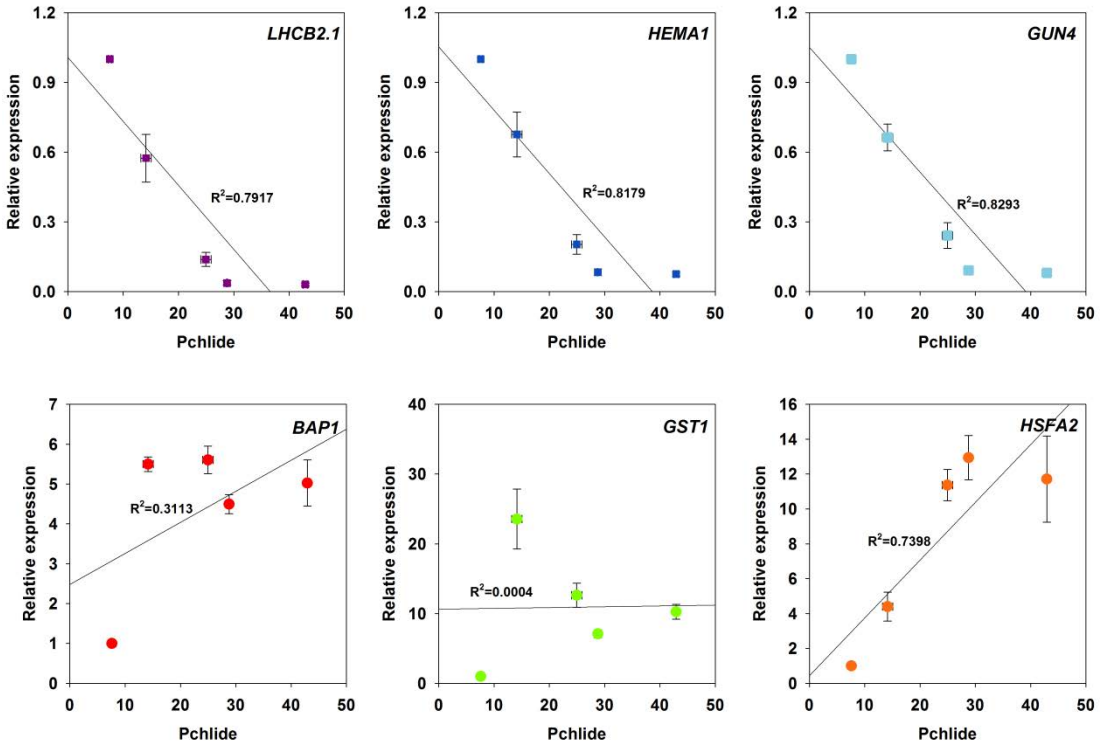

Figure 5.3 Correlation between white light expression of selected photosynthetic, tetrapyrrole, ROS and stress related marker gene and Pchlide accumulation in the dark after ALA treatment. WT (Col-0) seedlings were grown on 1% agar with ½ MS medium supplemented with 5 mM MES, without sucrose, and with or without different ALA concentration: 0-0.2 mM ALA for 4 d in D and 2 h in WLc (100 µmol m^{-2} s^{-1}). Pchlide levels were evaluated in dark grown seedlings before transfer to WL. Gene expression was measured 2 h after WL exposure by quantitative RT-PCR analysis relative to Col-0 grown without ALA, and normalised to *ACTIN DEPOLYMERIZING FACTOR 2* (*ADF2,* At3g46000*)*. Data shown are means ±SEM of three biological replicates.

In the next step, the accumulation of different ROS in cotyledons of seedlings grown on 0.1 mM ALA was monitored by fluorescence microscopy to examine if changes in gene expression observed earlier were correlated with $^1O_2$ production. Staining with Singlet Oxygen Sensor Green (SOSG) was used to test for the presence of $^1O_2$. As shown in Figure 5.4, strong SOSG fluorescence was detected in cotyledons of wild type seedlings treated with 0.1 mM ALA 0.5 h and 2 h after transfer to WLc. In contrast, no SOSG fluorescence was detected in *gun5-1* that is unable to accumulate Pchlide. In addition, no SOSG fluorescence was present in ALA-treated seedlings left in darkness, confirming that light excitation is required for singlet oxygen production after ALA-induced porphyrin accumulation. To determine whether singlet oxygen was produced specifically, seedlings were stained with the general oxidative stress indicator 2',7'-dichlorodihydrofluorescein diacetate (H_2DCFDA). As shown in Figure 5.5, there was no staining in seedlings bleaching in WL after ALA feeding in wild type or *gun5-1* cotyledons, indicating the absence of other ROS.

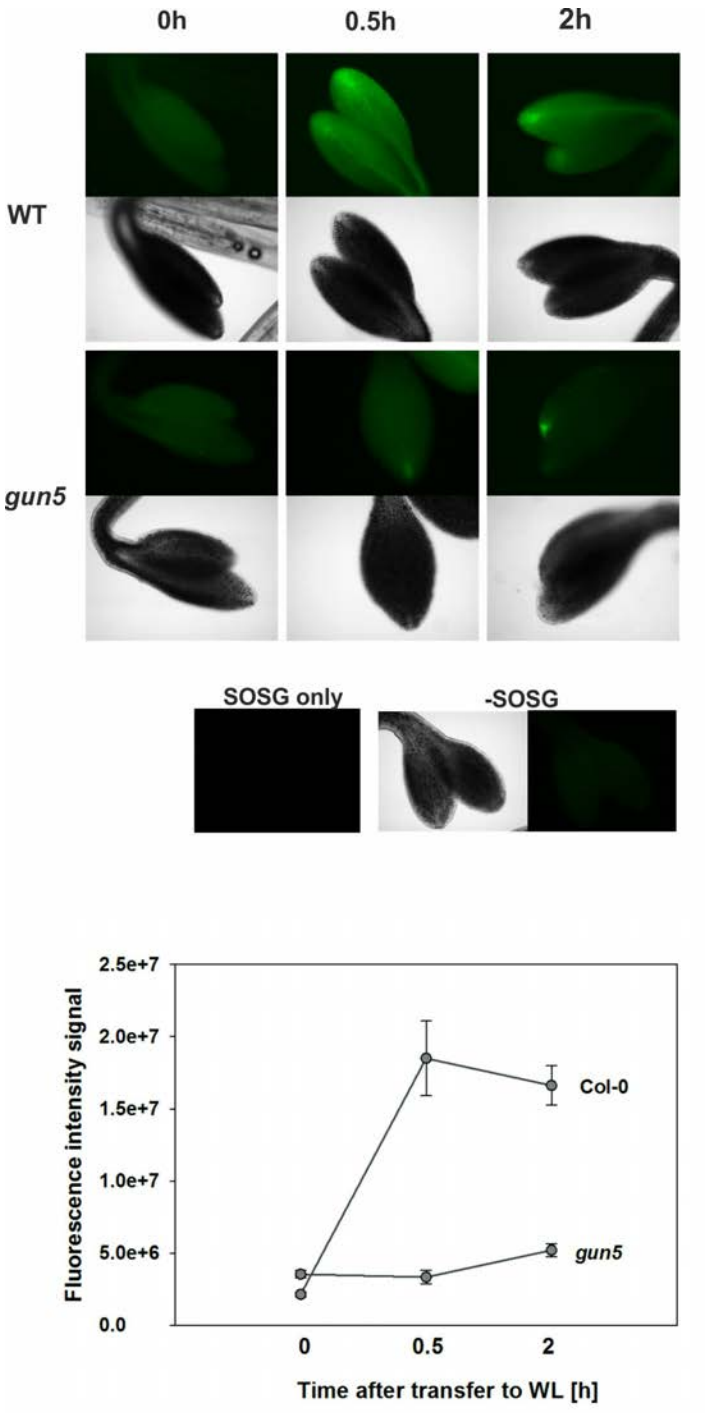

Figure 5.4 Imaging of singlet oxygen ($^1O_2$) levels in cotyledons of ALA-treated seedlings. WT (Col-0) and *gun5-1* seedlings were grown on 1% agar with ½ MS medium supplemented with 5 mM MES, without sucrose, and with or without 0.01 mM ALA concentration for 4 d in D and 0.5 or 2 h in WLc (100 µmol m^{-2} s^{-1}). Singlet oxygen was measured by SOSG fluorescence. Representative photographs are shown from 3 independent biological replicates. Lower panel: Image intensity analysis of SOSG staining outlined above.

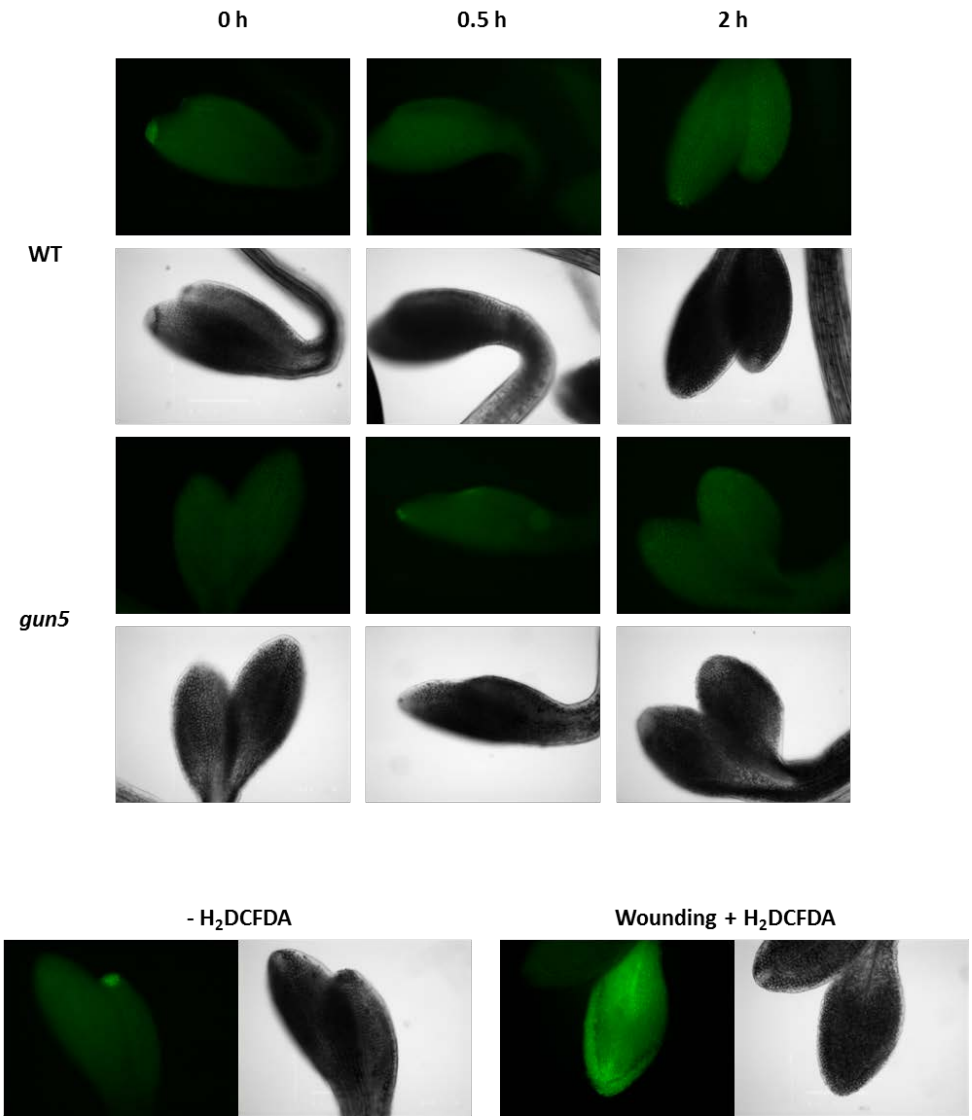

Figure 5.5 Imaging of ROS levels in cotyledons of ALA-treated seedlings. WT (Col-0) and *gun5-1* seedlings were grown on 1% agar with ½ MS medium supplemented with 5 mM MES, without sucrose, and with or without 0.01 mM ALA concentration for 4 d in D and 0.5 or 2 h in WLc (100 µmol m^{-2} s^{-1}). ROS was measured by H_2DCFDA fluorescence. Representative photographs are shown from 2 independent biological replicates.
Lower panel: negative control of seedling auto-fluorescence (left), and positive control of H_2DCFDA fluorescence after wounding stress (right).

To further examine the effect of ALA treatment on the production of singlet oxygen, the expression of different ROS and stress responsive genes was examined by qPCR (Figure 5.6). Three singlet oxygen-responsive genes *BAP1*, *NOD2* and *LTI30* (Op den Camp, 2003; Ramel et al., 2012) were up-regulated after 2 h transfer to WL in wild type fed with 0.1 mM ALA, while there was no induction for any of the H_2O_2 responsive genes: *FER1*, *APX1* or *CAT2* (Op den Camp, 2003; Ramel et al., 2012). Identical results were obtained when gene expression was normalised relative to the *ADF2* and *PRF1* (Ramel et al., 2012) reference genes (Figure 5.6). These results support the proposal that ALA-treatment leads to the induction of singlet oxygen signalling.

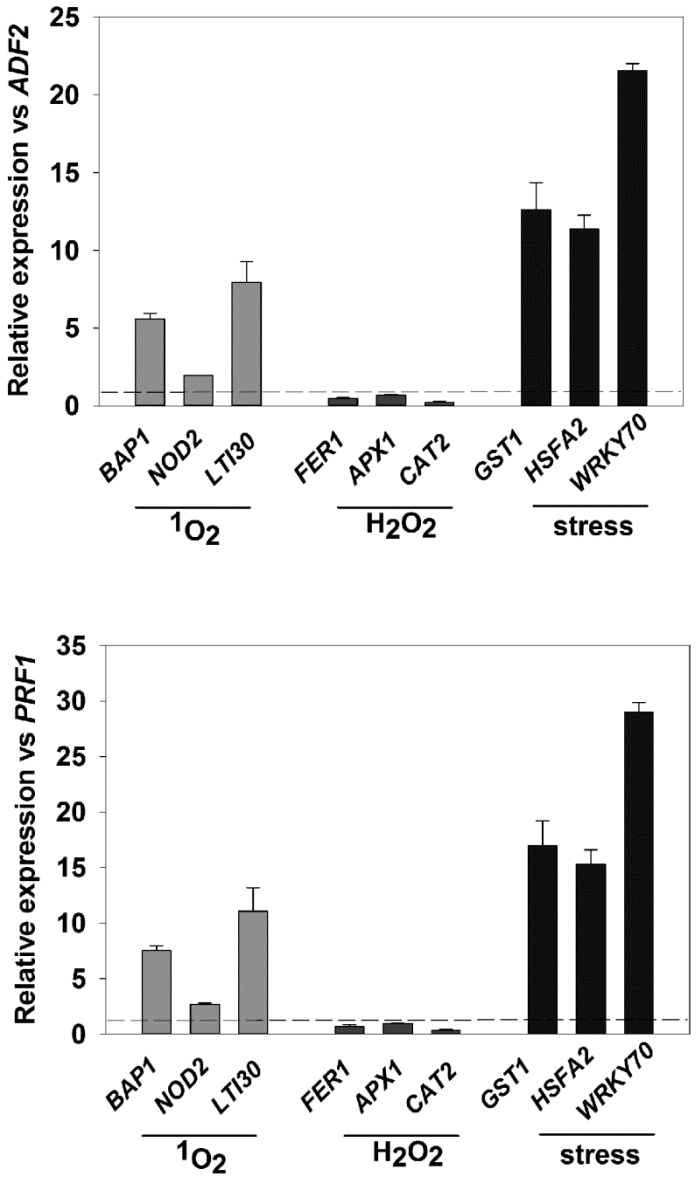

Figure 5.6 Expression of different ROS responsive genes in wild type seedlings after ALA treatment. WT (Col-0) seedlings were grown on 1% agar with ½ MS medium supplemented with 5 mM MES, without sucrose, and with or without different 0.01 mM ALA concentration for 4 d in D and 2 h in WLc (100 µmol m^{-2} s^{-1}). Gene expression was measured by quantitative RT-PCR analysis 2 h after WL exposure, and normalised to *ACTIN DEPOLYMERIZING FACTOR 2* (*ADF2,* At3g46000; A), or *PROFILIN 1* (*PRF1*, AT2G19760; B). Data shown are means +SEM of three biological replicates.

5.2.2 Induction of singlet oxygen response by FR pre-treatment

The FR pre-treatment was shown to cause seedling bleaching and block of chloroplast development during seedling photomorphogenesis (Barnes et al., 1996; McCormac and Terry 2002). Integration of this response with singlet oxygen retrograde signalling was examined in more detail to test for similarities with ALA-induced signalling. Firstly, the ability to accumulate Pchlide was examined in 2 d D grown Col-0 and *gun5-1* seedlings transferred to FR for 1-3 d or left in darkness. Consistent with other studies on FR pre-treatment described above, the data confirmed that exposure to FR resulted in a rapid (within one day) and strong increase in Pchlide levels in wild type, but not in *gun5-1* (Figure 5.7A). This was similar, to what was observed for ALA feeding to wild type, however longer exposure to FR (2.5-3 d) did not have such a pronounced effect on Pchlide accumulation in seedlings, in contrast to feeding with increasing doses of ALA in the dark (compare Figure 5.7A, B and Figure 5.1).

The association between length of the FR growth and induction of inhibitory retrograde signalling was further evaluated by measuring expression of two photosynthetic genes *LHCB2.1* and *HEMA1* in wild type and *gun5-1* seedlings after 1-3 d FR pre-treatment followed by 24 h WLc exposure (Figure 5.8A). The analysis confirmed that, as seen previously (McCormac and Terry, 2004; Page et al., 2017a), in Col-0 there was a strong down-regulation of *LHCB2.1* and *HEMA1* following FR pre-treatment and subsequent WLc exposure. Additionally, this effect was dependent on time of FR pre-irradiation (Figure 5.8B). At 1.5 d FR pre-treatment a strong, 3-5-fold repression of *LHCB2.1* and *HEMA1* was detected in wild type and expression diminished thereafter with longer FR pre-irradiation. In contrast, *gun5-1* rescued *HEMA1* and *LHCB2.1* expression. For *HEMA1,* the rescue of expression was complete after 2.5 d FR pre-treatment, while for *LHCB2.1* the rescue response was weaker (Figure 5.8B). These results indicate that progressive loss of transcription of photosynthetic gene expression following transfer to WL is tightly coupled with the accumulation of the phototoxic porphyrins in seedlings, and suggests an important role for singlet oxygen as a signalling component.

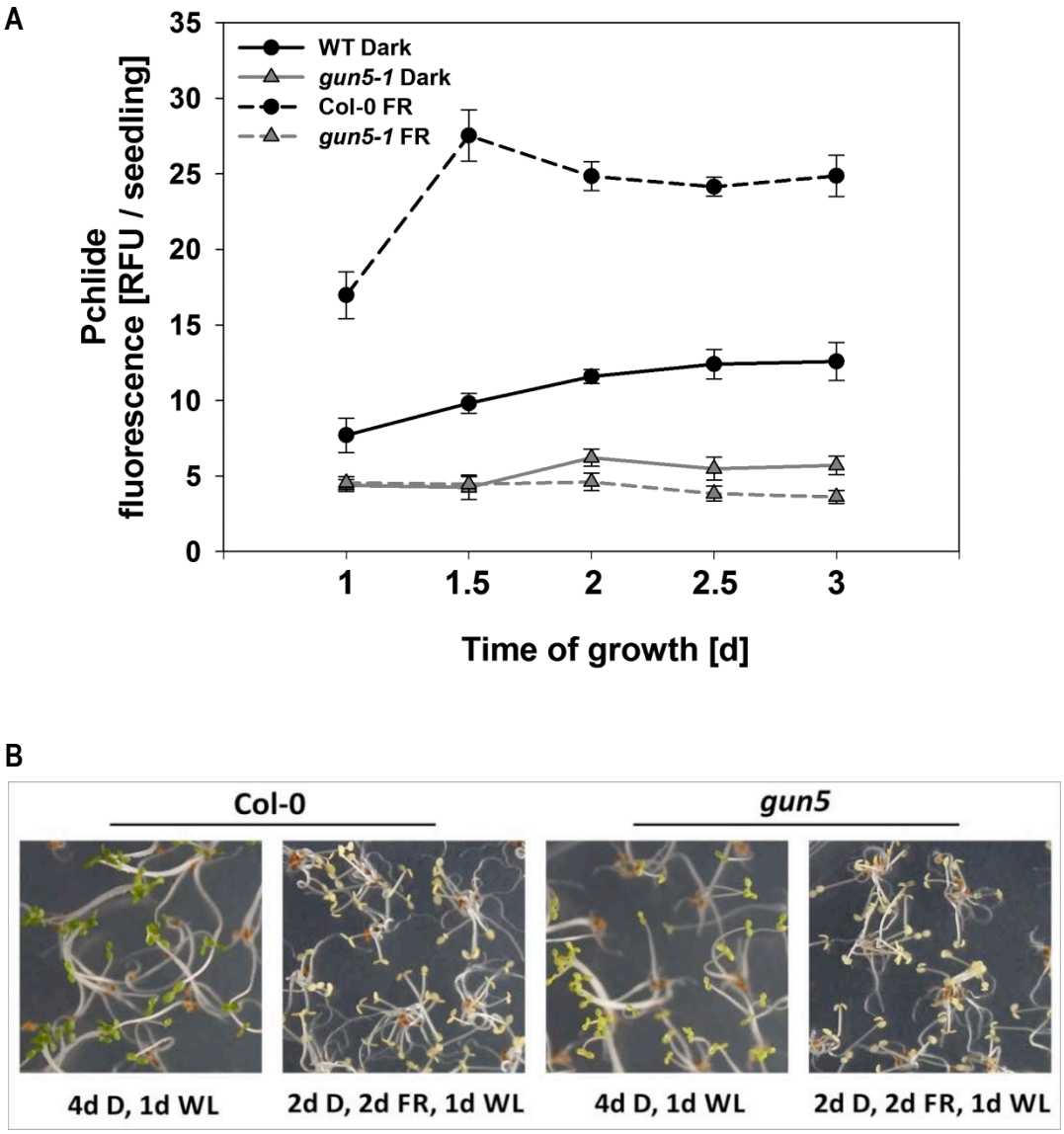

Figure 5.7 The response to a far red (FR) light pre-treatment. (A) Protochlorophyllide (Pchlide) accumulation in WT (Col-0) and *gun5-1* mutant seedlings grown on 1% agar, with ½ MS medium, without sucrose, for 2 d D and 1, 1.5, 2, 2.5 and 3 d FR. As a control, seedlings grown only in D for the corresponding time were used. Data are means ± SD of three independent biological replicates. (B) Phenotypes of 5 d old Col-0 and *gun5-1* etiolated seedlings grown under the following conditions: 2 d D + 2 d FR or 4 d D followed by 1 d in WLc (100 µmol m^{-2} s^{-1}).

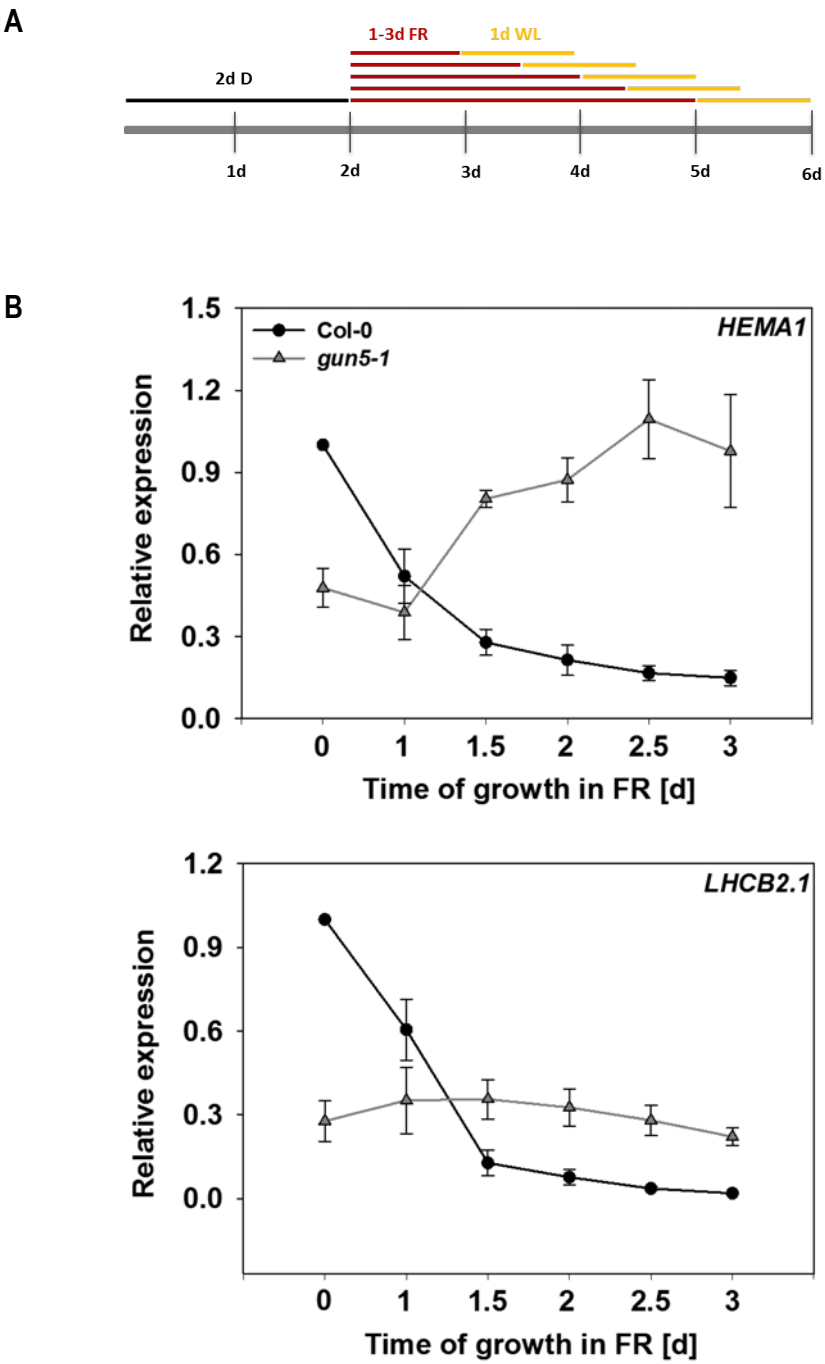

Figure 5.8 Time course for the effect of far red (FR) pre-treatment length on *LHCB2.1* and *HEMA1* expression. (A) A graphical representation of the experimental design, where: D – dark, FR –far red, WL- white light. (B) WT (Col-0) and *gun5-1* seedlings were grown on 1% agar, with ½ MS medium, without sucrose, for 2 d in D and transferred to FR for 1-3 d, each time followed by exposure to WLc (100 µmol m^{-2} s^{-1}) for 1 d. Gene expression was measured by quantitative RT-PCR analysis and normalised to *ACTIN DEPOLYMERIZING FACTOR 2* (*ADF2,* At3g46000) and to dark-grown Col-0. Data shown are means + SEM of three biological replicates.

To characterize further the ROS response of FR pre-treated seedlings transferred to WLc ROS levels were measured using H_2DCFDA and SOSG fluorescence.

Strong SOSG fluorescence, but no H_2DCFDA fluoresce, was detected in cotyledons of wild type, within hours of transfer from FR to WL (Figure 5.9A) indicting that the bleaching after FR pre-irradiation is due to a specific release of singlet oxygen. The increase in SOSG fluorescence was detected as early as 0.5 h after WL exposure and was the strongest after 2 h transfer to WL. These results are similar to those seen after ALA feeding (Figures 5.4 and 5.5). To examine whether singlet oxygen induced cellular damage resulted in a cell death, FR pre-treated Col-0 seedlings were stained with trypan blue, which can only enter dead cells. As shown in Figure 5.9B, a strong increase in trypan blue staining was detected in cotyledons of wild type with prolonged time of exposure to WLc after FR pre-irradiation.

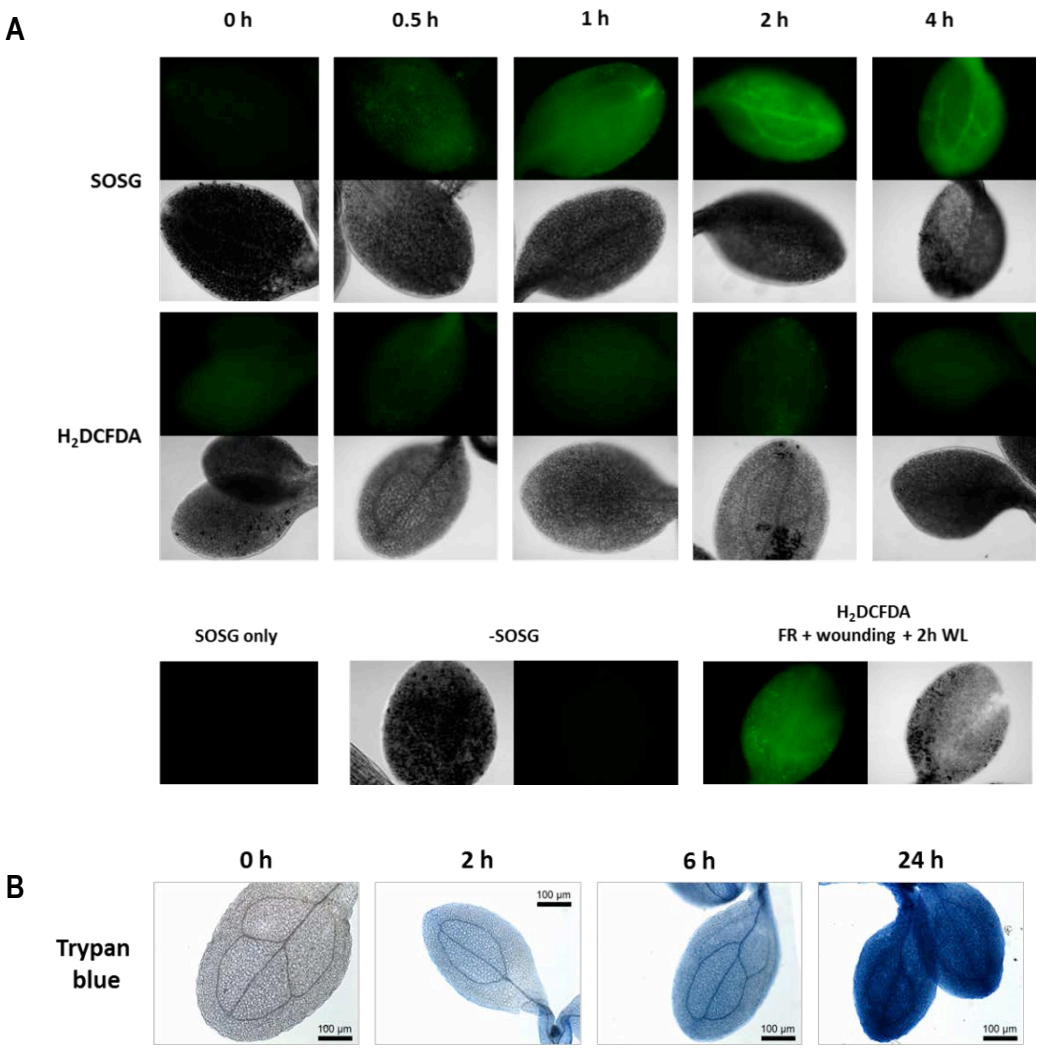

Figure 5.9 Cellular ROS and cell death induction in cotyledons of FR pre-treated seedlings. WT (Col-0) and *gun5-1* seedlings were grown on 1% agar with ½ MS medium supplemented, without sucrose, for 2 d in D and 2 d in FR followed by 0.5-24 h in WLc (100 µmol m^{-2} s^{-1}). (A) Singlet oxygen was determined by SOSG fluorescence. Other ROS were examined using H_2DCFDA fluorescence. (B) Effect of the FR pre-treatment on cell death induction investigated with trypan blue staining of Col-0 cotyledons after FR pre-treatment. Representative photographs are shown from 3 independent biological replicates.

5.2.3 Singlet oxygen signalling is dependent on Mg-porphyrin synthesis after ALA treatment

Results presented earlier in this section clearly indicate that increased porphyrin accumulation due to ALA feeding to dark-grown *Arabidopsis* seedlings induces singlet oxygen-dependent inhibitory retrograde signalling. To gain more understanding on the specificity of the ALA response, the impact of the ALA feeding on retrograde signalling was examined in *gun5-1* that is unable to accumulate high Mg-Proto IX or Pchlide levels, but can still potentially accumulate elevated levels of other phototoxic porphyrins like protoporphyrin IX. Thus, the *gun5-1* mutant was expected to rescue, at least partially, the effects of ALA treatment. As shown in Figure 5.10, *gun5-1* mutant was unable to accumulate high Pchlide levels after feeding with 0.1-0.2 mM ALA in the dark compared to wild type. This was accompanied by a very strong rescue from the inhibitory effect of ALA on the light induction of *LHCB2.1* and *HEMA1* photosynthetic gene expression in *gun5-1* measured 2 h after transfer to WLc. The reduced repression of photosynthetic gene expression in *gun5-1* after transfer to WLc was due to lower singlet oxygen production in the mutant, as demonstrated by lower *BAP1* induction compared to ALA treated wild type in WLc (Figure 5.10) and reduced SOSG fluorescence in ALA treated *gun5-1*, shown earlier (Figure 5.4). The *gun5-1* response to ALA treatment is consistent with the requirement for porphyrins for induction of singlet oxygen signalling. Importantly, the effect of ALA treatment was light dependent, as no down-regulation of *LHCB2.1* or *HEMA1*, and no induction of *BAP1* were detected in dark-grown wild type or *gun5-1*seedlings treated with ALA compared to dark-grown controls. Collectively, this data suggests that singlet oxygen inhibitory signalling resulting from ALA treatment is strongly dependent on Pchlide accumulation, but a contribution of other porphyrins in promotion of the singlet oxygen response cannot be excluded.

To determine how quickly changes in gene expression could be observed after transfer of FR-treated seedlings to WL a time course was performed in wild type and *gun5-1* seedlings (Figure 5.11). Changes in gene expression could be seen between wild type and *gun5-1* within 15 min of WL. This was clear for both *HEMA1* and *BAP1* gene expression profiles, although in this experiment no difference in expression profile for *LHCB2.1* was observed between FR pre-treated wild type and *gun5-1* (Figure 5.11). The *LHCB2.1* result, was different from that observed after ALA response (Figure 5.10) and in previous FR experiments (Figure 5.8).

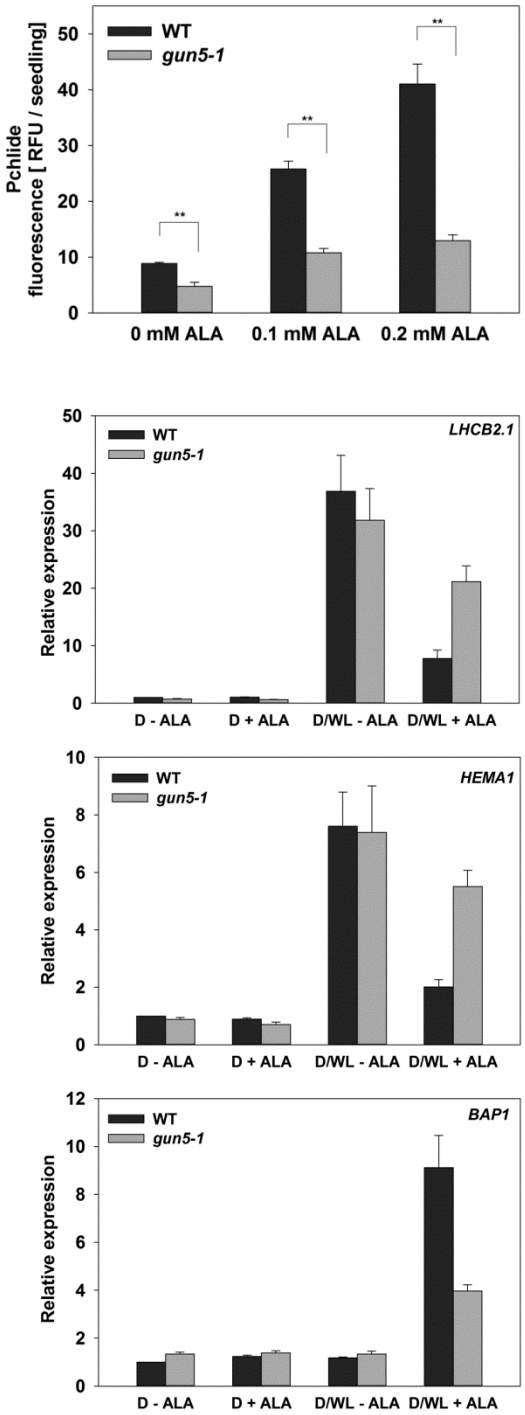

Figure 5.10 *gun5-1* rescues inhibition of gene expression induced by ALA treatment. WT (Col-0) and *gun5-1* seedlings were grown on 1% agar with ½ MS medium supplemented with 5 mM MES, without sucrose, and with or without 0.1-0.2 mM ALA for 4 d in D and 2 h in WLc (100 µmol m^{-2} s^{-1}). (A) Pchlide levels in 4 d D grown seedlings. 30 seedlings were harvested for each biological replicate. Data are means + SD of three biological replicates. (B) Gene expression measured 2 h after WLc exposure by quantitative RT-PCR analysis relative to Col-0 grown without ALA for 4 d D, and normalised to *ACTIN DEPOLYMERIZING FACTOR 2* (*ADF2*, At3g46000). Data shown are means +SEM of three biological replicates. Asterisks denote significant difference vs Col-0 for the same treatment (± ALA), Student's *t* test (*$p < 0.05$, **$p < 0.01$).

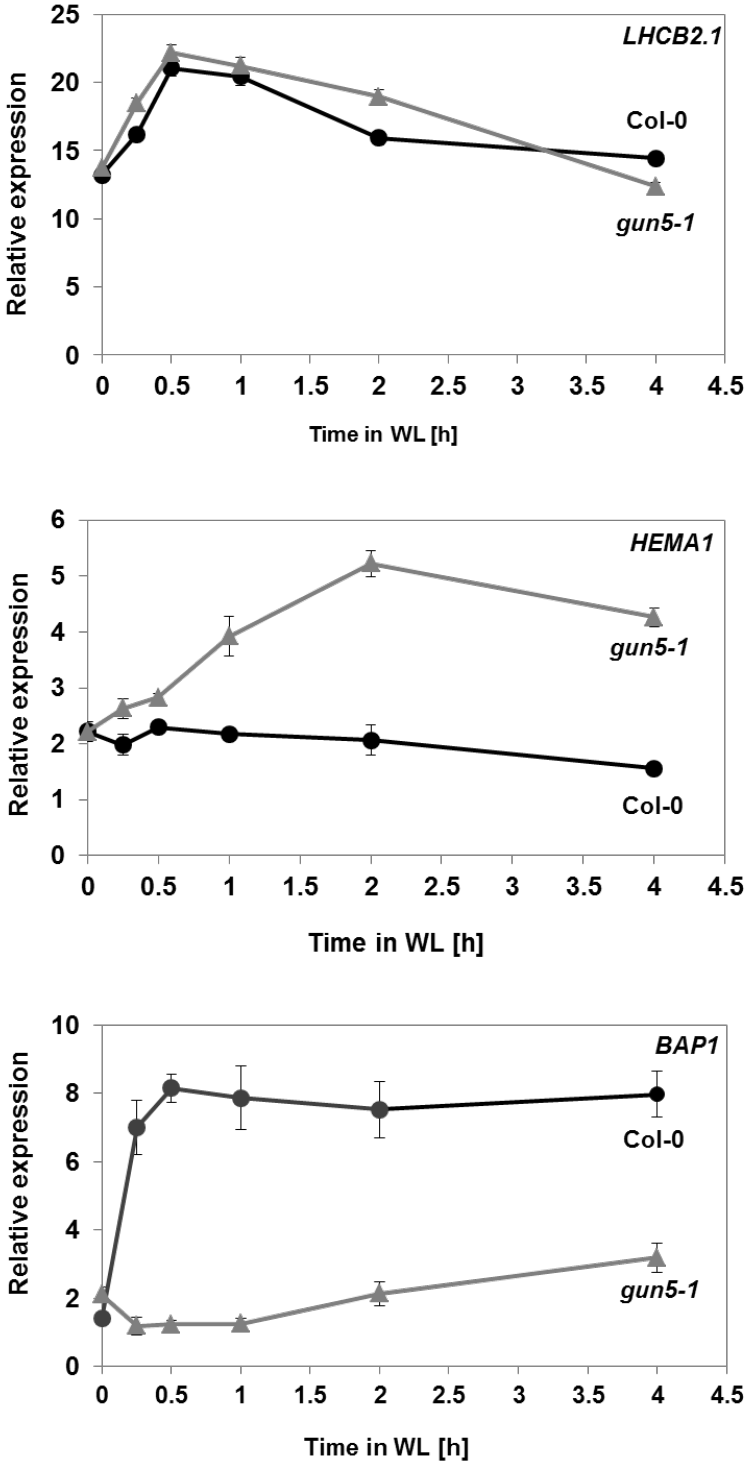

Figure 5.11 Expression of *LHCB2.1*, *HEMA1* and *BAP1* at early time points after transfer from far red (FR) to WLc. WT (Col-0) and *gun5-1* seedlings were grown on 1% agar, with ½ MS medium, without sucrose, for 2 d in D and 2 d FR and were transferred to WLc for 15 min to 4 h. Gene expression was measured by quantitative RT-PCR analysis and normalised to *ACTIN DEPOLYMERIZING FACTOR 2* (*ADF2,* At3g46000) and to Col-0 grown for 4 d D. Data shown are means ± SEM of three biological replicates.

5.2.4 Environmental regulation of singlet oxygen signalling

In this study, the ALA-induced singlet oxygen signalling was shown to be light dependent (Figure 5.10), thus the impact of the light intensity on regulation of this signalling was next examined. As shown in Figure 5.12, exposing 4 d old WT seedlings fed with 0.1 mM ALA in D to different WL intensities for 2 h had no strong effect on gene expression changes. Light induction of both, *LHCB2.1* and *HEMA1* was repressed to almost identical levels under 50-200 µmol $m^{-2}s^{-1}$ WL in ALA treated seedlings. Although under the low light intensity this repression was reduced, inhibition was still significant (p-value<0.05; Figure 5.12). This pattern was similar for *BAP1* expression, with *BAP1* highly up-regulated on ALA even under low WL and little further enhancement with increased WL intensity.

Studies indicate that temperature stresses can impact on chlorophyll biosynthesis through the reduction in porphyrin synthesis (Zhou et al., 2013). In order to examine if temperature stress responses can alter the expression response following ALA feeding, changes in gene expression were measured in dark grown WT seedlings treated with ALA and pre-treated with short cold stress or heat shock (HS) before exposure to 2 h of WL (see detail in Figure 5.13). Both temperature stresses were performed in darkness to separate them from additional light-dependent photooxidative effects. Analysis showed that while the short cold stress did not have any significant effect on the expression of genes inhibited and up-regulated by ALA treatment after transfer to WL, the HS pre-treatment disturbed the response to ALA. This was observed mostly, as the lack of induction of three singlet oxygen responsive genes *BAP1*, *NOD1* and *LTI30* in wild type seedlings treated with both ALA and HS, compared to seedlings treated with ALA only (Figure 5.13). Block of induction of these three genes could suggest that singlet oxygen signalling was inhibited by HS, however, no rescue of any photosynthetic gene expression was seen in ALA and HS treated seedlings compared with inhibition of these genes in WL by ALA treatment. This was because the HS treatment in D alone blocked very strongly the light induction of *LHCB2.1*, *GUN4* and *HEMA1* expression in control seedlings, and this response was not further enhanced by additional ALA treatment (Figure 5.13). To test whether this inhibitory response after HS treatment might be due to the increased H_2O_2 stress that is strongly implicated in the response to HS, expression of general ROS (*GST1*) and H_2O_2-responsive genes (*CAT2*, *APX1*) was measured under the same conditions as described above (Figure 5.13). Surprisingly, none of these 3 genes were up regulated by HS treatment in both control and ALA treated seedlings, with *CAT2* and *APX1* even repressed by the HS treatment.

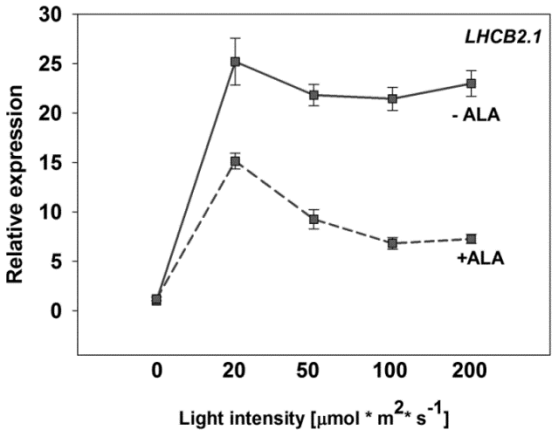

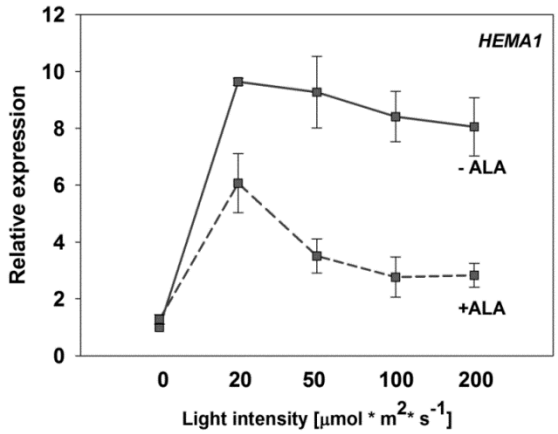

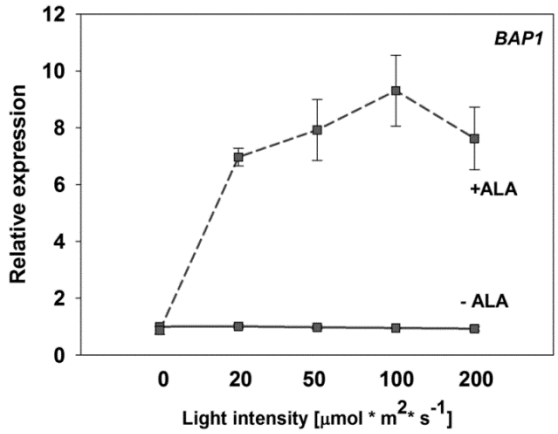

Figure 5.12 The effect of light intensity on expression of *LHCB2.1*, *HEMA1* and *BAP1* after ALA treatment. WT (Col-0) seedlings were grown on 1% agar with ½ MS medium supplemented with 5 mM MES, without sucrose, and with or without 0.1 mM ALA for 4 d in D. Seedlings were transferred to WLc for 2 h, under different light intensities (10-200 µmol $m^{-2}s^{-1}$), or were left in darkness. Gene expression was measured 2 h after WL exposure by quantitative RT-PCR analysis relative to Col-0 grown without ALA in darkness, and normalised to *ACTIN DEPOLYMERIZING FACTOR 2* (*ADF2,* At3g46000*)*. Data shown are means +/-SEM of three biological replicates.

Although this observation is difficult to explain, it is important to note that elevated expression of the heat stress marker genes *HSFA2*, *HSP17.6* in HS treated seedlings, and the cold stress marker gene *COR15a* in cold-treated seedlings was detected indicating both temperature stresses were effectively induced. The observation that *BAP1* was induced by the HS suggests the possibility that instead this treatment may be affecting singlet oxygen signalling.

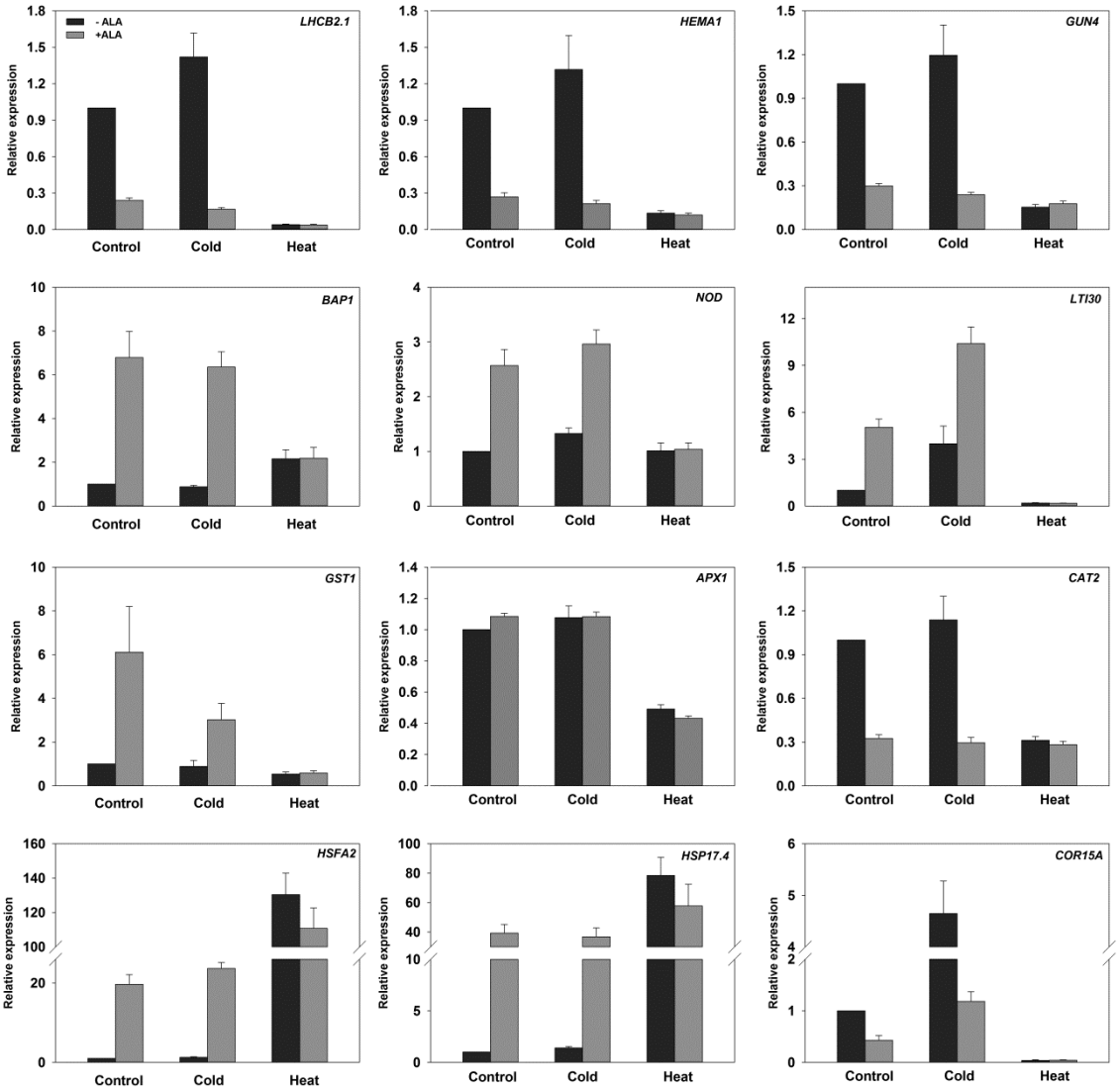

Figure 5.13 The effect of temperature stress on ALA–mediated regulation of nuclear gene expression. WT (Col-0) seedlings were grown on 1% agar with ½ MS medium supplemented with 5 mM MES, without sucrose, and with or without 0.1 mM ALA, under following conditions: 4 d in D and 2 h in WLc (100 µmol m^{-2} s^{-1}) at 22°C. For cold and heat stress treatments, before transfer to WL plates were treated with 4°C for 2 h or with 44°C for 1 h, respectively, in D. Gene expression was measured 2 h after WL exposure by quantitative RT-PCR analysis relative to Col-0 grown under standard temperature condition, without ALA (control), and normalised to *ACTIN DEPOLYMERIZING FACTOR 2* (*ADF2,* At3g46000*)*. Data shown are means +SEM of three biological replicates.

5.2.5 Induction of inhibitory retrograde signalling in *flu*

ALA feeding experiment could possibly result in ALA interaction with cellular components other than the tetrapyrrole pathway leading to the observed inhibition of gene expression. To analyse the role of tetrapyrrole-derived singlet oxygen signalling in regulation of nuclear gene expression under more specific conditions than an ALA treatment, the *flu* mutant was used.

In the dark, *flu* accumulated high Pchlide levels compared to wild type and this was accompanied by a complete block of the *flu* seedlings ability to green after transfer to WLc for 24 h (Figure 5.14A). This is consistent with previous characterization of the *flu* mutant (Meskauskiene et al.,2001), and is very similar with the response to ALA treatment described earlier in this chapter. The *flu* mutant bleaching phenotype has previously been shown to result from singlet oxygen production followed by an up-regulation of singlet oxygen specific genes (Meskauskiene et al.,2001; Op den Camp, 2003). It can be expected that inhibitory retrograde signalling is also induced in the *flu* mutant, however, this has not been examined before. As shown in Figure 5.14B, light induction of *LHCB2.1*, *HEMA1* and *GUN4* was severely repressed in the *flu* mutant compared to Col-0 2 h after transfer to WL. This response correlated with the significant up-regulation of singlet oxygen responsive genes *BAP1* and *LTI30* in *flu* compared to wild type. The same results were obtained when gene expression was normalised relative to *ADF2* and *PRF1* (Figure 5.14B, C). The identical pattern of gene expression to that observed earlier after ALA feeding (Figure 5.2) indicates that potentially the same signalling pathways were induced in both experimental systems. This observation provides further evidence for the requirement for porphyrin accumulation to induce a singlet oxygen signal and for an important role of this signal in the control of the photosynthetic gene expression in developing seedlings. Interestingly, D grown *flu* seedlings showed a moderate up-regulation of *HEMA1* and *GUN4* (but not *LHCB2.1*) compared to wild type, which could be the consequence of elevated tetrapyrrole accumulation activating the positive, heme-dependent signalling pathway.

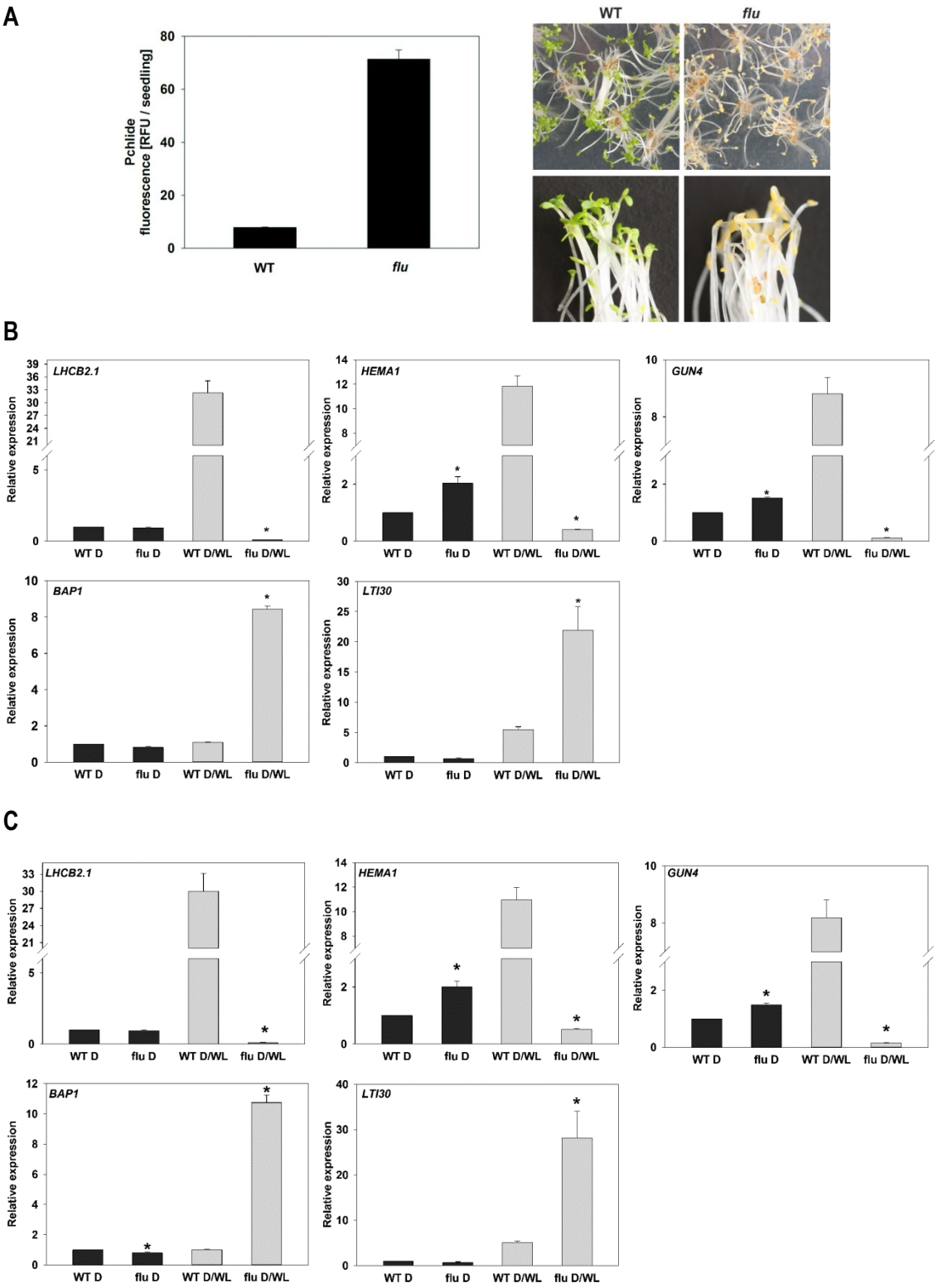

Figure 5.14 Changes in nuclear gene expression in dark-grown *flu* seedlings after transfer to WL. WT (Col-0) and *flu* seedlings were grown on 1% agar, with ½ MS medium, without sucrose under the following conditions: 4 d in D followed by transfer to WL (100 µmol m^{-2} s^{-1}) for 2 h or 24 h. (A) Pchlide accumulation in 4 d D grown Col-0 and *flu* (left) and seedling phenotype after transfer to WLc for 24 h (right). (B, C) Expression of selected photosynthetic, tetrapyrrole and $^1O_2$ marker genes measured before (D) and 2 h after WL exposure (D/WL) by quantitative RT-PCR analysis relative to Col-0 grown for 4 d in D, and normalised to *ACTIN DEPOLYMERIZING FACTOR 2* (*ADF2,* At3g46000; B*)* and to *PROFILIN 1* (*PRF1*, AT2G19760; C). Data shown are means +SEM of three biological replicates. Asterisks denote significant difference vs Col-0 for the same treatment (D or D/WL), Student's *t* test (*p < 0.05).

To examine the specificity of inhibitory signalling generated due to the singlet oxygen production in the *flu* mutant, global gene expression changes resulting from *flu* shifted from dark to WL were compared and classified for enriched functional terms (Figure 5.15). Two publicly available full transcriptome data sets for *flu* are available: WLc-grown Col-0 and *flu* mature plants (GSE10812; Op den Camp, 2003) and 4 d-old etiolated seedlings (GSE10812; Woodson et al., 2015), both transferred from D to WL for 2 h. These were downloaded and processed as described in Chapter 2 (see section 2.10), in order to find significantly down-regulated genes. Figure 15.5A shows the numbers of genes commonly repressed in the *flu* mutant by both treatments. Although twice as many genes were down-regulated in young *flu* seedlings transferred from D to WL than in mature plants, comparison between these 2 data sets showed significant overlap, with 260 genes (42 genes expected by chance) shared by the two treatments. This cohort of *flu* inhibited genes may be specific to singlet oxygen signalling and was further classified for enriched functional terms using the Classification SuperViewer tool at the Bio-Analytic Resource for Plant Biology (http://bar.utoronto.ca). Although, many metabolic processes were affected by *flu*, a high degree of specificity was also observed. Among the down-regulated genes, categories of photosynthesis (PS), tetrapyrrole synthesis and cell wall synthesis were the most highly enriched (Figure 5.15). Other significantly overrepresented terms included: abiotic stresses (misc), signalling, RNA and DNA processing, protein synthesis, transport and stress responses.

Bioinformatics analysis suggests the inhibitory singlet oxygen-dependent signal is not only important for the control of induction of photosynthetic gene expression in etiolated seedlings, as shown earlier in this chapter, but can also potentially operate in green plants, with developed chloroplasts. The original *flu* mutant characterisation is also supportive of the presence of singlet oxygen signatures in mature plants (Op den Camp, 2003). To test this hypothesis, increased Pchlide accumulation was induced transiently in 5-d old WLc-grown green seedlings, either by transferring *flu* plants to 24 h D, or by transferring WT seedlings to liquid ½ MS medium supplemented with 0.2 mM ALA for 24 h D (Figure 5.16). *BAP1* expression was monitored additionally as a specific indicator of singlet oxygen signalling. The results confirm that in the *flu* mutant and ALA treated WT seedlings there was a strong down-regulation in *LHCB2.1*, *HEMA1, GUN4* expression and up-regulation in *BAP1* expression following 2 h WL. This suggests that the singlet oxygen signal acts on both plastids and chloroplasts as a repressor of photosynthetic gene expression and contributes to regulation of seedling development and growth.

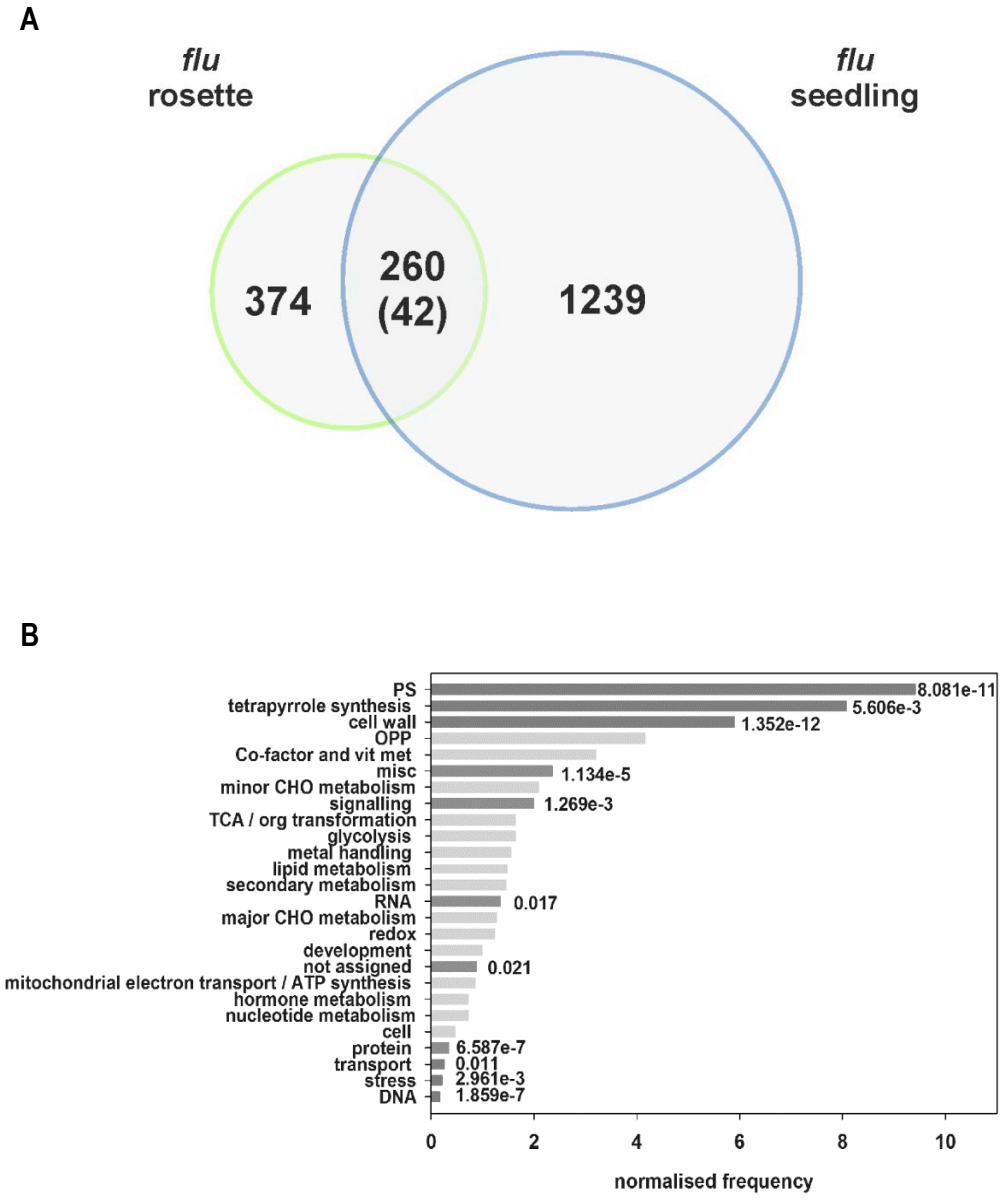

Figure 5.15 Bioinformatic analysis of genes down-regulated in *flu* after transfer from dark (D) to white light (WL). (A) Venn diagrams depicting common sets of genes down-regulated in mature *flu* plants (*flu* rosette, GSE10812) and *flu* seedlings (GSE10812) 2 h after a shift from D to WL. Number in parenthesis corresponds to genes overlapping by chance. (B) Gene ontology (GO) term enrichment for the set of 260 common genes identified in the two *flu* transcriptomes. GO terms were based on Mapman bins and were plotted relative to their frequency in the *Arabidopsis* gene set. Significant GO terms are marked in bold and p-values of the hypergeometric distribution are indicated.

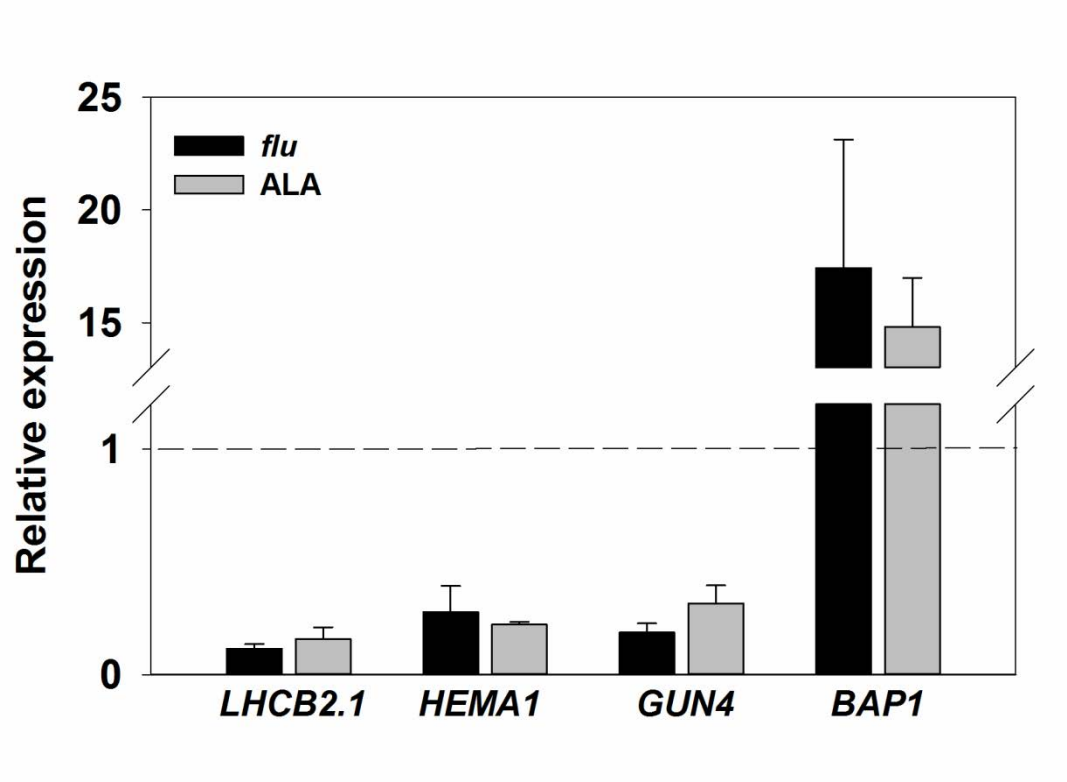

Figure 5.16 Induction of inhibitory retrograde signal in green *flu* seedlings or green WT seedlings treated with ALA. For *flu* experiment, WT and *flu* mutant seedlings were grown on 1% agar, with ½ MS medium, without sucrose, under the following conditions: 5 d in WLc (100 µmol m^{-2} s^{-1}) followed by 24 h D and 2 h WL exposure. For ALA treatment WT seedlings were grown on 1% agar, with ½ MS medium supplemented with 5mM MES, without sucrose under the following conditions: 2 d D and 3 d WLc (100 µmol m^{-2} s^{-1}). 5d old WT seedlings were transferred to liquid ½ MS medium supplemented with 5mM MES, with or without 0.2 mM ALA, and left in D for 24 h followed by a 2 h WL re-exposure. Gene expression was measured 2 h after WL re-exposure by quantitative RT-PCR analysis relative to WT transferred from D to WL and grown on agar ½ MS (*flu*) or treated with liquid ½ MS with MES only (ALA). Data were normalised to *ACTIN DEPOLYMERIZING FACTOR 2* (*ADF2,* At3g46000*)*. Data shown are means +SEM of three biological replicates.

5.2.6 Genetic regulation of ALA-induced singlet oxygen signalling

$^1O_2$ signalling induced by the ALA treatment is strongly associated with an excitation of tetrapyrrole precursor Pchlide accumulated in the dark. However, other porphyrins are able to induce singlet oxygen production and have been associated with single oxygen responses. For example, protoporphyrin IX (Proto IX) accumulated in *fc2-1* and *fc2-2* mutants transferred to dark and resulted in photobleaching on transfer to WL (Woodson et al., 2015). In order to verify the extent to which singlet oxygen signals derived from different pools of excited porphyrins contribute to the inhibition of photosynthetic gene expression, expression of selected nuclear genes was measured after 2 h of WL exposure in 4 d-old *fc1* and *fc2* mutants fed with ALA in the dark (Figure 5.17). In this experiment the lower (0.05 mM) ALA concentration was used that results only in a moderate photosynthetic gene repression in wild type seedlings (Figure 5.2), to ensure seedlings were still viable. Of the three ferrochelatase mutants tested, *fc2-1* and *fc2-2* showed a significantly stronger WL repression of *LHCB2.1* and *HEMA1* expression after ALA treatment compared to ALA treated wild type, while in ALA-treated *fc1-1* mutant this repression was weaker, with a significant rescue of *HEMA1* expression. The response of *fc1* and *fc2* mutants to ALA was not due to a different Pchlide level accumulation after ALA feeding although under control conditions dark-grown *fc2* mutants accumulated more Pchlide than WT (Figure 5.19). The hypersensitive phenotype of *fc2* was consistent with the higher induction of singlet oxygen responsive gene *BAP1* compared to wild type. The strong repression of *LHCB2.1* and *HEMA1* was also apparent in *fc2* mutants after transfer to WL without ALA treatment (Figure 5.17), but to a lesser extent then after ALA feeding. This phenotype is also consistent with the previous characterisation of Woodson et al., (2015). The response of the *fc2* mutant either with or ALA treatment suggests that singlet oxygen response derived through excitation of different Proto IX can also contribute to an inhibition of tetrapyrrole and photosynthetic gene expression. Interestingly, in the*fc1-1* mutant an enhanced induction of the singlet oxygen-responsive gene *BAP1* was uncoupled from Pchlide-dependent repression of photosynthetic gene expression (Figure 5.17, 5.19). This suggests that FC1 is also involved in regulation of singlet oxygen signalling although its precise role is not clear.

To examine further the genetic mechanisms that might contribute in mediating ALA-induced singlet oxygen signalling, the effect of known $^1O_2$ mutants on *LHCB2.1*, *HEMA1* and *BAP1* expression was tested (Figure 5.18). Gene expression was examined 24 h after transfer to WLc in seedlings treated with 0.1 mM ALA.

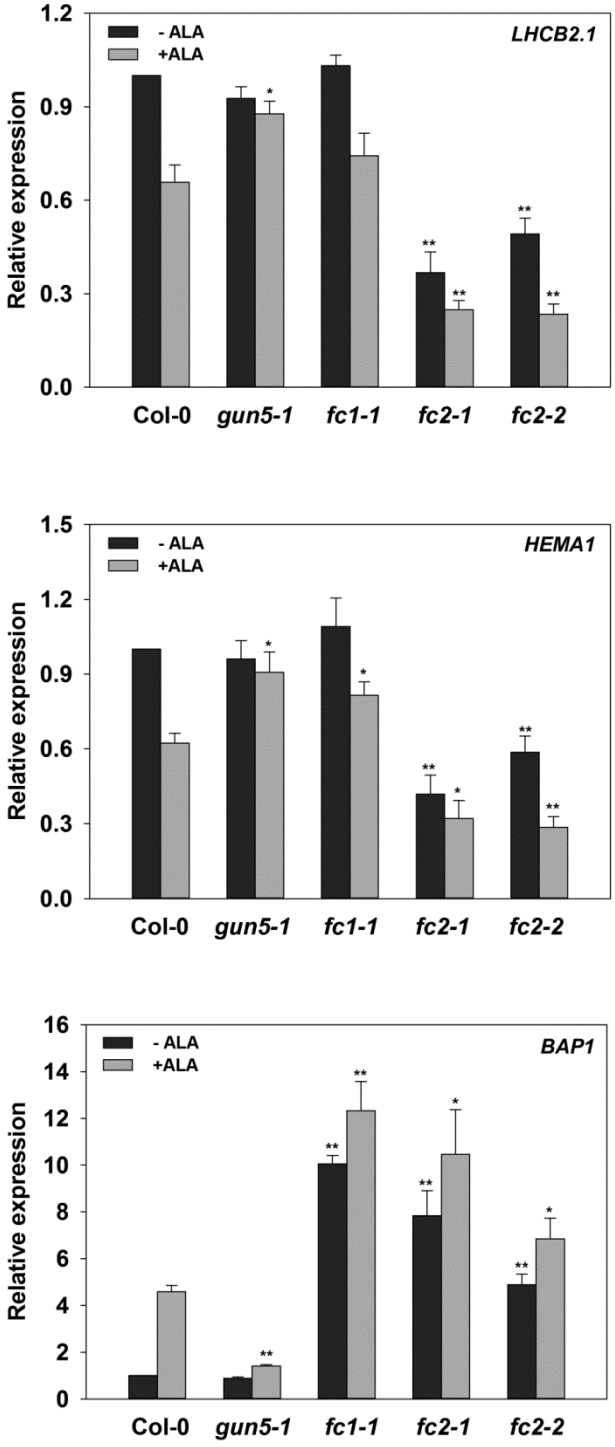

Figure 5.17 Expression of selected nuclear genes in ferrochelatase 1 and 2 (FC1, FC2) mutants after ALA treatment. WT (Col-0), *gun5-1*, *fc1-1*, *fc2-1* and *fc2-2* seedlings were grown on 1% agar with ½ MS medium supplemented with 5 mM MES, without sucrose, and with (+ALA) or without (-ALA) 0.05 mM ALA under the following conditions: 4 d in D followed by transfer to WL (100 µmol m^{-2} s^{-1}) for 2 h. Gene expression was measured by quantitative RT-PCR analysis relative to Col-0 grown without ALA, and normalised to *ACTIN DEPOLYMERIZING FACTOR 2* (*ADF2,* At3g46000*)*. Data shown are means +SEM of three biological replicates. Asterisks denote significant difference vs Col-0 for the same treatment (± ALA), Student's *t* test (*$p < 0.05$, **$p < 0.01$).

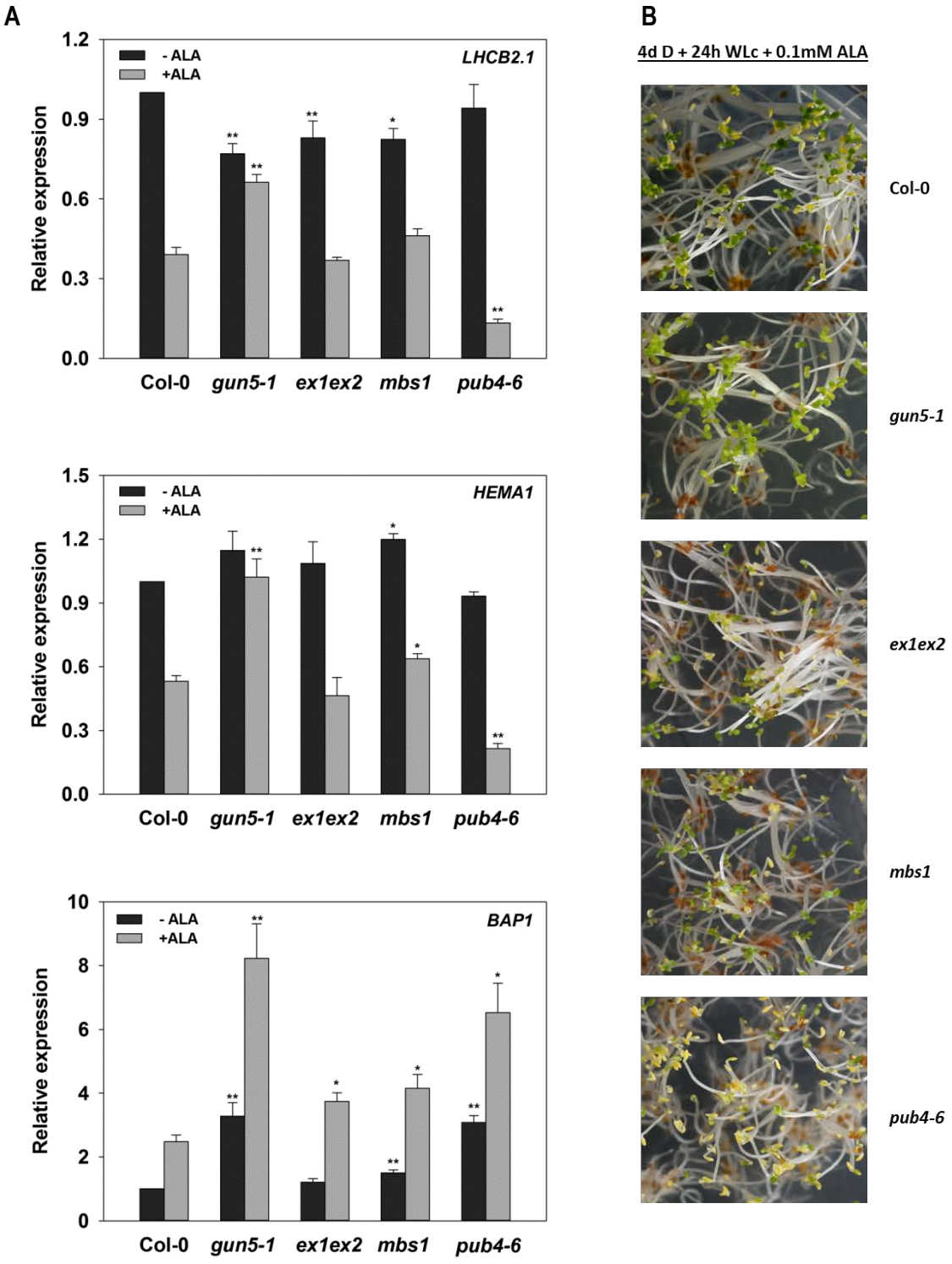

Figure 5.18 Response of known singlet oxygen signalling mutants to ALA treatment. WT (Col-0), *gun5-1*, *ex1/ex2*, *mbs1-1* and *pub4-6* seedlings were grown on 1% agar with ½ MS medium supplemented with 5 mM MES, without sucrose, and with (+ALA) or without (-ALA) 0.05 mM ALA under the following conditions: 4 d in D followed by transfer to WLc (100 µmol m^{-2} s^{-1}) for 24 h. (A) Expression of *LHCB2.1*, *HEMA1* and *BAP1* measured 24 h after WLc exposure by quantitative RT-PCR analysis relative to Col-0 grown without ALA and normalised to *ACTIN DEPOLYMERIZING FACTOR 2* (*ADF2,* At3g46000*)*. Data shown are means +SEM of three biological replicates. Asterisks denote significant difference vs Col-0 for the same treatment (± ALA), Student's *t* test (*p < 0.05, **p < 0.01). (B) Phenotypes of seedlings grown on 0.1 mM ALA in D for 4 d and transferred to WLc for 24 h.

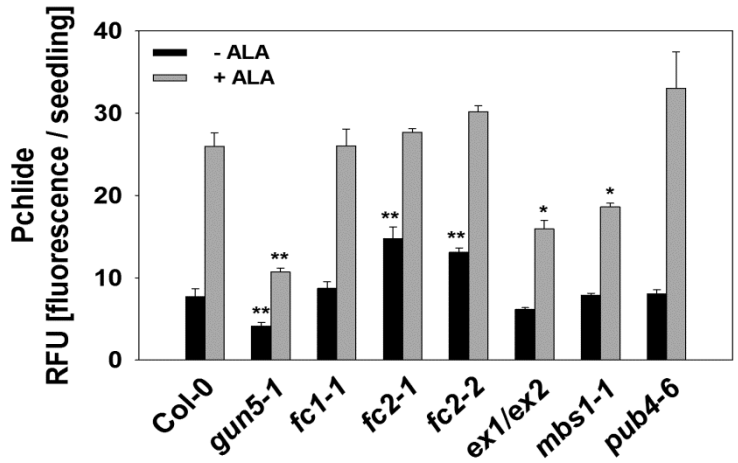

Figure 5.19 Protochlorophyllide (Pchlide) level in various mutants after treatment with ALA. WT (Col-0), *gun5-1*, *fc1-1*, *fc2-1*, *fc2-2*, *ex1ex2*, *mbs1-1* and *pub4-6* mutant seedlings were grown on 1% agar with ½ MS medium supplemented with 5 mM MES, without sucrose, and with (+ALA) or without (-ALA) 0.1 mM ALA for 4 d in D. Data shown are means + SD of three independent biological replicates. 30 seedlings were harvested for each biological replicate. Asterisks denote significant difference vs WT for the same treatment (-/+ALA), Student's *t* test (*$p < 0.05$, **$p < 0.01$).

Among all mutants tested only the control *gun5-1* rescued almost completely *LHCB2.1* and *HEMA1* expression, and greening after ALA treatment (Figure 5.18). Even though *ex1ex2* and *mbs1-1* mutants accumulated less Pchlide in D after ALA feeding (Figure 5.19) they both showed little difference from WT for *LHCB2.1* and *HEMA1* expression and greening after ALA treatment with just *HEMA1* in *mbs1-1* showing any significant rescue (Figure 5.18A, B). BAP1 expression was also a little higher in *ex1ex2* and *mbs1-1*than wild type (Figure 5.18A). These results therefore suggest that neither EX1, EX2 nor MBS1 have a major role in mediating singlet oxygen response induced by ALA treatment. After ALA treatment, expression of *LHCB2.1* and *HEMA1* was significantly lower, and expression of *BAP1* significantly higher, in the*pub4-6* mutant compared to WT (Figure 5.18A) which correlated with the complete block of greening in this mutant (Figure 5.18 B). This was not due to a strong elevation in Pchlide accumulation after ALA feeding (Figure 5.19).

The phenotype of *pub4-6* and *mbs1-1* mutants was additionally tested using a FR pre-treatment to induce singlet oxygen signalling with the standard conditions of 2 d D and 2 d FR followed by 24 h WL. After a FR pre-treatment, expression of *LHCB2.1*, *HEMA1* and *GUN4* was significantly higher in *pub4-6*, but not in *mbs1-1* compared to WT (Figure 5.20A). The *pub4-6* mutant was also characterised by a partial rescue of greening (Figure 5.20B, C). The rescue phenotype of *pub4-6* was not due to the lower Pchlide level (Figure 5.20C). In contrast no up regulation of *BAP1* expression was seen in *pub4-6* suggesting these two gene expression responses had been uncoupled.

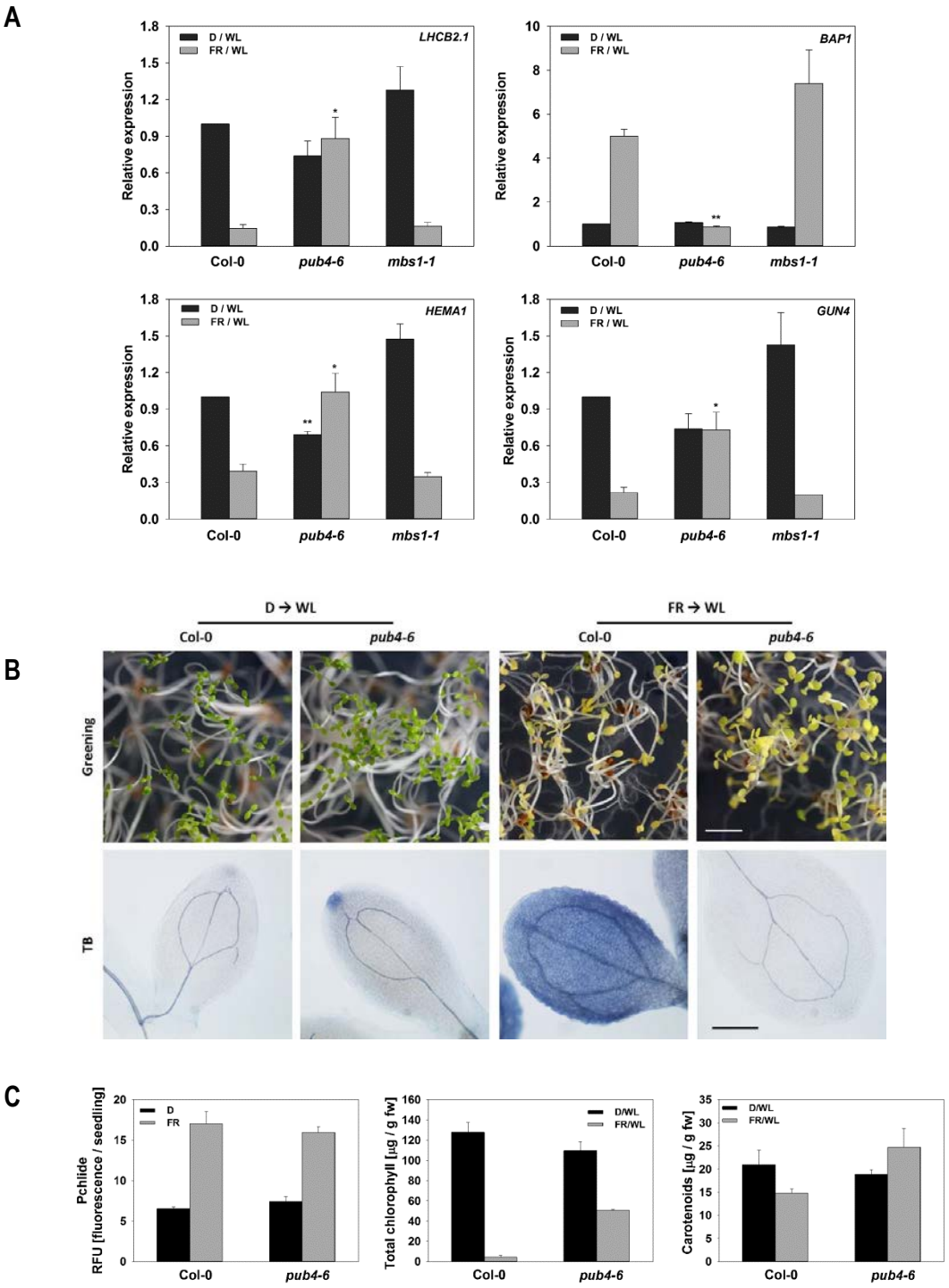

Figure 5.20 White light (WL) response of *pub4-6* and *mbs1-1* to a FR pre-treatment. WT (Col-0), *pub4-6* and *mbs1-1* seedlings were grown on 1% agar with ½ MS medium, without sucrose under the following conditions: 2 d D and 2 d FR or 4 d D followed by transfer to WLc (100 µmol m^{-2} s^{-1}) for 24 h. (A) Expression of *LHCB2.1*, *HEMA1, GUN4* and *BAP1* measured 24 h after WL exposure by quantitative RT-PCR analysis relative to Col-0 transferred from D to WLc normalised to *ACTIN DEPOLYMERIZING FACTOR 2* (*ADF2,* At3g46000*)*. Data shown are means +SEM of three biological replicates. Asterisks denote significant difference vs Col-0 for the same treatment (± FR), Student's *t* test (*p < 0.05, **p < 0.01). (B) Phenotypes of Col-0 and *pub4-6* seedlings pre-treated with FR ant transferred to WLc for 24 h. (C) Pchlide and chlorophyll levels in D or FR grown and WLc transferred seedlings, respectively. 30 seedlings were harvested for each biological replicate. Data are means + SD of three biological replicates.

5.2.7 CAS is not involved in singlet oxygen-mediated retrograde signalling in young seedlings

The ALA and FR pre-treatments examined in this chapter both induce $^1O_2$ signalling in developing chloroplasts. Due to the short half-life of $^1O_2$ it can be expected that this signalling involves additional chloroplast localized components. The chloroplast localized calcium-sensing receptor (CAS) could be a potential candidate for mediating $^1O_2$-dependent inhibitory retrograde signalling, as it has been shown to control nuclear and chloroplast gene expression during pathogen defence (Nomura et al., 2012). To test this hypothesis, the global gene expression data for *cas-1* regulated genes and FR pre-treatment induced retrograde signalling were compared, and the effect of *CAS* knock-out and overexpression on inhibition of photosynthetic gene expression after ALA treatment and a FR pre-treatment was measured.

Full transcriptome analysis of genes up- and down-regulated in flagellin (flg22)-treated *cas-1* mutant identified by Nomura et al., (2012), and the FR-pre-treatment (GSE6169) revealed an overlap of the regulated genes, with 135 genes regulated by both pathways (Figure 5.21). A third of the FR up-regulated genes were also down-regulated in the *cas-1* mutant and one quarter of the down-regulated genes after a FR pre-treatment were up-regulated in *cas-1*. This substantial overlap suggests that CAS might be involved in singlet oxygen signalling and this was tested directly using ALA and FR treatments.

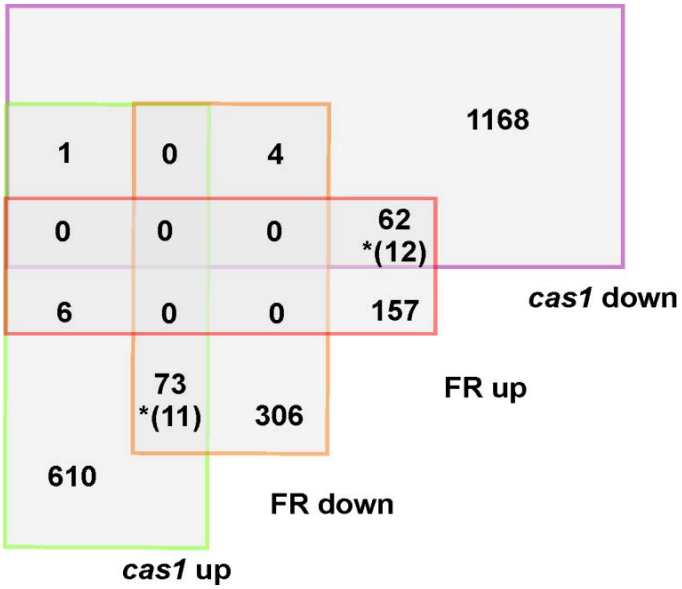

Figure 5.21 Bioinformatic analysis of genes regulated by a FR pre-treatment and *CAS*. Venn diagram depicting common sets of genes down-regulated (down) or up-regulated (up) in seedlings treated with FR and transferred to WLc for 24 h and in flagellin (flg22)-treated *cas-1* mutant plants (*cas1*) (data for *cas-1* come from Nomura et al., 2012). Numbers in parenthesis correspond to the number of genes expected to overlap by chance. (*) denotes statistically significant overlap between tested sets.

Figure 5.22 shows that both the *cas-1* mutant and CAS overexpressor (CASox) displayed little difference in inhibition of tetrapyrrole and photosynthetic gene expression or the induction of singlet oxygen specific *BAP1* expression compared to WT with either treatment. The only exception was a small, but significant rescue of *LHCB2.1* and *HEMA1* after ALA treatment in the CASox line (Figure 5.22A). CAS is therefore unlikely to be important element involved in regulation of singlet oxygen-dependent inhibitory retrograde signalling in developing seedlings.

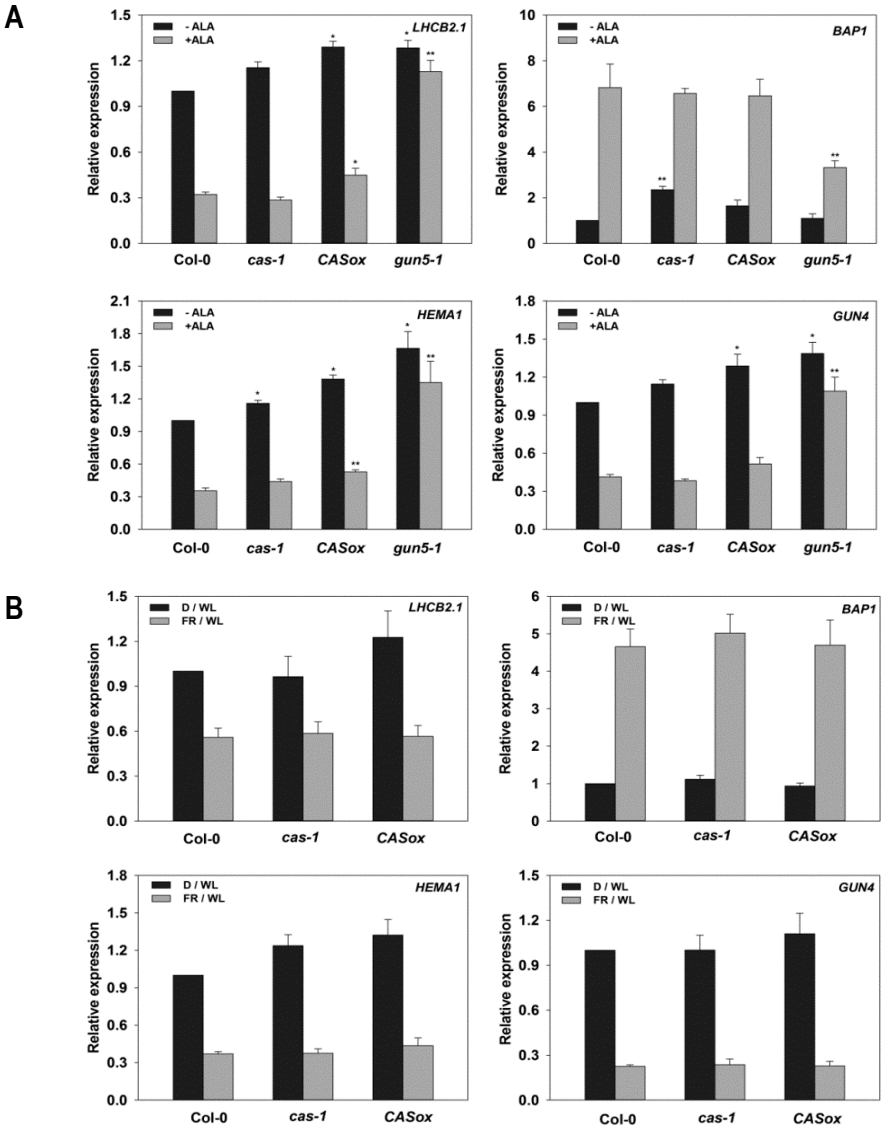

Figure 5.22 Expression of selected nuclear genes in CAS mutant and overexpressor lines after ALA treatment and FR pre-treatment. (A) For ALA treatment, WT (Col-0), *gun5-1*, *cas-1* and *CASox* seedlings were grown on 1% agar with ½ MS medium supplemented with 5 mM MES, without sucrose, and with (+ALA) or without (-ALA) 0.1 mM ALA under the following conditions: 4 d in D followed by transfer to WL (100 µmol m^{-2} s^{-1}) for 2 h. (B) For FR pre-treatment, Col-0, *cas-1* and *CASox* seedlings were grown on 1% agar with ½ MS medium, without sucrose under the following conditions: 2 d D and 2 d FR or 4 d D followed by transfer to WL (100 µmol m^{-2} s^{-1}) for 2 h. For both treatments gene expression was measured by quantitative RT-PCR analysis relative to Col-0 grown without ALA (-ALA) or without FR pre-treatment (D/WL) and normalised to *ACTIN DEPOLYMERIZING FACTOR 2* (*ADF2,* At3g46000*)*. Data shown are means +SEM of three biological replicates. Asterisks denote significant difference vs Col-0 for the same treatment (± ALA or +/- FR), Student's *t* test (*p < 0.05, **p < 0.01).

5.3 Discussion

Two previous sections focused on the investigation of the role of the FC1-derived, heme-dependent positive signal promoting photosynthetic gene expression during seedling development. As shown in earlier experiments, the existence of a single signal promoting gene expression does not always seem to provide enough explanation for the phenotypes that we can observe during seedling development. Any signal accumulating in excess can be dangerous and therefore additional compensating mechanisms must be activated during seedling photomorphogenesis to assure accurate regulation. With the two tetrapyrrole biosynthesis branches, one leading to the heme synthesis and the second resulting in porphyrin production, it seems sensible to speculate that there must be a second repressive signal, and chlorophyll precursors are plausible candidates. This hypothesis would be in agreement with a pivotal role of tetrapyrroles in signalling to the nucleus, proposed by many researchers in the past years. In this section this possibility was investigated in more detail by analysing the consequence of feeding dark-grown seedlings with the tetrapyrrole precursor ALA to increase porphyrin accumulation in seedlings. The results obtained in this Chapter are supportive of the model for tetrapyrrole-mediated retrograde signalling, with both positive and inhibitory pathways, proposed earlier by Terry and Smith (2013).

5.3.1 ALA treatment blocks nuclear gene expression in WL but not in the dark

The data presented here provide further evidence for the role of porphyrins as a source of an inhibitory retrograde signal and provide a possible explanation for some of the inconsistencies present in the literature. ALA feeding experiments have been used before by other researchers, in a similar system to that used here. There are also studies analysing the consequence of feeding ALA to mature plants, but these will not be discussed here as this may be a very different system. In developing seedlings, feeding ALA to WT and the *hy1* mutant resulted in a down-regulation of *LHCB1* expression in D and under FR in both cases (Vinti et al., 2000). This was opposite to the result obtained here, as no down-regulation of *LHCB2.1*, or any other tetrapyrrole gene was seen in Col-0 or *gun5* seedlings grown on ALA in the dark (Figure 5.10, Figure 5.12), even though the range of ALA concentrations used overlapped in both experiments (0.1 mM). Intriguingly, strong down-regulation of *LHCB1.2* in 3 d-old etiolated seedlings was also reported by Czarnecki et al. (2012), using quantitative RT-PCR analyses. One explanation for the difference between experiments from this work and Vinti et al. (2000) is the detection method as the authors used RNA gel blot analyses. Actually, when they tested *LHCB1* promoter-driven GUS activity they could not detect a signal decrease other than at the highest

ALA concentrations (1-3 mM). Another explanation could be the growth conditions, as Vinti et al. (2000), kept seedlings on the agar medium supplemented with 20 mM HEPES buffer at pH 7.2. It is possible that seedling growth was compromised by the high pH and/or high buffer concentration that could induce nonspecific pleiotropic effects, especially in combination with a high ALA dose. In the current experiments a low concentration of 5 mM MES buffer was used to overcome problems with the acid nature of ALA, and it was confirmed that this buffer concentration was sufficient to stabilise growth medium pH at 5.6-5.8 up to 0.2 mM ALA supplementation, thus maintaining optimal growth conditions. At this concentration MES did not have any negative effect on seedling de-etiolation. It is, however, worth noting that under the conditions used here 0.2 mM ALA resulted in an inhibition of hypocotyl length, which was also noted by Vinti et al. (2000). The repression of *LHCB1.2* reported in Czarnecki et al. (2012), is more difficult to explain, as they used the same detection method and ALA concentration as used here. It cannot be excluded that in the Czarnecki et al. (2012), experiment, the etiolated seedlings were not maintained in complete darkness, for example during harvesting, which would result in $^1O_2$ production and gene expression inhibition. It was shown here that production of $^1O_2$ followed by an inhibition of photosynthetic genes can be seen within 15 min after transfer to WL, and the strong inhibition is apparent even under low light intensity (Figures 5.12 and 5.13; Page et al., 2017a). Finally, in this work *LHCB1.2* expression was not tested, instead the *LHCB2.1* transcript was analysed routinely. Still it is very unlikely that the *LHCB1.2* transcript, or other *LHCB* transcripts, could show such a divergent pattern of expression and account for this difference.

In contrast to the two studies discussed above, and closer to findings presented here, are the studies described by Woodson et al. (2011; 2013), where supplementation with high ALA concentration rescued photosynthetic gene expression on NF or in *sig2-2*. It is expected that ALA feeding increases flux through the whole tetrapyrrole pathway, including heme and thus might be expected to increase a promotive heme signal. Under the experimental conditions tested here any promotive effect of a heme-dependent signal was presumably masked by a rapid and substantial singlet oxygen production following transfer from D to WL (Figure 5.4). It is likely that in the Woodson et al. (2011; 2013) studies singlet oxygen was also produced, but in these experiments seedlings were maintained under constant low WL and low levels of $^1O_2$ could be quenched directly by the cell scavenging system. Alternatively, it is possible that in the presence of NF, or the *sig2-2* mutant that singlet oxygen production derived from excited porphyrins is diminished (e.g. Figure 3.7C) and thus the inhibitory signal remains insufficient to reduce the positive signal promoted by ALA feeding. Production of $^1O_2$ in WL after ALA treatment (from increased porphyrins levels) that results in inhibition of photosynthetic gene expression could also

explain some earlier observations suggesting that Mg-proto IX was a signalling molecule promoting loss of gene expression (Strand et al., 2003; Zhang et al., 2011).

5.3.2 ALA treatment induces $^1O_2$ in WL in *Arabidopsis* seedlings

Under the ALA treatment conditions tested here, production of singlet oxygen was detected in seedlings cotyledons after transfer to WL (Figure 5.4). It was assumed that this was derived from the photo-excitation of Pchlide (and to a lesser extent, possibly other porphyrins), which accumulated to high levels in the dark after ALA treatment (Figure 5.1). Porphyrins are known to produce $^1O_2$ after light excitation in the presence of O_2 due to their specific chemical structure. They are formed with 4 pyrrole rings conjugated by carbon methane bridges, which creates a delocalized electron path. Although they are not toxic in the dark, they can absorb light very strongly and their high energy excited state is then transferred to molecular oxygen in the ground state that leads to $^1O_2$ generation. All porphyrins and chlorins can potentially result in singlet oxygen production (Fernandez et al., 1997; Kimel et al., 1989) and $^1O_2$ production has been experimentally confirmed in plants as a result of photo-excited Pchlide (op den Camp, 2003; Page et al., 2017a) and Proto-IX (Kennedy and Pottier, 1992; Woodson et al., 2015; Tarahi Tabrizi et al., 2016) accumulation.

The ROS generated by transferring ALA treated seedlings to the light was specific to $^1O_2$, as no strong fluorescence of H_2DCFDA (indicating presence of other ROS) could be detected (Figure 5.5). Although this was not investigated earlier for the *fc2-1* mutant (Woodson et al., 2015) or after a FR pre-treatment (Page et al., 2017a), it was re-examined here for the FR pre-treatment with the same result (Figure 5.9). It could be argued that small levels of other ROS, including H_2O_2, are still produced under the conditions tested, but that the florescence dye used was not sensitive enough, or their production increases at later point after WL exposure. Performing additional staining experiments for H_2O_2 production with diaminobenzidine tetrahydrochloride (DAB), or superoxide anion with nitroblue tetrazolium (NBT), with more time points after WL exposure could be used to test this possibility. Further support for the specificity of singlet oxygen production comes from the observation that there was no induction of H_2O_2 responsive genes, with *FER1* and *CAT2* expression even showing some down-regulation. The specific pattern of $^1O_2$ and H_2O_2 gene expression detected after ALA treatment and transfer to WL for 2 h was fully consistent to previous reports investigating induction of singlet oxygen response (op den Camp, 2003; Woodson et al., 2015; Page et al., 2017a), clearly demonstrating that under the conditions tested here a $^1O_2$-specific response was induced.

5.3.3 ALA treatment supports the role of $^1O_2$ in plastid to nucleus communication

ALA feeding results in $^1O_2$ production in WL, and this was shown here to be accompanied by an inhibition of WL-induction of photosynthetic gene expression (Figure 5.2). The question can be asked if this was simply the effect of cellular oxidative damage or the consequence of singlet oxygen-initiated signalling. A clear separation between these processes is very challenging due to the high reactivity of ROS and their ability to interact with many cellular components including DNA, lipids and proteins (Foyer and Noctor, 2005; Van Breusegem and Dat, 2006). Previous studies using the *flu* mutant of Arabidopsis have provided evidence for $^1O_2$ signalling in plants by proving it can be a genetically controlled process (Meskauskiene et al., 2001; op den Camp et al., 2003). Using a FR pre-treatment, it was proposed that singlet oxygen produced from excited Pchlide initiates a signal that controls photosynthetic gene expression during seedling development (Page et al., 2017a). The ALA treatment described here was very similar to the situation in these studies with high Pchlide accumulation in D grown seedlings and $^1O_2$ production in WL. Similar to the FR pre-treatment, ALA-treated seedlings under WL showed a strong and clear down-regulation of *LHCB2.1*, *HEMA1* and *GUN4*. Although it was reported earlier that different systems for $^1O_2$ induction in plants differ, at least partially, in terms of their induced global transcriptomic responses (e.g. the *flu* and *fc2-1* array data comparison analysed in Woodson et al., 2015), the inhibitory effect on selected photosynthetic and tetrapyrrole genes is common for all these systems. This was demonstrated in this study by the quantitative RT-PCR experiments for the *flu, fc2-1* and *fc2-2* mutants (Figures 5.14 and 5.17). The observation that the cohort of genes commonly down-regulated in mature *flu* plants and seedlings, transferred from dark to WL, includes many photosynthetic and tetrapyrrole genes (Figure 5.15) is also in agreement with the role of porphyrins as a source of an inhibitory signal, and $^1O_2$ is likely to induce this response. It would be interesting to know what global transcriptomic changes result from ALA treatment. This information would permit a more comprehensive comparison between this response and other $^1O_2$ systems described so far in the literature.

Based on the gene expression experiments shown in this Chapter it can be concluded that induction of $^1O_2$ response was dependent on Mg-porphyrin synthesis, as the *gun5* mutant was able to rescue photosynthetic gene expression and has reduced induction of *BAP1* (Figures 5.10 and 5.11). This observation was in agreement with McCormac and Terry (2004), Woodson et al. (2015), and Page et al. (2017a). Moreover, correlation plots (Figure 5.3) suggest that induction of the $^1O_2$ response is strongly dependent on the amount of porphyrin accumulated before WL exposure (Figures 5.2, 5.3 and 5.8). It is not known if this response is also dependent on the amount of singlet oxygen produced after the transfer to WL, and results presented so far

are not clear enough to draw such a conclusion (Figures 5.4 and 5.9; Page et al., 2017a). This is partly due to the technical difficulties with ROS measurements. It was also shown here that although the $^1O_2$ response is induced by WL, it is essentially independent from WL intensity (Figure 5.12). This was in agreement with the earlier report on FR pre-treatment response (McCormac and Terry, 2002b), where there was no difference in loss of greening under low and normal light intensity. This might seem a surprising result, as there is evidence in literature for the induction of $^1O_2$ in green plants by high light (in combination with low temperature; Zhang et al., 2014). Based on the data from Chapter 3 it could be also expected that the hypersensitivity of *gun1-1* to high light could be at least partially a result of $^1O_2$ generation, although there is no direct evidence for this (discussed earlier in Chapter 3). However, in green plants $^1O_2$ is produced mostly from over-excited chlorophylls at the PS II reaction centres (Triantaphylides and Havaux, 2009) and high light intensity would be required to generate this over excitation. If we accept that in our experimental system the rate limiting step for the induction of the $^1O_2$ response is availability of porphyrins then, in contrast to the situation in green plants, any light excitation might be expected to induce this response. The independence from WL intensity also supports the suggestion that inhibition of photosynthetic gene expression is a direct consequence of a signalling response and not a secondary effect of oxidative damage as this would be expected to increase with increased light intensity. Importantly, inhibition of photosynthetic and tetrapyrrole gene expression derived from excess porphyrin accumulation in the D can also be induced in green seedlings with developed chloroplasts using either *flu* or ALA feeding in the D (Figures 5.15 and5.16). This suggests that perhaps signalling pathways induced by $^1O_2$ derived from different sources can be partially integrated. Interestingly, in mature *Arabidopsis* plants treated with the carotene oxidation product ß-cyclocitral, there was also an inhibition of some photosynthetic and tetrapyrrole genes such as *HEMA1*, *GUN4*, *CHLH*, *LHCB2.4* (Ramel et al, 2012). The possible interaction between these responses would need to be investigated in more detail in the future.

One of the major differences between ALA treatment and other treatments described here to induce $^1O_2$ signalling is that none of the mutants described so far to block induction of $^1O_2$ responses could rescue the inhibitory effects of ALA (Figure 5.18). This was apparent for *ex1ex2*, *pub4-6* and *mbs1-1*. Interestingly, some of these mutations including *ex1ex2* and *pub4-6* were shown to rescue greening and inhibition of photosynthetic gene expression after FR pre-treatment (Figure 5.20; Page et al., 2017a). There is a possibility that genetic regulation of the response to ALA-treatment is simply independent and distinct from EX1, EX2 and PUB4. However, the ALA assay was performed using dark-grown seedlings with undeveloped chloroplasts and it is possible that these proteins may only be functional in chloroplasts and thus

were not present in dark-grown seedlings to influence the response on transfer to WL. Consistent with this idea, both EX1 and EX2 were induced by FR light (Page et al., 2017a) and this could account for differences in the *ex1ex2* response to ALA and a FR pre-treatment.

The CAS protein does not seem to be involved in control of $^1O_2$ signalling of photosynthetic gene expression, as shown by WT-like phenotype of *cas* mutant and *CAS*ox lines under ALA and FR pre-treatment conditions (Figures 5.21 and 5.22). As a chloroplast membrane protein that controls Ca^{2+} signatures, CAS could be considered as a strong candidate for the regulation of $^1O_2$ signalling (Nomura et al., 2012). The significant overlap between transcripts affected by FR pre-treatment and the flg22-treated *cas* transcriptome might be more related with induction of general defence responses and not $^1O_2$. The original *flu* experiments showed there is an induction of many stress and hormone genes after a shift from dark to WL (op den camp, 2003), and possible cross-talk between $^1O_2$ signalling and environmental regulation cannot be excluded. Also it is possible that a role for CAS in the regulation of $^1O_2$ responses is restricted only to mature plants (Nomura et al., 2012). These last results suggest that more detailed genetic studies on components regulating the ALA-response should be undertaken in the future to broaden our understanding on the consequences of $^1O_2$ production in the very early stages of seedling development.

Chapter 6 Role of plastid retrograde signalling in the response of *Arabidopsis* seedlings to abiotic stress

6.1 Introduction

Retrograde signalling has increasingly been linked to stress signalling. Chloroplasts, acting as environmental sensors, control nuclear gene expression in response to changes in light, temperature and oxidation levels by triggering redox and stress-related reactive oxygen species (ROS) signalling pathways (Pogson et al., 2008; Galvez-Valdivieso and Mullineaux, 2010; Karpinski et al., 2013). Redox changes at the plastoquinone (PQ) pool in relation to both genetic and metabolic components were shown to be involved in crosstalk between signalling pathways in response to light induced excess excitation energy (EEE) and pathogen stresses (Mühlenbock et al., 2008). These results also indicate the importance of chloroplast signalling for systemic acquired acclimation (SAA) and systemic acquired resistance (SAR). Other chloroplast-derived signals such as SAL1-PAP (Estavillo et al., 2011) and MEcPP (Xiao et al., 2012) are involved in drought and generic stress responses respectively and chloroplast-specific hydrogen peroxide (H_2O_2) overproduction was also shown to down-regulate expression of genes connected to cold and pathogen stresses (Maruta et al., 2012). However, these examples, and most of the analyses performed to study plant response to abiotic stress, focus on mature plants. Young seedlings can also experience environmental perturbation and how they cope with this will be critical for their development and survival. There are examples of a role for chloroplasts in stress responses in young seedlings. Environmental regulation will also be critical during chloroplast biogenesis and there is evidence that cold (Yang et al., 2005), heat (Yu et al., 2012) and drought stress (Cheng et al, 2011; Miller et al., 2010) all impact on development via effects on chloroplast signalling. For heat stress, chloroplast ribosomal protein S1 (RPS1) was recently shown to control expression of *HSFA2* and its target genes in response to heat (Yu et al., 2012). Another heat shock protein, HSP90 was proposed to be involved in regulation of plastid signalling-mediated photosynthetic gene expression during oxidative stress (Kindgren et al., 2012). Cold treatment has also been shown to block seedling ability to green and this was accompanied by the inhibition of expression of homologues of *Arabidopsis LHCB* genes (Yang et al., 2005). Finally, it cannot be excluded that temperature stresses may impact on excitation of chlorophyll precursors and thus indirectly modulate signalling to the nucleus.

In the era of rapid environmental changes, understanding the role of chloroplast signals in seedling development will be critical in the context of crop productivity and bioenergy. The aim of this study is to examine if activation of plastid retrograde signalling is involved in the response

of young seedlings to different abiotic stresses. This will be achieved by comparing global plastid signalling transcriptomic datasets with those for abiotic stress signalling to identify overlaps in the gene expression profiles. Treatments with the strongest overlap will be further verified experimentally for their ability to compromise chloroplast signalling to the nucleus. Additionally, selected mutants, with altered responses to abiotic stresses will be tested for their impact on plastid signalling.

6.2 Results

6.2.1 The effect of abiotic stresses on expression of tetrapyrrole pathway genes

The original discovery of the *gun* mutants and their characterization, including results presented in Chapters 4 and 5, strongly supports the role of tetrapyrroles as key regulators of plastid-to-nucleus retrograde signalling (Strand et al., 2003, Woodson et al., 2011, Terry and Smith 2013). Additionally, there is increasing interest in a role for tetrapyrrole metabolism in regulation of plant tolerance to abiotic stresses such as drought (Nagahatenna et al., 2015). To investigate if there is a relationship between tetrapyrrole-dependent retrograde signalling and abiotic stresses, the effect of different environmental conditions on the expression of tetrapyrrole pathway genes was first analysed using *Arabidopsis* eFP Browser (based on data from Zeller et al., 2009). Time-dependent fold changes in expression of 25 tetrapyrrole biosynthesis genes in response to temperature stresses (cold and heat), as well salt and osmotic stresses, are presented in logarithmic scale in Figure 6.1 and Figure 6.2, respectively.

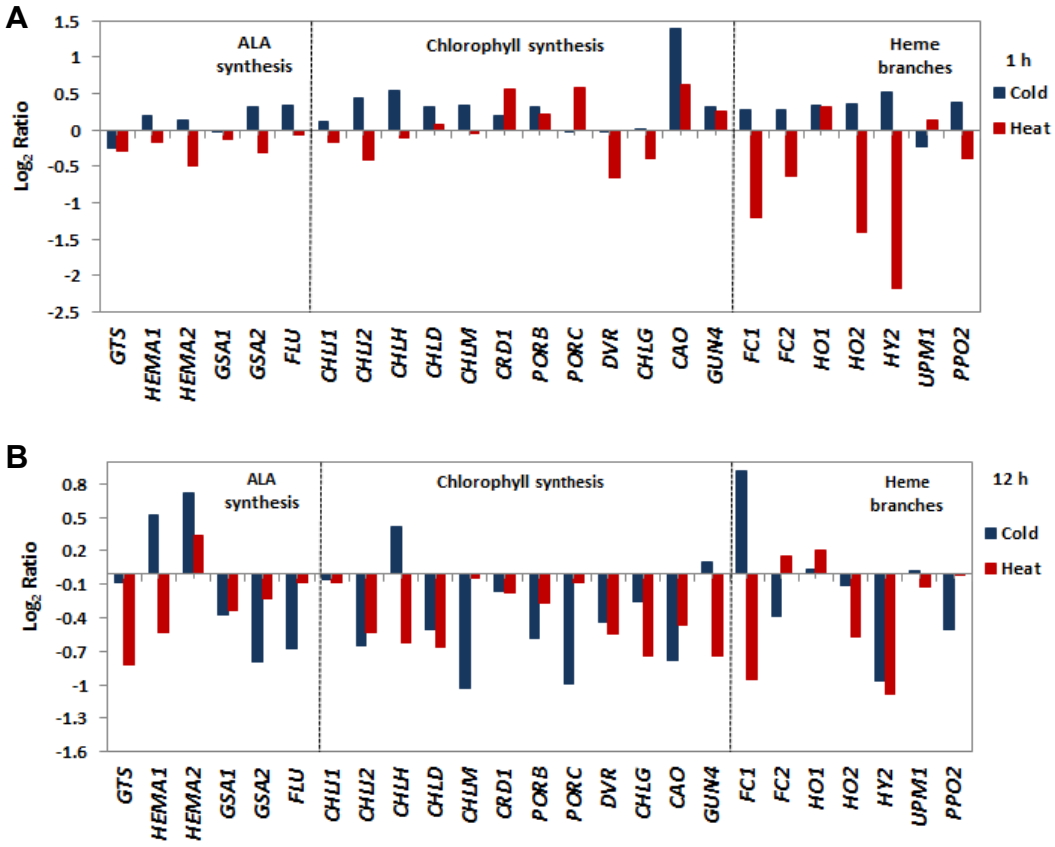

Figure 6.1 The effect of temperature stress treatments on expression of selected genes encoding the tetrapyrrole pathway. Young seedlings were exposed to a temperature of 8°C and 30°C for the cold and heat stresses, respectively. Graphs represent changes in gene expression at 1h (A) and 12h (B) after the stress exposure. The average values for the gene expression were collected from *Arabidopsis* eFP browser and presented as $\log_2$ ratios.

Analysis showed that short exposure to cold and heat for 1h, did not have a severe effect on tetrapyrrole genes expression, with the exception of 3 genes dedicated to heme synthesis. Ferrochelatase 1 (*FC1*), Heme Oxygenase 2 (*HO2*), and Elongated Hypocotyl 2*(HY2*), all showed a more than 2-fold decrease in expression after exposure to heat (Figure 6.1A). 12h heat and cold treatment resulted in a global down-regulation in the expression of most analysed tetrapyrrole genes, however; these changes were relatively moderate (no higher than 2-fold decrease in gene expression, Figure 6.1B). Interestingly, 12h of heat and cold exposure had an antagonistic effect on the expression of *HEMA1*, *CHLH* and *FC1*genes, which all were up-regulated by cold and down-regulated by heat. These genes might be potentially important in cross-talk between temperature stresses.

Changes in tetrapyrrole biosynthesis gene expression after salt and osmotic stresses showed comparable trends to those for temperature stresses. Almost all genes were unaffected by 1h of salt and osmotic treatment, with the exception of the gene encoding chlorophyll oxygenase (*CAO*), which was 1.7-1.9-fold up-regulated by both treatments (Figure 6.2A). In contrast, 12h salt and osmotic stress treatment resulted in a general inhibition in tetrapyrrole gene expression, but only for some genes was repression higher than 1.5-fold (Figure 6.2B). This is similar to the effect of NF treatment, which has been shown to strongly down-regulate the expression of most of genes in the tetrapyrrole pathway (Moulin et al., 2008).

The repressive effect of salt and osmotic stresses was observed mainly for the genes belonging to the chlorophyll synthesis branch of the pathway (Figure 6.2B). In addition, salt stress seemed to have a stronger effect on the inhibition of gene expression than osmotic stress. This is not surprising perhaps, as salt stress combines osmotic and ionic disturbance. Genes that were the most strongly repressed by salt (≥2-fold) include: *GSA2* (ALA synthesis), *CHLI2*, *CHLD*, *CHLM*, *PORC*, *CAO*, *GUN4* (chlorophyll branch) and *HY2* (heme branch). Overall, these data suggest that some of the components of tetrapyrrole biosynthesis can be important for regulation of seedling response to abiotic stresses.

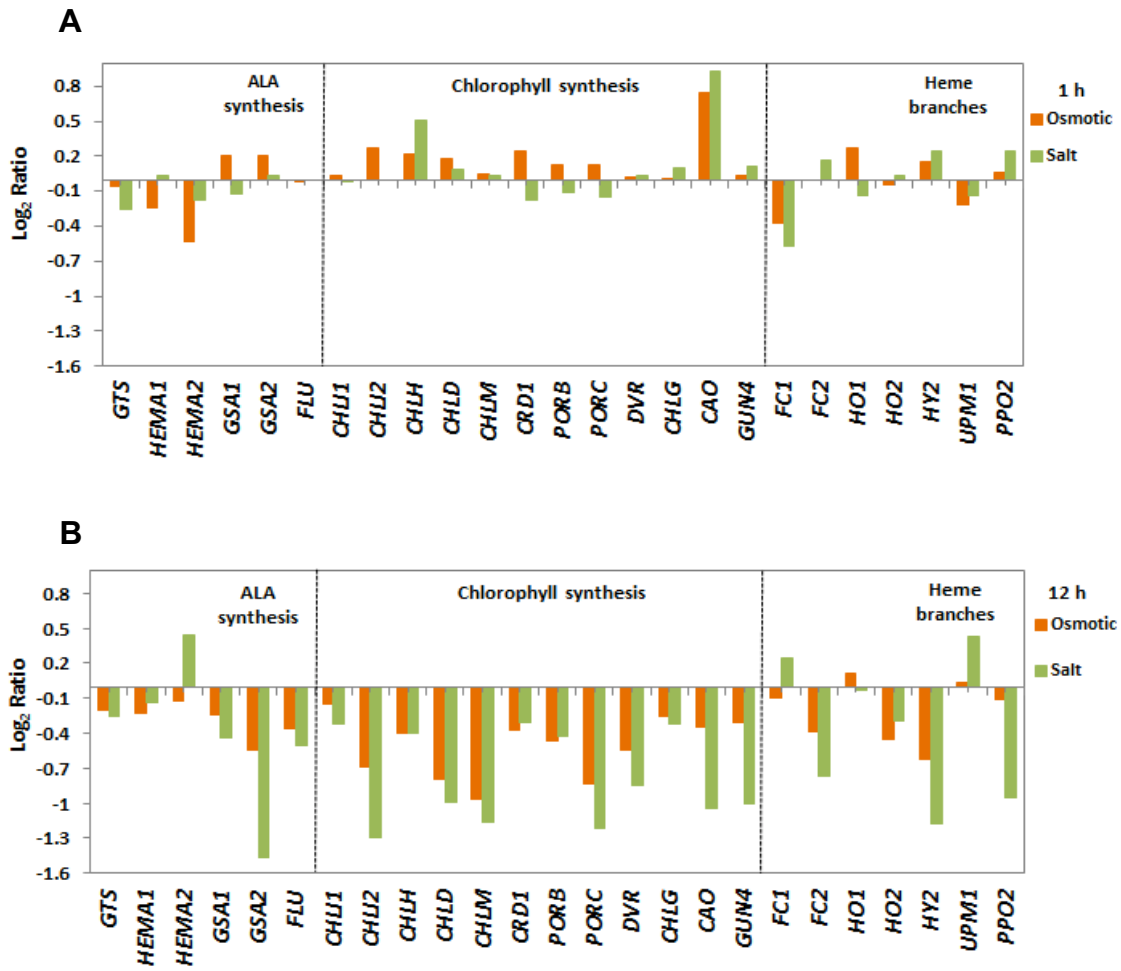

Figure 6.2 The effect of salt and osmotic stress treatments on expression of selected genes encoding the tetrapyrrole pathway. Young seedlings were treated with 300 mM mannitol and 200 mM NaCl for the osmotic and drought stresses, respectively. Graphs represent changes in gene expression at 1h (A) and 12h (B) after the stress exposure. The average values for the gene expression were collected from *Arabidopsis* eFP browser and presented as $\log_2$ ratios.

6.2.2 Bioinformatics analysis of the interaction between singlet oxygen signalling and heat stress signalling

The gene expression analysis from the previous chapter showed that the heat stress can change the transcriptional response to the ALA treatment (Figure 5.13). As shown above, temperature stresses can affect expression of some tetrapyrrole genes and thus potentially can impact on retrograde plastid signalling pathways. To test this, first, the publicly available full transcriptome data for FR pre-treatment and heat stress, as well other abiotic stresses (including cold, drought and salt) were compared, to look for significant overlaps. Figure 6.3 shows numbers of genes commonly induced and repressed by each treatment. Because changes in gene expression in response to abiotic stresses are very dynamic, analyses were performed separately at different time points after applying cold (1 h, 24 h, 7 d; Figure 6.3A) and heat (20 min and 1 h; Figure 6.3B). Comparison with different abiotic stress treatments showed that many genes up-regulated by the heat stress were also found to be up-regulated by FR pre-treatment (Figure 6.3B), suggesting similarity for induced signalling signatures. For the two different exposure times of 20 min and 1 h, 32 or 41 genes (2 or5 expected by chance, respectively) were common for the heat and FR induced genes. An overlap was not seen for the down-regulated genes. Many genes for heat shock proteins (e.g. *HSP17.4*, *HSP70*) and heat specific transcription factors (*HSFA2*) were up-regulated in 20 min and 1 h heat-stressed seedlings in a FR pre-treatment dependent manner. Interestingly, FR pre-treatment also shows some degree of overlap for genes down-regulated by a long cold stress (Figure 6.3A). However, previous experiments showed no significant effect of cold on changes in gene expression resulting from ALA treatment, which is expected to induce a similar singlet oxygen signalling response to FR (Figure 5.13). There was also a significant and strong overlap for the FR pre-treatment dataset with drought and salt stresses, for both down- and up-regulated genes (Figure 6.3C). However, this was partially due to the more severe effect of these two stresses, with thousands of genes being down- and up-regulated by drought and salt, and only hundreds of genes affected by the FR pre-treatment. Collectively, these results show that significant numbers of genes affected by FR pre-treatment are stress responsive genes, many of which encode heat shock proteins.

The overlap between genes regulated by a FR pre-treatment and heat stress was investigated further by performing a GO term enrichment analyses for genes up-regulated by FR using the ATCOECIS resource (http://bioinformatics.psb. ugent.be/ATCOECIS/). The original FR pre-treatment array also used the *gun1gun5* double mutant (Page et al., 2017a). The *gun1gun5* double mutant rescue both the induction and repression of a subset of the FR pre-treated genes and it has been demonstrated that these changes are primarily due to the loss of GUN5 (Page et

al., 2017a; this study). Among 225 genes selected initially as induced by the FR pre-treatment in wild type, 169 were unchanged or down-regulated in the *gun1gun5* double mutant suggesting their regulation is singlet oxygen-dependent, and this cohort of genes was subjected to the analysis. As shown in Figure 6.4, of the 28 GO terms that fall into the selection criteria, response to heat was one of the top classified. The 21 genes annotated as response to heat encoded marker genes for heat acclimation or general stress responses, and most of these genes are known to be involved in protein metabolism, or possess a DNA-binding activity e.g.: *HSP101*, *HSP17.4*, *HSP70*, *HSP20-like*, *HSFA2*, *ZAT12*. Moreover, apart from the response to heat, many of the 169 genes differently regulated in the *gun1,5* mutant were related to general stress response, regulation of transcription, response to light, or reactive oxygen species. These genes, especially those with the transcription factor activity, might be potentially important regulators of cross-talk between heat and singlet oxygen-dependent retrograde signalling.

To test if significant overlap of FR pre-treatment and heat stress up-regulated genes was specific to singlet oxygen signalling, the cohort of genes induced by 1 h heat stress was compared to genes up-regulated in other singlet oxygen signalling array experiments (Figure 6.5). Three array datasets were tested: the response to treatment by ß-cyclocitral, a carotenoid degradation product proposed to act downstream of singlet oxygen (Ramel et al., 2012), and the dark to light transition of the *fc2-1* (Woodson et al., 2015) and *flu* (Op den Camp et al., 2003) mutants. In all three of these datasets the overlap with heat stress up-regulated genes was small and lower than observed for FR pre-treatment, although still higher than would be expected by chance.

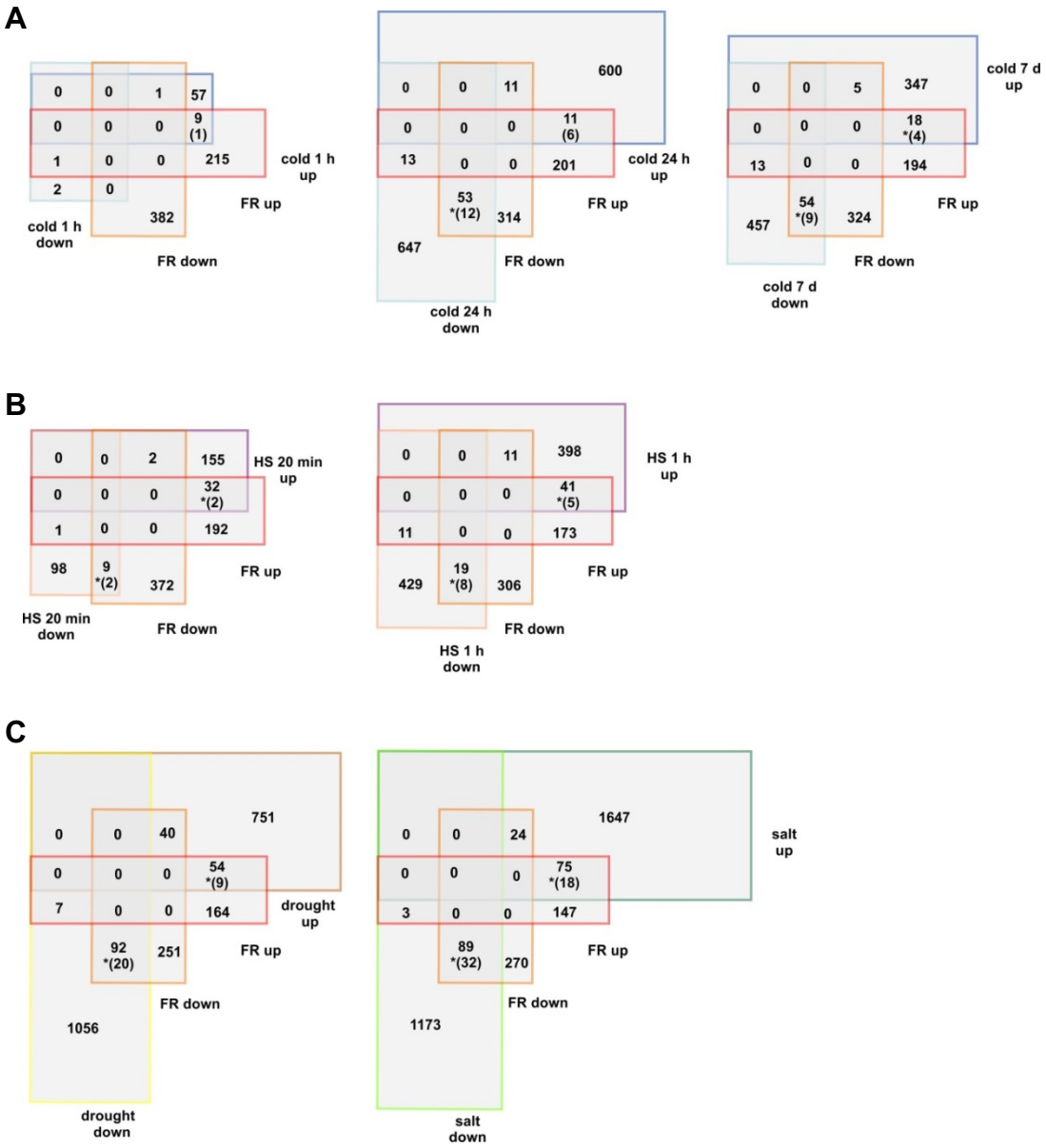

Figure 6.3 Comparison between transcripts regulated after transfer from FR to WL and various abiotic stresses. Venn diagram presenting numbers of down- and up-regulated genes by FR pre-treatment and cold stress (A), heat stress, HS (B) and drought and salt stress (C). A log fold change cut-off of 1 and p-value ≤ 0.05 were applied to define differently regulated genes. Numbers in parenthesis represent genes expected to overlap by chance and (*) indicates statistically significant overlap, p-value < 0.0001.

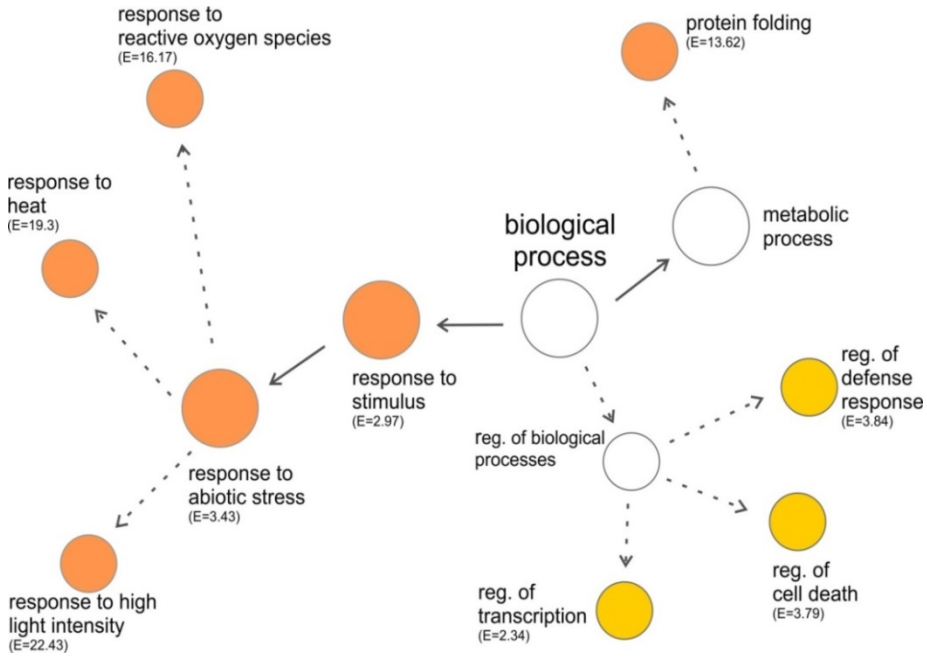

Figure 6.4 GO term enrichment for the set of genes up-regulated after transfer from FR to WL and not up-regulated in *gun1, gun5*. A subset of wild type FR induced genes considered as significant was compared with publicly available data for *gun1,5* after FR pre-treatment (GSE6169). Only categories with a p-value ≤ 0.05 and fold enrichment higher than 1.5 were chosen. Numbers in parenthesis indicate fold enrichment colours indicate significant p-value (more orange for lower p-value).

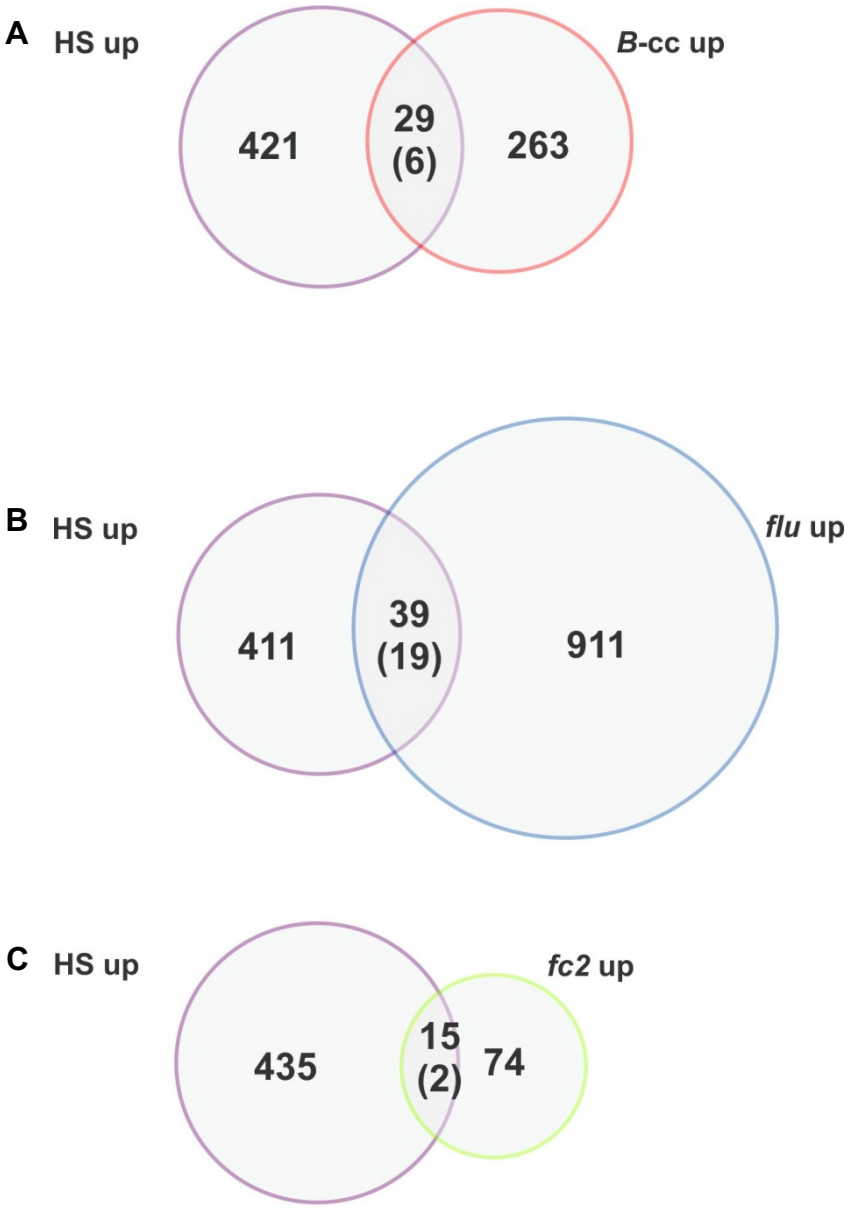

Figure 6.5 Comparison between transcripts up-regulated by heat stress (HS) and in various singlet oxygen-related array experiments. Venn diagram presenting numbers of commonly up-regulated genes 1 h after HS and 2 h after treatment with ß-cyclocitral (ß-cc, A), *flu* mutant transferred from D to WL for 2 h (*flu*, B) and *fc2-1* mutant transferred to WL for 2 h (C). A log fold change cut-off of 1 and p-value ≤ 0.05 were applied to define differently regulated genes. Numbers in parenthesis represent genes expected to overlap by chance. Circle size represent total number of genes up-regulated by the treatment.

6.2.3 Interaction of heat stress signalling and singlet oxygen signalling

Based on the strong overlap observed for the FR pre-treatment and heat stress transcriptomes, it was tested experimentally whether a prior heat stress treatment can alter changes in gene expression resulting from the FR response. Thus, a time point experiment was performed in which gene expression was analysed 2h, 4h and 24h after WLc exposure in wild type and *gun5-1* seedlings that had received a heat shock (HS), a FR pre-treatment of both (Figure 6.6). Analysis showed that 1 h HS treatment inhibited the response to a FR pre-treatment, as seen by a reduced induction of *BAP1* expression in WT seedlings observed at early and late time points after WLc exposure. Reduced induction of *BAP1* in WT did not correlate with a rescue of *HEMA1* expression, which remained low after an additional HS. This response was very similar to the effect of HS on ALA-induced changes in gene expression seen previously (Figure 5).

Although *gun5-1* inhibited the FR response, the ability to recue *HEMA1* expression was almost completely lost in this mutant after an additional HS treatment (Figure 6.6), suggesting that inhibition of tetrapyrrole gene expression after a FR pre-treatment and HS might be at least partially independent. The *gun5-1* mutant did not alter the HS response, as no significant difference in gene expression changes between wild type and *gun5-1* exposed to a single HS was seen (Figure 6.6), suggesting that a HS response is induced independently of *gun* signalling.

Singlet oxygen and hydrogen peroxide have been proposed to function antagonistically in the regulation of gene expression (Laloi et al., 2007). To examine if H_2O_2 can inhibit the response to a FR pre-treatment in a similar way to a HS, gene expression was analysed by qPCR in 4d D grown or 2 d D and 2 d FR pre-treated wild type seedlings immersed in H_2O_2 and exposed to 2h of WL (Figure 6.7). Interestingly, a FR pre-treatment and H_2O_2 had a slight additive effect on gene expression. H_2O_2 application resulted in a moderate inhibition of *LHCB2.1*, *HEMA1* and induction of *BAP1* in WL, and these trends were stronger in after a FR pre-treatment (Figure 6.7). *BAP1* in particular showed a strong additive response to the two treatments.

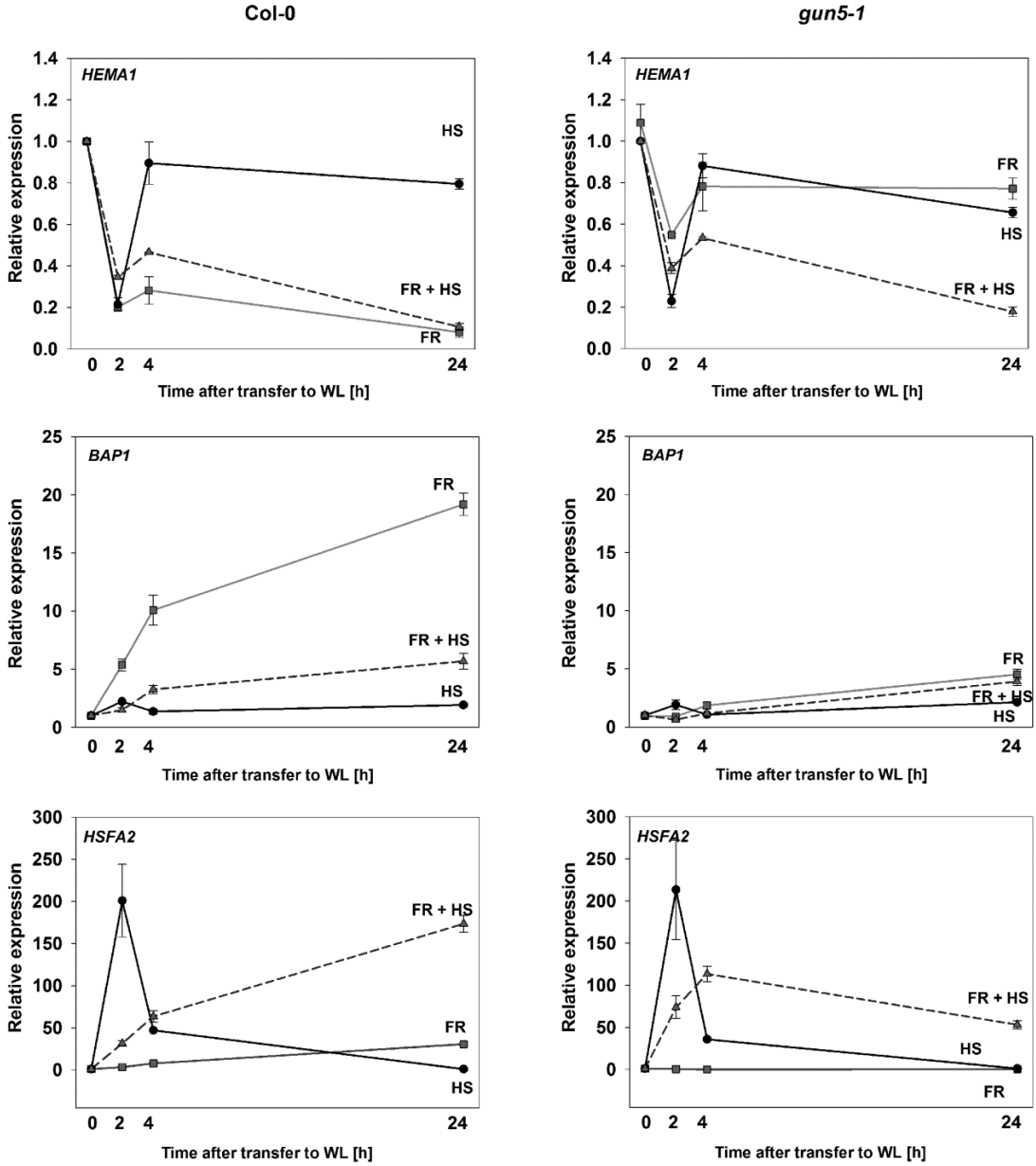

Figure 6.6 Time course of *HEMA1*, *BAP1* and *HSFA2* gene expression in WT (Col-0) and *gun5-1* mutant seedlings treated with either a FR pre-treatment (FR), a heat shock (HS) or both. Col-0 and *gun5-1* seedlings were grown on 1% agar, with ½ MS medium, without sucrose, for 2 d in D and 2 d in FR or 4 d in D followed by an exposure to constant white light under 100 µmol m^{-2} s^{-1} intensity for 2h. For the heat shock, plates were treated with 44°C in standard WL (100 µmol m^{-2} s^{-1}) for 1 h after transfer from dark (HS) or FR (FR+HS) and then returned to control conditions (22°C, 100 µmol m^{-2} s^{-1}) for an additional 1 h. Gene expression was measured by quantitative RT-PCR analysis and normalised to *ACTIN DEPOLYMERIZING FACTOR 2* (*ADF2,* At3g46000) reference gene and to the 4 d D grown Col-0 transferred to WL for 2h. Data shown are means +/- SEM of three biological replicates.

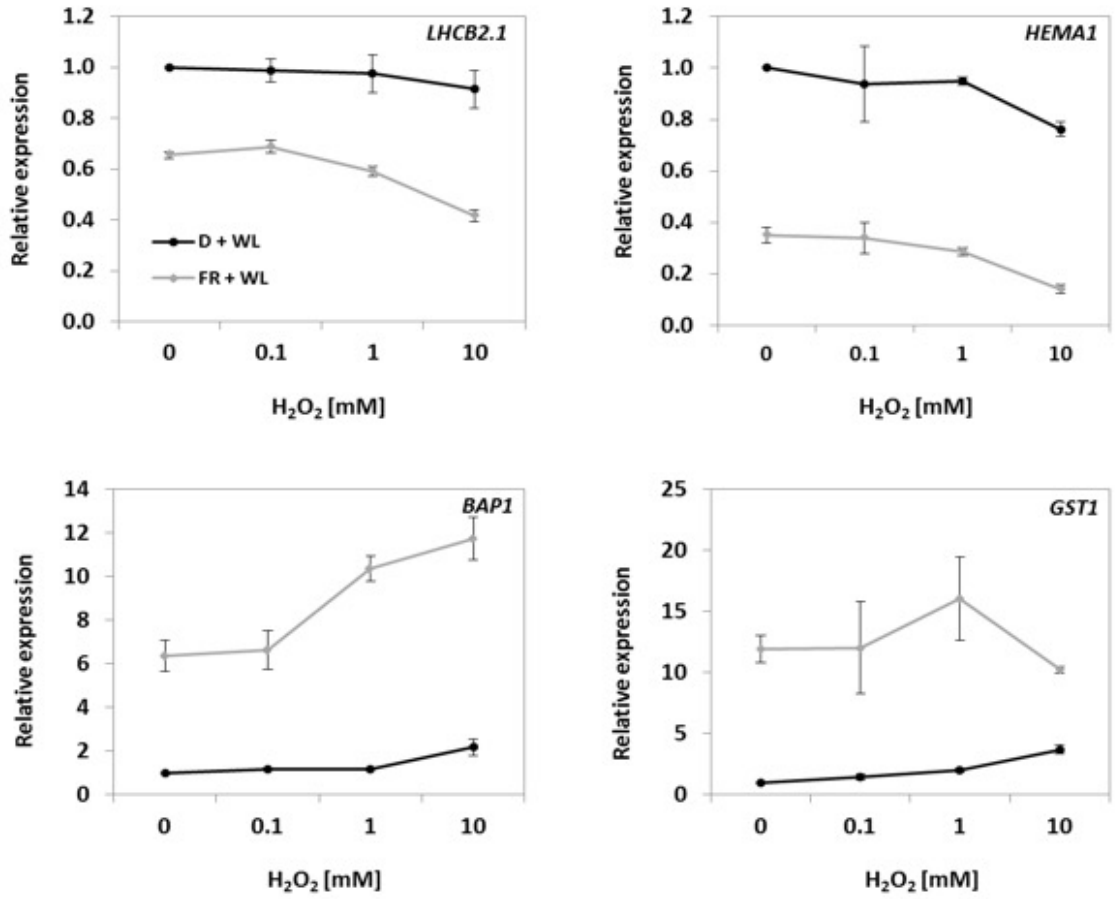

Figure 6.7 Effect of H_2O_2 on $^1O_2$ response induced by a far red (FR) pre-treatment. WT (Col-0) seedlings were grown on 1% agar, with ½ MS medium, without sucrose, for 2 d in D and 2 d in FR or 4 d in D followed by WLc (100 µmol m^{-2} s^{-1}) for 2 h. Directly before the shift from D or FR to WL, seedlings were immersed in a solution containing ½ MS and different concentrations of H_2O_2. Gene expression was measured by quantitative RT-PCR analysis and normalised to *ACTIN DEPOLYMERIZING FACTOR 2* (*ADF2,* At3g46000) and to 4 d D grown Col-0 without H_2O_2. Data shown are means +/- SEM of three biological replicates.

To further examine if the phenotypes observed after HS and ALA or FR pre-treatments was directly linked with the perturbation in ROS production, the accumulation of $^1O_2$ and other ROS was examined by fluorescence microscopy in cotyledons of seedlings treated with single ALA to WL, FR to WL, or HS treatments and a combination of these treatments (Figure 6.8). Fluorescence was recorded before (0 h) and 2 h after transfer to WL. A strong SOSG fluorescence was detected in cotyledons of 0.1 mM ALA treated and FR pre-treated Col-0 after 2 h transfer to WL, but not before, consistent with the ability of these two conditions to induce $^1O_2$ production in WL. SOSG fluorescence after ALA and FR treatments was weaker, when seedlings were additionally pre-treated with HS (Figure 6.8A). This indicates that HS can reduce WL production of $^1O_2$ derived from excess protochlorophyllide, a result that is consistent, with changes in *BAP1* expression observed in earlier experiments (Figure 5.13 and Figure 6.6).

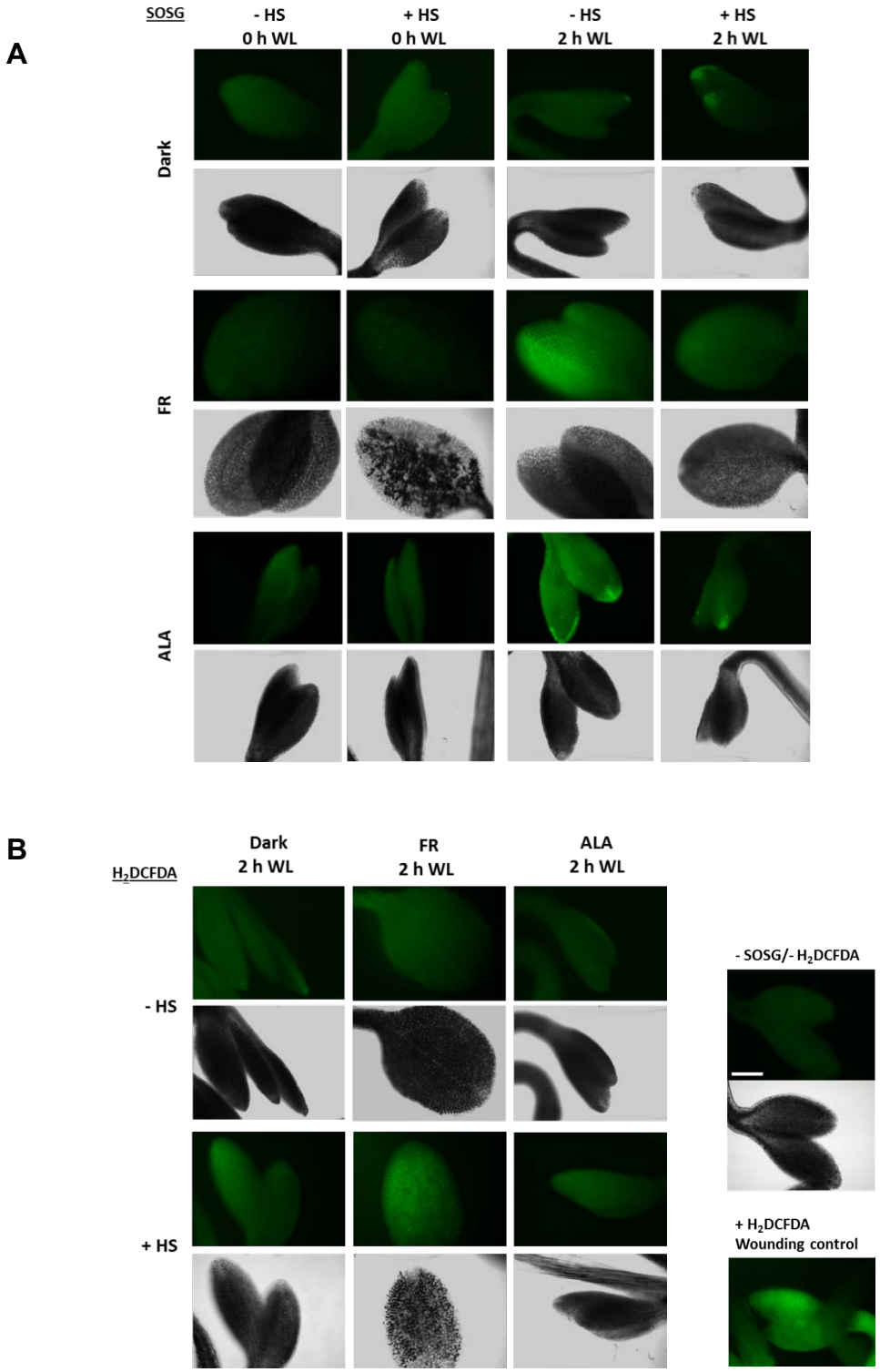

Figure 6.8 Cellular singlet oxygen ($^1O_2$) levels in cotyledons of far red (FR) pre-treated, ALA and heat shock (HS) treated seedlings. WT (Col-0) seedlings were grown on 1% agar with ½ MS medium supplemented with 5 mM MES, without sucrose, and with or without 0.01 mM ALA concentration for 4 d in D (ALA) or 2 d D + 2 d FR (FR) were transferred to WL (100 µmol m^{-2} s^{-1}) for 2 h. For the HS treatment, plates were treated with 44°C for 1 h in D before transfer to WL. (A) Singlet oxygen was determined by SOSG fluorescence. (B) Other ROS were examined using H_2DCFDA fluorescence. Representative photographs are shown from 2 independent biological replicates. Scale bar is 200 µm.

No $^1O_2$ production by HS alone was seen independent of the light treatment and growth conditions. The production of other ROS was measured by H_2DCFDA florescence (Figure 6.8B). Surprisingly only weak increase in H_2DCFDA florescence was detected for any treatment tested, even when a HS applied solely (Figure 6.8), suggesting that inhibition of $^1O_2$ production observed in this experiment was not due to concurrent action of other ROS species.

While results presented so far might be difficult to explain mechanistically, they clearly demonstrate that heat stress can affect the response to ALA and FR pre-treatment. A reciprocal approach was then undertaken, where selected mutants known to be involved in regulation of different aspects of the heat stress response including mutants for transcription factors (*mpk6*, *hsfa2*), autophagy (*atg5*) and heat shock proteins with a role in protein transport and folding (*cphsc70-1*, *chip*) were screened for their response to ALA treatment. Their possible involvement in tetrapyrrole-dependent retrograde signalling was then examined.

Firstly, a series of alleles of *hsfa2-1, atg5-1, cphsc70-1* and *chip-1* mutants were isolated from the SALK and SAIL T-DNA collections. A schematic representation of gene models including T-DNA insertion sites and primers used for confirmation of homozygosity and knockout of gene expression is presented in Figure 6.9. The homozygous lines (see Chapter 2, Table 2.1 for detail on insert name) were selected by PCR screening from a heterozygous population, with primer pairs binding specifically to the gene tested and to the T-DNA insert, as indicated in Figures 6.10 and 6.11. The RT-PCR reaction confirmed that no *HSFA2, ATG5, cpHSC70-1* and *CHIP* transcript could be detected in selected homozygous lines (Figure 6.11). The *mpk6* mutant was already available and was originally obtained from the SALK collection.

Quantitative PCR analysis was performed to establish the effect of the selected mutations in different heat stress responses on photosynthetic gene expression. Using optimised ALA conditions of 4 d dark growth on 0.1 mM ALA, the *atg5-1*, *mpk6-3*, *hsfa2-1* and *chip-1* mutants showed a strong and significant rescue of inhibition of *HEMA1*, *LHCB2.1* and *GUN4* expression 24 h after transfer to WLc (Figure 6.12). All these mutants were also showed elevated *BAP1* expression on ALA similar to the wild type response level and in some cases had higher *BAP1* expression in the absence of ALA feeding. Interestingly, one of the mutants examined, *cphsc70-1,* was characterised by a hypersensitive response to ALA treatment, with stronger repression of photosynthetic genes (significant for *LHCB2.1*) and a greater induction of *BAP1* (Figure 6.12).

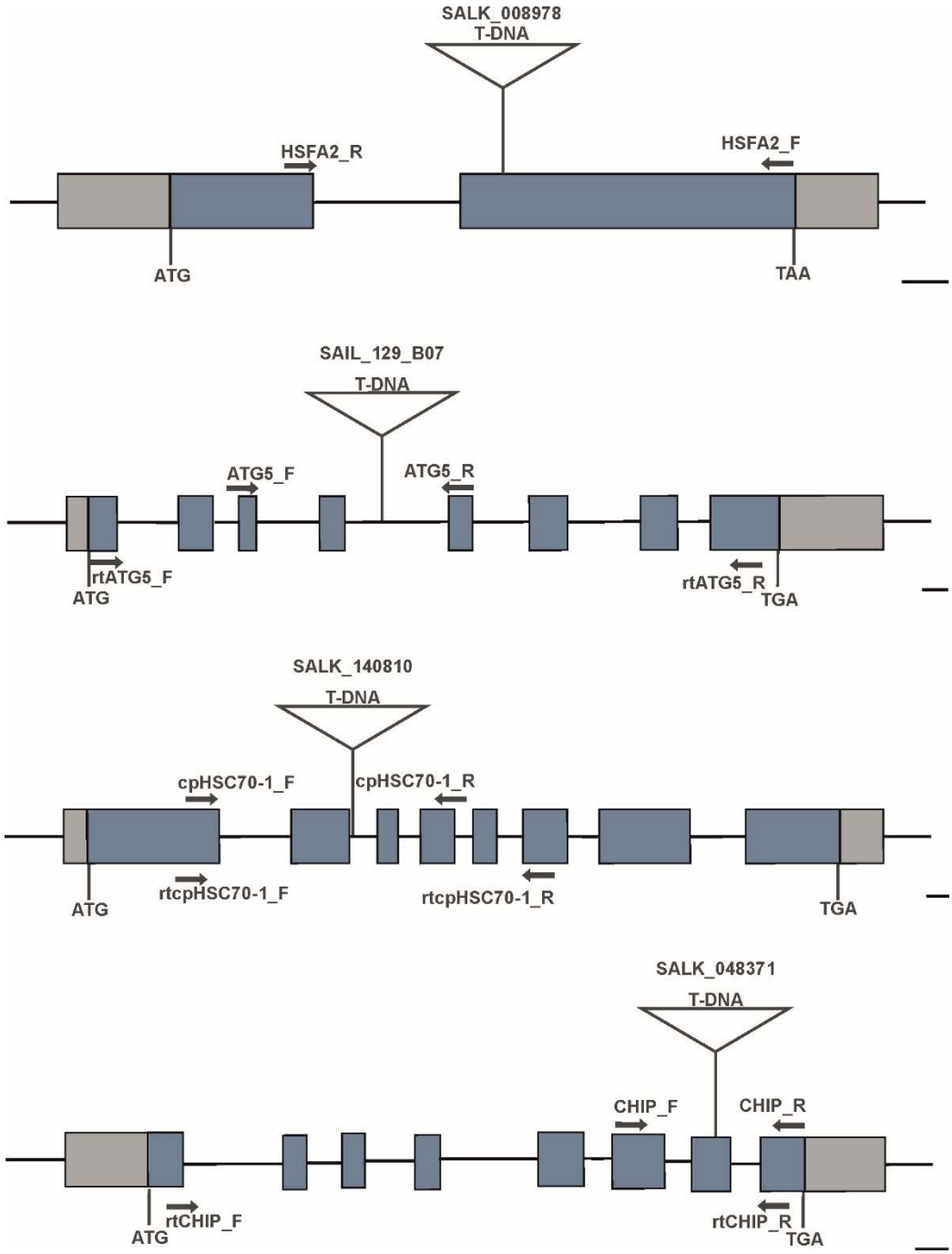

Figure 6.9 Schematic representations of *hsfa2-1*, *atg5-1*, *cphsc70-1* and *chip-1* mutant alleles. Blue boxes represent exons, grey boxes represent UTR regions, and black lines represent introns. Start (ATG) and stop (TGA/TAA) codon of translation are also indicated. Scale bar for each scheme represents 100 bp. PCR and RT-PCR primers used for genotyping are indicated by black arrows. T-DNA insertions and primer pairs are not drawn to scale.

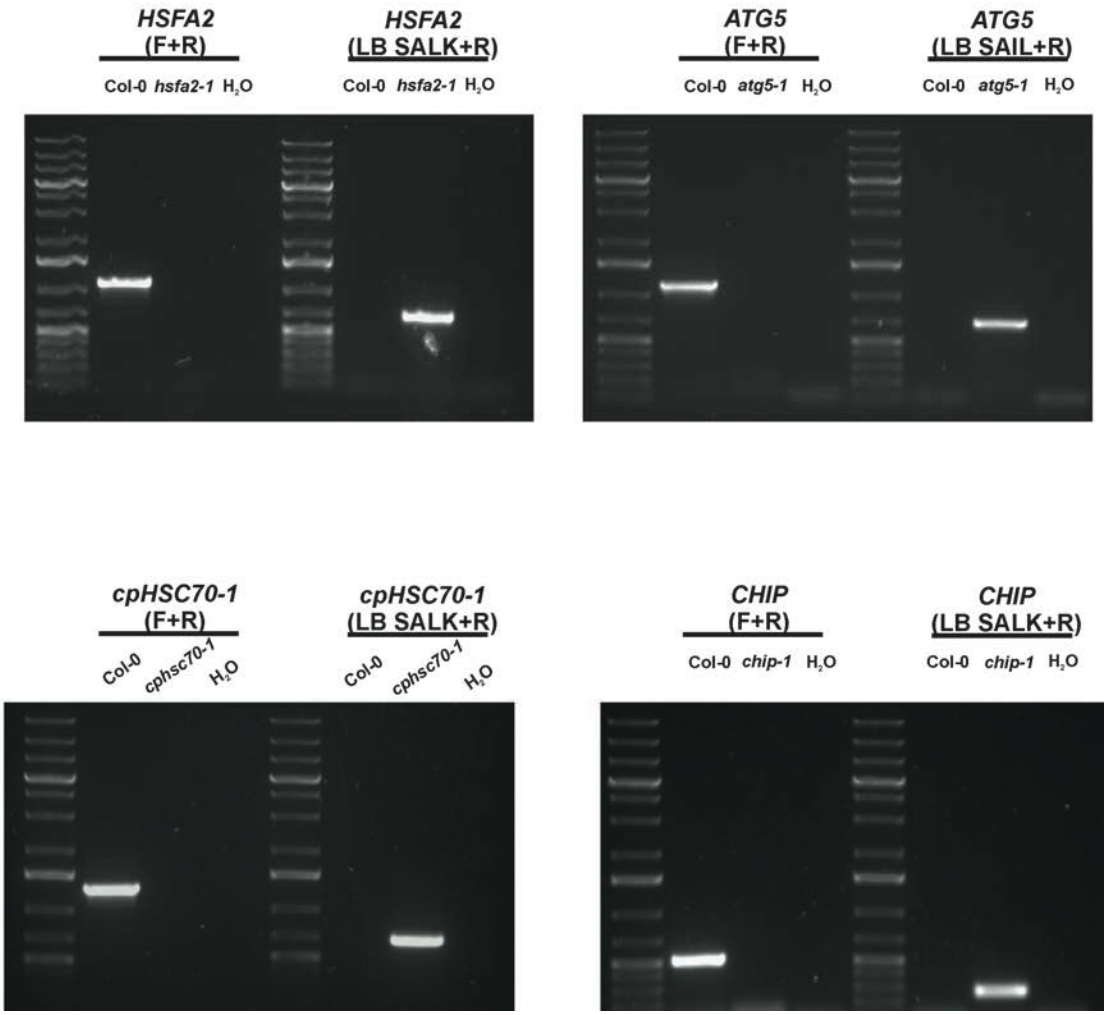

Figure 6.10 Analysis of the T-DNA insertion alleles of *hsfa2-1*, *atg5-1*, *cphsc70-1* and *chip-1* mutants. Confirmation of the T-DNA insertion by PCR amplification. Genomic DNA from WT (Col-0) and *hsfa2-1*, *atg5-1*, *cphsc70-1* and *chip-1* plants was amplified using gene specific primers (indicated in Figure 6.9) and a left border specific primer (LB SAIL or LB SALK).

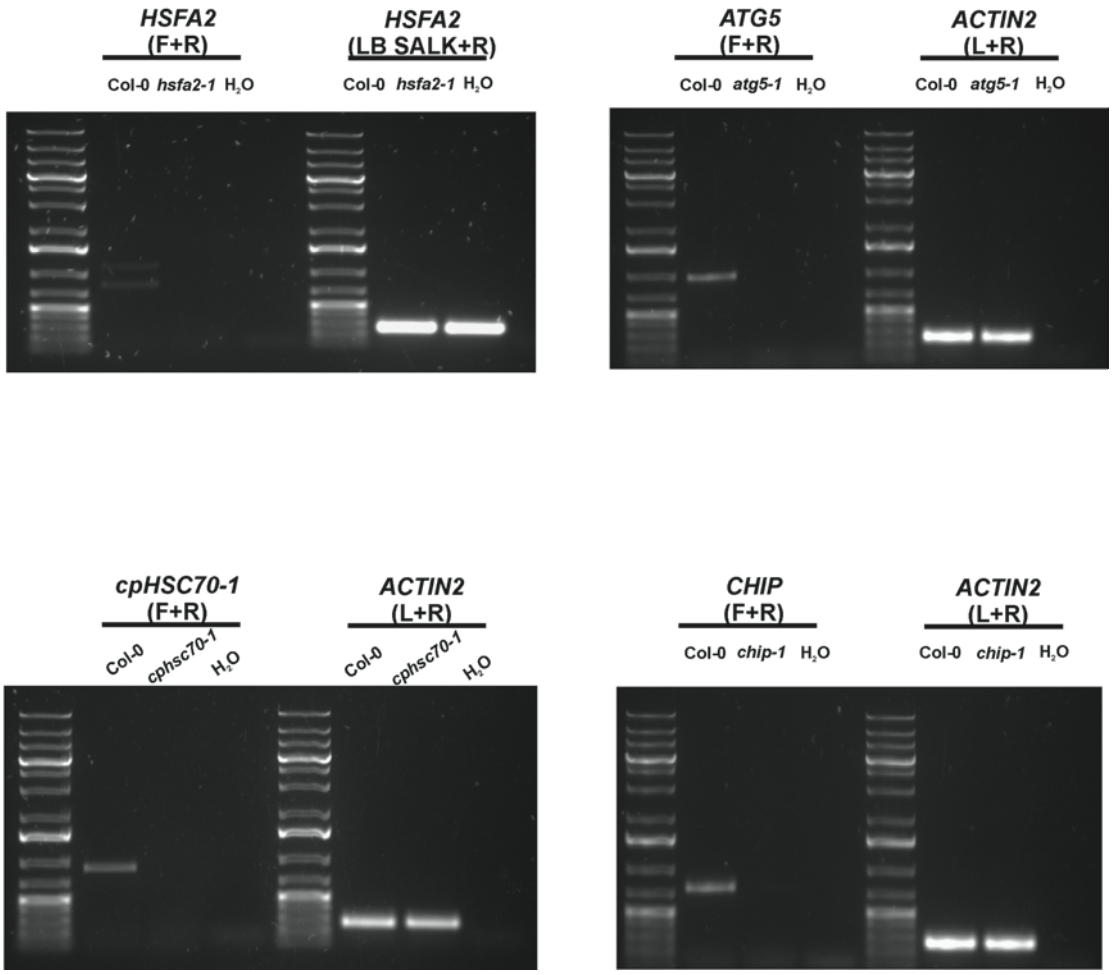

Figure 6.11 Analysis of the T-DNA insertion alleles of *hsfa2-1*, *atg5-1*, *cphsc70-1* and *chip-1* mutants. RT-PCR analysis of disrupted *HSFA2, ATG5, cpHSC70-1* and *CHIP* genes in selected homozygous T-DNA insertion lines using primers binding to the selected exons (detail on primers location are depicted in Figure 6.9). *ACTIN2* transcripts were used as a positive control.

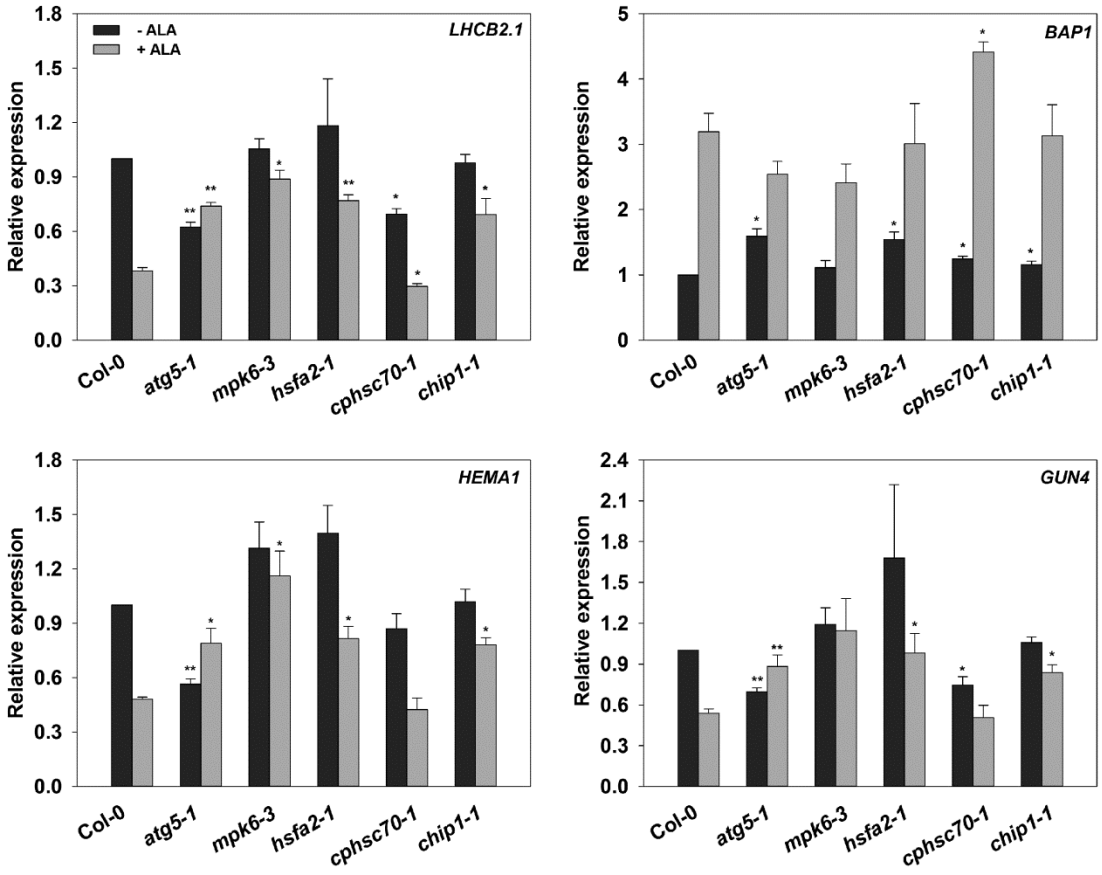

Figure 6.12 Expression of selected nuclear genes in etiolated heat stress mutants after 5-aminolevulinic acid (ALA) treatment. WT (Col-0), *atg5-1*, *mpk6-3, hsfa2-1*, *cphsc70-1* and *chip-1* seedlings were grown on 1% agar with ½ MS medium supplemented with 5 mM MES, without sucrose, and with (ALA) or without (-ALA) 0.01 mM ALA for 4 d in D and 24 h in WLc (100 µmol m^{-2} s^{-1}). Gene expression was measured by quantitative RT-PCR analysis relative to Col-0 without ALA and normalised to *ACTIN DEPOLYMERIZING FACTOR 2* (*ADF2,* At3g46000). Data shown are means +SEM of three biological replicates.

The results presented here and in Chapter 5 show that heat stress can inhibit photosynthetic and tetrapyrrole gene expression in WL when given in the first 1 h of the WL period. To gain more understanding of the response to heat stress, WL-induced gene expression was measured in seedlings after treatment with 1 h HS in the dark. Figure 6.14 shows that although heat stress can be effectively induced in the dark-grown seedlings, as seen by induction of *HSFA2* and *BAP1* expression at time point 0, the HS blocked only light induction of *HEMA1* and *LHCB2.1*, while there was no strong effect on repression of these genes before transfer to WL. The reduced expression of photosynthetic and tetrapyrrole genes was not due to the reduced Pchlide after the HS, as this accumulated in the dark at a comparable level to the unstressed wild type seedlings (Figure 6.15A). However, the HS treatment did reduce seedling greening, as reduced chlorophyll accumulation was seen in stressed seedlings 1 d after transfer to WLc (Figure 6.15A). Between 1 and 3 d the rate of greening was slightly slower in seedlings that had received a HS. To test if the HS inhibitory response could be due to the functional impairment of PORs, expression of *PORA* and *PORB*, as well the dark accumulation of PORA protein were investigated in HS stressed WT seedlings. In fact, HS resulted in a rapid up-regulation of *PORA* and *PORB* expression in the dark and delayed the light-induced down-regulation of these transcripts (Armstrong et al., 1995). No effect was seen on PORA protein accumulation in the time of the HS treatment (Figure 6.15B).

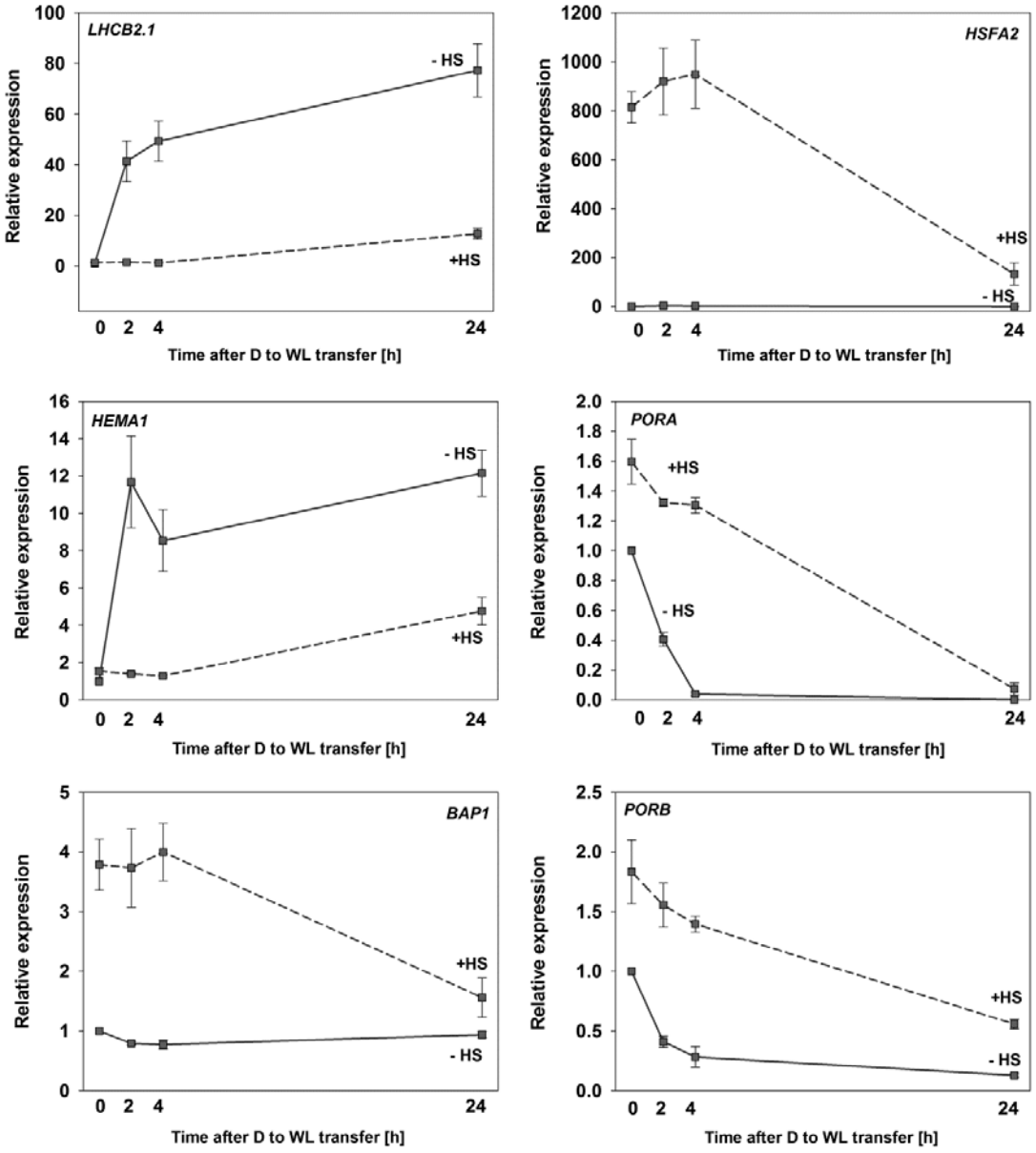

Figure 6.13 Time course of expression of selected nuclear genes in WT (Col-0) seedlings pre-treated with a heat shock (HS) in dark. WT (Col-0) seedlings were grown on 1% agar, with ½ MS medium, without sucrose, for 4 d in D followed by an exposure to WLc (100 µmol m^{-2} s^{-1}) for 0, 2, 4 and 24 h. For the heat shock (+HS), plates were treated with 44°C for 1 h in the dark just before transfer to WL, while the control plates were left in darkness in at 22°C (-HS). Gene expression was measured by quantitative RT-PCR analysis and normalised to *ACTIN DEPOLYMERIZING FACTOR 2* (*ADF2,* At3g46000) and to 4 d D grown Col-0 (-HS). Data shown are means +/- SEM of three biological replicates.

A

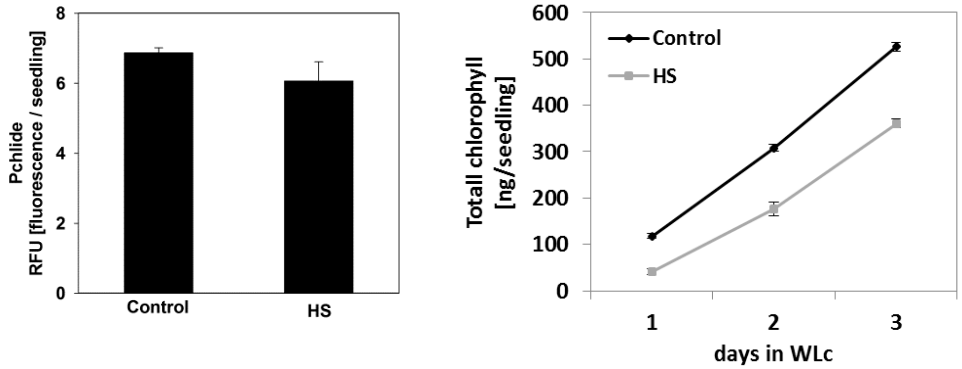

B

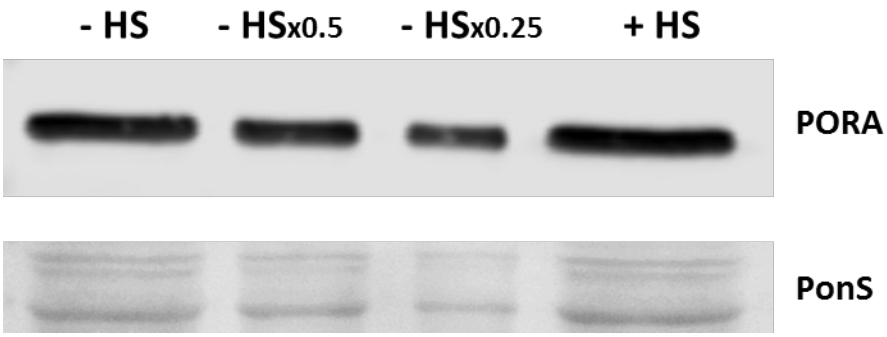

Figure 6.14 The effect of heat stress applied in darkness on the tetrapyrrole pathway. (A) Protochlorophyllide (Pchlide) and time course for the total chlorophyll accumulation after transfer to WLc (100 µmol m^{-2} s^{-1}) in WT (Col-0) grown on 1% agar, with ½ MS medium, without sucrose, for 3d D with and without a HS for 1 h at 44°C in D. (B) Western blot analysis of PORA under the same conditions. A representative blot from 3 independent biological replicates is shown, with similar results in each replicate.

6.2.4 Interaction of retrograde signalling with drought and salt stresses

In recent years, microarray datasets have become available for the effect of NF on nuclear genes expression in young seedlings (Alluru et al., 2009; Woodson et al., 2012, Moulin et al., 2008). To investigate whether retrograde signalling responses may be important in the response to environmental stress, the full NF transcriptome datasets were compared to publically-available datasets for responses to drought, salt, cold and heat in *Arabidopsis* seedlings. These datasets were processed to identify differentially expressed genes using ± 1-log fold change as a cut-off (see Chapter 2 for detailed procedures). Figure 6.16A shows the summary of this analysis comparing number of genes commonly repressed or induced by these treatments. Salt and drought stresses resulted in the strongest transcriptomic changes, with more than a thousand of genes being inhibited or induced. Among all analysed abiotic stresses, drought shared the highest similarity with genes down-regulated after NF treatment (Figure 6.16A, B).

Although 3 different NF treatments tested in this study resulted in down-regulation of similar number of genes (between 645-834 genes), a surprisingly small proportion of these genes were common to all treatments (159 genes). Of these 159 genes common for all NF-treatments, 72 and 43 genes were also inhibited during drought and salt stresses, respectively (Figure 16.6B, C). Many of the overlapping genes inhibited by NF and drought were related with photosynthesis, encoded energy or electron transport pathways, or were involved in cell organisation, transport and protein metabolism (e.g. photosystem II–related genes *PSBQ-1*, *PPL2,* the gene for light harvesting complex, *LHCA5;* chlorophyll synthesis genes *PORB*, *HEMA1; CP12-2* encoding a Calvin cycle protein, and *J20* functioning in protein folding).

No strong overlap was found between genes differently regulated by NF and HS. However, prolonged exposure to cold treatment (24 h and 7 d) resulted in a high and significant overlap with all 3 NF datasets tested, for both down and up regulated genes (Figure 6.16A, C). Among common down-regulated genes many were involved in photosynthesis, while overlapping up-regulated genes were involved in RNA and protein metabolism.

A

DRG		NF_In house	NF_Woodson	NF_Aluru
overlap	DRG No	645	834	716
Drought	1156	190	300	196
Salt	1866	121	168	123
HS 20 min	108	6	19	25
HS 1 h	459	43	36	71
Cold 1 h	3	0	0	0
Cold 24 h	709	92	119	96
Cold 7 d	524	104	125	90

URG		NF_In house	NF_Woodson	NF_Aluru
overlap	URG No	316	500	326
Drought	848	0	0	0
Salt	1747	20	46	75
HS 20 min	189	10	5	9
HS 1 h	450	16	22	11
Cold 1 h	67	2	1	2
Cold 24 h	627	79	106	39
Cold 7 d	397	42	47	24

B

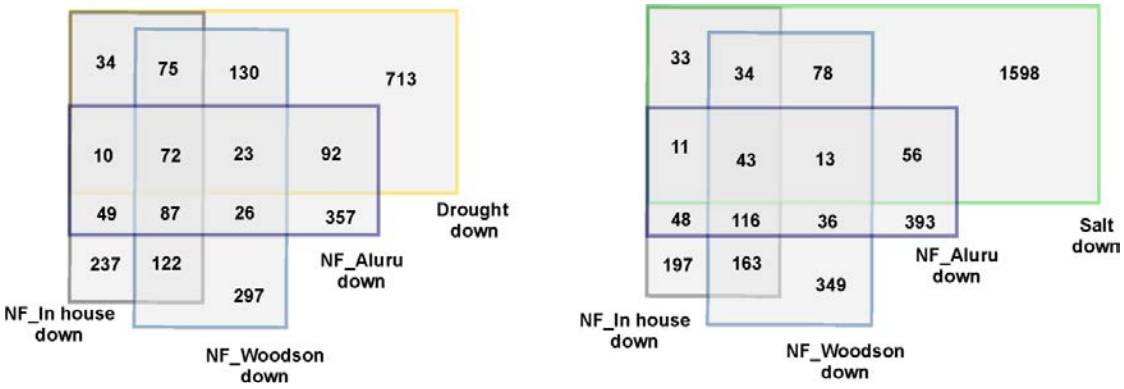

C

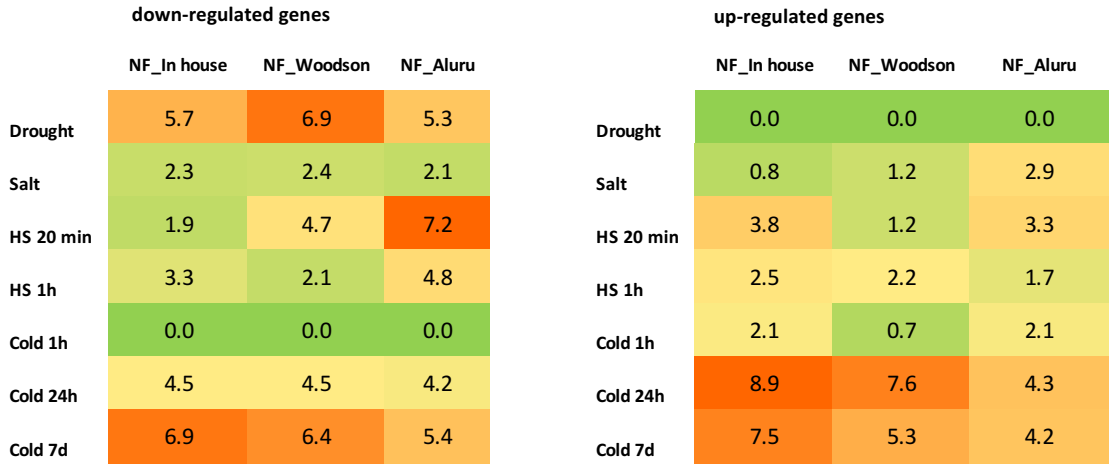

Figure 6.15 Comparison between transcripts down- and up-regulated by norflurazon (NF) and different abiotic stresses. (A) Number of genes overlapping between datasets tested. A log fold change cut-off 1 was applied to define differently regulated genes. (B) Selected Venn diagrams showing numbers of commonly regulated genes for NF and drought or salt stresses. (C) Significance of the overlap between NF and different abiotic stresses. Numbers represent ratios between the number of overlapping genes and the number of genes that would be expected by chance and are additionally depicted in a colour scale.

The array analysis suggests that drought and salt stresses have the highest potential to interact with the positive retrograde signalling pathways operating during chloroplast biogenesis. To test if these abiotic stresses can compromise the ability of the plastids to signal the nucleus gene expression was measured in wild type and *gun5-1* and *gun6-1D* mutant seedlings exposed to a combination of NF and salt treatments (Figure 6.17).

To induce salt stress, seedlings grown for 2 d D and 3 d WLc were immersed for 6 h in liquid MS supplemented with 150 mM NaCl and/or 1µM NF. As shown in Figure 6.17 a very strong induction of salt and drought marker gene expression (*RD29B*, *KIN1* and *bHLH92*) was observed in all analysed genotypes after NaCl treatment, indicating that the conditions used in this study were successful in induction of salt stress. Expression of these genes after NaCl treatment was enhanced in the *gun5-1* compared to wild type and may indicate that the mutant was more susceptible to the salt stress treatment. Interestingly, induction of these 3 genes by salt stress was strongly repressed when plastid signalling was blocked by NF (Figure 6.17). Additionally, in the *gun5-1* and *gun6-1D* mutants, this block of gene induction was rescued. As expected, both *gun5-1* and *gun6-1D* mutants showed higher expression of*HEMA1*, *LHCB2.1* and *CP12-2* after a NF treatment compared to wild type (Figure 6.17). Intriguingly, the ability of *gun5-1* and *gun6-1D* to rescue expression of these photosynthetic genes on NF was actually further enhanced when additional salt stress was applied. Overall these data suggest that there is a requirement for a functional chloroplast to induce responses to salt stress.

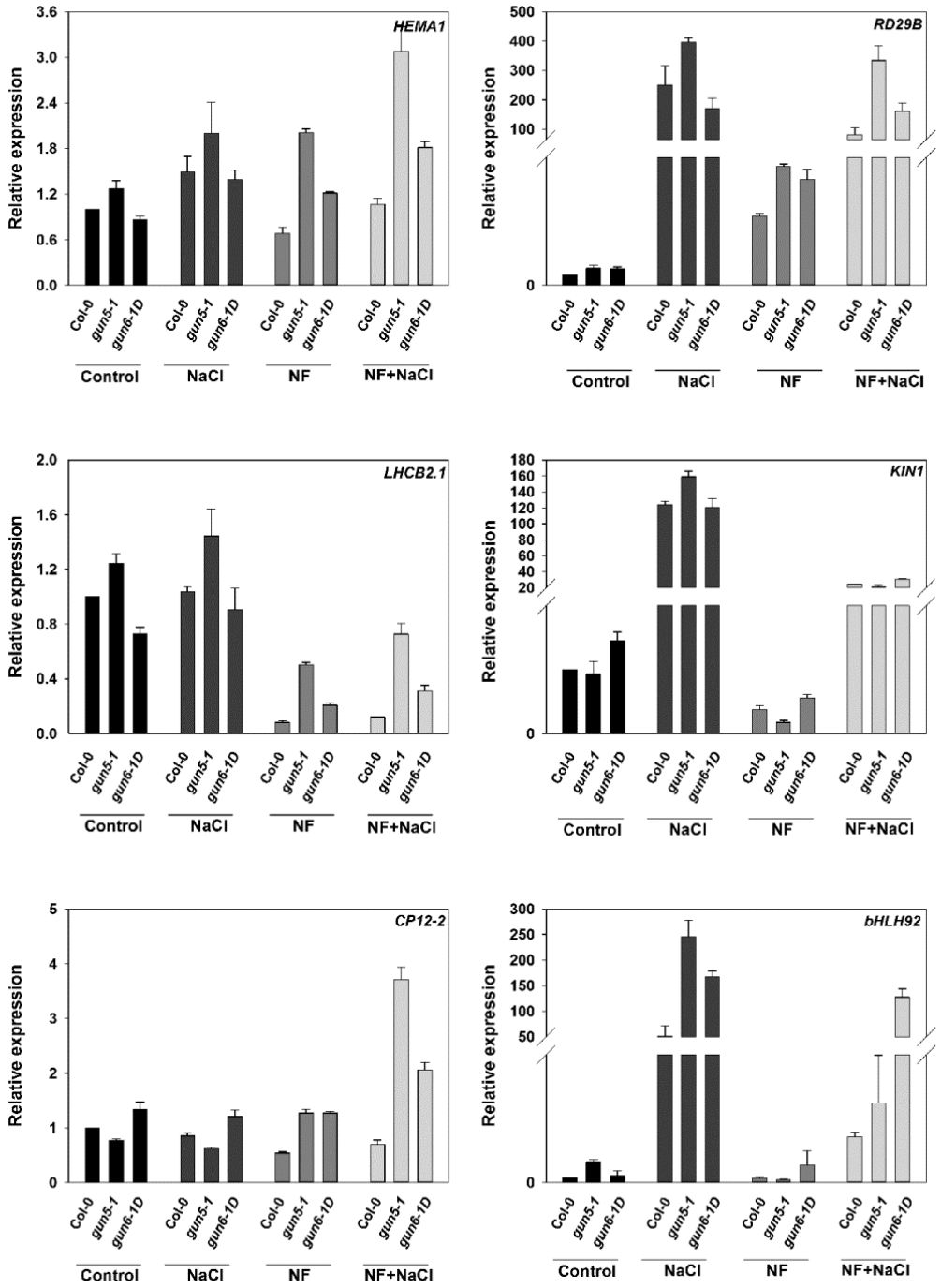

Figure 6.16 Expression of selected nuclear genes in WT (Col-0), *gun5-1* and *gun6-1D* seedlings treated with norflurazon (NF) and salt stress (NaCl). Seedlings were grown on ½ MS medium with 1% agar (pH 5.6) and with or without 1 µM NF under the following conditions: 2 d dark, 3 d WLc (100 µmol m^{-2} s^{-1}). For the final 6 h of WLc growth, seedlings were transferred to liquid ½ MS supplemented with: 1 µM NF (NF), 150 mM NaCl (NaCl), both 1 µM NF and 150 mM NaCl (NF+NaCl), or with 0.02% DMSO as a control. Expression is shown relative to WT control samples and normalised to *YELLOW LEAF SPECIFIC GENE 8* (*YLS8*, At5g08290). Data shown are means +SEM of three independent biological replicates.

It is well established that induction of many drought or salt responsive genes belonging to the CBF regulon is an ABA-dependent (see Introduction). Because NF treatment blocks ABA synthesis, it is possible that the phenotype observed in WT seedlings after the salt and NF treatments (Figure 6.17) resulted from a reduced ABA response to NaCl treatment. To test this, a Lin treatment was used to inhibit chloroplast function in a manner that is not thought to block ABA synthesis. In this case, and in contrast to the previous experiment, induction of the salt stress responsive genes *RD29B* and *KIN1* was not inhibited by growing seedlings on Lin (Figure 6.18A). However, *bHLH92* induction by salt stress was still abolished after Lin treatment. Thus, the phenotype observed earlier in WT seedlings treated with NF and salt could not be fully explained by a block of ABA synthesis. Interestingly, NaCl treatment rescued significantly the repression of *HEMA1*, *LHCB2.1* and *CP12-2* by Lin, resulting in a *gun*-like phenotype.

If the gene expression phenotype of NF- and NaCl-treated wild type seedlings resulted from the ABA disruption, then it might be expected that feeding with ABA should rescue this response. In order to test this, seedlings grown on NF were immersed in 10µM or 100µM ABA and gene expression was analysed by quantitative RT-PCR after 6h ABA treatment. Both ABA concentrations could successfully induce *RD29B* and *KIN1* expression in the presence or absence of NF, but no induction of *bHLH9 2*was observed (Figure 6.18B). These results are consistent with the previous observation that on Lin only *bHLH92* was still inhibited after a salt treatment (Figure 6.18A). If the disruption in ABA accounts for the NF-treated wild type phenotype, then the rescue of the tetrapyrrole and photosynthetic gene expression by ABA could also be expected. Figure 6.18B shows this is not the case, as none of three retrograde signalling marker genes (*HEMA1*, *LHCB2.1*, *CP12-2*) were rescued by ABA treatment. On the contrary, immersing NF-grown seedlings in 100µM ABA with 1µM NF enhanced the repressive effect of NF treatment alone (Figure 6.18B).

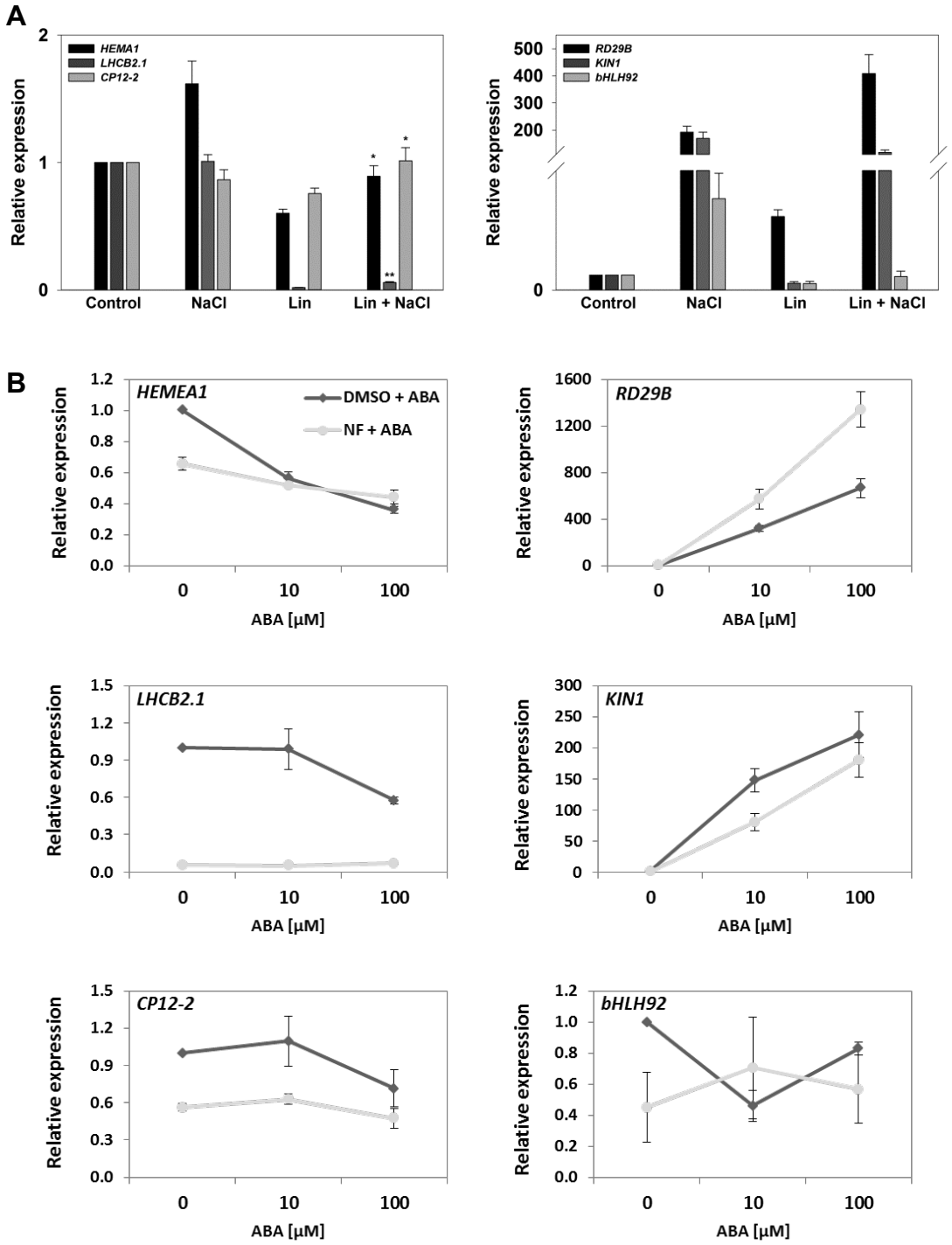

Figure 6.17 Expression of selected nuclear genes in WT seedlings treated with lincomycin (Lin) and salt stress (NaCl) or norflurazon (NF) and abscisic acid (ABA). (A) WT (Col-0) seedlings were grown on ½ MS medium with 1% agar (pH 5.6) and with or without 0.5 mM lincomycin (Lin) under the following condition: 2 d D and 3 d WLc (100 µmol m^{-2} s^{-1}). For the final 6 h of WLc growth, seedlings were transferred to liquid ½ MS supplemented with 0.5 mM Lin (Lin), 150 mM NaCl (NaCl), or both 0.5 mM Lin and 150 mM NaCl (Lin+NaCl). Control plants were immersed in liquid ½ MS supplemented with water. (B) Col-0 seedlings were grown on ½ MS medium with 1% agar (pH 5.6) and with (NF) or without (DMSO) 1 µM NF under the following conditions: 2 d dark, 3 d WLc (100 µmol m^{-2} s^{-1}). For the final 6 h of WLc growth seedlings were transferred to liquid ½ MS supplemented with or without 10 and 100 µM ABA, with additional supplementation of 1 µM NF (NF+ABA), or DMSO (DMSO+ABA). Expression is shown relative to WT control samples and normalised to *YELLOW LEAF SPECIFIC GENE 8* (*YLS8*, At5g08290). Data shown are means +SEM of three independent biological replicates. Asterisks in (A) denote a significant difference vs. Col-0 treatment with Lin alone, Student's *t*-test (*p<0.05, **p < 0.01).

6.3 Discussion

Many chloroplast-derived signals are implicated in plant responses to abiotic stresses (for detailed examples, see earlier introduction sections). Mature plants respond to environmental perturbation through activation of complex signalling networks that involve many factors that have complex interdependencies. The proposed tetrapyrrole-dependent model for plastid retrograde signalling during seedling development provides an opportunity to directly analyse the contribution of plastid signals to the response to abiotic stress in a potentially simpler system. Results from this study provide new information about the mechanisms that regulate response to stress, with a focus on the critical early stages of seedling development.

6.3.1 Possible role of tetrapyrrole signalling in abiotic stress signalling

Tetrapyrrole-dependent retrograde signalling was the main focus of this work and there is a strong body of evidence in the literature to support an important role of tetrapyrrole biosynthesis enzymes in plant responses to different abiotic stresses. The observation that the expression of tetrapyrrole biosynthesis genes can change in response to both temperature and salt and drought stresses (Figures 6.1 and6.2) is also in agreement with these findings. For example, changes in *HO1* (*HY1*) expression levels were shown to affect drought and salt stress tolerance (Xie et al., 2011; Wang et al., 2014, Wu et al., 2015). Higher *HEMA1* expression and ALA synthesis rates were observed in transgenic rice plants overexpressing *PPO,* which conferred resistance to drought stress (Thu-Ha et al., 2011). Both *Arabidopsis* ferrochelatase have also been proposed to play a role in salt stress responses. A study on stress tolerance (including salt stress and flagellin treatment) of two plant ferrochelatase mutants *fc1-1* and *fc2-1* suggested that heme produced by FC2 is involved in regulation of plant stress resistance, since mutation in *FC1* had only a marginal effect on the response to stresses compared to control plants (Scharfenberg et al., 2014). In contrast, gene expression analyses suggest that *FC1* and *FC2* are characterised by a divergent expression pattern under stress conditions (Scharfenberg et al., 2014; Figures6.1. and 6.2), with *FC1* expression slightly more responsive to environmental perturbation. FC1, and not FC2, was additionally shown to be involved in response to wounding and pathogen infection (Singh et al., 2002). In agreement with the above examples, expression of *FC1* and *HEMA1* selected genes were shown in this work to be more strongly affected by abiotic stress than other genes encoding the tetrapyrrole pathway (Figures 6.1 and6.2). It is possible that some of these genes are operating independently of biogenic retrograde signalling and their function relies more on an indirect effect i.e. towards modifying cellular ROS homeostasis or growth responses. This is a plausible explanation, since heme is a cofactor for antioxidant enzymes including catalases (CAT),

superoxide dismutase (SOD) and peroxidases (APX) (Sharma et al., 2012). Heme might also act via other heme binding proteins like TSPO, which is also known to be involved in stress responses and its expression is strongly modulated by different stresses (Guillaumot et al., 2009). Moreover, *HO1,* in addition to its anti-oxidative role, was shown to be important for induction of stomatal closure and stomata movement (Cao et al., 2007; Xie et al., 2016).

Testing for an overlap between genes regulated by abiotic stress and retrograde signalling using with array datasets seems to be a good strategy to investigate the potential role of chloroplast signalling in stress signalling. However, proving a clear link between these two might be challenging, due to the complexity of stress responses, with potentially many different signalling pathways being involved. It is known that many abiotic stresses result it divergent transcriptome changes, with only a small proportion of genes induced by multiple different treatments (Chinnusamy et al., 2004; Rasmussen et al., 2013). These genes can be potentially important for the improvement of plant stress tolerance; however, it should be emphasized that, in general, many regulators of stress resistance act via independent and complex mechanisms. Even though, no strong overlap between plastid signalling and abiotic stress treatments was seen, in some cases it was still significant. For example, there was overlap between drought or salt and NF inhibited genes, and between genes up-regulated by a FR pre-treatment and heat (in both cases p-value < 0.0001; Figures6.3 and6.15), and these interactions were studied in more detail. It should be noted that simultaneous application of plastid signalling and selected abiotic stress treatments could potentially result in a completely different transcriptome signature compared with that observed after exposure only to a single treatment. The final response can require an additive, or antagonistic interaction between genes, while by analysing the effect of only single treatments this information is partially lost. This is supported by the recent global transcriptome comparison between responses to single and double abiotic stress treatments, where it was observed that approximately 61% of transcripts responded in a different way (including combinatorial, cancelled or opposite gene expression responses) to a combined double stress treatment (Rasmussen et al., 2013).

6.3.2 The role of tetrapyrrole signalling in drought and salt stresses

The strong overlap detected between NF treatment and drought and salt stresses datasets is not surprising, since plastid signalling has been increasingly linked with ABA signalling. This is supported by the studies of Koussevitzky et al. (2007), Wu et al. (2009) and Voigt et al. (2010) described earlier. It is also supported by the fact that the consequence of both NF and salt or drought is a global down-regulation of tetrapyrrole genes (Figure 6.2; Moulin et al., 2008),

which might suggest at least some cross-talk between the signalling pathways controlling these responses. Interestingly, among photosynthetic genes inhibited by NF and rescued by the *gun1,5* mutant in the array experiment conducted by Moulin et al. (2008), there was a significant enrichment in many ABA-responsive *cis*-acting elements (ABREs), with the core sequence ACGTG (analysis performed for this work). Many photosynthetic genes inhibited after NF treatment were also inhibited by drought or salt stresses (Figure 6.15). Additionally, out of 72 genes found to be common for drought and NF (Figure 6.15), 65 were also inhibited on Lin. This cohort of genes can potentially represent key targets responding to stresses in a plastid signalling-dependent manner. If this is the case, then regulation of this gene cohort via ABRE *cis*-elements might be one of the mechanisms explaining this interaction. On the other hand, it was shown in this work (Chapter 3) that *abi4* mutant is not a *gun* mutant, which would not support this idea, because ABI4 targets ABRE cis-elements. Other, not yet defined transcription factors may be involved in this regulation. Although it was shown before that ABA treatment can result in a *gun* phenotype on NF (Voigt et al., 2010), no rescue of gene expression was seen here (Figure 6.17). One of the reasons for the difference between Voigt et al., (2010) and this work is the time of ABA treatment. Voigt et al. (2010) fed seedlings with ABA for days, while only a short 6 h treatment was applied in this study. Short ABA treatments might be closer to reflecting the actual consequence of disturbed signalling than a prolonged treatment for days that can induce additional pleiotropic effects. Since the ABA treatment used in this work resulted in repression on photosynthetic gene expression and induction of some stress responsive genes (*RD29B*, *KIN1*), and this was not changedfurther by NF treatment, it can be proposed that retrograde signalling could be uncoupled from ABA. Detailed quantitative PCR analyses for salt and NF or Lin (Figures 6.16 and6.17) confirmed that disturbed plastid signalling can compromise the ability of seedlings to respond to salt stresses, however this effect seems to be partially dependent on NF-mediated inhibition of ABA synthesis. Different pools of genes that are regulatedby salt and drought stress control may have different requirements for functional chloroplast status. The observation that *gun* mutants including *gun6-1D* could rescue from the effects of NF and salt treatment is supportive for the role of tetrapyrroles in regulation of stress signalling. If we accept the FC1-derived heme pool is necessary for control over nuclear gene expression, it would be interesting to investigate the effect of NF (and other chemicals that block plastid signalling) on salt and drought stress responses in other *FC1*ox lines and ferrochelatase mutants. There is some evidence in the literature for *fc* mutants being affected in salt stress tolerance (Scharfenberg et al., 2014) and transgenic rice plants that overexpress ferrochelatase can confer salt and drought resistance (Kim et al., 2014). The fact that ALA feeding in many crop plants can have a similar result is certainly intriguing (for the review see Nagahatenna et al., 2015). Although the precise

mechanism for this response is not well understood it may be related to an activation of retrograde signalling either mediated the heme pathway or perhaps via effects on ROS metabolism.

6.3.3 Heat stress impacts on $^1O_2$– dependent inhibitory retrograde signalling

It was noted in this work that many stress responsive genes were induced by the FR pre-treatment, including heat shock (HS) proteins and transcription factors. Further bioinformatics analyses with this microarray dataset confirmed a significant overlap with heat stress datasets (Figures 6.3 and 6.4). Although this overlap was not as strong for other arrays related to $^1O_2$ signalling (Figure 6.5), it is interesting to note that among 37 genes proposed by Woodson et al., (2015), as being *fc2*-specifically induced during etiolation, there were many encoding HS proteins e.g. *HSP22*, *HSP18.2*, *MBF1C*, *HSP100*. The detailed analysis of gene expression after HS and FR pre-treatment or ALA treatment (Figure 5.13 from Chapter 5, Figure 6.6) confirmed that these two responses are integrated, with HS most probably blocking production of $^1O_2$ derived from photo-excited porphyrins (Figure 6.8). On the other hand, *BAP1* was shown in this work to be induced by solely by a HS treatment, which might suggest that HS can induce $^1O_2$ production; however, this was not detected by SOSG analysis (Figure 6.8). It cannot be excluded that the HS induced small amounts of $^1O_2$, but that this could not be detected by fluorescence analysis in whole cotyledons. Perhaps these $^1O_2$ signatures were more localised and not necessarily related to the chloroplast. There is some evidence for $^1O_2$ production by heat in *C. reinhardtii* (Prasad et al., 2016).

Another possibility for an inhibition of *BAP1* expression after HS and FR or ALA treatments is the antagonistic effect of H_2O_2. This type of interaction between these two ROS species was previously revealed on the basis of a study with the *flu* mutant overexpressing thylakoid bound ascorbate peroxidase (Laloi et al., 2007). Heat stress is additionally very strongly implicated with H_2O_2 and a fast (within 15 minutes) increase in intracellular levels of H_2O_2 after heat exposure in darkness has been shown in *Arabidopsis* cell cultures (Volkov et al., 2006). Fluorescence analysis of H_2DCFDA confirmed the production of ROS, most probably H_2O_2, after the HS (Figure 6.8), but did not inhibit *BAP1* induction. Thus, antagonism between these two signalling pathways is unlikely to account for the HS effect. In fact, H_2O_2 actually increased *BAP1* expression, especially in the presence of singlet oxygen and this may account for the induction of *BAP1* after a HS. Ha et al. (2017), reported that prolonged growth of etiolated seedlings in moderate heat resulted in $^1O_2$ production and a block of greening due to disturbed POR stabilisation. This is a different situation to the one in this study as no negative effect of HS on

Pchlide and dark PORA accumulation was seen (Figure 6.14), most probably because of the difference in the duration of the heat treatments used in the two experiments. Interestingly, many mutants that show perturbed responses to heat and are affected in heat signalling or HS protein accumulation rescued $^1O_2$-dependent inhibition of photosynthetic gene expression (Figure 6.12). This could be because of the reduced capacity to accumulate Pchlide in the dark after ALA feeding and therefore singlet oxygen, which would weaken an inhibitory response. Additional Pchlide and singlet oxygen measurements for these lines need to be performed. On the other hand, *BAP1* induction was detected in all these lines indicating that $^1O_2$ signalling was induced (though see discussion above). Alternatively, it is possible that mutants in heat stress response proteins already suffer from cellular perturbation and are insensitive to $^1O_2$ stress. The rescue from ALA treatment in the autophagy mutant *atg5-1* is very interesting as there is evidence for autophagosomal-mediated turnover of whole, damaged chloroplasts to the vacuole (Izumi et al., 2017). Whether chloroplast turnover could be one of the mechanisms mediating $^1O_2$-dependent inhibitory retrograde signalling needs to be investigated in the future.

Chapter 7 Final discussion

7.1 Regulation of the plastid-to-nucleus retrograde signalling

The basic term "retrograde signalling" can be defined as the ability of chloroplasts or mitochondria to generate signals, which modulate nuclear gene expression. Decades of research attempting to explain regulation of chloroplast-to-nucleus retrograde signalling has focused on identifying gene products that are potentially key mediators of plastid signalling pathways. However, despite extensive studies, precise mechanisms underlying organellar communication are still poorly understood, and what we mostly understand is the final consequence of disturbing retrograde signals. It seems now well accepted that at least two main signalling pathways are involved in mediating plastid retrograde signalling in developing seedlings: one including tetrapyrrole biosynthesis pathway intermediates, and the second one associated with the organellar gene expression (discussed in section 1.7 and 4.1). Despite significant progress in the field, it is still not clear how exactly biogenic retrograde signals are triggered, especially under the real physiological conditions, what the mechanisms of action for retrograde signalling molecules are, and how these signals are mediated to the nucleus.

The critical role of tetrapyrrole metabolism in the control of retrograde signalling was evidenced early by the genetic screen for multiple *gun* mutants (Susek et al., 1993; Mochizuki et al., 2001), and subsequently confirmed in many further studies (e.g. Vinti et al., 2000; Strand et al., 2003; Voigt et al., 2010; Czarnecki et al., 2011, Sun et al., 2016). Despite of all these studies, different models for the role of tetrapyrroles in retrograde signalling have been suggested, but without a clear consensus. As with other metabolite-based regulation systems, biogenic retrograde signalling can be affected by negative feedback inhibition of tetrapyrrole synthesis (see section 1.6), which complicates the interpretation of experimental perturbations. Critical for defining retrograde signalling is also development of advanced methods for the precise detection of tetrapyrrole precursors. This was illustrated well by experiments that disproved an earlier retrograde signalling model, in which disturbed chloroplast development by NF was proposed to induce an inhibitory retrograde signal, wrongly assigned to Mg-proto IX accumulation (Strand et al., 2003; Mochizuki et al., 2008; Moulin et al., 2008). Undoubtedly, a major breakthrough in our understanding of biogenic retrograde signalling was demonstrating genetically that a FC1-derived heme-related signal operates as a positive signal to promote nuclear gene expression (Woodson et al., 2011). In the current work, de-repression of photosynthetic gene expression under different NF conditions was confirmed for the *gun6-1D* mutant that overexpresses *FC1* (Chapter 3, Chapter 6) supporting the requirement for a FC1-derived signal to positively regulate the

chloroplast development. Interestingly, a weak *gun* phenotype was also observed in the loss of function *fc2-1* mutant (Figure 3.3) suggesting that the substrate availability for the FC1 might be the important regulatory point. To test further how strongly these phenotypes are related to tetrapyrrole (and, more precisely, heme) metabolism it would be interesting to examine if the *fc2-1* rescue on NF could be actively modulated, and potentially enhanced by additional feeding with ALA, or by crossing the *fc2-1* mutant with *gun6-1D*, or other *FC1* overexpressor lines. It has been hypothesized that a specific FC1-derived heme pool (Woodson et al., 2011), possibly related to a very small portion of unbound free heme (Terry and Smith, 2013), could operate as a direct retrograde signal or initiate such a signal. However, precise quantification techniques for the regulatory heme measurements are missing to date, which limits further evaluation of these hypotheses. Reduced total heme levels on NF were demonstrated for WT plants, but under the same conditions heme content was not significantly higher in most *gun* mutants including the *gun6-1D* (Woodson et al. 2011; Espinas et al., 2012). Reduction of the total heme by NF treatment is not surprising due to the strong repression of the *FC2* gene (e.g. Moulin et al., 2008), and the loss of photosynthetic protein abundance (e.g. Voigt et al. 2010). Confusingly, experiments using different acetone-based extraction methods and chemiluminescence detection have repeatedly observed an increase in a free heme pool after NF treatments (Voigt et al., 2010; Espinas et al., 2012). Since classic NF experiments are performed after a few days' treatment, it is possible that the regulatory free heme signal was transient or it was subsequently metabolised and already lost at this time point and a more detailed investigation into heme metabolism is required in the future.

In the past years, a number of novel molecular factors were identified as mediating biogenic retrograde signals, such as down-stream regulators of photosynthetic gene expression including different transcription factors, light signalling components, or the recently identified PTM (discussed in Chapter 1.5, 1.7). Two were considered as the most promising candidates: PTM, which could operate as a mobile signal in the GUN1 pathway, as it undergoes proteolytic cleavage during disturbed chloroplast development with its N-terminal fragment relocating from chloroplasts to the nucleus, and ABI4, which is targeted by the PTM fragment, and was shown to inhibit *LHCB* expression by competitive binding to its promoter region (Sun et al., 2011; Zhang et al., 2013). Both were also of particular interest in this study, but despite a thorough evaluation, neither the *abi4* mutant alleles or the *ptm* mutant rescued photosynthetic gene expression on NF or Lin (Chapter 3), which contradicts earlier studies (Koussevitzky et al., 2007; Sun et al., 2011), and strongly indicates that neither play a role in plastid retrograde signalling. Additional retrograde signalling candidates for the transcriptional control of nuclear gene expression are two

critical regulators of chloroplast development, GLK1 and GLK2 (Waters et al., 2009). A number of observations are in favour of this concept. Firstly, *GLK1* and *GLK2* expression is inhibited by mutations or treatments affecting biogenic retrograde signalling such as NF and Lin (Waters et al., 2009; Leister and Kleine 2016). Secondly, the GLK1 protein was shown to bind to the promoter region of many photosynthetic and tetrapyrrole genes via the conserved CCAATC motif (Waters et al., 2009). And thirdly, both GLK constitutive overexpressor lines were shown to have a *gun* phenotype on NF and Lin (Leister and Kleine 2016). However, the double *glk1glk2* mutant has also been reported to show a weak *gun* phenotype and de-repress *CA1* and *RbcS* expression on NF (Waters et al., 2009). This might reflect the complex interaction between light and retrograde signalling and possible cross talk between anterograde and retrograde signals. The *gun* phenotype of GLKs overexpressors is not surprising, since they are down-stream transcription factors, and the photosynthetic and tetrapyrrole nuclear gene expression is already promoted in these lines under control conditions irrespective of the up-stream events (Waters et al., 2009; Leister and Kleine 2016). In a similar manner, the *pifQ* mutant has been shown to rescue nuclear gene expression on Lin in dark-grown seedlings; however, the *pifQ* mutant shows constitutive induction of light signalling, and consequently has an elevated expression of photosynthetic transcripts in darkness (Martin et al., 2016). The DP treatment strongly inhibited the elevated photosynthetic gene expression of dark-grown *pifQ*, but had a minor repressive effect in the wild type (Figure 3.6) suggesting the constitutive photomorphogenic phenotype of *pifQ* might be potentially dependent on bilin synthesis. Photosynthetic genes, which are down-stream targets for retrograde signals, have different light responsive elements in their promoter regions, and these elements serve as interaction sites for multiple transcription factors (Yu et al., 2014). It might be difficult to clearly define the relative contribution of GLKs, or light regulators, like HY5, PIFs, to different retrograde signals. With no more candidates for retrograde signalling molecules confirmed by independent examination, existing models for organellar communication are challenged. It might be speculated that biogenic retrograde signalling does not involve any master cytosolic- or nuclear-localised signalling components, as such molecular factors should have been identified earlier in genetic screens along with the original *gun* mutants (Susek et al., 1993). Other EMS screens aimed at identifying new mutants with increased nuclear gene expression during disturbed chloroplast development after NF or Lin treatment were performed by Ruckle et al. (2007), who isolated the blue light receptor mutant *cry1*, and by Sun et al. (2016), who isolated the *coe1* mutant with a mutation in Mitochondrial Transcription Termination Factor 4 (mTERF4). A series of mutants named *hon* (happy on NF) were additionally identified as rescuing greening and *LHCB* expression on a low NF concentration and under low light intensity (Saini et al., 2011). One of the *hon* mutations affected the ClpR4 protein of the Clp protease complex. Neither ABI4 nor

PTM were identified through these genetic screens. Another possibility is that the down-stream molecular events during retrograde signalling involve coordinated action of multiple mitochondrial, cytosolic and/or nuclear molecular factors. Heme-binding proteins could be potentially implicated with such a mechanism of organellar communication, however more work needs to be undertaken to test this hypothesis.

Another problem in the study of plastid biogenic signalling is that it involves severe treatments resulting in seedling photo-oxidative damage. It is then argued that additional pleiotropic effects are induced and that the observed response does not only reflect the action of the actual plastid retrograde signal (e.g. Voigt et al., 2010; Schlicke et al., 2014). However, it should be noted that, at least for NF treatment, a very high proportion of down-regulated genes that are de-repressed in *gun* mutants are photosynthesis-related and tetrapyrrole-related (Moulin et al., 2008), which could indicate some level of specificity. The DP treatment tested here (Figure 3.5) affects chloroplast function in a more direct way by inhibiting heme synthesis. Similarly to the NF response, exposure to DP resulted in a down-regulation of photosynthetic and tetrapyrrole genes, clearly supporting the hypothesis of a heme-dependent signal. We can expect that this promotive pathway can be blocked by any condition (chemical or genetic) that represses chloroplast development and this seems to be the case with inhibition of chloroplast transcription, editing and translation all reducing nuclear gene expression (see Chapter 4.1). No de-repression of *LHCB* expression on NF has been shown for a number of mutants with disturbed early enzymatic steps in the tetrapyrrole synthesis pathway upstream of Proto-IX, and some of these mutants were rather hypersensitive to the NF treatment (Voigt et al., 2010; Woodson et al., 2011), which is also in agreement with a positive heme-dependent signal. Surprisingly, mutations in plastid transcription (*sig2-2* and *sig6-1*) and plastid translation (*prpl11-1*) were shown here to promote the expression of selected nuclear genes, rather than inhibit them (Figures 3.7 and 4.1). Different researchers apply NF treatments in a very distinct ways, with different doses at different seedling developmental ages (Koussevitzky et al., 2007; Moulin et al, 2008; Woodson et al., 2011; Kim and Apel 2013). This could account perhaps for differences in the *sig2-2* and *sig6-1* phenotypes, with a general gene down-regulation in the mutants proposed by Woodson et al. (2013) and elevated expression of *HEMA1* and a *gun* phenotype on NF shown in this study (Figure 3.7). Although the hypothesis for the role of a heme-derived signal in the promotion of photosynthetic gene expression is strongly supported by the results from this work, it cannot be excluded that other mechanisms are involved in the regulation of retrograde signalling. Since FC1-derived heme is a cofactor of anti-oxidative enzymes it is possible that the *gun* phenotype of FC1ox lines is a result of enhanced tolerance to ROS imbalance. It was hypothesised that NF-

induced perturbation of tetrapyrrole synthesis may result in a localized ROS production or modification of the plastid redox state, and that could control plastid signalling (Moulin et al., 2008). However, Voigt et al. (2010) did not detect any difference in regulation of distinct ROS marker genes between WT and *gun* mutants grown on NF. Interestingly, *sig2-2* and *sig6-1* mutants grown on low NF conditions retain the ability to green, in contrast to wild type and other known *gun* mutants (Figure 3.7). The *prpl11* mutant also maintains the ability to green in low NF conditions (data not included).

An important convergence point between plastid gene expression signalling and tetrapyrrole-based signalling is represented by the plastid-transcribed $tRNA^{GLU}$, which is involved in plastid protein synthesis, but also serves as a substrate for synthesis of ALA, an initial precursor of tetrapyrrole biosynthesis (Beale et al. 1990). Loss of the *PRPL11* gene was shown in this work to promote selected expression of tetrapyrrole genes as well accumulation of the GluTR, CHLH and HO1 tetrapyrrole enzymes. It is possible that at least part of this phenotype is related to promotion of $tRNA^{GLU}$ distribution towards the tetrapyrrole synthesis pathway (or increased $tRNA^{GLU}$ availability), as a direct or indirect consequence of blocked plastid translation. However, results from Chapter 4 provide strong evidence for PRPL11 interaction with tetrapyrrole synthesis, perhaps as a possible regulator of Mg-chelatase (Table 4.1). Interestingly, only prolonged and continuous silencing of *CHLH* or *CHLM* in *Arabidopsis* green seedlings for 1 to 4 days modulated nuclear gene expression, observed as a subtle increase of *LHCB1.2*, *HEMA1*, *GUN4* and *FC1* expression (Schlicke et al., 2014). The elevated *HEMA1* and *CP12-2* expression in *prprl11-1* was also demonstrated to be time-dependent (Figure 4.5) suggesting complex mechanisms are involved in control over nuclear gene expression. Transcriptomic changes in *CHLH* and *CHLM* RNAi lines correlated with the moderate elevation of Proto-IX levels and concurrent repression of the accumulation of other chlorophyll precursors (Schlicke et al., 2014), which might suggest that a FC1-dependent signal was promoted in these lines due to increased substrate availability. Although Pchlide accumulation in dark-grown *prprl11-1* seedlings was reduced (Figure 4.9) it would be interesting to investigate the level of other chlorophyll precursors in this mutant, especially Proto-IX, during prolonged WLc exposure. Regulation of tetrapyrrole synthesis would provide an explanation for the gene expression phenotype of the *prpl11* mutant and a mechanism by which PRPL11, or the ribosome itself, can modulate nuclear gene expression. It is possible that all the major chloroplast protein complexes are able to feed information into such a signal through an interaction with the tetrapyrrole pathway, either directly or indirectly. It will be interesting to test this further.

It has been often proposed that retrograde signalling involves a combination of many different signals (e.g. Leister, 2012; Pfannschmidt, 2010). GUN1 has been described as functioning to integrate these signals (e.g. Koussevitzky et al., 2007), but the exact mechanism of GUN1 action is still not well understood. Early examinations were focused on GUN1 interaction with DNA (Koussevitzky et al., 2007), however there is increasing evidence in the literature that GUN1 might act through protein-protein interactions (Tadini et al., 2016), or as a general coordinator of protein homeostasis (Llamas et al., 2017). Based on the work in Chapter 3, it can be proposed that GUN1 might also be acting through the regulation of the tetrapyrrole-dependent retrograde signalling and that this is the basis of its rescue of organellar gene expression-dependent signalling. The *gun1* mutant was shown here to accumulate more Pchlide in the dark on ALA and *gun1* rescue of gene expression on Lin was lost after DP treatment. Combining these results with the earlier evidence that GUN1 can interact with FC1 and Mg-chelatase (Tadini et al., 2016), it can be proposed that GUN1 operates as a general repressor of tetrapyrrole biosynthesis. Since *prpl11* inhibited the capacity to accumulate Pchlide, PRPL11 may operate as a positive regulator of Mg-chelatase. Figure 7.1 shows an updated model for retrograde signalling that includes these recent conclusions as well as omitting PTM and ABI4 as major components of the pathway based on the results in Chapter 3.

If a positive tetrapyrrole signal leads to an up-regulation of the tetrapyrrole pathway, then there is a danger that the seedling will over produce tetrapyrroles, many of which are dangerous and lead to $^1O_2$ production and ultimately cell death (Meskauskiene et al., 2001, Danon et al., 2005). It was shown previously that $^1O_2$ production can also lead to down-regulation of tetrapyrrole (and other photosynthetic) genes. Here it was demonstrated that analysis of nuclear gene expression after an ALA treatment and in the *flu* and *fc2* mutants, examined in Chapter 5, are fully supportive of an $^1O_2$ - mediated inhibitory response (Figure 7.1). Lin has been shown before to partially rescue repression of gene expression after a FR pre-treatment (McCormac and Terry, 2004), and it was evidenced in this work that Lin blocks Pchlide accumulation (Figure 4.2), therefore preventing $^1O_2$ production. An additive interaction between NF and FR treatments was showed by McCormac and Terry, (2004), but rather surprisingly, these two treatments were demonstrated later to repress largely different sets of genes by microarray analysis (Page et al., 2016a). Since the $^1O_2$ – initiated signal is proposed to balance the positive - heme related pathway (Terry and Smith 2013), they might be expected to target a similar cohort of genes. The overlap between genes inhibited by NF and $^1O_2$ is higher once compared with the array data for *flu* seedlings transferred from dark to WL. Out of the 356 genes repressed in seedlings by two independent NF treatments (Moulin et al., 2008 and Woodson et al., 2011; for overlap between

arrays see Figure 6.15B), 234 genes are also repressed in *flu* seedlings transferred to WL (GSE10812). The severity of all these treatments, as well different time points for the data analysis, may account for observed inconsistencies. More work is needed to evaluate the interaction between the positive and the negative tetrapyrrole-dependent signals. The ALA treatment characterised in Chapter 5 is another strategy that can be used for this purpose.

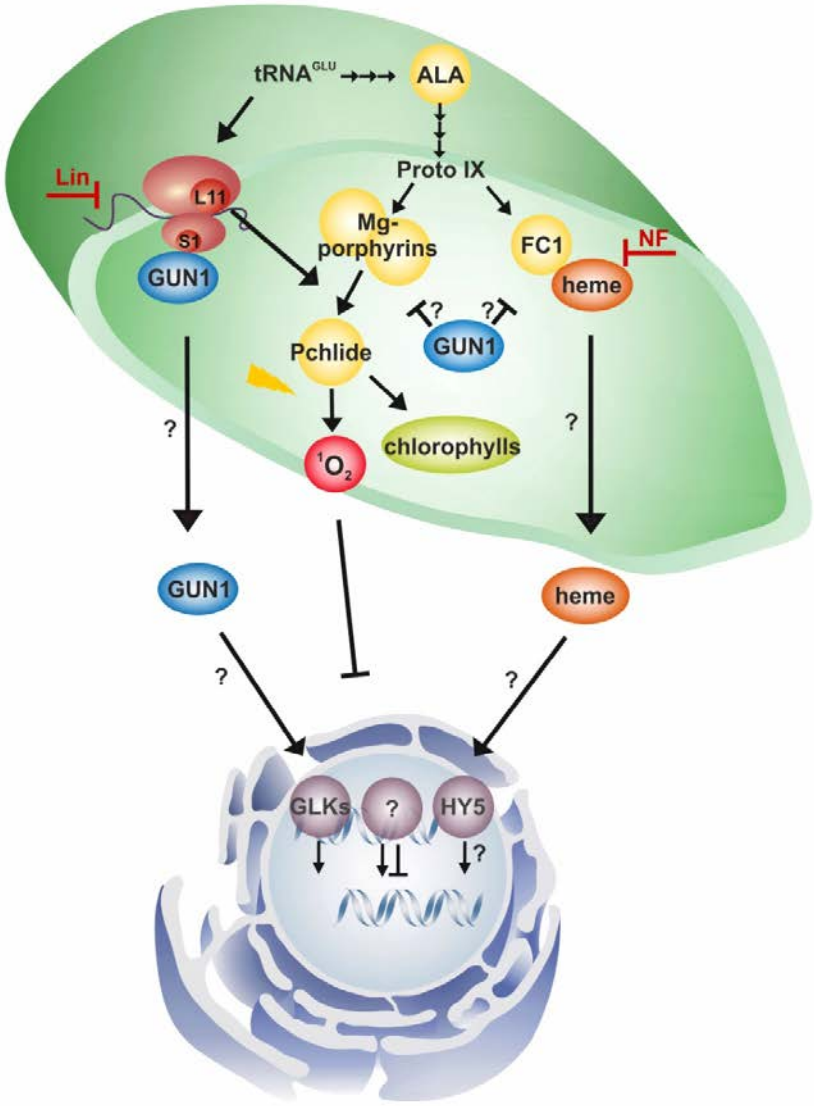

Figure 7.1 A working model for chloroplast-to-nucleus signalling during chloroplast biogenesis. In this model there are two signalling pathways proposed. A positive heme-related signal, mediated by ferrochelatase 1 (FC1) and an inhibitory light-dependent signal that is mediated by singlet oxygen ($^1O_2$). GUN1 acts a general repressor of seedling development and inhibits both positive and negative signalling pathways via an effect on FC1 and Mg-chelatase. PRPL11 (L11) promotes Mg-chelatase and controls the direction of metabolic flux through the two tetrapyrrole branches. Abbreviations: $tRNA^{Glu}$, glutamic acid transfer RNA; GUN1, GENOMES UNCOUPLED 1; ALA, 5-aminolevulinic acid; FC1, ferrochelatase 1; $^1O_2$, singlet oxygen; L11, PLASTID RIBOSOMAL PROTEIN L11; S1 PLASTID RIBOSOMAL PROTEIN S1; GLKs, Golden-like proteins; HY5, LONG HYPOCOTYL 5; NF, norflurazon; Lin, lincomycin.

7.2 Integration of plastid retrograde signalling with plant responses to abiotic stresses

The biggest challenge for plastid retrograde signalling research is the absence of a clearly defined nature of the biogenic retrograde signals and mechanisms for these signals targeting to the nucleus. This limits further investigations on how plastid retrograde signalling can be integrated with plant responses to environmental changes. In the past years, chloroplasts were proven to respond actively to environmental stresses by eliciting many signalling molecules of different chemical nature (discussed in Chapter 1.9). Despite the high importance and increasing interest in regulatory and stress acclimatory responses triggered by plant organelles, there has not been a lot of research on the role of biogenic retrograde signalling in young developing seedlings, which are also exposed to environmental stresses.

By analysing publically available transcriptomic datasets it seemed apparent that plastid retrograde signalling might be involved in drought and salt stress signalling. This was hypothesized based on a significant overlap between genes down-regulated by drought or salt and those blocked after NF treatment (Chapter 6). Analysis of selected photosynthetic and stress-responsive transcripts under both conditions were supportive for this interaction (Figure 6.16, 6.17). For example, NaCl treatment significantly rescued photosynthetic gene expression on NF or Lin in wild-type seedlings compared to treatments with the plastid signalling inhibitors alone. At the same time, the *gun* phenotype of *gun5-1* and *gun6-1D* was also enhanced by stress exposure. Based on this finding, it could be speculated that salt or drought stress can promote the heme-dependent retrograde signalling pathway, and indeed *HEMA1* expression was elevated almost 2-fold by a single NaCl treatment (Figure 6.16). Alternatively, due to a severe perturbation of plastids by abiotic stresses, more of the free regulatory heme might be released from proteins where it was bound non-covalently or even covalently. If such a signal controlled the expression of genes other than those related to photosynthesis, then it would impact on plant acclimation to drought stress. One candidate protein implicated in both stress responses and retrograde signalling is ABI4. However, the work from Chapter 3, discussed above, shows *abi4* is not a *gun* mutant. The roles of other transcriptional regulators in mediating retrograde signals is still under discussion. One overlap that is particularly intriguing is the recent suggestion that heme synthesis is important in controlling nuclear gene expression in response to drought (Nagahattena et al., 2015). In contrast to other organisms there is no evidence for direct heme regulatory activity in the nucleus in plants. Interesting candidates for future study are therefore transcription factors from the nuclear factor-Y class (NF-Y), which were shown to positively regulate plant resistance to drought stress in an ABA- independent manner (Nelson et al., 2007). These factors are known

to bind *CCAAT*-cis elements, and are also known as Heme Activator Proteins (HAP; Nardini et al., 2013).

Although there are examples in the literature of improved drought tolerance after ALA feeding, possibly via promotion of chlorophyll synthesis, photosynthetic performance and ROS detoxification (Nagahattena et al., 2015), the ALA treatment to dark-grown seedlings was designed in this work to induce a specific $^1O_2$-dependent retrograde signal (Chapter 5). While the $^1O_2$-initiated changes in gene expression after ALA treatment or FR pre-treatment were light dependent, some stresses applied in darkness, like wounding, drought or flaggelin22 treatment also induce $^1O_2$ signalling in different plant compartments including mitochondria, peroxisomes and the nucleus (Mor et al., 2014). However, the authors provided information only on the induction of gene expression. It would be interesting to test whether the inhibition of photosynthetic gene expression initiated by $^1O_2$ in the current work is also present in the dark-grown stressed plants. Lack of such an inhibitory effect could indicate that the $^1O_2$ signal related to porphyrin accumulation is controlled by a plastid specific factor. Since ROS are strongly implicated in plant responses to abiotic stresses, the impact of $^1O_2$-initiated signalling on stress signalling was particularly interesting. Based on the analysis from Chapters 5 and 6, it can be concluded that both heat signalling and $^1O_2$ signalling impact on each other in a manner that is difficult to fully explain. Heat shock in dark-grown seedlings was shown here to inhibit photosynthetic gene expression, probably independent from tetrapyrrole synthesis (Figure 5.13, 6.6, 6.13) and independent from $^1O_2$ accumulation. On the other hand, under conditions that initiate $^1O_2$ signalling, induction of stress responsive genes like *HSFA2* or *COR15A* was reduced providing further support for the partial coordination of stress responses via chloroplast functional status, in a similar manner to that observed for the salt and NF treatments (see section 6.3.2).

In summary, two main signalling pathways were proposed to control plastid-to-nucleus retrograde signalling: heme and $^1O_2$-dependent signals derived through tetrapyrrole synthesis and signals related to chloroplast gene expression. How these signals are transmitted to the nucleus is still not well understood. The current project has helped to provide new evidence to develop these existing models for retrograde signalling, with the focus on defining possible integration sites for different signalling regulators. The significance of the environmental control over plastid signals was additionally addressed in this work, which can be used in future research to improve plant resistance to abiotic stresses.

Chapter 8 References

Aarti, D., Tanaka R., Ito, H., Tanaka, A. (2007). High light inhibits chlorophyll biosynthesis at the level of 5-aminolevulinate synthesis during de-etiolation in cucumber (*Cucumis sativus*) cotyledons. Photochem. Photobiol. 83:171-176.

Abe, H., Urao, T., Ito, T., Seki, M., Shinozaki, K. and Yamaguchi-Shinozaki, K. (2003). Arabidopsis AtMYC2 (bHLH) and AtMYB2 (MYB) Function as Transcriptional Activators in Abscisic Acid Signaling. Plant Cell 15: 63-78.

Adamska, I. (1995). Regulation of early light-Inducible protein gene expression by blue and red light in etiolated seedlings involves nuclear and plastid factors. Plant Physiol. 107: 1167-1175.

Allen, J. F. (2003). Why chloroplasts and mitochondria contain genomes. Comp. Funct. Genomics. 4: 31–36.

Al-Sady, B., Ni, W., Kircher, S., Schafer, E. and Quail, P. H. (2006). Photoactivated phytochrome induces rapid PIF3 phosphorylation prior to proteasome-mediated degradation. Mol. Cell 23: 439-446.

Alban, C., Tardif, M., Mininno, M., Brugiere, S., Gilgen, A., Ma, S., et al. (2014). Uncovering the protein lysine and arginine methylation network in *Arabidopsis* chloroplasts. PLoS ONE 9: e95512.

Albertson P. (2001). A quantitative model of the domain structure of the photosynthetic membrane. Trends Plant Sci. 6: 349-358.

Alfonso, M., Perewoska, I. and Kirilovsky, D. (2000). Redox Control of psbA Gene Expression in the *Cyanobacterium Synechocystis* PCC 6803. Involvement of the Cytochrome b_6/f Complex Complex. Plant Physiol. 122: 505-516.

Allison, L. A., Simon, L. C., Maliga, P. (1996). Deletion of rpoB reveals a second distinct transcription system in plastids of higher plants. EMBO J. 15: 2802–2809.

Allison, L. A. (2000). The role of sigma factors in plastid transcription. Biochimie, 82: 537-548.

Alsheikh, M. K., Heyen, B. J. and Randall, S. K. (2003). Ion Binding Properties of the Dehydrin ERD14 Are Dependent upon Phosphorylation. Journal of Biological Chemistry 278: 40882-40889.

Aluru, MR., Zola, J., Foudree, A., Rodermel, S. R. (2009). Chloroplast photooxidation-induced transcriptome reprogramming in Arabidopsis immutans white leaf sectors. Plant Physiol. 150:904-23.

Armstrong, G. A., Runge, S., Frick, G., Sperling, U., Apel, K. (1995). Identification of NADPH:protochlorophyllide oxidoreductases A and B: a branched pathway for light-dependent chlorophyll biosynthesis in Arabidopsis thaliana. Plant Physiol.108:1505-17.

Ankele, E., Kindgren, P., Pesquet, E. and Strand, A. (2007). In vivo visualization of Mg-protoporphyrin IX, a coordinator of photosynthetic gene expression in the nucleus and the chloroplast. Plant Cell 19: 1964-1979.

Apitz, J., Schmied, J., Lehmann, M. J., Hedtke, B., Grimm B. (2014). GluTR2 complements a hema1 mutant lacking glutamyl-tRNA reductase 1, but is differently regulated at the post-translational level**.** Plant Cell Physiol. 55:645-57.

Apitz J., Nishimura K., Schmied, J., Wolf, A., Hedtke, B., van Wijk, K. J., and Grimm, B. (2016). Posttranslational Control of ALA Synthesis Includes GluTR Degradation by Clp Protease and Stabilization by GluTR-Binding Protein. Plant Physiol. 170: 2040–2051.

Beale S. (1990). Biosynthesis of the tetrapyrrole pigment precursor, δ-aminolevulinic acid, from glutamate. Plant Physiol. 93: 1273–1279.

Barah, P., Jayavelu, N. D., Rasmussen, S., Nielsen, H. B., Mundy, J., Bones, A. M. (2013). Genome-scale cold stress response regulatory networks in ten *Arabidopsis thaliana* ecotypes. BMC Genomics 14: 1-16.

Barajas-Lopez Jde, D., Kremnev, D., Shaikhali, J., Pinas-Fernandez, A. and Strand, A. (2013). PAPP5 is involved in the tetrapyrrole mediated plastid signalling during chloroplast development. PLoS One 8: e60305.

Barbrook, A. C., Howe, C. J. and Purton, S. (2006). Why are plastid genomes retained in non-photosynthetic organisms? Trends Plant Sci. 11: 101-108.

Barkan, A. (1988). Proteins encoded by a complex chloroplast transcription unit are each translated from both monocistronic and polycistronic mRNAs. EMBO J. 7: 2637-2644.

Barkan, A. (1989). Tissue-dependent plastid RNA splicing in maize: transcripts from four plastid genes are predominantly unspliced in leaf meristems and roots. Plant Cell1: 437-445.

Barnes, S. A., Nishizawa, N. K., Quaggio, R. B., Whitelam, G. C. and H., C. N. (1996). Far-Red Light Blocb Greening of Arabidopsis a Phytochmme A-Mediated Change in Plastid Seedlings via Development. Plant Cell 8: 601-615.

Bradbeer, J. W., Atkinson, Y. E., Börner, T. and Hagemann, R. (1979). Cytoplasmic synthesis of plastid polypeptides may be controlled by plastid-synthesised RNA. Nature 279: 816-817.

Cahoon, A. B., Harris, F. M. and Stern, D. B. (2005). Analysis of developing maize plastids reveals two mRNA stability classes correlating with RNA polymerase type. EMBO Rep. 5: 801–806.

Cao, Z., Huang, B., Wang, Q., Xuan, W., Ling, T., Zhang, B., et al. (2007). Involvement of carbon monoxide produced by heme oxygenase in ABA-induced stomatal closure in Vicia faba and its proposed signal transduction pathway. Chin. Sci. Bull. 52: 2365–2373.

Chan, K. X., Phua, S. Y., Crisp, P., McQuinn, R., Pogson B. J. (2016). Learning the Languages of the Chloroplast: Retrograde Signaling and Beyond. Annu. Rev. Plant Biol. 67: 25-53.

Chang, C. C., Sheen, J., Niwa, Y., Lerbs-Mache, S., Stern, D. B. (1999). Functional analysis of two maize cDNAs encoding T7-like RNA polymerases. Plant Cell 11: 911–926.

Chang, C. C., Ball, L., Fryer, M. J., Baker, N. R., Karpinski, S. and Mullineaux, P. M. (2004). Induction of ASCORBATE PEROXIDASE 2 expression in wounded Arabidopsis leaves does not

involve known wound-signalling pathways but is associated with changes in photosynthesis. Plant J. 38: 499-511.

Chuartzman, S. G., Nevo, R., Shimoni, E., Charuvi, D., Kiss V., Ohad, I., Brumfeld, V., Reich Z. (2008). Thylakoid membrane remodeling during state transitions in *Arabidopsis*. Plant Cell 20: 1029–1039.

Chinnusamy, V., Ohta, M., Kanrar, S., Lee, B. H., Hong, X., Agarwal, M., Zhu, J. K. (2003). ICE1: a regulator of cold-induced transcriptome and freezing tolerance in *Arabidopsis*. Genes Dev. 17: 1043-54.

Chinnusamy, V., Schumaker, K., and Zhu, J. K. (2004). Molecular genetic perspectives on cross-talk and specificity in abiotic stress signalling in plants. J. Exp. Bot. 55: 225–236.

Chinnusamy, V., Zhu, J. K. and Sunkar, R. (2010). Gene regulation during cold stress acclimation in plants. Methods Mol. Biol. 639: 39-55.

Chow, K. S., Singh, D. P., Walker, A. R., Smith, A. G. (1998). Two different genes encode ferrochelatase in Arabidopsis: mapping, expression and subcellular targeting of the precursor proteins. Plant J. 15:531-41.

Chua, NH., Blobel, G., Siekevitz, P. (1973). Isolation of cytoplasmic and chloroplast ribosomes and their dissociation into active subunits from *Chlamydomonas reinhardtii*. J. Cell Biol. 57: 798-814.

Chung, J. S., Zhu, J. K., Bressan, R. A., Hasegawa, P. M. and Shi, H. (2008). Reactive oxygen species mediate Na+-induced SOS1 mRNA stability in Arabidopsis. Plant J. 53: 554-565.

Cline, K., Henry, R. (1996). Import and routing of nucleus-encoded chloroplast proteins. Annu Rev. Cell. Dev. Biol. 12: 1-26.

Colletti, K. S., Tattersall, E. A., Pyke, K. A., Froelich, J. E., Stokes, K. D., Osteryoung, K. W. (2000). A homologue of the bacterial cell division site-determining factor MinD mediates placement of the chloroplast division apparatus. Curr Biol. 10: 507-516.

Cornah, J. E., Terry, M. J., Smith, A. G. (2003). Green or red: what stops the traffic in the tetrapyrrole pathway? Trends Plant Sci. 8:224-30.

Cottage, A., Mott, E. K., Kempster, J. A., Gray, J. C. (2010) The *Arabidopsis* plastid-signalling mutant *gun1* (genomes uncoupled1) shows altered sensitivity to sucrose and abscisic acid and alterations in early seedling development.J. Exp. Bot. 61: 3773-3786.

Cottage, A. and Gray, J. C. (2011). Timing the switch to phototrophic growth. Plant Signal.Behav. 6: 578–582.

Czarnecki, O., Hedtke, B., Melzer, M., Rothbart M., Richter, A., Schroter, Y., Pfannschmidt T., Grimm B. (2011). An *Arabidopsis* GluTRbinding protein mediates spatial separation of 5-aminolevulinic acid synthesis in chloroplasts. Plant Cell 23: 4476-4491.

Czarnecki, O., Gläßer, C., Chen, J.-G., Mayer, K. F. X. and Grimm, B. (2012). Evidence for a Contribution of ALA Synthesis to Plastid-To-Nucleus Signaling. Front Plant Sci. 3:1-19.

Danon, A., Miersch, O., Felix, G., Camp, R. G. and Apel, K. (2005). Concurrent activation of cell death-regulating signaling pathways by singlet oxygen in *Arabidopsis thaliana*. Plant J. 41: 68-80.

de Longevialle, A. F., Small, I. D., Lurin, C. (2010). Nuclearly encoded splicing factors implicated in RNA splicing in higher plant organelles. Mol Plant 3: 691–705.

Deshpande, N. N., Bao Y., Herrin, D. L. (1997). Evidence for light/redox-regulated splicing of psbA pre-RNAs in Chlamydomonas chloroplasts. RNA 3: 37-48.

Dos Santos, P. C., Smith, A. D., Frazzon, J., Cash, V. L., Johnson, M. K., Dean, D. R. (2004). Iron-sulfur cluster assembly: NifU-directed activation of the nitrogenase Fe protein.J. Biol. Chem. 279: 19705-11.

Duggan, J., Gassman, M. (1974). Induction of porphyrin synthesis in etiolated bean leaves by chelators of iron. Plant Physiol.53: 206-15.

Edwards, K., and Kössel, H. (1981). The rRNA operon from *Zea mays* chloroplasts*:* nucleotide sequence of *23S* rDNA and its homology with *E*. *coli* 23S rDNA. Nucleic Acids Res. 9: 2853-69.

Edwards, K., Bedbrook, J., Dyer, T. and Kossel, H. (1981). 4.5S rRNA from *Zea Mays* chloroplasts shows structural homology with the 3'end of prokaryotic 23S rRNA. Biochem. Int. 2: 533–538.

Ellis, R. J. (1970). Further similarities between chloroplast and bacterial ribosomes. Planta 91: 329—335.

Escoubas, J. M., Lomas, M., LaRoche, J. and Falkowski, P. G. (1995). Light intensity regulation of cab gene transcription is signaled by the redox state of the plastoquinone pool. Proc. Natl. Acad. Sci. USA 92: 10237–10241.

Estavillo, G. M., Chan, K. X., Phua, S. Y. and Pogson, B. J. (2013). Reconsidering the nature and mode of action of metabolite retrograde signals from the chloroplast. Front Plant Sci. 3: 1-9.

Estavillo, G. M., Crisp, P. A., Pornsiriwong, W., Wirtz, M., Collinge, D., Carrie, C., Giraud, E., Whelan, J., David, P., Javot, H., Brearley, C., Hell. R., Marin, E., Pogson, B. J. (2011). Evidence for a SAL1-PAP chloroplast retrograde pathway that functions in drought and high light signaling in Arabidopsis. Plant Cell 23: 3992-4012.

Favory, J. J., Kobayshi, M., Tanaka, K., Peltier, G., Kreis, M., Valay, J. G., Lerbs-Mache, S. (2005). Specific function of a plastid sigma factor for ndhF gene transcription. Nucleic Acids Research 33: 5991-5999.

Fernandez, E., Bilgin, M. D., Grossweiner, L. I. (1997) Singlet oxygen generation by hotodynamic agents. Photochem. Photobiol. B. Biol. 37:131-140.

Fey, V., Wagner, R., Brautigam, K., Wirtz, M., Hell, R., Dietzmann, A., Leister D., Oelmüller R., Pfannschmidt, T. (2005). Retrograde plastid redox signals in the expression of nuclear genes for chloroplast proteins of *Arabidopsis thaliana*. J. Biol. Chem. 280: 5318-5328.

Fischer, B. B., Krieger-Liszkay, A., Hideg, E., Snyrychova, I., Wiesendanger, M. and Eggen, R. I. (2007). Role of singlet oxygen in chloroplast to nucleus retrograde signaling in Chlamydomonas reinhardtii. FEBS Lett. 581: 5555-5560.

Forreiter, C., Apel K. (1993). Light-independent and light-dependent protochlorophyllide-reducing activities and two distinct NADPH-protochlorophyllide oxidoreductase polypeptides in mountain pine (*Pinus mugo*). Planta 190: 536-45.

Foyer, C. H., Noctor, G. (2005). Redox homeostasis and antioxidant signaling: a metabolic interface between stress perception and physiological responses. Plant Cell.17:1866-75.

Franklin, K. A., Linley, P. J., Montgomery, B. L., Lagarias, J. C., Thomas, B., Jackson, S. D., Terry M. J. (2003). Misregulation of tetrapyrrole biosynthesis in transgenic tobacco seedlings expressing mammalian biliverdin reductase. Plant J. 35:717-28.

Franklin, K. A., Larner, V. S., Whitelam, G. C. (2005). The signal transducing photoreceptors of plants. Int J Dev Biol. 49: 653-664.

Fuentes, I., Karcher, D. and Bock, R. (2012). Experimental reconstruction of the functional transfer of intron-containing plastid genes to the nucleus. Curr. Biol. 22: 763-771.

Gadjev, I., Vanderauwera, S., Gechev, T. S., Laloi, C., Minkov, I. N., Shulaev, V., Apel ,K., Inzé, D., Mittler, R., Van Breusegem, F. (2006). Transcriptomic footprints disclose specificity of reactive oxygen species signaling in *Arabidopsis.* Plant Physiol. 141: 436-445.

Galvez-Valdivieso, G., Mullineaux, P.M. (2010). The role of reactive oxygen species in signalling from chloroplasts to the nucleus. Physiol . Plant. 138: 430-9.

Gerace E. and Moazed D. (2015). Affinity Pull-Down of Proteins Using Anti-FLAG M2 Agarose Beads. Methods Enzymol.559: 99-110.

Geisler, M., Kleczkowski, L. A., Karpinski S. (2006). A universal algorithm for genome-wide in silicio identification of biologically significant gene promoter putative cis-regulatory-elements; identification of new elements for reactive oxygen species and sucrose signaling in *Arabidopsis*. Plant J. 45: 384–398.

Gilmour, S. J., Fowler, S. G. and Thomashow, M. F. (2004). Arabidopsis transcriptional activators CBF1, CBF2, and CBF3 have matching functional activities. Plant Mol.Biol. 54: 767-781.

Giraud, E., Van Aken, O., Ho, L. H., Whelan, J. (2009). The transcription factor ABI4 is a regulator of mitochondrial retrograde expression of ALTERNATIVE OXIDASE1a.Plant Physiol. 150: 1286-1296.

Goslings, D., Meskauskiene, R., Kim, C., Lee, K. P., Nater, M. and Apel, K. (2004). Concurrent interactions of heme and FLU with Glu tRNA reductase (HEMA1), the target of metabolic feedback inhibition of tetrapyrrole biosynthesis, in dark- and light-grown *Arabidopsis* plants. Plant J. 40: 957-967.

Graf, M., Arenz, S., Huter, P., Dönhöfer, A., Novácek, J., Wilson, D. N. (2017). Cryo-EM structure of the spinach chloroplast ribosome reveals the location of plastid-specific ribosomal proteins and extensions. Nucleic Acids Res. 45: 2887-2896.

Gray, J. C., Sullivan, J. A., Wang, J. H., Jerome, C. A. and MacLean, D. (2003). Coordination of plastid and nuclear gene expression. Philos. Trans. R. Soc. Lond.B Bio. Sci. 358: 135-144.

Griffiths, W. T. (1991) Protochlorophyllide photoreductionIn H Scheer, ed, Chlorophylls. CRC Press, Boca Raton, FL: 433–449.

Guillaumot, D., Guillon, S., Déplanque, T., Vanhee, C., Gumy, C., Masquelier, D., Morsomme, P., Batoko, H. (2009). The *Arabidopsis* TSPO-related protein is a stress and abscisic acid-regulated, endoplasmic reticulum-Golgi-localized membrane protein. Plant J. 60: 242–256.

Guo, H, Feng, P., Chi, W., Sun, X., Xu, X., Li, Y., Ren, D., Lu, C., David Rochaix, J., Leister, D., Zhang, L. (2016). Plastid-nucleus communication involves calcium-modulated MAPK signaling. Nature Communications. 7: 12173

Guisinger, M. M., Kuehl, J. V., Boore, J. L., Jansen, R. K. (2011). Extreme reconfiguration of plastid genomes in the angiosperm family Geraniaceae: rearrangements, repeats, and codon usage. Mol Biol Evol. 28: 583-600.

Ha, J. H., Lee, H. J., Jung, J. H., Park, C. M. (2017). Thermo-Induced Maintenance of Photo-oxidoreductases Underlies Plant Autotrophic Development. Dev Cell. 41:170-179.

Haake, V., Cook, D., Riechmann, J. L., Pineda, O., Thomashow, M. F. and Zhang, J. Z. (2002). Transcription factor CBF4 is a regulator of drought adaptation in *Arabidopsis*. Plant Physiol. 130: 639-648.

Haitao Zhang, H., Li, J., Yoo, J., Yoo, S., Cho, S., Koh, H., Seo, H., Paek, N. (2006). Rice Chlorina-1 and Chlorina-9 encode ChlD and ChlI subunits of Mg-chelatase, a key enzyme for chlorophyll synthesis and chloroplast development. Plant Mol. Biol. 62: 325–337.

Hajdukiewicz, P. T., Allison, L. A., Maliga, P. (1997). The two RNA polymerases encoded by the nuclear and the plastid compartments transcribe distinct groups of genes in tobacco plastids. EMBO J. 16: 4041-4048.

Hanaoka, M., Kanamaru, K., Fujiwara, M., Takahashi, H. and Tanaka, K. (2005). GlutamyltRNA mediates a switch in RNA polymerase use during chloroplast biogenesis. Embo Reports 6: 545-550.

Harb, A., Krishnan, A., Ambavaram, M. M. and Pereira, A. (2010). Molecular and physiological analysis of drought stress in *Arabidopsis* reveals early responses leading to acclimation in plant growth. Plant Physiol. 154: 1254-1271.

Hedtke, B., Borner, T., and Weihe, A. (2000). One RNA polymerase serving two genomes. Embo Reports 1: 435-440.

Heins, L., Mehrle, A., Hemmler, R., Wagner, R., Küchler, M., Hörmann, F., Sveshnikov, D. and Soll, J. (2002). The preprotein conducting channel at the inner envelope membrane of plastids. EMBO J. 21: 2616–2625.

Hiltbrunner, A., Bauer, J., Vidi, P. A., Infanger, S., Weibel, P., Hohwy, M., Kessler, F. (2001b). Targeting of an abundant cytosolic form of the protein import receptor at Toc159 to the outer chloroplast membrane. J. Cell Biol. 154: 309–316.

Hinnah, S. C., Wagner, R., Sveshnikova, N., Harrer, R., Soll, J. (2002). The chloroplast protein import channel Toc75: pore properties and interaction with transit peptides. Biophys J. 83: 899-911.

Hoecker, U., Tepperman, J. M., Quail, P. H. (1999). SPA1: A WD-repeat protein specific to phytochrome A signal transduction. Science 284: 496-499.

Horlitz, M. and Klaff, P. (2000). Gene-specific trans regulatory functions of magnesium for chloroplast mRNA stability in higher plants. J. Biol. Chem. 275: 35638-35645.

Hricova, A., Quesada, V., Micol, J. L. (2006). The SCABRA3 nuclear gene encodes the plastid RpoTp RNA polymerase, which is required for chloroplast biogenesis and mesophyll cell proliferation in Arabidopsis. Plant Physiol. 141: 942-956.

Hu, J., Bogorad L. (1990). Maize chloroplast RNA polymerase: the 180-, 120-, and 38-kilodalton polypeptides are encoded in chloroplast genes. Proc. Natl. Acad. Sci. USA. 87: 1531-1535.

Hu, X., Page, M., Sumida, A., Tanaka, A., Terry, M., Tanaka R. (2017). The iron–sulfur cluster biosynthesis protein SUFB is required for chlorophyll synthesis, but not phytochrome signalling. Plant J. 89: 1184-1194.

Huq, E., Al-Sady, B., Hudson, M., Kim, C., Apel, K. and Quail, P. H. (2004). Phytochrome-interacting factor 1 is a critical bHLH regulator of chlorophyll biosynthesis. Science 305: 1937.

Ikeda, T. M., Gray, M. W. (1999). Characterization of a DNA-binding protein implicated in transcription in wheat mitochondria. Mol. Cell Biol. 19: 8113-8122.

Ilag, L. L., Kumar, A. M., Soll, D. (1994). Light regulation of chlorophyll biosynthesis at the level of 5-aminolevulinate formation in *Arabidopsis*. Plant Cell 6:265–75.

Ishizaki, Y., Tsunoyama, Y., Hatano, K., Ando, K., Kato, K., Shinmyo, A., Kobori, M., Takeba, G., Nakahira, Y., and Shiina, T. (2005). A nuclear-encoded sigma factor, *Arabidopsis* SIG6, recognizes sigma-70 type chloroplast promoters and regulates early chloroplast development in cotyledons. Plant J. 42: 133-144.

Itoh, R., Fujiwara, M., Nagata, N., Yoshida, S. (2001). A chloroplast protein homologous to the eubacterial topological specificity factor minE plays a role in chloroplast division. Plant Physiol. 127: 1644-1655.

Ivey, R. A. Subramanian, C., Bruce, B. D. (2000). Identification of a Hsp70 recognition domain within the rubisco small subunit transit peptide. Plant Physiol. 122: 1289-1299.

Izumi, M., Ishida, H., Nakamura, S., Hidema J. (2017). Entire Photodamaged Chloroplasts Are Transported to the Central Vacuole by Autophagy. Plant Cell 28:1-43.

Jackson, D. T., Froehlich, J. E. and Keegstra, K. (1998). The hydrophilic domain of Tic110, an inner envelope membrane component of the chloroplastic protein translocation apparatus, faces the stromal compartment. J. Biol. Chem. 273: 16583–16588.

Janská, A., Marsik, P., Zelenkova, S. and Ovesna, J. (2010). Cold stress and acclimation - what is important for metabolic adjustment? Plant Biol. 12: 395-405.

Jarvis, P. and Robinson, C. (2004). Mechanisms of protein import and routing in chloroplasts. Curr. Biol. 14: 1064–1077.

Jensen, P.E., Gibson, L. C. and Hunter, C.N. (1999). ATPase activity associated with the magnesium-protoporphyrin IX chelatase enzyme of *Synechocystis* PCC6803: Evidence for ATP hydrolysis during Mg2+ insertion, and the MgATP-dependent interaction of the ChlI and ChlD subunits. Biochem. J. 339: 127–134.

Jensen, P. E., Reid, J. D., Hunter, C. N. 2000. Modification of cysteine residues in the ChlI andChlH subunits of magnesium chelatase results in enzyme inactivation. Biochem. J. 352:435–441.

Jeong, J., Kim, K., Kim, M.E., Kim, H.G., Heo, G.S., Park, O.K., Park, Y.I., Choi, G., and Oh, E. (2016). Phytochrome and ethylene signaling integration in *Arabidopsis* occurs via the transcriptional regulation of genes co-targeted by PIFs and EIN3.Front. Plant Sci. 7: 1055.

Jiang, Y., Liang ,G., Yu, D. (2012). Activated expression of WRKY57 confers drought tolerance in *Arabidopsis*. Mol. Plant 5: 1375-1388.

Johanningmeier, U. and Howell, S. H. (1984). Regulation of light-harvesting chlorophyll-binding protein mRNA accumulation in *Chlamydomonas reinhardi*.Possible involvement of chlorophyll synthesis precursors. J. Biol. Chem. 259: 13541-13549.

Josse E. M., Halliday K. J. (2008). Skotomorphogenesis: the dark side of light signalling. Curr Biol. 18:R1144-6.

Jung, H. S. and Chory, J. (2010). Signaling between chloroplasts and the nucleus: can a systems biology approach bring clarity to a complex and highly regulated pathway? Plant Physiol. 152: 453-459.

Jung, JH., Domijan, M., Klose, C., Biswas, S., Ezer, D., Gao, M., Khattak, A. K., Box, M.S., Charoensawan, V., Cortijo, S., Kumar, M., Grant, A., Locke, J.C. Schäfer,E., Jaeger, K. E., Wigge P. A. (2016). Phytochromes function as thermosensors in *Arabidopsis*. Science. 354:886-889.

Kahlau, S., and Bock, R. (2008). Plastid transcriptomics and translatomics of tomato fruit development and chloroplast-to-chromoplast differentiation*:* chromoplast gene expression largely serves the production of a single protein*.* Plant Cell. 20: 856-74.

Kakizaki, T., Matsumura, H., Nakayama, K., Che, F. S., Terauchi, R., Inaba, T. (2009). Coordination of plastid protein import and nuclear gene expression by plastid-to-nucleus retrograde signaling. Plant Physiol. 151 1339–1353.

Kakizaki, T., Yazu, F., Nakayama, K., Ito-Inaba, Y., Inaba, T. (2012). Plastid signalling under multiple conditions is accompanied by a common defect in RNA editing in plastids. J. Exp. Bot. 63:251-60.

Kanamaru, K., Nagashima, A., Fujiwara, M., Shimada, H., Shirano, Y., Nakabayashi, K., Shibata, D., Tanaka, K. and Takahashi, H. (2001). An *Arabidopsis* Sigma Factor (SIG2)-Dependent Expression of Plastid-Encoded tRNAs in Chloroplasts. Plant Cell Physiol. 42: 1034-1043.

Karpinski, S., Reynolds, H., Karpinska, B., Wingsle, G., Creissen, G. and Mullineaux, P. (1999). Systemic signaling and acclimation in response to excess excitation energy in Arabidopsis. Science 284: 654-657.

Karpiński, S., Szechyńska-Hebda, M., Wituszyńska, W., Burdiak, P. (2013). Light acclimation, retrograde signalling, cell death and immune defences in plants. Plant Cell Environ. 36:736-44.

Kennedy, J. C., Pottier, R. H. (1992). Endogenous protoporphyrin IX, a clinically useful photosensitizer for photodynamic therapy.J. Photochem.Photobiol. B. 14:275-92.

Kessler, F., Blobel, G., Patel, H. A., Schnell D. J. (1994). Identification of two GTP-binding proteins in the chloroplast protein import machinery. Science 266: 1035–1039.

Kim, C. and Apel, K. (2013).$^1O_2$-mediated and EXECUTER-dependent retrograde plastid-to-nucleus signaling in norflurazon-treated seedlings of *Arabidopsis thaliana*. Mol. Plant 6: 1580-1591.

Kim, C., Lee, K. P., Baruah, A., Nater, M., Gobel, C., Feussner, I. and Apel, K. (2009). $^1O_2$-mediated retrograde signaling during late embryogenesis predetermines plastid differentiation in seedlings by recruiting abscisic acid. Proc. Natl. Acad. Sci. USA 106: 9920-9924.

Kim, J.-G., Back, K., Lee, H.Y., Lee, H.-J., Phung, T.-H., Grimm, B. and Jung, S. (2014) Increased expression of Fe-chelatase leads to increased metabolic fluxinto heme and confers protection against photodynamically inducedoxidative stress. Plant Mol. Biol. 86, 271–287.

Kimel, S., Tromberg, B.J., Roberts, W.G., Berns, M.W. (1989). Singlet oxygen generation of porphyrins, chlorins, and phthalocyanines. Photochem Photobiol. 50:175-83.

Kimura M., Yamamoto Y.Y., Seki M., Sakurai T., Sato M., Abe T., Yoshida S., Manabe K., Shinozaki K., Matsui M. (2003). Identification of *Arabidopsis* genes regulated by high light-stress using cDNA microarray. Photochem. Photobio. 77: 226-33.

Kindgren, P., Norén, L, López Jde, D., Shaikhali, J., Strand, A. (2012). Interplay between Heat Shock Protein 90 and HY5 controls PhANG expression in response to the GUN5 plastid signal. Mol. Plant 5: 901-913.

Kerchev, P.I., Pellny, T.K., Vivancos, P.D., Kiddle G., Hedden, P., Driscoll, S., Vanacker, H., Verrier, P., Hancock, R.D. and Foyer, C.H. (2011). The transcription factor ABI4 Is required for the ascorbic acid-dependent regulation of growth and regulation of jasmonate-dependent defence signaling pathways in *Arabidopsis.* Plant Cell 23: 3319-3334.

Kourtz, L., Ko, K. (1997). The early stage of chloroplast protein import involves Com70. J Biol Chem. 272: 2808-2813.

Koussevitzky, S., Nott, A., Mockler, T. C., Hong, F., Sachetto-Martins, G., Surpin, M., Lim, J., Mittler, R., Chory, J. (2007). Signals from chloroplasts converge to regulate nuclear gene expression. Science 316: 715-719.

Kumar, A., M., Csankovszki, G., Soll, D. 1996. A second and differentially expressed glutamyltRN reductase gene from *Arabidopsis thaliana*. Plant Mol. Biol. 30: 419–26.

Kusumi, K., Yara, A., Mitsui, N., Tozawa, Y., Iba, K. (2004). Characterization of a rice nuclear-encoded plastid RNA polymerase gene OsRpoTp. Plant Cell Physiol. 45: 1194–1201.

Kwak, K., J., Kim, Y., O., Kang, H. (2005). Characterization of transgenic *Arabidopsis* plants overexpressing GR-RBP4 under high salinity, dehydration, or cold stress J. Exp. Bot. 56: 3007-3016.

Kwok, E. Y. and Hanson, M. R. (2004). Plastids and stromules interact with the nucleus and cell membrane in vascular plants. Plant Cell Rep. 23: 188-195.

Laby, R. J., Kincaid, M. S., Kim, D., Gibson, S. I. (2000). The Arabidopsis sugar-insensitive mutants sis4 and sis5 are defective in abscisic acid synthesis and response. Plant J. 23:587-96.

Leister, D., Kleine T. (2016). Definition of a core module for the nuclear retrograde response to altered organellar gene expression identifies GLK overexpressors as gun mutants. Physiol. Plant. 157: 297-309.

Laloi, C., Stachowiak, M., Pers-Kamczyc, E., Warzych, E., Murgia, I., Apel, K. (2007). Cross-talk between singlet oxygen- and hydrogen peroxide-dependent signaling of stress responses in *Arabidopsis thaliana*. Proc. Natl. Acad. Sci. USA 104: 672-677.

Larkin, R. M., Alonso, J. M., Ecker, J. R. and Chory, J. (2003). GUN4, a regulator of chlorophyll synthesis and intracellular signaling. Science 299: 902-906.

Larkin, R. M. and Ruckle, M. E. (2008). Integration of light and plastid signals. Curr.Opin. Plant Biol. 11: 593–599.

Lee B. H., Henderson D. A., Zhu J. K. 2005. The *Arabidopsis* cold-responsive transcriptome and its regulation by ICE1.Plant Cell 17: 3155-75.

Lee, J., He, K., Stolc, V., Lee, H., Figueroa, P., Gao, Y., Tongprasit, W., Zhao, H., Lee, I., Deng, X. W. (2007). Analysis of transcription factor HY5 genomic binding sites revealed its hierarchical role in light regulation of development. Plant Cell 19: 731-749.

Leister, D. (2012). Retrograde signaling in plants: from simple to complex scenarios. Front. Plant. Sci. 3: 135.

Leivar, P., Tepperman, J.M., Monte, E., Calderon, R. H., Liu, T. L., Quail, P. H. (2009). Definition of early transcriptional circuitry involved in light-induced reversal of PIF-imposed repression of photomorphogenesis in young *Arabidopsis* seedlings. Plant Cell21:3535-53.

Lerbs-Mache, S. (1993). The 110-KDa polypeptide of spinach plastid DNA-dependent RNApolymerase - single-subunit enzyme or catalytic core of multimeric enzyme complexes. Proc. Natl. Acad. Sci. USA 90: 5509-5513.

Leustek, T., Smith, M., Murillo, M., Singh, D. P. Smith, A. G., (1997). Siroheme biosynthesisin higher plants. Analysis of an S-adenosyl-L-methionine-dependent uroporphyrinogenIII methyltransferase from *Arabidopsis thaliana*. J. Biol. Chem. 272: 2744–52.

Li, J., Wang, Y., Chai, J. Wang, L., Wang, C., Long, W., Wang, D. Zheng M. (2013). Green-revertible Chlorina 1 (grc1) is required for the biosynthesis of chlorophyll and the early development of chloroplasts in rice. Journal of Plant Biology. 56: 326–335.

Li, Q., Zhu, F. Y., Gao, X., Sun, Y., Li, S., Tao, Y., Lo, C., Liu, H. (2014). Young Leaf Chlorosis 2 encodes the stroma-localized heme oxygenase 2 which is required for normal tetrapyrrole biosynthesis in rice. Planta. 240:701-12.

Lichtenthaler H. K. (1987). Chlorophylls and carotenoids, the pigments of photosynthetic biomembranes. Methods in Enzymology: 148: 350-382.

Liere, K., Maliga, P. (1999). In vitro characterization of the tobacco *rpoB* promoter reveals a core sequence motif conserved between phage-type plastid and plant mitochondrial promoters. EMBO J. 18: 249-57.

Lindoy L. F. and Livingstone S. E. (1967). Complexes of iron(II), cobalt(II) and nickel(II) with α-diimines and related bidentate ligands. Coordination Chemistry Reviews. 173-193.

Liu, Y., Zhang, C., Chen, J., Guo, L., L,i X., Li, W., Yu, Z., Deng, J., Zhang, P., Zhang, K., Zhang, L. (2013). *Arabidopsis* heat shock factor *HsfA1a* directly senses heat stress, pH changes, and hydrogen peroxide via the engagement of redox state. Plant Physiol. Biochem. 64: 92-98.

Liu, D., Li W., Cheng, J., Hou L. (2014). Expression analysis and functional characterization of a cold-responsive gene *COR15A* from *Arabidopsis thaliana*. Acta Phys. Plant. 36: 2421-2432.

Lübeck J., Soll, J., Akita, M., Nielsen, E. and Keegstra, K. (1996). Topology of IEP110, a component of the chloroplastic protein import machinery present in the inner envelope membrane. EMBO J. 15: 4230–4238.

Lv F., Zhou J., Zeng L., Xing D. (2015). β-cyclocitral upregulates salicylic acid signalling to enhance excess light acclimation in *Arabidopsis*.J. Exp. Bot. 66: 4719-32.

Ma, L., Li, J., Qu, L., Hager, J., Chen, Z., Zhao, H. and Deng, X. W. (2001). Light Control of Arabidopsis Development Entails Coordinated Regulation of Genome Expression and Cellular Pathways. Plant Cell 13: 2589–2607.

Ma, L., Zhao, H., Deng, X. W. (2003). Analysis of the mutational effects of the COP/DET/FUS loci on genome expression profiles reveals their overlapping yet not identical roles in regulating *Arabidopsis* seedling development. Development 130: 969-981.

Manuell, A. L., Quispe, J., and Mayfield, S. P. (2007). Structure of the chloroplast ribosome: novel domains for translation regulation. PLoS Biol. 5: e209.

Marri, L., Zaffagnini, M., Collin, V., Issakidis-Bourguet, E., Lemaire, S.D., Pupillo, P., Sparla, F., Miginiac-Maslow, M. and Trost, P. (2009). Prompt andeasy activation by specific thioredoxins of calvin cycle enzymes of *Arabidopsis thaliana* associated in the GAPDH/CP12/PRK supramolecularcomplex. Mol. Plant 2: 259–269.

Martin, W. (2003). Gene transfer from organelles to the nucleus: frequent and in big chunks. Proc. Natl. Acad. Sci. USA 100: 8612-8614.

Martin, T., Sharma, R., Sippel, C., Waegemann, K., Soll J., Vothknecht, U. C. (2006). A protein kinase family in A*rabidopsis* phosphorylates chloroplast precursor proteins. J Biol Chem 281: 40216–40223.

Martin, G., Leivar, P., Ludevid, D, Tepperman, J. M., Quail, P. H., Monte E. (2016). Phytochrome and retrograde signalling pathways converge to antagonistically regulate a light-induced transcriptional network. Nat. Commun. 7: 11431.

Maruta, T., Noshi, M., Tanouchi, A., Tamoi, M., Yabuta, Y., Yoshimura, K., Ishikawa, T., Shigeoka, S. (2012). H_2O_2-triggered Retrograde Signaling from Chloroplasts to Nucleus Plays Specific Role in Response to Stress. Journal of Biological Chemistry 287: 11717-11729.

Masood, M. S., Nishikawa, T., Fukuoka, S., Njenga, P. K., Tsudzuki, T. and Kadowaki, K. (2004). The complete nucleotide sequence of wild rice (*Oryza nivara*) chloroplast genome: first genome wide comparative sequence analysis of wild and cultivated rice. Gene 340: 133-139.

Mathis, P., Butler, W. L. and Satoh, K. (1979). Carotenoid triplet state and chlorophyll fluorescence quenching in chloroplasts and subchloroplast particles Photochemistry and Photobiology 30: 603-614.

Matsumoto F., Obayashi T., Sasaki-Sekimoto Y., Ohta H., Takamiya K., Masuda T. (2004) Gene expression profiling of the tetrapyrrole metabolic pathway in *Arabidopsis* with a mini-array system, Plant Physiol. 135: 2379-2391.

May, T., Soll, J. (2000). 14-3-3 proteins form a guidance complex with chloroplast precursor proteins in plants. Plant Cell. 12: 53-64.

Mayfield, S. P. and Taylor, W. C. (1984). Carotenoid-deficient maize seedlings fail to accumulate light-harvesting chlorophyll a/b binding protein (LHCP) mRNA. Eur. J. Biochem. 144: 79-84.

McCormac, A. C., Fischer, A., Kumar, A. M., Soll, D., Terry, M. J. 2001. Regulation of HEMA1 expression by phytochrome and a plastid signal during de-etiolation in *Arabidopsis* thaliana. Plant J. 25:549–61.

McCormac, A. C. and Terry, M. J. (2002a). Light-signalling pathways leading to the co-ordinated expression of HEMA1 and Lhcb during chloroplast development in *Arabidopsis thaliana*. Plant J. 32: 549-559.

McCormac, A. C. and Terry, M. J. (2002b). Loss of nuclear gene expression during the phytochrome A-mediated far-red block of greening response. Plant Physiol. 130: 402-414.

McCormac, A. C. and Terry, M. J. (2004). The nuclear genes Lhcb and HEMA1 are differentially sensitive to plastid signals and suggest distinct roles for the GUN1 and GUN5 plastid-signalling pathways during de-etiolation. Plant J. 40: 672-685.

Meskauskiene, R., Nater, M., Goslings, D., Kessler, F., op den Camp, R., and Apel, K. (2001). FLU: a negative regulator of chlorophyll biosynthesis in *Arabidopsis thaliana*. Proc. Natl. Acad. Sci. USA 98: 12826–12831.

Meskauskiene, R., Wursch, M., Laloi, C., Vidi, P. A., Coll, N. S., Kessler, F., Baruah, A., Kim, C., Apel, K. (2009). A mutation in the *Arabidopsis* mTERF-related plastid protein SOLDAT10 activates retrograde signaling and suppresses $^1O_2$-induced cell death. Plant J. 60: 399-410.

Miller, G., Mittler, R. (2006). Could heat shock transcription factorsfunction as hydrogen peroxide sensors in plants? Ann. Bot. 98:279-288.

Miller, G., Suzuki, N., Rizhsky, L., Hegie, A., Koussevitzky S., and Mittler R.(2007). Double Mutants Deficient in Cytosolic and Thylakoid Ascorbate Peroxidase Reveal a Complex Mode of Interaction between Reactive Oxygen Species, Plant Development, and Response to Abiotic Stresses. Plant Physiol. 144: 1777–1785.

Mittler, R., Vanderauwera, S., Gollery, M. and Van Breusegem, F. (2004). Reactive oxygen gene network of plants. Trends Plant Sci. 9: 490-498.

Mittler, R., Vanderauwera, S., Suzuki, N., Miller, G., Tognetti, V. B., Vandepoele, K., Gollery, M., Shulaev, V., Van Breusegem, F. (2011). ROS signaling: the new wave? Trends Plant Sci. 16: 300-309.

Mochizuki, N., Susek, R. and Chory, J. (1996). An intracellular signal transduction pathway between the chloroplast and nucleus is involved in de-etiolation. Plant Physiol .112: 1465–1469.

Mochizuki, N., Brusslan, J. A., Larkin, R., Nagatani, A. and Chory, J. (2001). Arabidopsis*genomes uncoupled5* (*GUN5*) mutant reveals the involvement of Mg-chelatase H subunit in plastid-to-nucleus signal transduction. Proc. Nat. Acad. Sci. USA 98: 2053-2058.

Mochizuki, N., Tanaka, R., Tanaka, A., Masuda, T. and Nagatani, A. (2008). The steady-state level of Mg-protoporphyrin IX is not a determinant of plastid-to-nucleus signaling in Arabidopsis. Proc. Natl. Acad. Sci. USA 105: 15184-15189.

Mochizuki, N., Tanaka, R., Grimm, B., Masuda, T., Moulin, M., Smith, A. G. (2010). The cell biology of tetrapyrroles: a life and death struggle. Trends. Plant Sci. 15: 488–498.

Mor, A., Koh, E., Weiner, L., Rosenwasser, S., Sibony-Benyamini, Fluhr, R. (2014). Singlet oxygen signatures are detected independent of light or chloroplasts in response to multiple stresses. Plant Physiol .165: 249–261.

Moulin, M., McCormac, A. C., Terry, M. J. and Smith, A. G. (2008). Tetrapyrrole profiling in *Arabidopsis* seedlings reveals that retrograde plastid nuclear signaling is not due to Mg-protoporphyrin IX accumulation. Proc. Natl. Acad. Sc. USA 105: 15178-15183.

Mazzoleni M., Figuet S., Martin-Laffon J., Mininno M., Gilgen A., Leroux M., Brugière S., Tardif M., Alban C., Ravanel S. (2015). Dual Targeting of the Protein Methyltransferase PrmA Contributes to Both Chloroplastic and Mitochondrial Ribosomal Protein L11 Methylation in Arabidopsis.Plant Cell Physiol. 56: 1697-710.

Mubarakshina, M. M., Ivanov, B. N., Naydov, I. A., Hillier, W., Badger, M. R. and Krieger-Liszkay, A. (2010). Production and diffusion of chloroplastic H_2O_2 and its implication to signalling. J. Exp. Bot. 61: 3577-3587.

Muhlenbock, P., Szechynska-Hebda, M., Plaszczyca, M., Baudo, M., Mateo, A., Mullineaux, P. M., Parker, J.E., Karpinska, B., Karpinski, S. (2008). Chloroplast signaling and LESION SIMULATING DISEASE1 regulate crosstalk between light acclimation and immunity in *Arabidopsis*. Plant Cell 20: 2339-2356.

Munchel, S. E., Shultzaberger, R.K., Takizawa, N., Weis K. (2011). Dynamic profiling of mRNA turnover reveals gene-specific and system-wide regulation of mRNA decay. Mol. Biol. Cell 22: 2787 – 2795.

Nada, A. and Soll, J. (2004). Inner envelope protein 32 is imported into chloroplasts by a novel pathway. J. of Cell Sci. 117: 3975–3982.

Nagahatenna, D. S. K., Langridge, P., and Whitford, R. (2015). Tetrapyrrole-based drought stress signalling. Plant Biotechnology Journal 13: 447–459.

Nagai, S., Koide, M., Takahashi, S., Kikuta, A., Aono, M., Sasaki-Sekimoto, Y, Ohta, H., Takamiya, K. and Tatsuru Masuda (2007). Induction of Isoforms of Tetrapyrrole Biosynthetic Enzymes, AtHEMA2 and AtFC1, under Stress Conditions and Their Physiological Functions in A*rabidopsis*. Plant Physiol. 144: 1039–1051.

Nakashima, K., Yamaguchi-Shinozaki, K., Shinozaki K. (2014). The transcriptional regulatory network in the drought response and its crosstalk in abiotic stress responses including drought, cold, and heat. Front. Plant Sci. 5: 170.

Nardini, M., Gnesutta, N., Donati, G., Gatta, R., Forni, C., Fossati, A., et al. (2013). Sequence-specific transcription factor NF-Y displays histone-like DNA binding and H2B-like ubiquitination. Cell 152: 132–143.

Nelson, D. E., Repetti, P. P., Adams, T. R., Creelman, R. A., Wu, J., Warner, D. C., … Heard, J. E. (2007). Plant nuclear factor Y (NF-Y) B subunits confer drought tolerance and lead to improved corn yields on water-limited acres. Proc. Natl. Acad. Sci. U.S.A. 104: 16450–16455.

Nielsen, E., Akita, M., Davila-Aponte, J. and Keegstra, K. (1997). Stable association of chloroplastic precursors with protein-translocation complexes that contain proteins from both envelope membranes and a stromal Hsp100 molecular chaperone. EMBO J. 16: 935–946.

Nishimura, K., Asakura, Y., Friso, G., Kim, J., Oh, S.H., Rutschow, H., Ponnala, L., van Wijk, K.J. (2013). ClpS1 is a conserved substrate selector for the chloroplast Clp protease system in *Arabidopsis*. Plant Cell. 25: 2276-301.

Nomura, H., Komori, T., Uemura, S., Kanda, Y., Shimotani, K., Nakai, K., Furuichi, T., Takebayashi, K., Sugimoto, T., Sano, S., Suwastika, I. N., Fukusaki, E., Yoshioka, H., Nakahira, Y., Shiina, T. (2012). Chloroplast-mediated activation of plant immune signalling in Arabidopsis. Nat. Commun. 3: 926.

Norris, S. R., Barrette, T. R. and DellaPenna, D. (1995). Genetic dissection of carotenoid synthesis in arabidopsis defines plastoquinone as an essential component of phytoene desaturation. Plant Cell 7: 2139-2149.

Ochsenbein, C., Przybyla, D., Danon, A., Landgraf, F., Göbel, C., Imboden, A., Feussner, I., Apel K. (2006). The role of EDS1 (enhanced disease susceptibility) during singlet oxygen-mediated stress responses of Arabidopsis. Plant J. 47: 445-56.

Oelmüller, R. and Mohr, H. (1986). Photooxidative destruction of chloroplasts and its consequences for expression of nuclear genes. Planta 167: 106-113.

Oh, S. and Montgomery B. L. (2013). Phytochrome-induced SIG2 expression contributes to photoregulation of phytochrome signalling and photomorphogenesis in *Arabidopsis thaliana*. J. Exp. Bot. 64: 5457–5472.

op den Camp, R. G., Przybyla, D., Ochsenbein, C., Laloi, C., Kim, C., Danon, A., Wagner, D., Hideg, E., Göbel, C., Feussner, I., Nater, M. Apel, K. (2003). Rapid induction of distinct stress responses after the release of singlet oxygen in *Arabidopsis*. Plant Cell 15: 2320-2332.

Osterlund, M. T., Wie, N., Deng, X. W. (2000b). The roles of photoreceptor systems and the COP1-targeted destabilization of HY5 in light control of *Arabidopsis* seedling development. Plant Physiol 124: 1520–1524.

Osteryoung, K., W., Stokes, K. D., Rutherford, S. M., Percival, A. L, Lee, W. Y. (1998). Chloroplast division in higher plants requires members of two functionally divergent gene families with homology to bacterial ftsZ. Plant Cell 10: 1991-2004.

Paddock, T. N., Mason, M. E., Lima, D. F. and Armstrong, G. A. (2010). *Arabidopsis* protochlorophyllide oxidoreductase A (PORA) restores bulk chlorophyll synthesis and normal development to a porB porC double mutant. Plant Mo. Biol. 72: 445-457.

Paddock, T., Lima, D., Mason, M. E., Apel, K, Armstrong G. A. (2012) Arabidopsis light-dependent protochlorophyllide oxidoreductase A (PORA) is essential for normal plant growth and development. Plant Mol. Biol. 78:447–460.

Page, M. T., McCormac, A. C., Smith, A. G., Terry, M. J. (2017a). Singlet oxygen initiates a plastid signal controlling photosynthetic gene expression. New Phytol. 213: 1168–1180.

Page, M. T., Kacprzak, S. M., Mochizuki, N., Okamoto, H., Smith, A. G. and Terry M. J. (2017b). Seedlings Lacking the PTM Protein Do Not Show a *genomes uncoupled* (g*un*) Mutant Phenotype. Plant Physiol. 174: 21–26.

Palmer, J. D., Osorio, B., Aldrich, J., Thompson, W. F. (1987). Chloroplast DNA evolution among legumes: loss of a large inverted repeat occurred prior to other sequence rearrangements. Curr Genet. 11: 275–286.

Pattanayak G. K. and Tripathy B. C. (2016). Modulation of biosynthesis of photosynthetic pigments and light-harvesting complex in wild-type and gun5 mutant of Arabidopsis thaliana during impaired chloroplast development. Protoplasma.253:747-52.

Patel, D. and Franklin, K. A. (2009). Temperature-regulation of plant architecture. Plant Signal Behav. 4: 577-579.

Peltier, J.B., Cai, Y. , Sun, Q., Zabrouskov, V. , Giacomelli, L. , Rudella, A. , Ytterberg, A. J. , Rutschow, H. and van Wijk , K. J. (2006). The oligomeric stromal proteome of Arabidopsis thaliana chloroplasts. Mol. Cell. Proteomics 5: 114 – 133.

Pesaresi, P., Varotto, C., Meurer, J., Jahns, P., Salamini, F., Leister, D. (2001). Knock-out of the plastid ribosomal protein L11 in Arabidopsis: effects on mRNA translation and photosynthesis. Plant J. 27: 179-89.

Pesaresi, P., Masiero, S., Eubel, H., Braun, H-P., Bhushan, S., Glaser, E., Salamini, ., LFeister, D. (2006). Nuclear Photosynthetic Gene Expression Is Synergistically Modulated by Rates of Protein Synthesis in Chloroplasts and Mitochondria. Plant Cell 18: 970–991.

Pesaresi, P., Hertle, A., Pribil, M., Kleine, T., Wagner, R., Strissel, H., Ihnatowicz, A., Bonardi, V., Scharfenberg, M., Schneider, A., Pfannschmidt, T., Leister, D. 2009. *Arabidopsis* STN7 kinase

provides a link between short- and long-term photosynthetic acclimation. Plant Cell 21: 2402-2423.

Pfannschmidt, T., Nilsson, A., Tullberg, A., Link, G., Allen, J. F. (1999a). Direct transcriptional control of the chloroplast genes psbA and psaAB adjusts photosynthesis to light energy distribution in plants. IUBMB Life 48: 271–276.

Pfannschmidt, T., Allen, J. F. and Oelmuller, R. (2001). Principles of redox control in photosynthesis gene expression. Physiol. Plant. 112: 1-9.

Pfannschmidt, T. (2003). Chloroplast redox signals: how photosynthesis controls its own genes. Trends Plant Sci. 8:33-41.

Pfannschmidt, T. (2010). Plastidial retrograde signaling – a true "plastid factor" or just metabolite signatures? Trends Plant Sci. 15: 427–435.

Pfannschmidt, T., Blanvillain, R., Merendino, L., Courtois, F., Chevalier, F., Liebers, M., Grübler, B., Hommel, E., Lerbs-Mache, S. (2015). Plastid RNA polymerases: orchestration of enzymes with different evolutionary origins controls chloroplast biogenesis during the plant life cycle. J. Exp. Bot. 66: 6957–6973.

Pogson, B. J. and Albrecht, V. (2011). Genetic dissection of chloroplast biogenesis and development: an overview. Plant Physiol. 155: 1545-1551.

Pogson, B. J., Woo, N. S., Forster, B. and Small, I. D. (2008). Plastid signalling to the nucleus and beyond. Trends Plant Sci .13: 602-609.

Pontoppidan, B., Kannangara, C. G. (1994). Purification and partial characterisation of barley glutamyl-tRNAGlu reductase, the enzyme that directs glutamate to chlorophyll biosynthesis. Eur . J. Biochem. 225: 529–537.

Prasad, T. K., Anderson, M. D., Martin, B. A. and R., S. C. (1994). Evidence for Chilling-Induced Oxidative Stress in Maize Seedlings and a Regulatory Role for Hydrogen Peroxide. Plant Cell 6: 65–74.

Prasad, A., Ferretti, U., Sedlářová, M., Pospíšil, P. (2016). Singlet oxygen production in *Chlamydomonas reinhardtii* under heat stress. Sci. Rep. 6 20094

Puthiyaveetil, S., Kavanagh, T. A., Cain, P., Sullivan, J. A., Newell, C. A., Gray, J. C., Robinson, C., van der Giezen, M., Rogers, M. B., Allen, J. F. (2008). The ancestral symbiont sensor kinase CSK links photosynthesis with gene expression in chloroplasts. Proc. Natl. Acad. Sci. USA 105: 10061-6.

Ramel, F., Birtic, S., Ginies, C., Soubigou-Taconnat, L., Triantaphylidès, C. and Havaux, M. (2012). Carotenoid oxidation products are stress signals that mediate gene responses to singlet oxygen in plants. Proc. Natl. Acad. Sci. USA 109: 5535-5540.

Ramel, F., Ksas, B., Akkari, E., Mialoundama, A. S., Monnet, F., Krieger-Liszkay, A, Ravanat, J-L., Mueller M. J., Bouvier F., Havaux M. (2013). Light-inducedacclimation of the *Arabidopsis* chlorina1 mutant to singlet oxygen. Plant Cell25: 1445–1462.

Rasmussen, S., Barah, P., Suarez-Rodriguez, M. C., Bressendorff, S., Friis P., Costantino, P., Bones, A. M., Nielsen, H. B., Mundy, J. (2013). Transcriptome responses to combinations of stresses in *Arabidopsis.* Plant Physiol. 161: 1783-1794.

Rial, D. V., Arakaki, A. K., Ceccarelli, E. A. (2000). Interaction of the targeting sequence of chloroplast precursors with Hsp70 molecular chaperones. Eur J Biochem. 267: 6239-6248.

Romani, I., Tadini, L., Rossi, F., Masiero, S., Pribil, M., Jahns, P., Kater, M., Leister, D., Pesaresi, P. (2012). Versatile roles of Arabidopsis plastid ribosomal proteins in plant growth and development. Plant J. 72: 922-934.

Ruckle, M. E., DeMarco, S. M., Larkin, R. M. (2007). Plastid signals remodel light signaling networks and are essential for efficient chloroplast biogenesis in *Arabidopsis*. Plant Cell.19:3944-60.

Ruckle, M. E., Burgoon, L. D., Lawrence, L. A., Sinkler, C. A. and Larkin, R. M. (2012). Plastids are major regulators of light signaling in *Arabidopsis*. Plant Physiol.159: 366-390.

Ruf, M., Kossel, H. (1988). Occurrence and spacing of ribosome recognition sites in mRNAs of chloroplasts from higher plants. FEBS Lett. 240 : 41-44.

Saini, G., Meskauskiene, R., Pijacka, W., Roszak, P., Sjogren, L. L., Clarke, A. K., et al. (2011). 'happy on norflurazon' (hon) mutations implicate perturbance of plastid homeostasis with activating stress acclimatization and changing nuclear gene expression in norflurazon-treated seedlings. Plant J. 65: 690–702.

Sakuma, Y., Maruyama, K., Osakabe, Y., Qin, F., Seki, M., Shinozaki, K. and Yamaguchi-Shinozaki, K. (2006). Functional analysis of an *Arabidopsis* transcription factor, DREB2A, involved in drought-responsive gene expression. Plant Cell 18: 1292-1309.

Saltveit, M., E., Morris, L., L. (1990). Overview of chilling injury of horticultural crops. [in]: Wang, C., Y. Chilling injury of horticultural crops. CRC Press, Boca Raton, FL: 3–15.

Scharfenberg, M., Mittermayr, L., VON Roepenack-Lahaye, E., Schlicke, H., Grimm, B., Leister, D., Kleine T. (2013). Functional characterization of the two ferrochelatases in *Arabidopsis thaliana*. Plant Cell Environ. 38:280-98.

Schattat, M. H., Griffiths, S., Mathur, N., Barton, K., Wozny, M. R., Dunn, N., Greenwood, J.S., Mathur, J. (2012). Differential coloring reveals that plastids do not form networks for exchanging macromolecules. Plant Cell 24: 1465-1477.

Schlicke, H., Hartwig, A. S., Firtzlaff, V., Richter, A. S., Glässer, C., Maier, K., Finkemeier, I., Grimm, B. (2014). Induced deactivation of genes encoding chlorophyll biosynthesis enzymes disentangles tetrapyrrole-mediated retrograde signalling. Mol. Plant. 7: 1211-1227.

Schünemann D. (2007). Mechanisms of protein import into thylakoids of chloroplasts. Biol Chem. 388: 907-915.

Schwechheimer, C., and Deng, X. W. (2000). The COP/DET/FUS proteins-regulators of eukaryotic growth and development. Semin. Cell Dev. Biol. 11: 495-503.

Seki, M., Narusaka, M., Abe, H., Kasuga, M., Yamaguchi-Schinozaki, K., Carninci, P., Hayashizaki, Y. and Shinozaki, K. (2001). Monitoring the expression pattern of 1300 *Arabidopsis* genes under drought and cold stresses by using a full-length cDNA microarray. Plant Cell 13: 61–72.

Scharfenberg, M., Mittermayr, L., Von Roepenack-Lahaye, E., Schlicke, H., Grimm, B., Leister, D. (2015). Functional characterization of the two ferrochelatases in Arabidopsis thaliana. Plant Cell Environ. 38: 280–298.

Seedorf, M., Waegemann, K., Soll, J. (1995). A constituent of the chloroplast import complex represents a new type of GTP-binding protein. Plant J 7: 401–411.

Seo, H. S., Yang, J., Ishikawa, M., Bolle, B., Ballesteros, M. L., Chua, N. H. (2003). LAF1 ubiquitination by COP1 controls photomorphogenesis and is stimulated by SPA1. Nature 423: 995–999.

Serino, G., Maliga, P. (1998). RNA polymerase subunits encoded by the plastid *rpo* genes are not shared with the nucleus-encoded plastid enzyme. Plant Physiol. 117: 1165-70.

Shahnejat-Bushehri, S., Mueller-Roeber, B. and Balazadeh, S. (2012). *Arabidopsis* NAC transcription factor JUNGBRUNNEN1 affects thermomemory-associated genes and enhances heat stress tolerance in primed and unprimed conditions. Plant Signal.Behav. 7: 1518-1521.

Sharma, M. R., Wilson, D. N., Datta, P. P., Barat, C., Schluenzen, F., Fucini, P., Agrawal, R. K. (2007). Cryo-EM study of the spinach chloroplast ribosome reveals the structural and functional roles of plastid-specific ribosomal proteins. Proc. Natl. Acad. Sci. USA 104: 19315–19320.

Shin, J., Park, E., Choi, G. (2007). PIF3 regulates anthocyanin biosynthesis in an HY5-dependent manner with both factors directly binding anthocyanin biosynthetic gene promoters in *Arabidopsis*. Plant J. 49: 981-994.

Singh, D. P., Cornah, J. E., Hadingham, S., Smith, A. G. (2002). Expression analysis of the two ferrochelatase genes in *Arabidopsis* in different tissues and under stress conditions reveals their different roles in haem biosynthesis. Plant Mol. Biol. 50 773–788.

Sharma, P., Jha, A. B., Dubey, R. S., and Pessarakli, M. (2012). Reactive Oxygen Species, Oxidative Damage, and Antioxidative Defense Mechanism in Plants under Stressful Conditions. Journal of Botany, 1-26.

Shin, J., Kim, K., Kang, H., Zulfugarov, I. S., Bae, G., Lee, C. H., Lee, D., Choi, G. (2009). Phytochromes promote seedling light responses by inhibiting four negatively-acting phytochrome-interacting factors. Proc. Natl. Acad. Sci. USA 106: 7660-7665.

Shumbe L., Chevalier A., Legeret B., Taconnat L., Monnet F., Havaux M. (2016). Singlet Oxygen-Induced Cell Death in *Arabidopsis* under High-Light Stress Is Controlled by OXI1 Kinase. Plant Physiol. 170: 1757-71.

Siguira, M. (1992). The chloroplast genome. Plant Mol Biol. 19: 149-168.

Solfanelli, C., Poggi, A., Loreti, E., Alpo, A., Pirate, P. (2006). Sucrose-specific induction of the anthocyanin biosynthetic pathway in *Arabidopsis*. Plant Physiology 140: 637–646.

Stephenson, P.G., Terry, M.J. (2008). Light signalling pathways regulating the Mg-chelatase branchpoint of chlorophyll synthesis during de-etiolation in *Arabidopsis thaliana*. Photochem. Photobiol. Sci. 7: 1243–1252.

Stephenson, P. G., Fankhauser, C. and Terry, M. J. (2009). PIF3 is a repressor of chloroplast development. Proc. Natl. Acad. Sci. USA 106: 7654-7659.

Stern, S., Dror T., Stolovicki, E., Brenner, N., Braun, E. (2007). Genome-wide transcriptional plasticity underlies cellular adaptation to novel challenge. Mol. Syst. Biol. 3:106.

Stern, D. B., Goldschmidt-Clermont, M., Maureen, R. H. (2010). Chloroplast RNA metabolism. Annu. Rev. Plant Biol. 61: 125-155.

Strand, A., Asami, T., Alonso, J., Ecker, J. R. and Chory, J. (2003). Chloroplast to nucleus communication triggered by accumulation of Mg-protoporphyrinIX. Nature 421: 79-83.

Su, Q., Frick, G., Armstrong, G. and Apel, K. (2001). POR C of *Arabidopsis thaliana*: a third light- and NADPH-dependent protochlorophyllide oxidoreductase that is differentially regulated by light. Plant Mol. Biol. 47: 805–813.

Su, P. H., Li, H. M. (2010). Stromal Hsp70 is important for protein translocation into pea and *Arabidopsis* chloroplasts. Plant Cell 22: 1516-1531.

Sugira, M. (1992). The chloroplast genome. Plant Mol. Biol. 19: 149-168.

Sullivan, J. A. and Gray, J. C. (1999). Plastid translation is required for the expression of nuclear photosynthesis genes in the dark and in roots of the pea *lip1* mutant Plant Cell 11: 901-910.

Sun, X., Feng, P., Xu, X., Guo, H., Ma, J., Chi, W., Lin, R., Lu, C., Zhang, L. (2011). A chloroplast envelope-bound PHD transcription factor mediates chloroplast signals to the nucleus. Nat. Commun. 2: 477.

Sun, X., Xu D., Liu, Z., Kleine, T., Leister, D. (2016). Functional relationship between mTERF4 and GUN1 in retrograde signaling. J. Exp. Bot. 67: 3909-24.

Susek, R. E., Ausubel, F. M. and Chory, J. (1993). Signal transduction mutants of *Arabidopsis* uncouple nuclear CAB and RBCS gene expression from chloroplast development. Cell 74: 787-799.

Suzuki, T., Masuda, T., Singh, D. P., Tan, F. C., Tsuchiya, T. (2002). Two types of ferrochelatase in photosynthetic and nonphotosynthetic tissues of cucumber. Their difference in phylogeny, gene expression, and localization. J. Biol. Chem. 277: 4731–37.

Svensson, J. T., Crosatti, C., Campoli, C., Bassi, R., Stanca, A. M., Close, T. J., Cattivelli L. (2006). Transcriptome analysis of cold acclimation in barley *albina* and *xantha* mutants. Plant Physiol. 141: 257-70.

Tadini, L., Pesaresi, P., Kleine, T., Rossi, F., Guljamow, A., Sommer, F., Mühlhaus, T., Schroda, M., Masiero, S., Pribil, M., Rothbart, M., Hedtke, B., Grimm, B., Leister, D. (2016). GUN1 Controls Accumulation of the Plastid Ribosomal Protein S1 at the Protein Level and Interacts with Proteins Involved in Plastid Protein Homeostasis. Plant Physiol.170: 1817-30.

Takahashi, S., Murata, N. (2008). How do environmental stresses accelerate photoinhibition? Trends Plant Sci. 13: 178-182.

Tanaka,R., and Tanaka A. (2007). Tetrapyrrole biosynthesis in higher plants. Annu. Rev. Plant Biol. 58: 321–346.

Tang, J., Xia, H., Cao, M., Zhang, X., Zeng, W., Hu, S., Tong, W., Wang, J., Wang, J., Yu, J., Yang, H., Zhu, L. (2004). A comparison of rice chloroplast genomes. Plant Physiology 135: 412–42.

Tarahi Tabrizi, S., Sawicki, A., Zhou, S., Luo, M., Willows, R.D. (2016). GUN4-Protoporphyrin IX Is a Singlet Oxygen Generator with Consequences for Plastid Retrograde Signaling. J. Biol. Chem. 291: 8978-84.

Terry M. J., Wahleithner J A., Lagarias J C. (1993). Biosynthesis of the plant photoreceptor phytochrome. Arch. Biochem. Biophys.306:1-15.

Terry, M. J., Kendrick, R. E. (1996). The aurea and *yellow-green-2* mutants of tomato are deficient in phytochrome chromophore synthesis. J. Biol. Chem .271:21681–21686.

Terry, M. J., Ryberg, M., Raitt, C. E., and Page, A. M. (2001). Altered etioplast development in phytochrome chromophore-deficient mutants. Planta 214: pp. 314-325.

Terry, M. J. and Smith, A. G. (2013). A model for tetrapyrrole synthesis as the primary mechanism for plastid-to-nucleus signaling during chloroplast biogenesis. Front. Plant. Sci. 4: 1-14.

Tewari K. A. Tripathy B. C. (1998). Temperature-stress-induced impairment of chlorophyll biosynthetic reactions in cucumber and wheat. Plant Physiol. 117: 851-858.

Thu-Ha, P., Jung, H.-I., Park, J.-H., Kim, J.-G., Back, K. and Jung, S. (2011). Porphyrin biosynthesis control under water stress: sustained porphyrin statuscorrelates with drought tolerance in transgenic rice. Plant Physiol. 157: 1746–1764.

Tiller, N., Bock, R. (2014). The translational apparatus of plastids and its role in plant development. Molecular plant 7: 1105–1120.

Timmis, J. N., Ayliffe, M. A., Huang, C. Y. and Martin, W. (2004). Endosymbiotic gene transfer: organelle genomes forge eukaryotic chromosomes. Nat. Rev. Genet. 5: 123-135.

Tohdoh N., and Sugiura, M. (1982). The complete nucleotide sequence of a 16S ribosomal RNA gene from tobacco chloroplasts: Recombinant plasmid; sequence homology; stem and loop structure. Gene 17: 213-218.

Triantaphylides, C., Krischke, M., Hoeberichts, F. A., Ksas, B., Gresser, G., Havaux, M., Van Breusegem, F., Mueller, M. J. (2008). Singlet oxygen is the major reactive oxygen species involved in photooxidative damage to plants. Plant Physiol. 148: 960-968.

Triantaphylidès, C., Havaux, M. (2009). Singlet oxygen in plants: production, detoxification and signaling. Trends Plant. Sci. 14:219-28.

Tsunoyama, Y., Morikawa, K., Shiina, T., and Toyoshima, Y. (2002). Blue light specific and differential expression of a plastid σ factor, Sig5 in *Arabidopsis thaliana*. FEBS Lett. 516: 225–228.

Tsunoyama, Y., Ishizaki, Y., Morikawa, K., Kobori, M., Nakahira, Y., Takeba, G., Toyoshima, Y., and Shiina, T. (2004). Blue light-induced transcription of plastid-encoded psbD gene is mediated by a nuclear-encoded transcription initiation factor, AtSig5. Proceedings of the National Academy of Sciences of the United States of America 101: 3304-3309.

Turan, S., Tripathy, B. C. (2014). Salt-stress induced modulation of chlorophyll biosynthesis during de-etiolation of rice seedlings. Physiol Plant .153:477-91.

Ujwal, M. L., McCormac, A. C., Goulding, A., Kumar, A. M., Söll, D., Terry M. J. (2002). Divergent regulation of the HEMA gene family encoding glutamyl-tRNA reductase in *Arabidopsis thaliana*: expression of HEMA2 is regulated by sugars, but is independent of light and plastid signalling. Plant Mol. Biol. 50:83-91.

Van Breusegem, F., Dat, J. F.(2006). Reactive oxygen species in plant cell death. Plant Physiol. 141:384-90.

Verslues, P. E., Ober, E. S. and Sharp, R. E. (1998). Root growth and oxygen relations at low water potentials. Impact of oxygen availability in polyethylene glycol solutions Plant Physiol. 116: 1403-1412.

Villarejo, A., Burén, S., Larsson, S., Déjardin, A., Monné, M., Rudhe, C., Karlsson, J., Jansson, S., Lerouge, P., Rolland, N., von Heijne, G., Grebe, M., Bako, L., Samuelsson G. (2005). Evidence for a protein transported through the secretory pathway en route to the higher plant chloroplast. Nat. Cell. Biol. 7: 1224-31.

Vinti G., Hills A., Campbell S., Bowyer J.R., Mochizuki N., Chory J., López-Juez E. (2000). Interactions between hy1 and gun mutants of Arabidopsis, and their implications for plastid/nuclear signalling. Plant J. 24: 883-94.

Vitha, S., Froehlich, J. E., Koksharova, O., Pyke, K. A., van Erp H., Osteryoung, K. W. (2003). ARC6 is a J-domain plastid division protein and an evolutionary descendant of the cyanobacterial cell division protein Ftn2. Plant Cell. 15: 1918-1933.

Voigt, C., Oster, U., Bornke, F., Jahns, P., Dietz, K. J., Leister, D. and Kleine, T. (2010). In-depth analysis of the distinctive effects of norflurazon implies that tetrapyrrole biosynthesis, organellar gene expression and ABA cooperate in the GUN-type of plastid signalling. Physiol. Plant 138: 503-519.

Volkov, R. A., Panchuk, I. I., Mullineaux, P. M., Schöffl, F. (2006). Heat stress-induced H_2O_2 is required for effective expression of heat shock genes in *Arabidopsis*. Plant Mol. Biol. 61: 733-746.

von Heijne, G. (1986). Mitochondrial targeting sequences may form amphiphilic helices. EMBO J. 5:1335-1342.

von Heijne, G., Steppuhn, J., Herrmann, R. G. (1989). Domain structure of mitochondrial and chloroplast targeting peptides. Eur J Biochem. 180: 535-545.

Von Wettstein, D., Gough, S. and Kannangara, G. (1995). Chlorophyll Biosynthesis. Plant Cell 7: 1039-1057.

Wagner, D., Przybyla, D., OpdenCamp, R., Kim, C., Landgraf, F., Lee, K. P. (2004). The genetic basis of singlet oxygen induced stress responses of *Arabidopsis thaliana*. Science 306,1183–1185.

Wakasugi, T., Tsudzuki, T. and Sugiura, M. (2001). The genomics of land plant chloroplasts: Gene content and alteration of genomic information by RNA editing. Photosynth Res. 70: 107-118.

Walker, C. J., Willows, R. D. (1997) Mechanism and regulation of Mg-chelatase. Biochem J.327:321–333.

Walter, M., Kilian, J. Kudla, J. (2002). PNPase activity determines the efficiency of mRNA 3'-end processing, the degradation of tRNA and the extent of polyadenylation in chloroplasts. EMBO J. 21: 6905–6914.

Walter, M., Piepenburg, K., Schöttler, M. A., Petersen, K., Kahlau, S., Tiller, N., Drechsel, O., Weingartner, M., Kudla, J., Bock, R. (2010). Knockout of the plastid RNase E leads to defective RNA processing and chloroplast ribosome deficiency. Plant J. 64: 851-63.

Wang, L., Ma, F., Xu, S., Zheng, T., Wang, R., Chen, H. and Shen, W. (2014) Cloning and characterization of a heme oxygenase-2 gene from rice (*Oryzasativa L.*), and its expression analysis in response to some abiotic stresses. Acta. Physiol. Plant, 36: 893–902.

Waters, M. T. and Langdale, J. A. (2009). The making of a chloroplast. EMBO J. 28: 2861-2873.

Waters, M. T., Wang, P., Korkaric, M., Capper, R. G., Saunders, N. J. and Langdale, J. A. (2009). GLK transcription factors coordinate expression of the photosynthetic apparatus in *Arabidopsis*. Plant Cell 21: 1109-1128.

Weihe, A., Börner, T. (1999). Transcription and the architecture of promoters in chloroplasts. Trends Plant Sci. 4: 169-170.

Willows, R.D. and Beale, S.I. (1998). Heterologous expression of the *Rhodobacter capsulatus* BchI, -D, and -H genes that encode magnesium chelatase subunits and characterization of the reconstituted enzyme. J. Biol. Chem. 273: 34206–34213.

Wind, J. J., Peviani, A., Snel B, Hanson, J., Smeekens, S. C. (2013). ABI4: versatile activator and repressor. Trends Plant Sci. 18:125-32.

Wolfe, K. H., Morden, C. W., and Palmer, J. D. (1992). Function and evolution of a minimal plastid genome from a nonphotosynthetic parasitic plant. Proc. Natl. Acad. Sci. U.S.A. 89: 10648–10652.

Woodson, J. D., Perez-Ruiz, J. M. and Chory, J. (2011). Heme synthesis by plastid ferrochelatase I regulates nuclear gene expression in plants. Curr .Biol .21: 897-903.

Woodson, J. D., Perez-Ruiz, J. M., Schmitz, R. J., Ecker, J.R., Chory, J. (2013) Sigma factor-mediated plastid retrograde signals control nuclear gene expression. Plant J. 73:1-13.

Wu, F. Q., Xin, Q., Cao, Z., Liu, Z. Q., Du, S. Y., Mei, C., Zhao, C.X., Wang, X.F., Shang, Y., Jiang, T., Zhang, X. F., Yan, L., Zhao, R., Cui, Z. N., Liu, R., Sun, H. L., Yang, X. L., Su, Z.,

Wu, C. S., Lin, C. P., Hsu, C. Y., Wang, R. J., Chaw, S. M. (2011). Comparative chloroplast genomes of *pinaceae*: insights into the mechanism of diversified genomic organizations. Genome Biology and Evolution 3: 309–319.

Wu, H. Zheng, Y., Liu, J., Zhang, H., and Chen, H. (2015). Heme Oxygenase-1 Delays Gibberellin-Induced Programmed Cell Death of Rice Aleurone Layers Subjected to Drought Stress by Interacting with Nitric Oxide. Front. Plant Sci. 6: 1267.

Xiao, Y., Savchenko, T., Baidoo, E. E., Chehab, W. E., Hayden, D. M., Tolstikov, V., Corwin, J. A., Kliebenstein, D. J., Keasling, J. D., Dehesh, K. (2012). Retrograde signaling by the plastidial metabolite MEcPP regulates expression of nuclear stress-response genes. Cell 149: 1525-1535.

Xie, Y. J., Xu, S., Han, B., Wu, M. Z., Yuan, X. X., Han, Y., Gu, Q., Xu, D. K., Yang, Q., Shen, W. B. (2011). Evidence of *Arabidopsis* salt acclimation induced by up-regulation of HY1 and the regulatory role of RbohD-derived reactive oxygen species synthesis. Plant J. 66:280-92.

Xie, Y., Mao, Y., Duan, X., Zhou, H., Lai, D., Zhang, Y., Shen W. (2016). *Arabidopsis* HY1-Modulated Stomatal Movement: An Integrative Hub Is Functionally Associated with ABI4 in Dehydration-Induced ABA Responsiveness. Plant Physiol. 170: 1699-713.

Xiong, L., Lee, Bh., Ishitani, M., Lee, H., Zhang, C., Zhu, J. K. (2001). FIERY1 encoding an inositol polyphosphate 1-phosphatase is a negative regulator of abscisic acid and stress signaling in *Arabidopsis*. Genes Dev. 15: 1971-1984.

Xu X., Chi W., Sun X., Feng P., Guo H., Li J., Lin R., Lu C., Wang H., Leister, D., Zhang L. (2016). Convergence of light and chloroplast signals for de-etiolation through ABI4-HY5 and COP1. Nat. Plants. 9: 16066.

Yamaguchi-Shinozaki, K. and Shinozaki, K. (1994). A novel cis-acting element in an *Arabidopsis* gene is involved in responsiveness to drought, low-temperature, or high-salt stress. Plant Cell 6: 251-264.

Yamaguchi, K., von Knoblauch, K., Subramanian, A. R. (2000). The plastid ribosomal proteins. Identification of all the proteins in the 30 S subunit of an organelle ribosome (chloroplast). J Biol. Chem. 275: 28455–28465.

Yamaguchi, K., Subramanian, A. R. (2000). The plastid ribosomal proteins. Identification of all the proteins in the 50 S subunit of an organelle ribosome (chloroplast). J. Biol. Chem. 275: 28466–28482.

Yang, J., Lin, R., Sullivan, J., Hoecker, U., Liu, B., Xu, L., Deng, X. W., Wang, H. (2005). Light regulates COP1-mediated degradation of HFR1, a transcription factor essential for light signaling in *Arabidopsis*. Plant Cell 17: 804–821.

Yang, MT., Chen, S. L., Lin, C. Y., Chen, Y. M. (2005). Chilling stress suppresses chloroplast development and nuclear gene expression in leaves of mung bean seedlings. Planta 221: 374-85.

Yu, H., Chen, X., Hong, Y. Y., Wang, Y., Xu, P., Ke S. D., Liu, H. Y., Zhu, J. K., Oliver, D. J., Xiang, C. B. (2008). Activated expression of an *Arabidopsis* HD-START protein confers drought tolerance with improved root system and reduced stomatal density. Plant Cell 20: 1134-1151.

Yu, H., D., Yang, X. F., Chen, S.T., Wang, Y. T., Li, J. K., Shen, Q., Liu, X. L, Guo, F. Q. (2012). Downregulation of chloroplast RPS1 negatively modulates nuclear heat-responsive expression of HsfA2 and its target genes in *Arabidopsis*. PLoS Genet. 8: 1-18.

Zeller, G., Henz, S. R., Widmer, C. K., Sachsenberg, T., Rätsch, G., Weigel, D., Laubinger, S. (2009). Stress-induced changes in the *Arabidopsis* thaliana transcriptome analyzed using whole-genome tiling arrays. The Plant J. 58: 1068–1082.

Zeller, G., Henz, S. R., Widmer, C. K., Sachsenberg,T., Rätsch, G., Weigel, D., Laubinge,r S.(2009). Stress-induced changes in the *Arabidopsis* thaliana transcriptome analyzed using whole-genome tiling arrays. Plant J. 58:1068-82.

Zghidi, W., Merendino, L., Cottet, A., Mache, R., and Lerbs-Mache, S. (2007). Nucleusencoded plastid sigma factor SIG3 transcribes specifically the psbN gene in plastids. Nucleic Acids Research 35: 455-464.

Zhao, D. S., Zhang, C. Q., Li, Q. F., Yang, Q. Q., Gu, M. H., Liu, Q. Q. (2016). A residue substitution in the plastid ribosomal protein L12/AL1 produces defective plastid ribosome and causes early seedling lethality in rice. Plant Mol. Biol. 91: 161-77.

Zhang, X. P., Glaser, E. (2002). Interaction of plant mitochondrial and chloroplast signal peptides with the Hsp70 molecular chaperone. Trends Plant Sci. 7: 14-21.

Zhang, D. P. (2009). The magnesium-chelatase H subunit binds abscisic acid and functions in abscisic acid signaling: new evidence in *Arabidopsis*. Plant Physiol. 150: 1940-1954.

Zhang, Z-W., Yuan, S., Feng, H., Xu, F., Cheng, J., Shang, J., Zhang, D-W., Lin, H-H. (2011). Transient accumulation of Mg-protoporphyrin IX regulates expression of PhANGs – new evidence for the signaling role of tetrapyrroles in mature *Arabidopsis* plants. Journal of Plant Physiology 168: 714–721.

Zhang, S., Qi, Y., Liu, M., Yang, C., (2013). SUMO E3 ligase AtMMS21 regulates drought tolerance in *Arabidopsis thaliana*. J. Integr. Plant. Biol. 55: 83-95.

Zhang, Z. W., Feng, L. Y., Cheng, J., Tang, H., Xu, F., Zhu, F., Zhao, Z. Y., Yuan, M., Chen, Y. E., Wang, J. H. Yuan, S. Lin, H. H. (2013). The roles of two transcription factors, ABI4 and CBFA, in ABA and plastid signalling and stress responses. Plant Mol. Biol. 83:445-58.

Zhelyazkova, P., Sharma, C. M., Forstner, K. U., Liere, K., Vogel, J., Borner, T. (2012). The Primary Transcriptome of Barley Chloroplasts: Numerous Noncoding RNAs and the Dominating Role of the Plastid-Encoded RNA Polymerase. Plant Cell 24: 123-136.

Zhu, Q., Zhang, J., Gao, X., Tong, J., Xiao, L., Li, W., Zhang, H. (2010). The *Arabidopsis* AP2/ERF transcription factor RAP2.6 participates in ABA, salt and osmotic stress responses. Gene 457: 1-12.